

# SUPPRESSION OF PRO-INFLAMMATORY SIGNALLING PATHWAYS BY SULFORAPHANE

Danielle Lyn Folkard

Institute of Food Research

A thesis submitted for the degree of Doctor of Philosophy to the  
University of East Anglia

June 2014

©This copy of the thesis has been supplied on condition that anyone who consults it is understood to recognise that its copyright rests with the author and that use of any information derived there from must be in accordance with current UK Copyright Law.

In addition, any quotation or extract must include full attribution.

## Abstract

Low-grade inflammation has been associated with the risk of chronic pathologies including cancer, atherosclerosis and type 2 diabetes. Epidemiological studies demonstrate an inverse correlation between diets rich in cruciferous vegetables and risk of cancer, cardiovascular disease mortality and circulating levels of pro-inflammatory cytokines. Sulforaphane (SF), an isothiocyanate obtained from broccoli, has many biological functions. The aim of this thesis was to test whether SF was able to suppress pro-inflammatory signalling using *in vitro* models of chronic inflammation.

In human monocytes (PBMCs and THP-1 cells), physiologically relevant concentrations of SF significantly suppressed the production of LPS-induced cytokines IL-6, IL-1 $\beta$  and TNF $\alpha$ . The suppression was also observed with all genes induced by 1ng/ml LPS as measured by whole genome arrays. In addition, it was demonstrated that SF could directly interact with thiol groups of cysteine residues 609 and 246 within the LPS receptor, TLR4 under non-reducing conditions, to reduce the levels of inflammatory mediators that are produced in response to LPS.

The anti-inflammatory effect of SF was not restricted to the TLR4 pathway, and significant reductions were observed in NF- $\kappa$ B activity induced in response to TLR2 and NOD2 ligands. These findings were translated into a more complex *in vitro* model, investigating the effect of SF on lipid accumulation within adipocytes and adipose tissue inflammation in response to macrophage-conditioned medium (MaCM) using human SGBS adipocytes. SF at 10 $\mu$ M significantly reduced levels of lipid accumulation within adipocytes and increased the expression of carnitine palmitoyltransferase-1A (CPT1A), suggesting a role in energy metabolism, a process often disrupted in obesity. In addition, a significant suppression in SGBS adipocyte IL-1 $\beta$  and IL-6 expression was observed when adipocytes were exposed to MaCM from SF-treated macrophages, when SF was used at a concentration as low as 2 $\mu$ M.

This work demonstrates that concentrations of SF that could be achieved via reasonable broccoli consumption can suppress pro-inflammatory cytokine production, induced in response to a number of signalling pathways in addition to suppression of lipid accumulation and adipose tissue inflammation. The relevance of this data supports the concept that consumption of broccoli could lead to a reduction in the chronic inflammatory status *in vivo* as well as a suppression of lipid accumulation within adipocytes, to reduce the risk of developing chronic disease.

## Contents

<b>Abstract</b> .....	<b>i</b>
<b>Contents</b> .....	<b>ii</b>
<b>List of Figures</b> .....	<b>viii</b>
<b>List of Tables</b> .....	<b>xii</b>
<b>Abbreviations</b> .....	<b>xiii</b>
<b>Symbols</b> .....	<b>xvii</b>
<b>List of Publications</b> .....	<b>xviii</b>
<b>Acknowledgements</b> .....	<b>xix</b>
<b>Chapter One – General introduction</b> .....	<b>1</b>
1.0. Summary of the thesis.....	2
1.1. Inflammation.....	3
<i>1.1.1. Acute versus chronic inflammation</i> .....	4
<i>1.1.2. Inflammatory signalling pathways involved in chronic inflammation</i> .....	4
1.1.2.1. TLR4 and TLR2 signalling pathways.....	4
1.1.2.2. NOD2 signalling pathway.....	7
<i>1.1.3. The importance of chronic inflammation in diseases</i> .....	9
1.1.3.1. Cancer.....	10
1.1.3.2. Cardiovascular disease.....	10
1.1.3.3. Type 2 diabetes mellitus.....	11
1.1.3.4. Inflammatory bowel diseases.....	11
1.1.3.5. Involvement of obesity in chronic disease.....	12
<i>1.1.4. Characteristics of obesity</i> .....	13
1.1.4.1. Lipid metabolism.....	15
1.1.4.2. Adipose tissue inflammation.....	16
1.2. Epidemiological data for fruit and vegetable intake and chronic disease risk.....	17
1.3. Cruciferous vegetables.....	19
<i>1.3.1. Glucosinolates</i> .....	19
1.4. Sulforaphane.....	21
<i>1.4.1. Bioavailability</i> .....	21
<i>1.4.2. Targets of SF</i> .....	23
1.4.2.1. Phase 2 enzymes and oxidative stress.....	23
1.4.2.2. Cell metabolism.....	24
1.4.2.3. Cell cycle and apoptosis.....	25
1.4.2.4. Inflammation.....	25
1.5. Thesis Aims.....	26

---

<b>Chapter Two – General materials and methods</b> .....	<b>29</b>
2.1. General reagents.....	30
2.2. Cell culture.....	30
2.2.1. <i>Human monocytes</i> .....	30
2.2.2. <i>PRR-transfected cell lines</i> .....	31
2.2.3. <i>HT-29 colon adenocarcinoma cells</i> .....	32
2.2.4. <i>SGBS preadipocyte cells</i> .....	32
2.3. Cell viability assay.....	33
2.3.1. <i>Background</i> .....	33
2.3.2. <i>Measurement of cell viability</i> .....	34
2.3.3. <i>Data analysis and statistics</i> .....	35
2.4. Measuring cytokine secretion using enzyme-linked immunosorbant assay .....	35
2.4.1. <i>Background</i> .....	35
2.4.2. <i>Measurement of cytokine secretion</i> .....	37
2.4.3. <i>Statistics</i> .....	37
2.5. Gene expression using real-time reverse transcriptase – polymerase chain reaction .....	37
2.5.1. <i>Background</i> .....	37
2.5.2. <i>RNA extraction and quantification</i> .....	38
2.5.3. <i>Real-time RT-PCR</i> .....	38
2.5.4. <i>Statistics</i> .....	41
2.6. Whole genome expression analysis using microarray techniques.....	41
2.6.1. <i>Background</i> .....	41
2.6.2. <i>Assessment of RNA quality</i> .....	42
2.6.3. <i>Data analysis and statistics</i> .....	43
2.7. Western blotting.....	44
2.7.1. <i>Background</i> .....	44
2.7.2. <i>Sample preparation</i> .....	44
2.7.3. <i>Gel electrophoresis</i> .....	45
2.7.4. <i>Immunoblotting</i> .....	45
2.7.5. <i>Data analysis and statistics</i> .....	47
2.8. Analysis of SF modifications on TLR4 using liquid chromatography-tandem mass spectroscopy (LC-MS/MS).....	47
2.8.1. <i>Sample preparation</i> .....	47
2.8.1.1. <i>Recombinant TLR4 protein</i> .....	47
2.8.1.2. <i>Cytoplasmic and membrane protein extracts</i> .....	47

2.8.1.3. Immunoprecipitation of the TLR4 protein.....	47
2.8.2. <i>Gel digestion of protein bands</i> .....	49
2.8.3. <i>LC-MS/MS analysis</i> .....	50
2.8.4. <i>Data analysis and statistics</i> .....	50
2.9. Measure of NF- $\kappa$ B activity using QUANTI-Blue™ assay.....	51
2.9.1. <i>Background</i> .....	51
2.9.2. <i>QUANTI-Blue™ assay</i> .....	51
2.9.3. <i>Statistics</i> .....	52
2.10. Analysis of lipid accumulation and lipolysis in SGBS cells.....	52
2.10.1. <i>Background</i> .....	52
2.10.2. <i>Oil Red O staining</i> .....	53
2.10.3. <i>Glycerol release analysis</i> .....	54
2.10.4. <i>Data analysis and statistics</i> .....	55
2.11. Analysis of TCA intermediates in MaCM using LC-MS/MS analysis.....	55
2.11.1. <i>Sample preparation</i> .....	55
2.11.2. <i>LC-MS/MS analysis</i> .....	56
2.11.3. <i>Data analysis and statistics</i> .....	57
<b>Chapter Three – Effect of SF on LPS-induced cytokine production in human</b>	
<b>monocytes</b> .....	<b>58</b>
3.0. Introduction.....	59
3.1. Materials and Methods.....	60
3.2. Results.....	61
3.2.1. <i>PBMCs</i> .....	61
3.2.1.1. Effect of SF on LPS-induced cytokine secretion.....	61
3.2.1.2. Effect of SF on PBMC cell viability.....	65
3.2.2. <i>THP-1 monocytes</i> .....	65
3.2.2.1. Effect of SF on LPS-induced cytokine secretion.....	65
3.2.2.2. Effect of SF on THP-1 cell viability.....	69
3.2.2.3. Effect of SF on LPS-induced cytokine expression.....	70
3.3. Discussion.....	73
3.4. Conclusions.....	77
<b>Chapter Four – Effect of SF on global gene expression of THP-1 monocytes exposed to</b>	
<b>LPS</b> .....	<b>79</b>
4.0. Introduction.....	80
4.1. Materials and Methods.....	82
4.2. Results.....	82

---

4.2.1. <i>Effect of SF on THP-1 monocytes</i> .....	82
4.2.2. <i>Effect of LPS on THP-1 monocytes</i> .....	89
4.2.3. <i>Effect of SF on LPS-treated THP-1 monocytes</i> .....	91
4.3. Discussion.....	100
4.4. Conclusions.....	104
<b>Chapter Five – Investigations into the mechanism of SF on TLR4 signalling</b> .....	<b>105</b>
5.0. Introduction.....	106
5.1. Materials and Methods.....	107
5.2. Results.....	107
5.2.1. <i>Modification of TLR4 cysteine residues by SF under reducing and non-reducing conditions</i> .....	107
5.2.2. <i>Effect of SF at lower concentrations on TLR4 modification</i> .....	108
5.2.3. <i>Quantification of TLR4 protein in vitro</i> .....	111
5.2.4. <i>Investigations into SF modifications of TLR4 from HT-29 cells treated with SF in the presence or absence of LPS</i> .....	114
5.2.5. <i>Identification of potential SF-modified TLR4 using immunoprecipitation</i> ..	117
5.2.5.1. Immunoprecipitation and gel electrophoresis.....	117
5.2.5.2. LC-MS/MS analysis of gel digestion fragments.....	120
5.3. Discussion.....	120
5.4. Conclusion.....	123
<b>Chapter Six – Effect of SF on NF-<math>\kappa</math>B in PRR-expressing cell models</b> .....	<b>124</b>
6.0. Introduction.....	125
6.0.1. <i>L-SF versus DL-SF</i> .....	125
6.0.2. <i>Chronic inflammatory signalling pathways</i> .....	125
6.1. Materials and Methods.....	128
6.2. Results.....	129
6.2.1. <i>Effect of SF on cell viability of HEK293 cells</i> .....	129
6.2.2. <i>Effect of SF on NF-<math>\kappa</math>B activity in TLR4-expressing cells</i> .....	130
6.2.3. <i>Effect of SF on NF-<math>\kappa</math>B activity in transiently transfected TLR4 cells</i> .....	131
6.2.4. <i>Effect of SF on NF-<math>\kappa</math>B activity in TLR2-expressing cells</i> .....	134
6.2.5. <i>Effect of SF on NF-<math>\kappa</math>B activity in NOD2 wildtype and mutant G908R cells</i> .....	138
6.2.6. <i>Comparison of the effects of L-SF and DL-SF on NF-<math>\kappa</math>B activity</i> .....	143
6.3. Discussion.....	144
6.4. Conclusions.....	147



---

8.2.5.1. Effect of MaCM from SF-treated macrophages on cytokine expression in SGBS adipocytes.....	179
8.2.5.2. Quantification of cytokine levels in MaCM from SF-treated macrophages..	181
8.3. Discussion.....	182
8.4. Conclusion.....	187
<b>Chapter Nine – General discussion .....</b>	<b>189</b>
9.1. Summary of findings.....	190
9.2. How do these results compare with previous literature?.....	193
9.3. Limitations of the research.....	196
9.4. Future research .....	197
<b>References.....</b>	<b>201</b>

## List of Figures

Figure 1.1. Overview of TLR2 and TLR4 signalling.....	7
Figure 1.2. NOD2 signalling .....	9
Figure 1.3. Overview of changes in adipose tissue in obesity .....	14
Figure 1.4. Glucosinolate structure .....	19
Figure 1.5. Enzymatic breakdown of glucoraphanin .....	21
Figure 2.1. Conversion of WST-1 to formazan.....	34
Figure 2.2. Quantikine ELISA protocol.....	36
Figure 2.3. Protocol for immunoprecipitation of TLR4.....	48
Figure 2.4. Glycerol assay principle.....	53
Figure 2.5. Oil Red O staining protocol.....	54
Figure 3.1. Induction of IL-6 secretion with different LPS concentrations in human PBMCs.....	61
Figure 3.2. LPS significantly induces IL-6 secretion in human PBMCs over 24 hours.....	62
Figure 3.3. SF suppresses LPS-induced IL-6 secretion in PBMCs with a 2 hour pre-treatment (A) and 20 hour pre-treatment (B).....	63
Figure 3.4. SF significantly suppresses LPS-induced secretion of IL-6 (A), IL-1 $\beta$ (B) and TNF $\alpha$ (C) in PBMCs over time.....	64
Figure 3.5. Effect of SF on PBMC cell viability.....	65
Figure 3.6. Induction of IL-6 secretion with different LPS concentrations in THP-1 monocytes.....	66
Figure 3.7. LPS significantly induces IL-6 secretion in THP-1 monocytes over time.....	67
Figure 3.8. SF suppresses LPS-induced IL-6 secretion in THP-1 monocytes.....	67
Figure 3.9. SF significantly suppresses LPS-induced IL-6 secretion in THP-1 monocytes over 24 hours.....	68
Figure 3.10. SF significantly suppresses LPS-induced IL-1 $\beta$ (A) and TNF $\alpha$ (B) secretion in THP-1 monocytes.....	69
Figure 3.11. Effect of SF on THP-1 monocyte cell viability.....	70
Figure 3.12. LPS significantly induces IL-6 expression in THP-1 monocytes over time.....	71
Figure 3.13. SF significantly suppresses LPS-induced IL-6 expression in THP-1 monocytes over time.....	72
Figure 3.14. SF significantly suppresses LPS-induced IL-1 $\beta$ expression (A) and shows a trend for suppression of TNF $\alpha$ expression (B) in THP-1 monocytes.....	73

---

Figure 4.1. Overview of the TLR4 signalling pathway.....	81
Figure 4.2. Effect of SF on the expression of genes encoding enzymes involved in glycolysis and the pentose phosphate pathway.....	87
Figure 4.3. Effect of LPS in the presence or absence of SF on gene expression.....	92
Figure 4.4. 5µM SF suppresses all changes induced by 1ng/ml LPS.....	93
Figure 5.1. SF directly modifies cysteine 609 (A) and cysteine 246 (B) within the extracellular domain of TLR4 under non-reducing conditions.....	110
Figure 5.2. Intensity of SF-modified peptides containing Cys609 (A) or Cys246 (B) in response to varying SF concentrations under non-reducing conditions.....	111
Figure 5.3. TLR4 is expressed as a soluble and membrane bound protein.....	113
Figure 5.4. Densitometry blots of the gels for digestion.....	114
Figure 5.5. Analysis of immunoprecipitation product by gel electrophoresis with coomassie blue stain (A) and western blot analysis (B) for TLR4.....	118
Figure 5.6. Quantification of the bands of interest from the immunoprecipitation product.....	119
Figure 6.1. Overview of the TLR4, TLR2 and NOD2 signalling pathways.....	127
Figure 6.2. Effect of SF on viability of HEK293 cells.....	129
Figure 6.3. LPS significantly induces NF-κB activity in HEK-Blue™-hTLR4 cells.....	130
Figure 6.4. L-SF and DL-SF significantly suppress LPS-induced NF-κB activity in HEK-Blue™-hTLR4 cells.....	131
Figure 6.5. LPS significantly induces NF-κB activity in cells transiently transfected with wildtype or mutant TLR4.....	132
Figure 6.6. L-SF and DL-SF significantly suppress LPS-induced NF-κB activity in cells transiently transfected with wildtype or mutant TLR4.....	133
Figure 6.7. No significant differences were seen in the response to L-SF (A) or DL-SF (B) by cells transiently transfected with either wildtype or mutant TLR4.....	134
Figure 6.8. Pam3CSK4 significantly induces NF-κB activity in HEK-Blue™-hTLR2 cells.....	135
Figure 6.9. L-SF and DL-SF are able to significantly suppress Pam3CSK4-induced NF-κB activity in HEK-Blue™-hTLR2 cells.....	136
Figure 6.10. FSL-1 significantly induces NF-κB activity in HEK-Blue™-hTLR2 cells.....	137
Figure 6.11. L-SF and DL-SF are able to significantly suppress FSL-1-induced NF-κB activity in HEK-Blue™-hTLR2 cells.....	138

Figure 6.12. MDP significantly induces NF- $\kappa$ B activity in cells expressing wildtype (A) and mutant G908R (B) NOD2.....	139
Figure 6.13. Mutant G908R NOD2 cells are less responsive to MDP induction of NF- $\kappa$ B activity.....	140
Figure 6.14. L-SF and DL-SF are able to significantly suppress MDP-induced NF- $\kappa$ B activity in HEK-Blue <sup>TM</sup> -hNOD2 wildtype cells.....	141
Figure 6.15. L-SF and DL-SF are able to significantly suppress MDP-induced NF- $\kappa$ B activity in NOD2 G908R cells.....	142
Figure 6.16. Significant differences were seen in the response L-SF (A) and DL-SF (B) by cells expressing either the wildtype or mutant G908R NOD2 receptor.....	143
Figure 6.17. L-SF and DL-SF show no significant differences between their effects on ligand-induced NF- $\kappa$ B activity.....	144
Figure 7.1. Effect of SF on SGBS cell viability.....	152
Figure 7.2. Intracellular lipids accumulate within SGBS cells during differentiation..._	153
Figure 7.3. Intracellular lipid accumulation increased over the differentiation process of SGBS cells.....	154
Figure 7.4. 10 $\mu$ M SF significantly suppresses lipid accumulation of SGBS cells.....	155
Figure 7.5. Lipid accumulation was reduced in SGBS adipocytes differentiate in the presence of 10 $\mu$ M SF.....	156
Figure 7.6. 10 $\mu$ M SF significantly induces CPT1A expression in SGBS cells.....	157
Figure 7.7. SF caused no significant changes in the levels of glycerol released by SGBS cells.....	158
Figure 8.1. THP-1 cell morphology.....	165
Figure 8.2. SF significantly suppresses LPS-induced IL-6 (A + B), IL-1 $\beta$ (C + D) and TNF $\alpha$ (E + F) secretion in THP-1 macrophages.....	166
Figure 8.3. Effect of SF on cell viability of THP-1 macrophages.....	167
Figure 8.4. SF significantly suppresses LPS-induced IL-6 (A + B), IL-1 $\beta$ (C + D) and TNF $\alpha$ (E + F) expression in THP-1 macrophages.....	168
Figure 8.5. 50% MaCM significantly reduces cell viability of SGBS adipocytes.....	169
Figure 8.6. MaCM significantly suppresses differentiation of SGBS cells.....	170
Figure 8.7. SF significantly suppresses MaCM-induced IL-1 $\beta$ expression in SGBS cells.....	171
Figure 8.8. SF significantly suppresses MaCM-induced IL-6 expression in SGBS cells.....	172

---

Figure 8.9. TCA intermediate levels increase dose-dependently in MaCM from THP-1 macrophages.....	173
Figure 8.10. TCA intermediates are not responsible for the induction in IL-6 expression seen in response to MaCM.....	174
Figure 8.11. TNF $\alpha$ induces IL-1 $\beta$ expression in SGBS cells and when co-treated with 10 $\mu$ M SF, there was an additional induction.....	176
Figure 8.12. TNF $\alpha$ induces IL-6 expression in SGBS cells while SF has no significant effect.....	177
Figure 8.13. SF significantly suppresses MaCM-induced IL-1 $\beta$ expression in SGBS cells when used as a pre-treatment.....	178
Figure 8.14. SF had no consistent significant effects on MaCM-induced IL-6 expression in SGBS cells when used as a pre-treatment.....	179
Figure 8.15. MaCM from SF-treated macrophages demonstrates significantly reduced levels of IL-1 $\beta$ gene expression induction.....	180
Figure 8.16. MaCM from SF-treated macrophages demonstrates significantly reduced levels of IL-6 gene expression induction.....	181
Figure 8.17. SF significantly suppresses cytokine secretion of macrophages.....	182
Figure 9.1. Targets of SF for suppression of chronic inflammation.....	192

---

**List of Tables**

Table 2.1. Primer and probe sequences for genes analysed.....	40
Table 2.2. LC-MS/MS parameters for analytes measured.....	57
Table 4.1. Number of genes differentially expressed in response to SF.....	83
Table 4.2. Pathway analysis of genes differentially expressed in response to SF.....	84
Table 4.3. Genes differentially expressed in response to SF involved in detoxification pathways .....	85
Table 4.4. Genes differentially expressed in response to SF involved in carbohydrate cell metabolism.....	86
Table 4.5. Genes differentially expressed in response to SF involved in pathways in cancer.....	88
Table 4.6. Genes differentially expressed in response to SF involved in inflammatory signalling pathways.....	89
Table 4.7. Number of genes differentially expressed in response to LPS.....	90
Table 4.8. Pathway analysis of genes differentially expressed in response to LPS.....	90
Table 4.9. Number of genes differentially expressed in response to LPS and SF co-treatment.....	91
Table 4.10. Effect of SF on genes differentially expressed in response to LPS (with > 2-fold change) with functions in inflammatory signalling pathways.....	94
Table 4.11. Effect of SF on genes differentially expressed in response to LPS (with > 2-fold change) with miscellaneous functions.....	97
Table 5.1. Cysteine residues bound by SF with and without DTT treatment.....	108
Table 5.2. Proteins identified by LC-MS/MS from gel digestion samples*.....	116
Table 6.1. IC <sub>50</sub> for L-SF and DL-SF on HEK293 cells.....	130
Table 8.1. Levels of cytokines quantified in MaCM.....	175
Table 9.1. Animal studies using SF supplementation.....	198

---

## Abbreviations

4-AAP	4-aminoantipyrine
ABC	Ammonium bicarbonate
AcMaCM	Activated macrophage-conditioned medium
ADP	Adenosine diphosphate
AMPK	Adenosine monophosphate-activated protein kinase
ANOVA	Analysis of variance
AP	Alkaline phosphatase
AP-1	Activator protein-1
ARE	Antioxidant response element
Arg	Arginine
ATM	Adipose tissue macrophage
ATP	Adenosine triphosphate
AUC	Area under the curve
BCA	Bicinchoninic acid
Bis-Tris	Bis-(2-hydroxyethyl)-amino-tris(hydroxymethyl)-methane
BMI	Body mass index
BSA	Bovine serum albumin
CARD	Caspase-recruitment domain
CD14	Cluster of differentiation 14
CD36	Cluster of differentiation 36
CD68	Cluster of differentiation 68
CDF	Common data format
CDK	Cyclin-dependent kinase
C/EBP $\alpha$	CCAAT/enhancer-binding protein alpha
CoA	Coenzyme A
COX-2	Cyclooxygenase-2
CPT	Carnitine palmitoyltransferase
CRP	C-reactive protein
C <sub>T</sub>	Threshold cycle
Cys	Cysteine
CVD	Cardiovascular disease
DAMP	Damage-associated molecular pattern
DAVID	Database for annotation, visualisation and integrated discovery
DIO	Diet-induced obesity
DL-SF	DL-sulforaphane
DMEM	Dulbecco's Modified Eagle's medium
DMSO	Dimethyl sulfoxide
DNA	Deoxyribonucleic acid
D-SF	D-sulforaphane
DTT	Dithiothreitol
EC	Electron coupling agent
ECACC	European Collection of Cell Culture
EDTA	Ethylenediaminetetraacetic acid
ELISA	Enzyme-linked immunosorbant assay
EPHX1	Epoxide hydrolase 1

---

ESI	Electrospray ionisation
ESPA	N-ethyl-N-(3-sulfopropyl)- <i>m</i> -anisidine
FADH	Flavin adenine dinucleotide
FAM	6-carboxyfluorescein
FAS	Fatty acid synthase
FBS	Foetal bovine serum
FFA	Free fatty acid
G6PD	Glucose 6-phosphate dehydrogenase
GCLM	Glutamate-cysteine ligase, modifier subunit
GI	Gastrointestinal
Glu	Glutamic acid
Gly	Glycine
GPI	Glycosylphosphatidylinositol
GSH	Glutathione
GSL	Glucosinolate
GSR	Glutathione reductase
GST	Glutathione S-transferase
H <sub>2</sub> O <sub>2</sub>	Hydrogen peroxide
HBSS	Hank's balanced salt solution
HEK	Human embryonic kidney
HIF	Hypoxia inducible factor
His	Histidine
HMOX1	Hemoxygenase decycling 1
HO-1	Hemoxygenase-1
HPLC	High performance liquid chromatography
HRP	Horseradish peroxidase
IBD	Inflammatory bowel disease
IBMX	Isobutylmethylxanthine
IC <sub>50</sub>	half maximal inhibitory concentration
ICAM-1	Intracellular adhesion molecule 1
IFN	Interferon
IFN $\beta$	Interferon beta
IgG	Immunoglobulin G
I $\kappa$ B	Inhibitor of NF- $\kappa$ B
IKK $\gamma$	Inhibitor of NF- $\kappa$ B kinase-gamma
IL-1 $\beta$	Interleukin-1 beta
IL-6	Interleukin-6
IL-8	Interleukin-8
IL-10	Interleukin-10
IL-12	Interleukin-12
iNOS	Inducible nitric oxide synthase
IP	Immunoprecipitation
IP-10	Interferon- $\alpha$ inducible protein
IRF3	Interferon regulatory factor 3
ITC	Isothiocyanate
Keap1	Kelch-like associated protein 1
LBP	LPS binding protein

---

LC-MS/MS	Liquid chromatography-tandem mass spectroscopy
LDL	Low-density lipoprotein
Leu	Leucine
LPS	Lipopolysaccharide
LRR	Leucine-rich repeat
L-SF	L-sulforaphane
Lys	Lysine
MaCM	Macrophage-conditioned medium
MAPK	Mitogen-activated protein kinase
MCP-1	Monocyte chemotactic protein-1
MD2	Myeloid differentiation 2
MDP	Muramyl dipeptide
MEF	Mouse embryonic fibroblasts
Met	Methionine
MGST1	Microsomal glutathione S-transferase
MI	Myocardial infarction
MIAME	Minimum information about a microarray experiment
MIF	Macrophage migratory inhibitory factor
MOPS	3-(N-morpholino)-propanesulfonic acid
mRNA	Messenger ribonucleic acid
MSTR	Mitochondrial succinate-tetrazolium reductase system
Myb28	Myb-related protein-28
MyD88	Myeloid differentiation primary response gene (88)
NAC	N-acetylcysteine
NADH	Nicotinamide adenine dinucleotide
NADPH	Nicotinamide adenine dinucleotide phosphate
NF- $\kappa$ B	Nuclear factor kappa-light-chain-enhancer of activated B cells
NLR	NOD-like receptor
NOD2	Nucleotide-binding oligomerisation domain-containing protein-2
NQO1	NADPH dehydrogenase quinone 1
Nrf2	Nuclear factor (erythroid-derived 2)-like 2
NTC	No template control
OD	Optical density
OxLDL	Oxidised low-density lipoprotein
PAMP	Pattern-associated molecular pattern
PBMC	Peripheral blood mononuclear cells
PBS	Phosphate-buffered saline
PGD	Phosphogluconate dehydrogenase
PGN	Peptidoglycan
PMA	Phorbol 12-myristate 13-acetate
PPAR $\gamma$	Peroxisome proliferator-activated receptor-gamma
PRR	Pattern recognition receptor
RICK	Receptor-interacting serine/threonine kinase
RIN	RNA integrity number
RIP1	Receptor-interacting serine/threonine-protein kinase 1
RLR	RIG-I-like receptor
RMA	Robust multi-array analysis

---

RNA	Ribonucleic acid
RT-PCR	Reverse transcriptase-polymerase chain reaction
SD	Standard deviation
SDS-PAGE	Sodium dodecyl sulphate polyacrylamide gel electrophoresis
SEAP	Secreted embryonic alkaline phosphatase
Ser	Serine
SF	Sulforaphane
SGBS	Simpson-Golabi-Behmal Syndrome
SNP	Single nucleotide polymorphism
SOD1	Superoxide dismutase 1
SREBP	Sterol regulatory element binding protein
SRXN1	Sulfiredoxin 1
STAT1	Signal transducer and activator of transcription 1
SVF	Stromal vascular fraction
T2DM	Type 2 diabetes mellitus
T <sub>3</sub>	Triiodothyronine
TALDO1	Transaldolase
TAMRA	6-carboxytetramethylrhodamine
TBST	Tris-buffered saline tween-20
TCA	Tricarboxylic acid
Thr	Threonine
THP-1	Tamm-Horsfall Protein-1
TIR	Toll/IL-1R
TIRAP	TIR-domain-containing adapter protein
TKT	Transketolase
TLR	Toll-like receptor
TNF $\alpha$	Tumor necrosis factor alpha
TRAM	TIR-domain-containing adapter-molecule 2
TRIF	TIR-domain-containing adapter-inducing interferon- $\beta$
Tris	Tris(hydroxymethyl)aminomethane
Trp	Tryptophan
TXN	Thioredoxin
TXNRD1	Thioredoxin reductase
UC	Ulcerative colitis
VCAM-1	Vascular cell adhesion molecule 1
WST-1	4-[3-(4-iodophenyl)-2-(nitrophenyl)-2H-5-tetrazolio]-1,-benzene disulfonate

---

**Symbols**

°C	Degrees Celsius
CaCl <sub>2</sub>	Calcium chloride
cm	Centimetres
CO <sub>2</sub>	Carbon dioxide
Cu <sup>2+/1+</sup>	Copper (II)/(I)
Da	Daltons
H <sub>2</sub> O <sub>2</sub>	Hydrogen peroxide
HCl	Hydrochloric acid
kDa	Kilodaltons
µm	Micrometres
µM	Micromoles per litre
µg/ml	Micrograms per millilitre
M	Moles per litre
mg/l	Milligrams per litre
mg/ml	Milligrams per millilitre
ml	Millilitre
ml/min	Millilitres per minute
mm	Millimetres
mm <sup>3</sup>	Cubic millimetres
mM	Millimoles per litre
m/z	Mass to charge ratio
NaCl	Sodium chloride
NaPi	Sodium phosphate
ng/µl	Nanograms per microlitre
ng/ml	Nanograms per millilitre
nl/min	Nanolitres per minute
nm	Nanometre
nM	Nanomolar per litre
pg/ml	Picograms per millilitre
ppm	Parts per million
rpm	Revolutions per minute
V	Volts
v/v	Volume per volume
w/v	Weight per volume

## List of Publications

Folkard DL, Melchini A, Traka MH, Al-Bakheit A, Saha S, Mulholland F, Watson A and Mithen RF. '*Suppression of LPS-induced transcription and cytokine secretion by the dietary isothiocyanate sulforaphane*'. 2014. (Accepted by *Molecular Nutrition and Food Research*).

Folkard DL, Marlow G, Mithen RF and Ferguson LR. '*Effect of Sulforaphane on NOD2: Implications for Crohn's Disease*'. 2014. (Accepted by *Journal of Inflammation*).

Folkard DL, Melchini A, Traka MH, Wabitsch, M and Mithen RF. '*Sulforaphane modulates adipogenesis and the inflammatory response in human SGBS adipocytes*'. 2014. (In preparation).

## **Acknowledgements**

First and foremost I would like to thank my supervisor Prof. Richard Mithen for giving me this opportunity. Without his invaluable support, guidance and advice this thesis would not have been possible. The assistance and advice from my secondary supervisor Prof. Ian Johnson has been invaluable.

To the rest of the members of the research group, I could not have reached this point without your support. I am especially grateful to Dr. Antonietta Melchini, for teaching me from day one and being there with essential encouragement from both a professional and personal standpoint and Dr Ala'a Al-Bakheit who has been through the rollercoaster ride with me.

To Dr. Maria Traka for her expertise with the microarray analysis, Dr. Fran Mulholland for his essential help and support with the proteomic analysis of TLR4, Dr. Andrew Watson for help with the data analysis, Dr. Shikha Saha for her help with the TCA intermediate analysis and a special thanks to Dr. Joanne Doleman for personal encouragement and taking the time to read every chapter of this thesis. To Prof. Martin Wabitsch for providing the SGBS cells for an essential part of my thesis. Also, to BBSRC for funding my work.

Additionally, I would like to acknowledge Prof. Lynnette Ferguson and Dr. Gareth Marlow for giving me the opportunity of a three month placement at the University of Auckland. My experience in New Zealand was amazing!

I would like to thank all of my friends for always supporting me, not only though the Ph.D process, but in all of the stages before. To Simon, for putting up with me during the toughest, final stages of my Ph.D, your support has been essential.

I would also like to say a massive thank you to my family. Particularly to my sister for always being there for me and finally to my wonderful Dad, who is my rock and always will be. Without your love and support, this would never have been possible.

# Chapter One

---

General introduction

## 1.0. Summary of the thesis

This thesis contains the results of a research project that was concerned with investigating the hypothesis that sulforaphane (SF) would exert anti-inflammatory effects on a number of different inflammatory signalling pathway using physiologically relevant *in vitro* models of chronic inflammation. Cell culture models are often used in research and have both benefits and limitations. Cell models, either primary or immortalised can provide an alternative to *in vivo* experiments with few ethical issues, which allows for initial studies into the mechanistic details and efficacy of the test compound to be carried out. These models can present an indication of potential biological activities and can behave as a basis for designing *in vivo* studies with animals or humans. However, primary and immortalised cell lines are often homogenous cell populations which are not representative of the *in vivo* environment where a tissue is supported by multiple cell types. In addition, they are not cultured under hypoxic conditions and are not subjected to certain growth factors and proteins that would be present in the blood circulation. However, *in vitro* models are practically simple to use and can be well-controlled and demonstrate reproducibility.

Initially, human monocyte cell models were used to investigate whether physiologically relevant concentrations of SF were able to suppress lipopolysaccharide (LPS)-induced cytokine production measuring selected pro-inflammatory biomarkers interleukin-6 (IL-6), interleukin -1 beta (IL-1 $\beta$ ) and tumour necrosis factor alpha (TNF $\alpha$ ) in terms of the secretion level and also the transcriptional level. This was progressed into investigating the effect of SF on global gene expression induced by LPS at a low concentration of 1ng/ml, relevant to that found circulating in individuals with chronic disease. Next, investigations were carried out into the mechanistic details of the effects of SF and the aim was to determine whether SF was able to directly target the LPS receptor, Toll-like receptor (TLR) 4 via modification of thiol groups of cysteine residues present in the extracellular domain of the receptor, the area responsible for ligand binding, using cell-free and *in vitro* models. The scope of the investigations were broadened to investigate whether SF was able to target additional important inflammatory signalling pathways namely TLR2 and NOD2 (nucleotide-binding oligomerisation domain-containing protein 2), by measuring whether SF could target nuclear factor kappa B (NF- $\kappa$ B) activation in response to appropriate ligands. In the experiments with cell models expressing the individual inflammatory receptors, the two commonly studied forms of SF were compared, the L-SF and the DL-SF. The L-SF is the natural form of SF

extracted from broccoli while the DL-SF is a synthetic analogue of L-SF and it was hypothesised that these would behave to a similar extent.

The final stage of this thesis involved translating the multi-targeted anti-inflammatory effects of SF into a more complex *in vivo* model of obesity, a condition characterised by chronic inflammation. Firstly, it was investigated whether SF was able to exert effects on lipid accumulation and metabolism in human SGBS adipocytes, followed by studying whether physiologically relevant concentrations of SF could suppress SGBS adipocyte cytokine expression induced in response to macrophage-conditioned medium (MaCM) from human THP-1 macrophages.

The purpose of this general introduction is to introduce the concept of inflammation and how a low-grade, persistent state can impact on the development of chronic diseases including cancer, cardiovascular disease (CVD) and type 2 diabetes mellitus (T2DM). It will cover how diets rich in cruciferous vegetables have been shown to demonstrate beneficial effects on the risk of developing such pathologies, and will describe how glucosinolates (GSLs), which are found at high levels in cruciferous vegetables, may be responsible for the observed health benefits. The breakdown of GSLs to biologically active isothiocyanates (ITCs) will be explained with a particular focus on SF and its known functions. As the objectives of each chapter focuses on different aspects of the anti-inflammatory effects of SF, each results chapter will also provide an introduction to the literature relevant to the research aims of that chapter.

## **1.1. Inflammation**

Inflammation is a complex adaptive response that occurs in response to harmful stimuli in order to counteract the insult they are trying to exert. This process behaves to underlie a number of physiological and pathological disorders and while a great deal is understood about the cellular and molecular mechanisms involved in the response to infectious stimuli, much less is known about the instigators of systemic chronic inflammation. Nevertheless, a common explanation for inflammatory responses irrespective of the cause is the drive to restore homeostasis.

### **1.1.1. Acute versus chronic inflammation**

Classic triggers of an acute inflammatory response are infection and tissue injury. Macrophages sense the presence of the inflammatory stimulus leading to the recruitment of neutrophils to the site of insult [1, 2]. In the majority of cases, this process occurs over a short time course and is beneficial to the organism. However, if the process becomes disordered and the inflammatory response is unable to eradicate the pathogen, the inflammatory response persists replacing the neutrophils with additional macrophages and T lymphocytes. If this course of action is still insufficient, a chronic inflammatory state develops, with detrimental effects [3]. While the causes and mechanisms of localised chronic inflammation are partly understood, the development of systemic chronic inflammation, which occurs in a wide variety of diseases including cancer, CVD and T2DM, is less well understood. It is suggested that it is associated with a tissue malfunction where a number of fundamental physiological processes that are not necessarily directly related to tissue repair or the host defence response are disrupting the homeostatic balance [3].

### **1.1.2. Inflammatory signalling pathways involved in chronic inflammation**

Thus far, four different families of pattern recognition receptors (PRRs) have been identified, with the most commonly studied being the TLRs and the NOD-like receptors (NLRs). They behave to recognise exogenous microbial products known as pattern-associated molecular patterns (PAMPs) as well as endogenous molecules released from damaged cells, collectively known as damage-associated molecular patterns (DAMPs) [4]. Each class of PRRs have a number of family members which allows a certain level of specificity towards different microbial or non-microbial structures. Most relevant to the studies within this thesis, are the TLR4, TLR2 and NOD2 pathways.

#### **1.1.2.1. TLR4 and TLR2 signalling pathways**

The TLR family of PRRs consists of 10 family members in humans all of which are characterised by a common structure consisting of an N-terminal domain of leucine-rich repeats (LRRs), a region that spans the cell membrane, followed by a cytoplasmic Toll/IL-1R homology (TIR) domain [4]. The LRRs extend into the extracellular space of the cell and are responsible for the recognition of each specific ligand, which leads to the activation of the receptors and downstream signalling, a process controlled by the TIR domain [5]. A diverse array of the TLR family members are commonly identified on

cells that are involved in the immune response such as leukocytes and cells of the spleen. In addition, they are highly expressed in cells that are exposed to microbial pathogenic components such as those in the lungs, small intestine or colon [6]. TLR1, 2 and 4-6 are present on the plasma membrane, while TLR3, 8 and 9 are present intracellularly on endosomes or lysosomes [4].

The TLR4 molecule was identified as the receptor able to respond to LPS, an endotoxin that is present as a component of the outer membrane in Gram-negative bacteria [7]. The lipid portion of LPS known as lipid A is responsible for the pathogenic nature of this endotoxin and is the causative agent of septic shock [7]. When LPS is released from the cell wall of Gram-negative bacteria, it binds directly to the LPS-binding protein (LBP), present in circulation, which in turn interacts with CD14, a glycosylphosphatidylinositol (GPI)-anchored protein present at the cell membrane. This complex then facilitates the transfer of LPS to MD2, the co-receptor for TLR4 (**Figure 1.1**). The structure of LPS consists of six lipid chains, of which five bind within the hydrophobic pocket of MD2, with the remaining chain able to bind to the TLR4 [8]. This binding results in homodimerisation of two TLR4-MD2-LPS complexes which is necessary for downstream signal transduction [5].

The TLR2 receptor is able to recognise a number of different components from bacteria, mycoplasma, fungi and viruses, of which lipoproteins from bacteria and mycoplasma are most commonly described [4]. Unlike the TLR4 molecule, following ligand activation the TLR2 receptor undergoes heterodimerisation with either the TLR1 molecule to form a complex capable of recognising triacyl lipopeptides, or TLR6 in order to recognise diacyl lipopeptides (**Figure 1.1**) [4]. This specificity is as a result of different structures within the TLR dimers. The TLR2-TLR1 complex forms a structure where two acyl chains of a triacylated lipopeptide are able to interact with TLR2 and the third acyl chain is able to interact with the hydrophobic pocket of TLR1. In the TLR2-TLR6 dimer, the TLR6 molecule does not have a hydrophobic pocket and as a result can only recognise lipopeptides with two acyl chains [5].

In addition, TLR2 has the capability to interact with other cell surface receptors such as CD36, the principle receptor for oxidised low-density lipoprotein (oxLDL) (**Figure 1.1**) [9]. CD36 has a function analogous to CD14, in which it accentuates the response of TLR2 to diacylglycerides by binding with the ligand directly via its ectodomain [10, 11]. OxLDL is known to induce pro-inflammatory cytokine production with TLR2, CD36

and also TLR4 being necessary for this cell response [12]. This emphasises the important role of TLR2 in the recognition of endogenous ligands such as oxLDL which are crucial in chronic disease, most importantly in CVD.

Following ligand binding, downstream signalling is dependent on the recruitment of adaptor proteins. For TLR4 signalling, two pathways can be activated following the recruitment of MyD88 (myeloid differentiation primary response gene 88) and TRIF (TIR-domain-containing adapter-inducing interferon- $\beta$ ), while TLR2 signalling is specifically MyD88-dependent (**Figure 1.1**) [5]. The MyD88-dependent pathway is responsible for the activation of the transcription factors NF- $\kappa$ B (nuclear factor kappa-light-chain-enhancer of activated B cells) and AP-1 (activator protein-1), which control the expression of pro-inflammatory cytokines and chemokines [13]. In TLR4 signalling, following MyD88-dependent pathway activation, the TLR4-MD2-LPS homodimers undergo endocytosis which initiates the recruitment of TRIF. This MyD88-independent pathway ultimately activates interferon regulatory factor 3 (IRF3) which is responsible for controlling the expression of type I interferons (IFNs) and subsequently IFN-inducible genes [5]. Even though the TLR4 is able to activate these distinct signalling pathways, the expression of pro-inflammatory mediators is dependent on the activation of both pathways, for reasons which remain unknown [5].

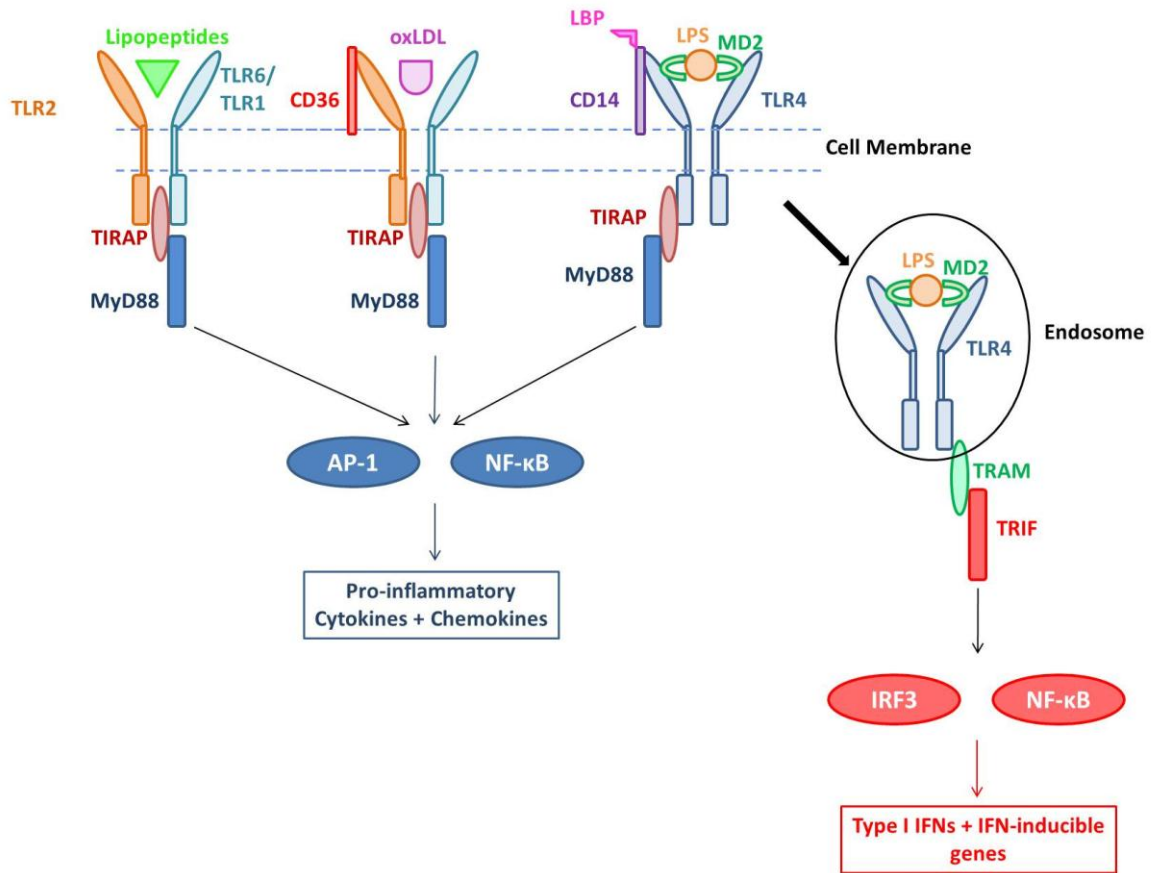


**Figure 1.1. Overview of TLR2 and TLR4 signalling.** During recognition by TLR4, LPS binds to the TLR4-MD2 complex with the aid of LBP and CD14 accessory proteins. The binding of LPS to the TLR4-MD2 complex results in homodimerisation and activation of an intracellular signalling cascade. This can be MyD88-independent or dependent. The MyD88-independent pathway occurs following internalisation of the TLR4-MD2-LPS complex, where it is retained within the endosome, leading to the recruitment of TRIF. This results in the early activation of IRF3 followed later by NF- $\kappa$ B which controls the expression of type I IFNs and IFN-inducible genes [5]. The MyD88-dependent pathway stimulates NF- $\kappa$ B and AP-1 resulting in pro-inflammatory cytokine and chemokine expression [5, 13, 14]. The MyD88-dependent pathway is also activated as a result of lipopeptides binding to TLR2 heterodimers with TLR1 and TLR6 and also in response to endogenous ligands such as oxLDL with the aid of CD36 [11, 12].

#### 1.1.2.2. NOD2 signalling pathway

The NLR family of receptors consists of cytoplasmic PRRs that share a conserved structure of a C-terminal LRR domain involved in ligand recognition, a central NOD domain that allows self-oligomerisation, in addition to a varying number of N-terminal caspase-recruitment domains (CARDs) involved in protein-protein interactions [15]. NOD2 is mainly expressed in the cytosol of antigen-presenting cells but also by epithelial cells at a lower level. The expression level of NOD2 is augmented by pro-

inflammatory cytokines including tumour necrosis factor- $\alpha$  (TNF $\alpha$ ), meaning once activated following ligand binding, NOD2 is able to control its own expression [15]. It behaves to specifically recognise muramyl dipeptide (MDP), a breakdown product of peptidoglycan (PGN) derived from both Gram-positive and Gram-negative bacteria. The ubiquitous nature of PGN presence, allows in principle, for NOD2 to respond all bacteria [15]. The way in which the cells are able to encounter the breakdown products of PGN is unclear, however one suggestion applicable to antigen-presenting cells is the notion that phagocytic cells such as macrophages are able to engulf the whole bacteria and digest them into their relevant peptides [16]. The same mechanism is not thought to apply to epithelial cells and instead it has been proposed that MDP is delivered to the receptor through a peptide transporter [17].

Once MDP is available to the NOD2 receptor, it is able to bind directly to the LRR domain of the receptor [15, 18]. Unlike with TLR signalling, there is no dimerisation with other members of the family and instead it is suggested that ligand binding induces a conformational change in the NOD2 receptor. It is this change in conformation that is responsible for the activation of the receptor and recruitment of RICK (receptor-interacting serine/threonine kinase) via a CARD-CARD interaction [19]. RICK is responsible for targeting the inhibitor of NF- $\kappa$ B (I $\kappa$ B)-kinase- $\gamma$  (IKK $\gamma$ ) for polyubiquitylation resulting in its degradation and the ultimate activation of NF- $\kappa$ B to allow production of pro-inflammatory cytokines (**Figure 1.2**) [19].

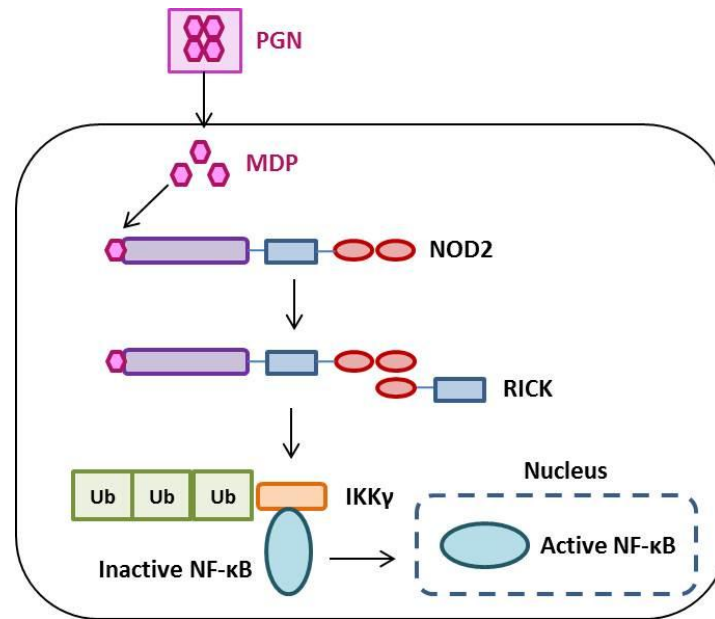


**Figure 1.2. NOD2 signalling.** PGN from both Gram-positive and Gram-negative bacteria is broken down into MDP. MDP is the specific ligand for NOD2 and interacts with the LRR domain (purple) of NOD2 in order to activate the receptor. This results in the recruitment of RICK which is able to interact with the NOD2 receptor through a CARD-CARD (red) interaction. RICK targets the principle regulator of the NF- $\kappa$ B inhibitor, IKK $\gamma$  for polyubiquitination and subsequent degradation. While NF- $\kappa$ B is sequestered in the cytosol it is inactive. Degradation of the IKK $\gamma$  leads to translocation of NF- $\kappa$ B to the nucleus leading to its activation and induction of pro-inflammatory cytokine expression [19].

### 1.1.3. The importance of chronic inflammation in disease

The complex signalling pathways that are necessary to maintain appropriate homeostasis of the immune system following an inflammatory attack may become less efficient with age and this in turn would lead to disorder in immune responses [20]. This lack of regulation presents itself with an increase in the levels of circulating inflammatory biomarkers including interleukin-6 (IL-6) and TNF $\alpha$ , observed in an elderly population as compared to a younger cohort, which could lead to unfavourable health consequences [21].

The link between a state of low-grade inflammation and the development of chronic pathologies such as CVD, cancer and T2DM has been widely studied in recent years. With the risk of developing these diseases largely increasing with age, it is possible that the elevation observed in the levels of pro-inflammatory cytokines in older populations may have an important role.

### **1.1.3.1. Cancer**

When a chronic inflammatory state persists, there is a cycle of consistent activation of macrophages resulting in a continued process of tissue damage, which in turn activates cell proliferation. A continued increase in the level of cell proliferation lends itself to the possibility of neoplasia [22]. Inflammation has been consistently associated with cancer development in recent years with a highlighted role of NF- $\kappa$ B, the transcription factor responsible for controlling the expression of pro-inflammatory cytokines including IL-6, TNF $\alpha$  and C-reactive protein (CRP) [23-25].

The role of circulating IL-6 in cancer was reviewed by Heikkila and colleagues involving the findings of 189 studies. Across the majority of the studies, there were consistent findings of elevated levels of circulating IL-6 in cancer patients compared to healthy controls, however this review was unable to determine any diagnostic capability due to few prospective studies included [26]. Aggarwal and colleagues also aimed to understand the link between pro-inflammatory cytokines and cancers at different sites. They identified an important role for IL-6 particularly in multiple myeloma, lymphoma, bladder, lung, breast and colon cancer risks, while with TNF $\alpha$ , the main association was with pancreatic cancer [25, 27, 28]. Furthermore, Il'yasova and colleagues discovered that the increased level of pro-inflammatory cytokines were more strongly associated with the risk of cancer mortality rather than cancer development [29].

As previously described, activation of TLR4, TLR2 and NOD2 signalling pathways results in the induction of pro-inflammatory gene expression. Interestingly, in patients suffering from multiple myeloma, a higher expression level of both TLR2 and TLR4 was observed in bone marrow-derived mononuclear cells [30].

### **1.1.3.2. Cardiovascular disease**

In terms of CVD, a widely accepted risk factor is elevated cholesterol levels which are highly predictive in younger populations. However, when studying elderly populations, this risk factor becomes less reliable [31]. It was hypothesised that this may be as a result of not accounting for the increased levels of pro-inflammatory cytokines within circulation of the older populations. This suggests that a state of low-grade inflammation has a more extensive role in the development of CVD in the ageing population [21]. In a large population of elderly men and women, it was observed that those diagnosed with sub-clinical or clinical CVD had elevated levels of IL-6, interleukin-1 $\beta$  (IL-1 $\beta$ ), TNF $\alpha$

and CRP [32, 33]. Additionally, these cytokines, in particular IL-6, had the ability to predict the risk of CVD incidence [34, 35].

Also of importance are the elevated expression levels of TLR2 and TLR4 that have been identified in human atherosclerotic plaques isolated from patients [36]. In combination with findings of significantly higher levels of endotoxin in patients diagnosed with carotid atherosclerosis than those observed in patients with no diagnosis, it is possible that the endotoxin could activate the TLR4 signalling pathway resulting in the elevation of pro-inflammatory markers seen in CVD [37].

#### **1.1.3.3. Type 2 diabetes mellitus**

Similarly, the development of T2DM has been linked to inflammation, due to the involvement of pro-inflammatory cytokines in the development of insulin resistance [21]. Elevated levels of IL-6, IL-1 $\beta$  and TNF $\alpha$  have been identified in subjects with T2DM compared to healthy controls [38-42]. It was also determined that those individuals that presented with the highest levels of circulating IL-6, were most likely to develop T2DM in the future [43]. Additionally, both TLR2 and TLR4 were up-regulated in obese patients suffering from T2DM compared to non-diabetic obese subjects [44]. The relevance of this increase may be further explained following the findings presented by Creely and Al-Attas, where levels of circulating endotoxin were elevated in those patients suffering from T2DM [45, 46].

#### **1.1.3.4. Inflammatory bowel diseases**

Crohn's disease and ulcerative colitis (UC) are collectively known as inflammatory bowel diseases (IBDs). The innate immune system is largely involved in these disorders and increased levels of a large range of pro-inflammatory cytokines including IL-6 and TNF $\alpha$  are often observed [47]. In addition, there is a significant increase in the expression levels of TLRs including the TLR2 and TLR4 receptors in patients suffering from IBDs [48-50].

Principally, the gene most commonly studied and linked to Crohn's disease is the NOD2 gene. Three polymorphisms in NOD2 were commonly identified in Crohn's disease, which collectively account for approximately 82% of all mutated alleles observed in sufferers [51, 52]. The Leu1007 (3020insC) insertion polymorphism results in a

frameshift mutation leading to the introduction of a premature stop codon and the translation of a truncated NOD2 protein with the final 33 amino acids missing [53]. The two other single nucleotide polymorphisms (SNPs) result in missense mutations Arg702Trp and Gly908Arg with a single amino acid substitution within the LRR of NOD2 [53]. TLR2 and TLR4 polymorphisms have also been identified as potential risk factors in Crohn's disease but with a much lower prevalence and the results are controversial [54-62].

#### **1.1.3.5. Involvement of obesity in chronic diseases**

An additional independent risk factor that may play a role in the increase in levels of pro-inflammatory cytokines within these chronic diseases is the coexistence of obesity [63-74]. Due to the knowledge that the likelihood of suffering from obesity increases with age [75], it is possible that this is in part responsible for the elevated levels of circulating pro-inflammatory cytokines found in elderly populations, which in turn, may result in an increased risk of developing chronic diseases.

In terms of the link with cancer, obesity has been consistently associated with cancers in many locations and it was found that with each increase of  $5\text{kg/m}^2$  in body mass index (BMI), a 30% increase was observed in all-cause mortality and a 10% increase in cancer mortality specifically was identified, highlighting the enormity of the obesity problem [76]. Further support for the link between obesity and cancer comes from evidence demonstrating that with weight loss as a result of bariatric surgery, the risk of developing cancer reduced by around 20% [77, 78]. A relationship is also observed between higher BMI status and risk for developing CVD [79]. This association as with cancer and obesity, was found to be also affected by bariatric surgery with individuals who had undergone surgery reducing their risks of cardiovascular adverse effects, specifically myocardial infarction (MI) and stroke [80]. With CVD, there is however a paradoxical nature to the relationship with evidence to suggest that in patients that have suffered a MI for example, have a better survival rate if overweight [81]. However while this may be true, this positive impact of obesity is at an endpoint e.g. after a MI. However, if these individuals were not overweight prior to the attack, it is possible that this event could have been prevented.

#### **1.1.4. Characteristics of Obesity**

Obesity is characterised by an increased fat mass, thought to be due to the hypertrophy of adipocytes in combination with the proliferation and differentiation of preadipocytes within the adipose tissue [82]. Two major processes involved in the symptoms and common accompanying conditions of obesity are disordered lipid metabolism and an increased inflammatory response (**Figure 1.3**).

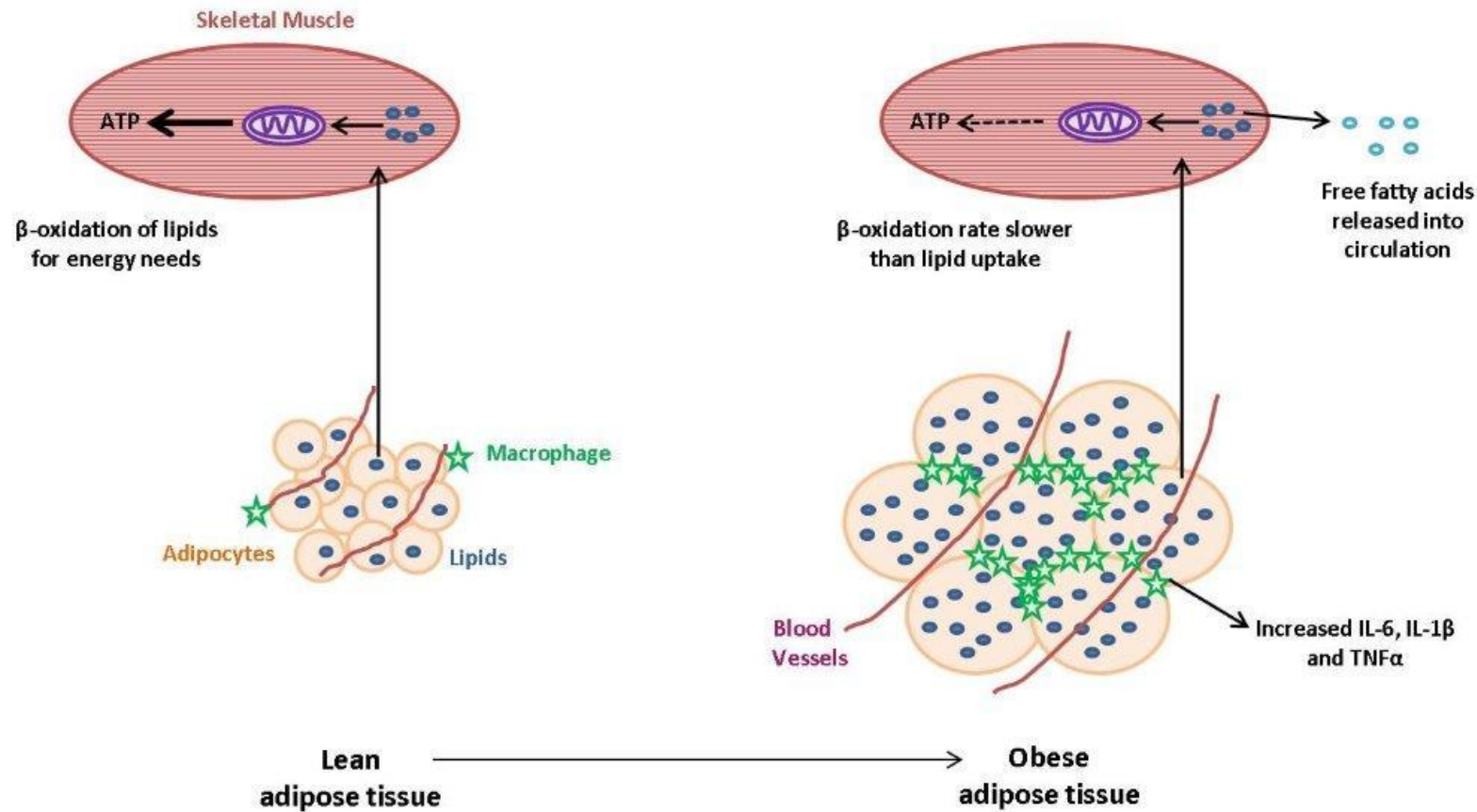


**Figure 1.3. Overview of changes in adipose tissue in obesity.** In lean individuals, the adipose tissue is able to control lipid metabolism for the body. The adipose tissue in a lean individual is composed of approximately 10% macrophages and they are found in close proximity to blood vessels [83]. When skeletal muscle tissue develops increased energy demand, lipids are supplied from the adipose tissue for  $\beta$ -oxidation and subsequent adenosine triphosphate (ATP) production [84]. In the adipose tissue of an obese individual, the adipocytes are larger in size as a result of increased lipid accumulation [82]. The level of macrophage infiltration can reach up to 40% of the stromal vascular fraction and they cluster around the adipocytes in crown-like structures. These macrophages secrete increased levels of pro-inflammatory cytokines [83]. Lipids are deposited into skeletal muscle tissue with the rate of uptake outweighing the rate of  $\beta$ -oxidation [84]. This results in release of free fatty acids (FFAs) into circulation.

#### 1.1.4.1 Lipid metabolism

Adipocytes are able to store triglycerides intracellularly as an energy source from dietary intake. The adipose tissue principally regulates lipid metabolism for the whole body. When energy is required, the adipocytes are able to induce the rapid hydrolysis of the stored triglyceride molecules for conversion to FFAs which can be transported to where they are required in the body in order to be metabolised as an energy source [84]. When these mechanisms become disrupted and the levels of triglyceride storage expands within the adipocytes as a result of increased consumption of saturated fat in the diet, lipolysis may be induced regardless of energy requirements, leading to increased levels of circulating FFAs [84]. A significant positive correlation has been consistently found between the elevated levels of circulating FFAs in patients with obesity and insulin resistance in addition to an increased level of fatty acids accumulating in skeletal muscle [85-87]. In a lean subject, fatty acids are deposited into skeletal muscle when energy is required from an alternative source to glycogen, which in some circumstances can account for 90% of the total energy demand [88].

When FFAs are taken up by the cells they are esterified into long-chain acyl coenzyme A (CoA) molecules, and require transport across the mitochondrial outer and inner membranes. This involves a complex of enzymes that enable conjugation of the long chain acyl-CoA molecules to carnitine by the enzyme carnitine palmitoyltransferase (CPT)-1, the rate-limiting enzyme which catalyses the production of acylcarnitines. Acylcarnitines are transported across the mitochondrial membranes by carnitine translocase. Once inside the mitochondrial matrix, CPT2 catalyses the conversion of the acylcarnitines back to their respective acyl-CoA and carnitine components. The long chain acyl-CoA is then able to enter  $\beta$ -oxidation [88, 89].

During the  $\beta$ -oxidation process, the long chain acyl-CoA molecule is shortened by two carbons each time resulting in the production of acetyl-CoA, NADH (nicotinamide adenine dinucleotide) and FADH (flavin adenine dinucleotide). These intermediates are able to enter the tricarboxylic acid (TCA) cycle and ultimately produce ATP following the electron transport chain process [88]. Due to increased uptake of lipids during obesity as a result of excessive dietary intake, the rate of lipid uptake outweighs the rate of  $\beta$ -oxidation which in turn leads to the export of FFAs into the systemic circulation [88].

The link between the increased level of lipid accumulation within the growing adipocytes and a heightened pro-inflammatory status may be due to the ability of FFAs to signal via the TLR4 as an endogenous stimulus, resulting in the activation of NF- $\kappa$ B and subsequent production of pro-inflammatory cytokines, as demonstrated in murine 3T3-L1 cells and BV-2 microglial cells [90, 91].

#### **1.1.4.2. Adipose tissue inflammation**

Elevated levels of pro-inflammatory mediators including TNF $\alpha$ , IL-6 and CRP have consistently been demonstrated within the adipose tissue of obese subjects [92-94]. While this elevation in pro-inflammatory cytokines is well documented, it was not until 2003 that Weisberg and colleagues reported that there were significantly higher levels of macrophage infiltration within the adipose tissue of obese individuals [83]. In research by Fain and colleagues it was determined that the production of particularly IL-6, IL-1 $\beta$  and TNF $\alpha$ , was by cells present in the stromal vascular fraction (SVF) of the adipose tissue and not the adipocytes themselves [95, 96]. Adipose tissue macrophages (ATMs), were found to constitute around 50% of the leukocytes found within the SVF [97] and Weisberg was able to provide some evidence that the pro-inflammatory cytokines identified within the adipose tissue were primarily produced by these ATMs [83].

A potential explanation for the observed increase in macrophage infiltration into adipose tissue of obese individuals was the induction of hypoxia [98, 99]. As the adipocytes grow in size, an increase in the tissue mass may result in the vasculature becoming insufficient to maintain normal oxygen conditions throughout the expanding adipose tissue. Hypoxic conditions thus induce an inflammatory response which leads to the infiltration of macrophages into the adipose tissue and subsequently the production of pro-inflammatory mediators in order to induce angiogenesis to improve available vasculature [99]. The notion of hypoxia-induced inflammation was confirmed via the exposure of stromal vascular cells to hypoxic conditions *in vitro* which resulted in a significant increase in pro-inflammatory cytokines such as IL-6 and TNF $\alpha$ , with the production dependent on the ATMs that had infiltrated the tissue [97, 100]. An *in vivo* study with the use of an obese murine model was able to demonstrate that the hypoxic conditions observed in the adipose tissue was responsible for up-regulating the levels of pro-inflammatory cytokines including IL-6, IL-1 $\beta$  and TNF $\alpha$  [98].

The adipose tissue of lean humans contains around 10% macrophages, compared to up to 40% in obese individuals [83]. While in lean individuals the present ATMs are identified as single cells in close proximity to endothelial cells [101], ATMs in obese subjects appear as aggregates and form ‘crown-like’ structures surrounding adipocytes [83, 100-102]. These macrophage aggregates were also found to exhibit high levels of intracellular lipids and resembled foam cells, which have distinct roles in the development of atherosclerosis [100, 101, 103]. Furthermore, the macrophages stained positively for CD68, a marker for phagocytic activity, suggesting an ability for these inflammatory cells to phagocytose adipocytes within adipose tissue [100, 101].

Evidence to support the idea of targeting obesity and its associated pro-inflammatory status in order to reduce the risk of developing more complex chronic diseases come from studies investigating the effect of weight loss on the pro-inflammatory status of obese individuals. In a study by Canello and colleagues, a significant reduction in the percentage of infiltrated macrophage as well as a change in the macrophage phenotype was observed, where an increase in the ATM expression of the anti-inflammatory cytokine interleukin-10 (IL-10) was observed in patients that had undergone gastric bypass surgery when compared to before surgery [101]. Further support for the importance of weight loss came from several studies that demonstrated a decrease in the serum levels of the pro-inflammatory mediators including IL-6 and soluble TNF $\alpha$  receptors, in combination with an increase in the levels of the anti-inflammatory adipokine, adiponectin [104-108].

The findings discussed in this section provide support for targeting pro-inflammatory cytokine production with pharmaceutical or dietary interventions as a potential mechanism to reduce the risk of developing chronic diseases.

## **1.2. Epidemiological data for fruit and vegetable intake and chronic disease risk**

It is not a recent concept that what we consume in our diets is able to largely influence our health. Currently, chronic diseases such as cancer and CVD are the leading cause for mortality in Western countries. Development of these diseases may involve genetic predisposition, but most importantly are dependent on a large array of environmental factors including physical exercise, dietary patterns, smoking and alcohol consumption.

Development of chronic disease as a result of these lifestyle factors is largely preventable by changing these influences, as demonstrated by the analysis of over 100,000 men and women where there was a significantly reduced risk of developing chronic disease, in particular CVD with individuals who closely adhered to dietary recommendations [109, 110].

A high intake of fruit and vegetables within the diet has been commonly associated with a lower risk of developing chronic diseases [111]. A disadvantage of these analyses is that by investigating the effect of fruit and vegetables as a whole, it may shadow potential specific associations with certain groups of fruit and vegetables. A considerable amount of data in the last 20 years has demonstrated a potential link between the risk of developing cancer and the consumption of cruciferous vegetables such as broccoli, Brussels sprouts, cabbage and cauliflower [112]. Based on the studies reviewed by Verhoeven in 1996, a more consistent decrease in risk of developing cancer of the lung and the gastrointestinal (GI) tract was observed [113]. In more recent studies, breast, prostate and pancreatic cancers have also been associated with decreased risk of development in individuals consuming high levels of cruciferous vegetables [114].

While the effect of cruciferous vegetable consumption has been studied widely in terms of its associations with cancer, there is very little known about effects of these vegetables on other chronic diseases such as CVD and T2DM. In one study by Zhang and colleagues, it was determined that increased fruit and vegetable consumption was inversely associated with total risk of mortality in both men and women. A more evident association was observed with cruciferous vegetable intake demonstrating a dose-dependent inverse relationship with the risk of CVD mortality [115]. Additional support for these findings comes from two studies that demonstrated a lower risk of MIs in individuals consuming a high level of cruciferous vegetables [116, 117]. In terms of T2DM, one prospective study demonstrated approximately a 20% reduction in the risk of developing the disease with men from a Japanese cohort who consumed high levels of cruciferous vegetables. This reduction was however, not statistically significant [118]. Furthermore, some indication of the involvement of cruciferous vegetable intake on the risk of developing T2DM came from a study where it was found that a higher incidence of T2DM was observed in individuals that followed a dietary pattern which included the low intake of cruciferous vegetables [119].

The most recent supporting evidence involving cruciferous vegetable intake and chronic inflammation came from a study by Jiang and colleagues who investigated whether there was an association between intake of cruciferous vegetables and circulating levels of pro-inflammatory cytokines. In a population of over 1000 middle-aged Chinese women, significant inverse correlations were found with increasing levels of cruciferous vegetable consumption and the circulating levels of IL-6, IL-1 $\beta$  and TNF $\alpha$  with between a 12-25% reduction in levels [120].

### 1.3. Cruciferous vegetables

Cruciferous or *Brassica* vegetables belong to the *Cruciferae* or *Brassicaceae* family which consists of some of the most highly consumed vegetables throughout Europe and Asia, including broccoli, cabbage, Brussels sprouts, cauliflower, kale, bok choy and Chinese cabbage [112]. These vegetables are a major source of GSLs, the phytochemicals that are thought to be responsible for the beneficial health effects seen in response to diets rich in cruciferous vegetables [113-115, 118-120].

#### 1.3.1. Glucosinolates

Different *Brassica* vegetables have different GSL compositions. While for broccoli the predominant GSL is glucoraphanin, for cabbage, sinigrin is found at high levels. In rocket high levels of glucoerucin can be found and in kale, high levels of glucoiberin are present. GSLs share a structure consisting of a sulphur-linked  $\beta$ -D-glucosepyranose moiety in addition to a variable side chain (**Figure 1.4**). The sulphate group is strongly acidic and as a result, GSLs accumulate within cells commonly as a potassium salt [121]. It is the variable side chain that is able to determine whether the GSL is characterised as aliphatic (methionine), aryl (phenylalanine) or indole (tryptophan) [122]. Thus far, 120 members of the GSL family have been identified [123].

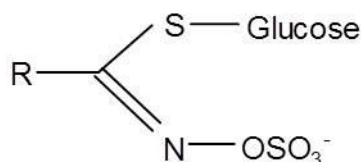


**Figure 1.4. Glucosinolate structure.** Each GSL contains a sulphur-linked  $\beta$ -D-glucosepyranose group, a sulphonated oxime group and a variable side chain that determines its aliphatic, aryl and indole characteristics [121].

When cruciferous vegetables are consumed, it is not the GSLs that are biologically active. Due to the chemical stability of GSLs within the plant, the hydrolysis process is controlled enzymatically by the only thioglucosidase enzyme known to be able to catalyse this reaction, namely myrosinase [122, 124]. The enzyme is physically separated from the GSLs within the plant but when the plant cells are damaged by chewing or mild cooking, the enzyme and GSLs can come into contact to allow the hydrolysis reaction to occur, however, the myrosinase enzyme may become denatured following long and high temperature cooking [114]. Tests investigating the stability of GSLs within the stomach have demonstrated that even in the highly acidic environment (pH 2) most are fairly stable and due to the potential denaturation of myrosinase during cooking practices, it is thought around 60% of GSLs reach the colon intact. Within the colon, it is possible for these GSLs to be hydrolysed by the gut microbiota demonstrating myrosinase-like behaviour, however the details are unclear [122].

Broccoli is now commonly available both fresh and frozen and evidence suggests that consumption of frozen broccoli, produced following blanching at 91°C for around 2.5 minutes, compared to lightly cooked fresh broccoli, can result in significantly less ITCs in the plasma. This is likely due to the degradation of the myrosinase enzyme, demonstrating that the source of the broccoli significantly affects the potential ITC concentration achieved [125]. A later study by Dosz and colleagues demonstrated that if the blanching process was carried out at a temperature of 86°C or higher, myrosinase was inactivated. However, if the blanching step was carried out at a temperature of 76°C, there was only an 18% loss observed in myrosinase conversion of glucoraphanin to SF [126]. These studies demonstrate the importance for using specific cooking practices to ensure the potential concentration of SF that can be reached in the plasma is achieved.

The enzymatic breakdown of GSLs can lead to the production of a number of different compounds depending on the reaction conditions such as ITCs, thiocyanates and nitriles [122]. At a neutral pH, the most common products are stable ITCs and while under acidic or alkaline conditions, nitriles are most commonly produced (**Figure 1.5**) [122].

## 1.4. Sulforaphane

SF is the most commonly studied ITC both *in vitro* and *in vivo*. It is derived from the GSL glucoraphanin, which is the predominant GSL found in broccoli [122] (**Figure 1.5**). Over the next few sections, its bioavailability and subsequent modes of actions will be introduced.

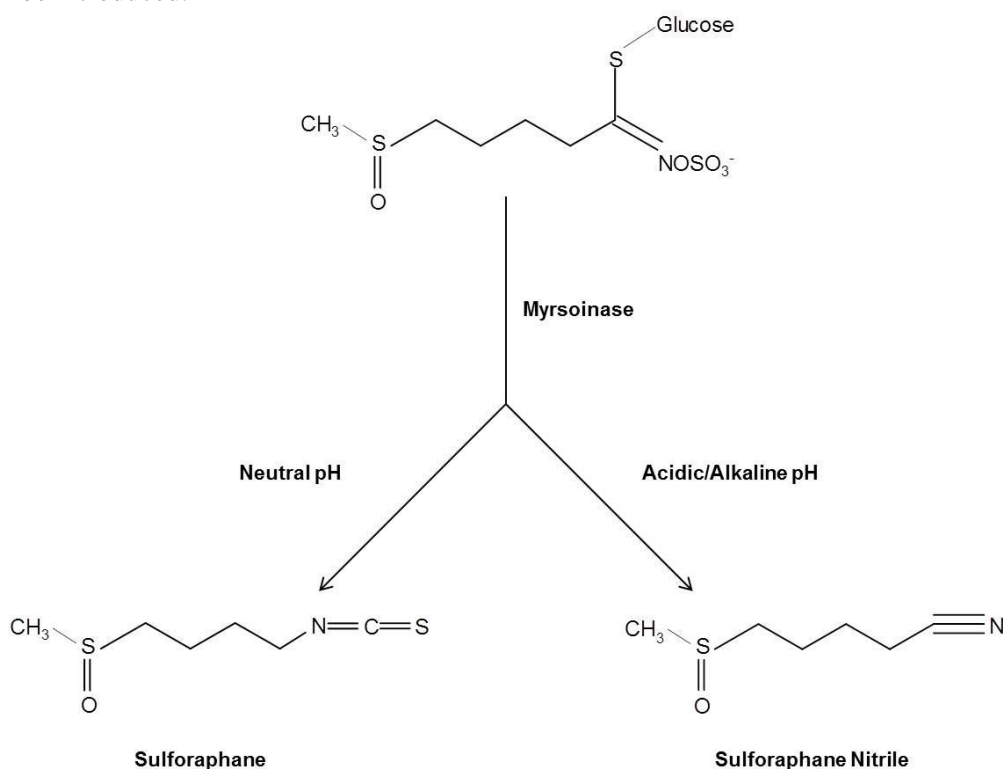


**Figure 1.5. Enzymatic breakdown of glucoraphanin.** Myrosinase behaves to cleave the thioglucose bond which results in the formation of an unstable aglycone. Depending on the pH of the environment, the ITC SF can be formed or following the loss of a sulphur, SF nitrile (Adapted from [121]).

### 1.4.1. Bioavailability

Once converted to SF, the ITC is readily conjugated to increase stability and allow distribution around the body. ITCs are known to accumulate intracellularly with the concentration reaching mM levels [127], much higher than that achieved in circulation following the consumption of broccoli. A study in rats found that except for the liver, GI tract and kidneys, the only other relatively high concentrations of ITCs and their metabolites were found within the blood [122]. In order to study the presence of ITCs within the plasma and urine, a cyclocondensation method was developed allowing quantification via HPLC. Within the plasma, different studies have reported varying levels of ITCs. In a study by Ye and colleagues, when individuals consumed a broccoli

sprout preparation supplying around 200µmoles of ITCs, predominantly SF, a peak concentration of 1µM SF was recorded after 1 hour indicating rapid absorption [128]. In a study by Gasper and colleagues, a higher level of SF was recorded with a peak concentration of 2µM at 2 hours following standard broccoli consumption and 7.4µM after consuming high-GSL broccoli [129].

The bioavailability of ITCs is limited due to the fact that after ITCs enter the cells, there is rapid conjugation to glutathione (GSH) to form dithiocarbamates, a reaction catalysed by glutathione-S-transferase enzymes (GSTs). The liver is the organ known to demonstrate the highest level of GST activity and also contains a high concentration of GSH [122]. These GSH conjugates are subsequently metabolised via the mercapturic acid pathway [130-132]. This pathway involves a number of sequential enzymatically controlled steps in which the ITC-GSH conjugate has the glutamine and glycine residues removed, before the remaining cysteine residue undergoes N-acetylation to ultimately form the N-acetylcysteine (NAC) conjugate [133]. The kidney is the principle organ involved in this conversion of ITC-GSH conjugates to NAC conjugates [122]. In terms of the ITC conjugates identified in urine, the NAC conjugate can account for up to 60% of the initial dose consumed [132]. However, the result of this conjugation means that the ITCs are modified at their electrophilic sulphur and consequently, the metabolites will have very low biological activity levels as many of the functions are reliant on a thiol modification.

The GST enzymes are categorised into cytosolic, mitochondrial and microsomal families. The cytosolic GSTs all exist as dimers and consist of at least 17 subunits which themselves are divided into 7 classes [134]. Of all the GSTs available, only a small subgroup have been investigated in terms of their effects on the conjugation of ITCs, namely GSTA1, M1, M4 and P1 [135]. Of these, the GSTM1 enzyme was most efficient at catalysing the conjugation reaction, followed by GSTP1. While aromatic ITCs were the favoured substrates, SF was the poorest [131, 135]. Based on their essential function in ITC conjugation, it is unsurprising that common polymorphisms within these enzymes have demonstrated variable rates in the response to SF. A null mutation in GSTM1 that results in the absence of a functional protein was thought to be as common as approximately 50% of the population potentially carrying the mutation [136]. When considering the presence of common mutations within the GST genes, epidemiological data found that GSTM1 positive individuals demonstrated greater reductions in the risk

of developing certain cancers, for example lung and prostate cancer [137-139]. However, these findings have been largely contradictory.

In a study by Gasper and colleagues, it was identified that individuals with the GSTM1 null genotype excreted a significantly higher proportion of SF from the broccoli consumed over a more rapid time course [129]. While these results are controversial compared to other studies, it may be an important factor to consider in terms of the effect of varying conjugation and excretion levels of SF, which may in turn impact on the level available to exert its beneficial actions.

### **1.4.2. Targets of SF**

Within the last 20 years a great deal of research has been carried out into the effects of SF and several modes of actions have been consistently demonstrated. While much of the research has been carried out *in vitro* with the pure compound, its effects *in vivo* using both mouse models and humans has also been studied, principally in relation to the effects on carcinogenesis but more recently, in terms of its anti-inflammatory effects. Over the next few sections, the common functions of SF are discussed including the ability of SF to induce phase 2 enzymes, reduce oxidative stress, effect cell metabolism, induce cell cycle arrest and apoptosis and also the reduction of inflammatory signalling.

#### **1.4.2.1. Phase 2 enzymes and oxidative stress**

Phase 2 enzymes detoxify xenobiotics and oxidants that may be encountered by the body allowing them to be rapidly excreted, preventing damaging effects to DNA and other molecules. Examples of phase 2 enzymes include the GSTs previously mentioned, NAD(P)H-quinone oxidoreductase (NQO1), superoxide dismutase 1 (SOD1) and hemoxygenase 1 (HO-1). These genes share a common mechanism for transcriptional regulation with each of the genes containing an antioxidant response element (ARE) within their promoters which are recognised by the transcription factor, nuclear factor (erythroid-derived)-like 2 (Nrf2). SF, along with several other agents with an electrophilic nature, is able to induce the activity of the Nrf2 transcription factor as demonstrated consistently by many groups *in vitro* and *in vivo* [140-153].

The mechanism, by which SF is able to induce Nrf2 activity, is via the targeting of its associated inhibitor Kelch-like ECH-associated protein 1 (Keap1). Keap1 behaves to

sequester the Nrf2 transcription factor to the cytoplasm where it is inactive and targeted for degradation. In response to SF, Nrf2 dissociates from Keap1, allowing translocation of the transcription factor to the nucleus where it is able to recognise and bind to AREs and activate the expression of its target genes [154, 155].

The structure of SF results in an electrophilic nature and SF is thus able to directly bind to the free thiol groups of the available cysteine residues within Keap1 to form thioacyl adducts [156, 157]. It is predicted that this mechanism results in Nrf2 being able to accumulate within the nucleus and subsequent induction of the transcription of its target genes however, due to the reversible nature of SF binding this is yet to be confirmed [157-159].

#### **1.4.2.2. Cell metabolism**

Recently, several papers have described evidence for a function of SF in cell metabolism. Following global gene expression analysis, a study in a non-cancerous breast cell line identified the up-regulation of a selection of enzymes involved in glycolysis and the pentose phosphate pathway [160]. Furthermore, SF has been shown to prevent adipogenesis which is reliant on the accumulation of lipids within adipocytes and moreover, in murine adipocyte-like cells, lipolysis was induced [161-164]. Thus far, the main pathway thought to be responsible for this function was the AMP-activated protein kinase (AMPK) pathway, which behaves to monitor the energy status of cells [165].

In a recent human intervention study, consumption of high-GSL broccoli for 12 weeks resulted in a significant alteration in the plasma metabolite profile, indicative of an improvement in the integration of fatty acid  $\beta$ -oxidation and TCA cycle activity [166]. The dysfunction of  $\beta$ -oxidation and TCA cycle activity is linked to the increased levels of FFAs in systemic circulation as well as cholesterol synthesis as a result of increased citrate. This link is supported by the findings that SF was able to induce a reduction in the levels of hepatic cholesterol in hamsters with dietary-induced hypercholesterolemia, hypothesised as a result of the down-regulation of the levels of enzyme fatty acid synthase (FAS) and sterol regulatory element-binding proteins (SREBP-1 and 2) [167]. While there are hypothetical links evident, more research should be carried out to further investigate the details of how SF can exert such profound effects on cellular metabolism.

### 1.4.2.3. Cell cycle and apoptosis

Another mechanism that has been explored in a number of different models e.g. prostate, colon and breast cells is the ability of SF to arrest the cell cycle. The cell cycle is made up of five phases: G<sub>0</sub> where the cells are senescent; G<sub>1</sub> where the cell increases in size; S which is responsible for DNA replication; G<sub>2</sub> where the cells prepare to divide; and M where the cells undergo mitosis. Each phase is regulated by a number of different molecules; the cyclin-dependent kinases (CDKs), cyclin proteins, and CDK inhibitors. SF has demonstrated the ability to inhibit the cell cycle at a number of phases with G<sub>2</sub>/M being commonly described in prostate cell lines [168-170]. This is thought to be as a result of altering the expression levels of cyclin B1 in addition to the cell cycle inhibitors including p21 and p27 [168, 171-176].

Furthermore, in some cases SF has been shown to induce apoptosis in a number of cell lines and in mouse models where an increase in transcription factors or proteins e.g. caspases involved in apoptosis are up-regulated [170, 172, 177, 178]. It is however, important to note that these results were achieved in studies with concentrations of SF in excess of 15µM which would require high levels of broccoli consumption or supplementation.

### 1.4.2.4. Inflammation

With most relevance to the research aims of this thesis, SF has been shown to exert anti-inflammatory effects through several mechanisms. In response to pro-inflammatory stimuli such as TNFα, IL-1 and more commonly LPS, SF was able to significantly suppress the expression of pro-inflammatory mediators: cytokines including IL-6, IL-1β and TNFα; inflammatory enzymes such as cyclooxygenase-2 (COX-2) and inducible nitric oxide synthase (iNOS) and proteins involved in vascular cells e.g. vascular cell adhesion molecule 1 (VCAM-1) and intercellular adhesion molecule-1 (ICAM-1) in a number of different cell models from both murine and human origin [179-189].

A number of different mechanisms have been suggested to explain these observations: induction of Nrf2, inhibition of NF-κB and targeting of the TLR4 molecule. In terms of Nrf2 induction, Lin and colleagues demonstrated a significant reduction in the levels of pro-inflammatory mediators induced in response to LPS when murine macrophages were treated with SF. However, the effect was seen to a much greater extent with macrophages derived from Nrf2 (+/+) mice as compared to Nrf2 (-/-) mice [185]. A

similar dependence was seen in endothelial cells where SF was able to significantly reduce VCAM-1 expression only in the Nrf2 wildtype animals and not in those without Nrf2 expression [190].

More commonly described is the finding that SF is able to significantly suppress the levels of the active subunit of NF- $\kappa$ B p65 observed in the nucleus, as well as its transcriptional activity and the reduction in the levels of its inhibitor I $\kappa$ B [184, 189, 191-194]. This is likely of fundamental importance in the anti-inflammatory effects of SF in response to LPS in particular, due to the downstream activation of the transcription factor in response to TLR4 activation (**Figure 1.1**). More recently, however, Youn and colleagues described the potential for SF to interact with the TLR4 receptor directly via free thiol groups of cysteine residues within the extracellular domain of the receptor, which resulted in the suppression of oligomerisation, a step required for downstream production of inflammatory mediators [195]. Further support for the targeting of SF at the ligand-receptor interaction, came from the same research group, which demonstrated an additional interaction between SF and a cysteine residue within the MD2 molecule, the co-receptor for TLR4 [196].

It is however, important to note that there is a requirement for the development of an *in vitro* experimental design which mimics a state of low-grade inflammation. As previously mentioned, endotoxin levels circulating in individuals suffering from a chronic inflammatory disorder is in the range of 1ng/ml, whereas the concentrations used in the experiments above are much higher, often surpassing those seen following acute inflammation [37, 45, 46, 197].

## **1.5. Thesis Aims**

Previously the majority of studies investigating inflammation *in vitro* use concentrations of LPS that are far in excess of that found in circulation of patients suffering from chronic disease. In addition, investigations of the anti-inflammatory effects of SF have principally been carried out in murine cell models with a reductionist approach of selecting only several biomarkers for measurement. The overall hypothesis of this thesis was that SF would suppress chronic inflammatory signalling via a multi-targeted approach at physiologically relevant concentrations. In order to test this overall aim, a number of different research questions were tested to progress the research from the present literature.

Within this thesis the following objectives were addressed:

1. The development of an *in vitro* model of chronic inflammation with human monocytes and physiologically relevant concentrations of both LPS and SF. Much of the previous literature investigating pro-inflammatory biomarker production has been carried out in cell lines of murine origin and with a concentration of inflammatory stimulus that is out of range of even acute inflammatory attack. With one of the main limitations of *in vitro* investigations being that it is difficult to translate the findings to an *in vivo* situation, this objective was fundamental in going some way to bridge this problem.
2. To investigate whether SF was able to target global gene expression in response to LPS and whether the mechanism was directly via TLR4 *in vitro*. While several pro-inflammatory biomarkers have been reported to be suppressed by SF in the presence of an inflammatory stimulus, little research has been carried out into the scope of this effect. SF alone has been studied on a global scale in a number of different cell models however, there have been no previous studies that investigated the effect of SF on inflammation on a global scale. Additionally, while the investigations into the global effect of SF can be potentially highly informative in terms of the capability of SF, it is important to try and elucidate the mechanism by which SF is able to have an effect on inflammation, by progressing previous research into the thiol modification of the TLR4.
3. To establish whether the anti-inflammatory effects of SF were restricted to TLR4 alone or if it was also able to target additional signalling pathways. The initial experiments all utilised LPS as the artificial inducer of pro-inflammatory biomarkers due to its relevance with chronic disease. However, a more informative approach would be to investigate whether effects of SF on LPS-signalling are able to be replicated in response to the activation of additional signalling pathways including the TLR2 which is important in the response to lipopeptides and the NOD2 pathway, which has been highly implicated in the IBD Crohn's disease.
4. To progress the methods used initially into a more complex model of chronic inflammation using human SGBS adipocytes and MaCM from human THP-1

macrophages to determine the effect of SF on adipogenesis and cytokine production as a result of adipose tissue inflammation. By using this more complex *in vitro* model of adipose tissue inflammation, different endpoints are able to be tested with disease relevance e.g. lipid accumulation in adipocytes and the inflammatory response to MaCM, mimicking the infiltration of macrophages within adipose tissue of obese individuals. This objective behaves to investigate the potential multi-targeting ability of SF in a disease-related context.

# Chapter Two

---

General materials and methods

---

## 2.1. General reagents

SF was supplied from LKT laboratories (L-SF; Cat. # S8046 and DL-SF; S8044, respectively). DL-SF was used in all chapters, while L-SF was only used in Chapter 6. A stock solution of each was prepared in dimethyl sulfoxide (DMSO). As the vehicle control for SF, it was ensured that the final concentration of DMSO added to the cell culture medium was below 0.1% (v/v). LPS from *Escherichia Coli* strain 055:B5 (Cat. # L6529, Sigma-Aldrich) and 0111:B4 (for experiments with PRR cell lines, Cat. # tlr1-ebpls, InvivoGen) were used in experiments to induce inflammation. LPS was prepared in phosphate buffered saline (PBS) to produce stock solutions. Pam3CSK4 (Cat. # tlr1-pms), FSL-1 (Cat. # tlr1-fsl) and MDP (Cat. # tlr1-mdp) were also supplied from InvivoGen. All stock solutions were prepared in sterile endotoxin-free water at concentrations of 1mg/ml, 100µg/ml and 5mg/ml, respectively. TNFα was supplied from R&D systems (Cat. # 210-TA-005). A stock solution was prepared in PBS at a concentration of 100µg/ml.

## 2.2. Cell culture

### 2.2.1. Human monocytes

Human peripheral blood mononuclear cells (PBMCs) were isolated from 10ml of whole blood provided by healthy, volunteer assay blood donors (male and female) from the Human Nutrition Unit of the Institute of Food Research. Ethical approval was obtained from the Human Research Governance Committee at the Institute of Food Research for optimisation of techniques and experimental design. Whole blood was anti-coagulated using EDTA-containing tubes and diluted 1:1 with PBS to improve the separation process. PBMCs were isolated from the whole blood using sterile, endotoxin-free Accuspin™ System-Histopaque® 1077 (Cat. # A7054, Sigma-Aldrich) according to manufacturer's instructions. From 10ml of whole blood, approximately 10-20 x 10<sup>6</sup> PBMCs were isolated. Cryopreserved PBMCs were also supplied from ZenBio (Cat. # SER-PBMC-F, Cambridge Biosciences). They were a pooled sample from 5 different donors, both male and female, ranging in age and ethnicity.

PBMCs were routinely cultured in RPMI-1640 medium with stable glutamine (Cat. # E15-840, PAA Laboratories) supplemented with 10% (v/v) foetal bovine serum (FBS; Cat. # 10270, Life Technologies) and 1% (v/v) penicillin/streptomycin (Cat. # 15140, Life Technologies).

Human monocytic THP-1 cells were obtained from the European Collection of Cell Culture (ECACC; Cat. # 88081201). THP-1 cells were originally isolated from the peripheral blood of a one year old male suffering from acute monocytic leukaemia [198]. THP-1 cells were routinely cultured in RPMI-1640 medium with stable glutamine supplemented with 10% (v/v) FBS and 1% (v/v) penicillin/streptomycin. THP-1 monocytes have the capability to be chemically differentiated into macrophages as a result of culturing the monocytes in serum-free RPMI-1640 medium in the presence of 125ng/ml phorbol 12-myristate 13-acetate (PMA; Cat. # P1585, Sigma-Aldrich) for 48 hours [199]. This differentiation process was monitored simply by following the morphological transition of the monocytes, which grow in suspension, becoming adherent as they differentiate in to macrophages.

### **2.2.2. PRR-transfected cell lines**

Human embryonic kidney (HEK)-Blue<sup>TM</sup> cells were obtained from InvivoGen (Cat. # hkb-htrl4, hkb-htrl2 and hkb-hnod2). All HEK-Blue<sup>TM</sup> cells were developed by stable transfection with the necessary receptors, TLR4, the MD2/CD14 co-receptors, TLR2 or NOD2, along with a secreted embryonic alkaline phosphatase (SEAP) reporter gene. The SEAP reporter gene is under the control of an IL-12 p40 minimal promoter fused to five NF- $\kappa$ B and AP-1 binding sites. Stimulation with the appropriate ligands activates NF- $\kappa$ B and AP-1 which induces the production of SEAP.

To generate the mutant G908R NOD2-expressing lines, HEK cells (Cat. # 293-null, InvivoGen) were co-transfected with a pSV- $\beta$ -Galactosidase control vector, pNifty2-SEAP (Cat. # pnifty2-seap, InvivoGen) and the mutant form of the receptor, pUNO-hNOD2a G908R, generated as a result of the substitution of the glycine residue at position 908 in the amino acid sequence for an arginine. For transient transfection experiments, 293-hMD2-CD14 cells (Cat. # hek-hmdcd, InvivoGen), prepared by the co-transfection of HEK cells with the MD2 and CD14 genes, were used and transiently transfected with TLR4 wildtype (pUNO-hTLR4-A) and mutant receptors D299G where an aspartate at position 299 has been exchanged for a glycine (pUNO-hTLR4-A, rs4986790) and T399I where a threonine at position 399 has been exchanged for an isoleucine (pUNO-hTLR4-A, rs4986791).

All PRR-expressing cell lines were maintained in DMEM medium with stable glutamine (Cat. # 41965, Gibco) supplemented with 10% (v/v) FBS and 1% (v/v)

penicillin/streptomycin, with variations in the necessary antibiotic combinations. The growth media for HEK-Blue™ TLR4 and TLR2 cell lines required the addition of 1% (v/v) penicillin, streptomycin, gentamicin cocktail, 0.18% (v/v) Normocin™ (Cat. # ant-nr, InvivoGen) and 1X HEK-Blue™ selection antibiotics (Cat. # hb-sel, InvivoGen). The NOD2 cell lines required 1% (v/v) penicillin, streptomycin, 0.06% (v/v) blasticidin (Cat. # ant-bl-5b, InvivoGen) and 0.1% (v/v) Zeocin™ (Cat # ant-zn, InvivoGen). The transiently transfected 293-hMD2-CD14 cells required 1% (v/v) penicillin, streptomycin, gentamicin cocktail and 0.05% (v/v) HygroGold™ (Cat. # ant-hg-1, InvivoGen).

To produce HEK cells transiently transfected with either the wildtype or mutant TLR4 receptors, 293-MD2-CD14 cells were grown to a confluency of 60-80% before being transfected using Lipofectamine 2000 (Cat. # 11668027, Invitrogen) according to the manufacturer's instructions. The cells were co-transfected with the wildtype or mutant plasmids and the reporter SEAP plasmid (pNifty2-SEAP) with optimised conditions (1µg TLR4 plasmids and 8µg pNifty2-SEAP).

### **2.2.3. HT-29 colon adenocarcinoma cells**

The human colon adenocarcinoma HT-29 cells were supplied by ECACC (Cat. # 91072201). They were isolated from a primary tumour in a 44 year old Caucasian female. These cells can form a well differentiated adenocarcinoma consistent with colonic primary grade I. The cells were routinely cultured in McCoy's 5A modified medium with stable glutamine (Cat. # M9309, Sigma-Aldrich) supplemented with 10% (v/v) FBS and 1% (v/v) penicillin/streptomycin.

### **2.2.4. SGBS preadipocyte cells**

The human preadipocyte SGBS cell line was kindly gifted by Prof. M. Wabitsch (University of Ulm, Germany). This cell line was isolated from an infant suffering from Simpson-Golabi-Behmel Syndrome (SGBS) which is characterised by enhanced prenatal and postnatal growth associated with large adipose tissue depots [200]. This cell line is characterised by the high capacity to be differentiated into mature adipocytes up to generation 60. SGBS preadipocyte cells were routinely cultured in DMEM/F12 (1:1) medium with stable glutamine and Hank's Balanced Salt Solution (HBSS; Cat. # 11330, Life Technologies) supplemented with 33µM biotin (Cat. # B4639, Sigma-Aldrich),

17 $\mu$ M pantothenate (Cat. # P5155, Sigma-Aldrich), 10% (v/v) FBS (not heat-inactivated) and 1% (v/v) penicillin/streptomycin.

In order to differentiate SGBS preadipocytes into mature adipocyte cells, the cells were cultured to reach 70-80% confluency before replacing the medium with basal growth medium (serum-free) supplemented with 0.01mg/ml transferrin (Cat. # T2252, Sigma-Aldrich), 20nM insulin (Cat. # I1507, Sigma-Aldrich), 0.1 $\mu$ M cortisol (Cat. # H0888, Sigma-Aldrich), 0.2nM triiodothyronine (T<sub>3</sub>; Cat. # T6397, Sigma-Aldrich), 25nM dexamethasone (Cat. # D1756, Sigma-Aldrich), 0.25mM isobutylmethylxanthine (IBMX; Cat. # I5879, Sigma-Aldrich) and 2 $\mu$ M rosiglitazone (Cat. # CAY71740, Caymen Chemicals) on day 0. On days 4, 8 and 12, the medium was replaced with basal growth medium (serum-free) supplemented with only 0.01mg/ml transferrin, 20nM insulin, 0.1 $\mu$ M cortisol and 0.2nM T<sub>3</sub> to continue differentiation. By day 14, the differentiation process was complete and the cells were treated as mature adipocytes. This process was monitored by following the increased accumulation of lipid droplets within the cells, giving clear morphological changes.

All cell lines used were maintained in a humidified atmosphere containing 5% CO<sub>2</sub> at 37°C and were routinely passaged to continue growth.

## 2.3. Cell viability assay

### 2.3.1. Background

The viability of all the cell lines described in the previous section was estimated in response to a number of different treatments using the WST-1 assay. This assay is based on the conversion of the tetrazolium salt WST-1 (4-[3-(4-iodophenyl)-2-(nitrophenyl)-2H-5-tetrazolio]-1,3-benzene disulfonate) into formazan by mitochondrial dehydrogenase enzymes (**Figure 2.1**). If a reduction of viability is observed as a result of the cell treatment, fewer cells will be metabolically active and therefore will be unable to carry out the conversion due to a reduction in the activity of mitochondrial dehydrogenases. The product of the enzymatic reaction, formazan is a deep red colour and this colour change enables a spectrophotometric assay to be used to allow quantitative determination of the number of viable cells.

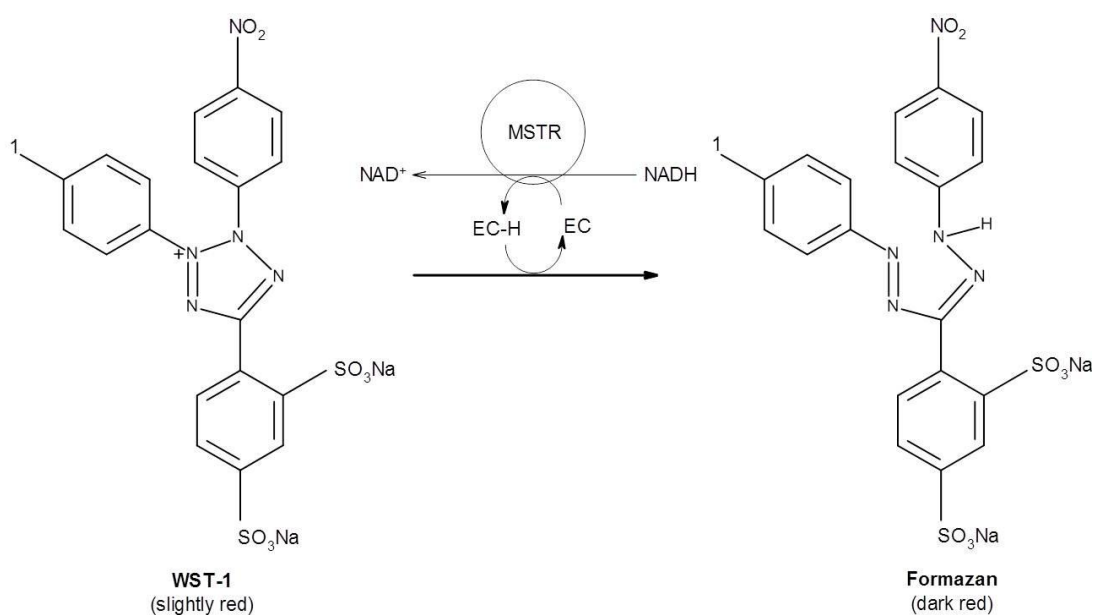


**Figure 2.1. Conversion of WST-1 to formazan.**

WST-1 can be reduced to formazan resulting in a colour change that is proportional to cell viability. (EC = electron coupling reagent; MSTR = mitochondrial succinate-tetrazolium reductase system). Figure adapted from product data sheet.

### 2.3.2. Measurement of cell viability

Cells were seeded into 96 well plates for this assay. For the adherent cell lines, (THP-1 macrophages, HEK-Blue™, HT-29 and SGBS) cells are grown to around 70-80% confluence. For THP-1 monocytes and PBMCs,  $1 \times 10^5$  cells and  $2.5 \times 10^5$  cells respectively, were seeded into 96 well plates and treated immediately. SGBS preadipocytes were seeded into 96 well plates and allowed to reach 70-80% confluence. For adipocytes, the preadipocytes at this point followed the differentiation process as described in section 2.2.4. THP-1 monocytes were differentiated into macrophages following the protocol explained in section 2.2.1. Cells were treated with concentrations of SF ranging from 1-200 $\mu$ M (vehicle control for SF = < 0.1% (v/v) DMSO) in six replicate wells.

For treatment with MaCM, THP-1 monocytes were differentiated by treating cells with 125ng/ml PMA for 48 hours in serum-free conditions. Once the differentiation of the macrophages was complete, the medium was replaced with serum-free RPMI-1640 containing 0.5% (w/v) bovine serum albumin (BSA; Cat. # A9418, Sigma-Aldrich) to stabilise the macrophage-secreted factors for a further 48 hours to produce the MaCM.

The MaCM was collected and cleared of cell debris by centrifugation. SGBS adipocytes were treated with doses of MaCM (10, 20 and 50%; v/v) in six replicate wells.

After 24 hours of cell treatments, 10 $\mu$ l (per 100 $\mu$ l media) of WST-1 reagent (Cat. # 05015944001, Roche) was added to each well. Cells were incubated in a humidified atmosphere containing 5% CO<sub>2</sub> at 37°C for up to 3 hours. The metabolic conversion of the WST-1 reagent to formazan was quantified by measuring the absorbance using a spectrophotometer at 450nm with a reference wavelength of 610nm. Medium only was used for the blank correction to compensate for any absorbance contribution of the basal colour from the phenol red present within the medium.

### **2.3.3. Data analysis and statistics**

Optical density (OD) values from 450nm reading (corrected with data from 610nm) were used to determine the percentage cell viability. For all treatments the percentage viability was calculated against the untreated control cells. The IC<sub>50</sub> (half maximal inhibitory concentration) was calculated using GraphPad Prism software including a logarithm transformation of the data and a non-linear analysis to determine the concentration at which 50% cell viability remained. The effect of the treatment was analysed using one-way analysis of variance (ANOVA) followed by Bonferroni multiple comparison tests.

## **2.4. Measuring cytokine secretion using enzyme-linked immunosorbant assay (ELISA)**

### **2.4.1. Background**

To determine the concentration of cytokines secreted in to the cell culture supernatant following cell treatments, Quantikine ELISA kits were used: IL-6 (Cat. # D6050); IL-1 $\beta$  (Cat. # DLB50) and TNF $\alpha$  (Cat. # DTA00C) kits were all purchased from R&D systems and carried out according to manufacturer's instructions (**Figure 2.2**). These kits all provide a standard of each compound in order to produce a calibration curve enabling quantification.

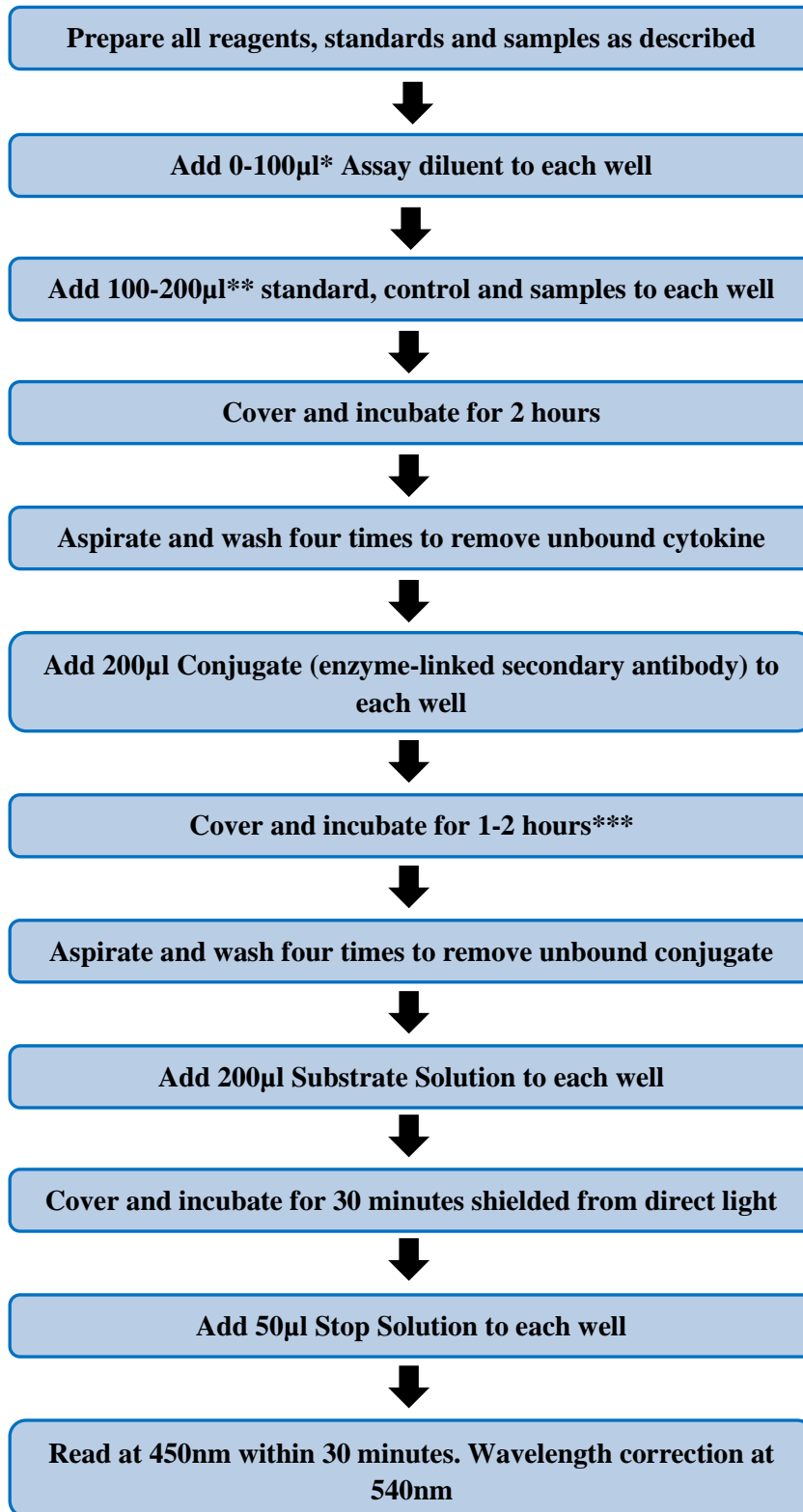


**Figure 2.2. Quantikine ELISA protocol.** Information taken from the protocol provided within the kits. Same protocol for all ELISA kits with the following variations. \*0µl Assay diluent added for IL-1 $\beta$ , 50µl for TNF $\alpha$  and 100µl for IL-6. \*\*100µl of standards, samples and controls for IL-6, 200µl for IL-1 $\beta$  and TNF $\alpha$ . \*\*\*Incubation for 1 hour for IL-1 $\beta$  and TNF $\alpha$ , 2 hours for IL-6.

### **2.4.2. Measurement of cytokine secretion**

Cells were seeded into 6, 12, 24 or 48 well plates depending on the cell type used and grown to 70-80% confluency. Cells were exposed to the treatments for varying times depending on the experimental design. Cell culture supernatant was collected and centrifuged at 13000rpm for 20 minutes at 4°C to remove any cell debris. Supernatants were stored at -20°C until required. On the day of use, the samples were thawed and inspected for the presence of precipitates. If visible, samples were centrifuged at 13000rpm for 10 minutes at 4°C and the supernatant was transferred to a fresh tube. Depending on the levels of cytokines expected to be present within the samples, necessary dilutions were carried out with the appropriate calibrator diluent provided in the kit to ensure the measurements remained within the calibration curve. After following the manufacturer's instructions, the levels of cytokines in the samples were quantified (**Figure 2.2**).

### **2.4.3. Statistics**

In experiments carried out with ranging doses of treatments, one-way ANOVA was performed followed by Bonferroni multiple comparison tests. In experiments with two variables (dose of treatment and time of exposure) two-way ANOVA was performed with Bonferroni multiple comparison tests. In experiments that were carried out over a period of time with single dose treatments, the area under the curve (AUC) was measured and Student t-tests carried out to statistically compare each time point.

## **2.5. Gene expression using real-time reverse transcriptase – polymerase chain reaction**

### **2.5.1. Background**

Real-time RT-PCR is a common technique used to quantify gene expression. A number of different companies provide products that allow detection of amplified target gene expression levels and for the present study, Taqman® was used (Applied Biosystems) which relies on the detection of the products via the generation of a fluorescent signal.

### **2.5.2. RNA extraction and quantification**

Total RNA was extracted from treated cells using the QIAGEN® RNeasy Mini Kit (Cat. # 74104, QIAGEN) according to manufacturer's instructions. Cells were initially lysed using the provided Buffer RLT and further homogenised using a QIAshredder (Cat. # 79654, QIAGEN). The differentiated SGBS adipocyte cells were the only exception in which total RNA was extracted from the cells using the QIAGEN® RNeasy Lipid Tissue Mini Kit (Cat. # 74804, QIAGEN) due to the high levels of intracellular lipid accumulation. Lysis of the SGBS adipocytes required the QIAzol Lysis Reagent provided with the kit. Additional steps were necessary to remove the lipid content from the homogenate. Chloroform was added to the homogenate to promote precipitation of the lipids and a centrifugation step was used to separate the aqueous layer containing the RNA for the subsequent steps.

RNA samples were quantified after extraction using the NanoDrop ND-1000 spectrophotometer. Triplicate readings for RNA quantification were performed per sample and the average was calculated. This technique also gives an indication of the purity of the RNA. Each sample receives a 260/280 absorbance ratio, where the 260nm reading is the wavelength absorbed by nucleic acids and the 280nm reading is indicative of protein absorbance. When the RNA is pure, you would expect a ratio of 2.0, however this does not necessarily mean that the RNA is of high quality due to the 280nm reading being susceptible to errors.

### **2.5.3. Real-time RT-PCR**

For the quantification of gene expression, the Taqman® RNA to C<sub>T</sub> 1-step kit was used (Cat. # 4392938, Life Technologies). This uses RNA extracted from the cells as its starting material and in one step produces the complimentary DNA strand based on the RNA sequence and amplifies the target genes. The fluorescent signal is generated through the use of dual-labelled probes. The probes are labelled with a reporter dye attached at the 5' end e.g. FAM (6-carboxyfluorescein) and a quencher dye at the 3' end e.g. TAMRA (6-carboxytetramethylrhodamine). When the probe is intact, the close proximity of the two dyes means that no fluorescent signal is generated. However, when the *Taq* polymerase extends the complementary DNA strand where the probe is bound, the 5' nuclease activity of the polymerase is able to cleave the probe resulting in the reporter and quencher dyes being decoupled and a fluorescent signal can occur. As each

cycle takes place, the fluorescent signal increases and this signal can be used to determine relative expression level of the target gene.

To prepare the samples for real-time RT-PCR, the CAS-1200 robot and Robotics 4 software was used (Corbett Life Sciences). MicroAmp Optical 96 well reaction plates (Cat. # N8010560, Life Technologies) were used for the ABI Prism 7500 Detection System (Applied Biosystems) and 96 well Semi-Skirted fast plates (Cat. # LW2214, Alpha Laboratories) were used for the ABI StepOne Plus machine (Applied Biosystems). A No Template Control (NTC) was loaded (double-autoclaved RNase-free water) to ensure there is no RNA contamination, followed by each of the samples of which there were three biological replicates and three technical replicates.

The ABI Prism 7500 Detection System or the ABI StepOne Plus instruments were used to quantify target mRNA expression levels under the following conditions: 48°C for 30 minutes to allow reverse transcription, 95°C for 10 minutes to activate the AmpliTaq™ Gold polymerase, followed by 40 cycles of 95°C for 15 seconds for denaturation and 60°C for 1 minute to anneal and extend the target gene DNA. Each of the reactions were performed in a volume of 20µl containing RNA, primers and probes either individually or as part of a prepared assay kit (IDT technologies), Taqman® Master Mix and the reverse transcriptase enzymes. **Table 2.1** gives the sequences of the primers and probes used for the assays.

**Table 2.1. Primer and probe sequences of genes analysed**

Gene Name	IDT kit I.D.	Sequence
IL-6		Forward: 5'-CTCTTCAGAACGAATTGACAAACAAAT-3' <sup>a</sup> Reverse: 5'-ATGTTACTCTTGTTACATGTCTTCTTTCTC-3' <sup>a</sup> Probe: 5'-FAM-TACATCCTCGACGGCATCTCAGCCC-TAMRA-3' <sup>b</sup>
IL-1 $\beta$	Hs.PT.51.20299051	Forward: 5'-AGGAGCACTTCATCTGTTTAGG-3' <sup>c</sup> Reverse: 5'-GCCAATCTTCATTGCTCAAGTG-3' <sup>c</sup> Probe: 5'-FAM-TTCACTGGCGAGCTCAGGTAATTC-TAMRA-3' <sup>b</sup>
TNF $\alpha$	Hs.PT.51.22572112.gs	Forward: 5'-CTCAGCTTGAGGTTTGC-3' <sup>c</sup> Reverse: 5'-CCTCTCTCTAATCAGCCCTCT-3' <sup>c</sup> Probe: 5'-FAM-CAGGCAGTCAGATCATCTTCTCGAACC-TAMRA-3' <sup>c</sup>
18S		Forward: 5'-GGCTCATTAATCAGTTATGGTTCCT-3' <sup>b</sup> Reverse: 5'-GTATTAGCTCTAGAATTACCACAGTTATCCA-3' <sup>b</sup> Probe: 5'-FAM-TGGTCGCTCGCTCCTCTCCAC-TAMRA-3' <sup>b</sup>
CPT1A	Hs.PT.56a.28218391	Forward: 5'-TGAAGACAACAAACGTGAACG-3' <sup>c</sup> Reverse: 5'-CAGAAGTGAAGACCCGGATAC-3' <sup>c</sup> Probe: 5'-FAM-CAAACCACCTGTCGTAACATCGGCC-TAMRA-3' <sup>c</sup>

<sup>a</sup>Primers were designed and purchased from Eurofins.

<sup>b</sup>Primers and probes were designed and purchased from Sigma-Aldrich.

<sup>c</sup>Pre-designed assay kits were purchased from IDT technologies.

The Applied Biosystems software calculated the threshold cycle ( $C_T$ ) values for each reaction and with the use of a standard curve of known total RNA quantities, the quantity of the target RNA was calculated. In order to normalise the expression of the specific target genes, an endogenous control, also known as a housekeeping gene, was used to account for potential differences in the total amount of RNA in each sample. For normalisation of the target genes used in the present study, 18S ribosomal RNA was used as the chosen housekeeping gene. The expression level of this gene should not vary with experimental treatment as it is very highly expressed and therefore the normalised data will allow demonstration of changes in target gene expression that are only as a result of experimental treatments.

The amplification efficiency is calculated using the standard curve and for all the genes considered, efficiencies were  $> 96\%$ . A reaction that has been 100% efficient will result in the gradient of the standard curve being  $-3.32$ , meaning the  $C_T$  difference between two sequential 2-fold dilutions will equal 1. The final essential parameter to take note of is the  $R^2$  value of the standard curve line of best fit. With an  $R^2$  value of 1, the value of Y (the  $C_T$ ) can be accurately from the X value. Values  $> 0.99$  are considered to be highly accurate.

#### **2.5.4. Statistics**

In experiments carried out with ranging doses of treatments, one-way ANOVA was performed followed by Bonferroni multiple comparison tests. In experiments with two variables (dose of treatment and time of exposure) two-way ANOVA was performed with Bonferroni multiple comparison tests. In the experiments that were carried out over a period of time with single dose treatments the AUC was measured and Student t-tests carried out to statistically compare each time point.

## **2.6. Whole genome expression analysis using microarray techniques**

### **2.6.1. Background**

In the present study, commercially available Affymetrix GeneChip® Human Exon 1.0ST arrays were used to analyse whole genome expression and has the capability to monitor expression at the exon level. Compared to the traditional 3' expression arrays

that have been commonly used, the Affymetrix GeneChip® Human Exon 1.0ST array contains probes that span the entire length of the gene and is not restricted to only the 3' end. In addition, with probes assigned to each individual exon, the expression of each exon within the gene can be measured allowing information on potential alternative splicing events.

The Affymetrix GeneChip® Human Exon 1.0ST array is made up of approximately 1.4 million probe sets and more than 5.5 million individual probes. Four individual probes comprise one probe set, with each probe set corresponding to individual exons. Depending on the length of the exon, more than one probe set may be assigned. While the 3' expression arrays contains 'mismatch probes', the Affymetrix GeneChip® Human Exon 1.0ST array contains only perfectly matched probes and the non-specific hybridisation is accounted for using background correction based on the GC content of the probes. Each of the probe sets specific for individual exons are grouped into transcript clusters. Gene level analysis is measured by considering all probes within a single transcript cluster. By focusing on the individual exons and not the gene as a whole, novel transcripts can be identified which may be present as a result of alternative splicing in response to factors within the experimental design. Many genes have a number of transcripts associated where the exons are spliced together in various combinations for example, certain exons may be missing from the final transcript. Each of the probe sets are categorised based on the level of characterisation of each exon. 'Core' probe sets are those which are annotated by RefSeq; 'extended' probe sets have mRNA evidence available and 'full' probes sets are those where there is a prediction based on bioinformatics for a particular exon. In the present study, the analysis was carried out using the 'core' probe sets (18708 transcripts, 284258 probe sets).

THP-1 monocytes ( $6 \times 10^6$  cells per 10cm dish) were treated with 1ng/ml LPS (vehicle control for LPS = PBS) in the presence or absence of 5 $\mu$ M SF (vehicle control for SF = < 0.1% (v/v) DMSO) for 12 hours with three biological replicates for each condition. RNA was extracted using the QIAGEN® RNeasy Mini Kit according to manufacturer's instructions and quantified as in section 2.5.2.

### **2.6.2. Assessment of RNA quality**

As explained in section 2.5.2, RNA quantity and purity was determined using the NanoDrop ND-1000 spectrophotometer. An absorbance ratio between 260nm and

280nm of 2 is indicative of highly pure RNA but this does not necessarily mean the RNA is of high quality. To measure the quality of RNA, the Agilent 2100 Bioanalyzer was used. The system uses an electrophoretic principle with quick separation on a chip system. The microchannels within the chip are filled with a sieving polymer and fluorescence dye. Once the wells are filled, the chip becomes part of an electrical circuit. When the dye molecules intercalate with the RNA, fluorescence occurs and this is measured and plotted graphically over time, in addition to a densitometry plot to show the two markers of ribosomal RNA, 28S and 18S. In order to quantitate the RNA quality a ladder was used and the ratio of the 28S and 18S ribosomal RNA markers was calculated to assess the integrity of the RNA. The 28S peak should have a larger area than 18S in samples of high quality. In addition, an RNA integrity number (RIN) can be used to estimate the quality and is based on the electrophoretic trace of the RNA sample. The RIN number ranges from 1-10 where 1 is a completely degraded sample and 10 is a perfect quality sample. All samples used for microarray analysis had a RIN value of  $\geq 9.6$ .

The RNA samples were sent to Nottingham *Arabidopsis* Stock centre and the Affymetrix GeneChip® Human Exon 1.0ST array was carried out according to manufacturer's protocols.

### **2.6.3. Data analysis and statistics**

For the analysis of the data from the microarray, the R/Bioconductor package was used. The raw signal intensity data was provided in .CEL files. The data was RMA (robust multi-array analysis)-background corrected and quantile normalised to determine if any outliers are present. Once complete, linear probe level models were fit to the data to analyse gene level summaries. For annotation of the data, the current file available at the *aroma.affymetrix* website (HuEx-1\_0-st-v2.na32.hg19.transcript.csv) was downloaded, which contains the information available for all transcripts and the core CDF probe set was selected. Subsequent statistical data analysis to identify differentially expressed genes was performed using *limma* [201]. Identification of genes that were differentially expressed were analysed for the level of statistical significance at different Benjamini and Hochberg adjusted p-values, to account for the potential false discovery rate.

To highlight pathways that were largely represented by the differentially expressed genes, functional analyses using the Database for Annotation, Visualisation and Integrated Discovery v6.7 (DAVID; <http://david.abcc.ncifcrf.gov>) was used [202, 203].

Microarray data generated in this study were compliant to MIAME (Minimum information about a microarray experiment) criteria and were made publicly available through ArrayExpress (Accession E-MEXP-3931, Date of Release: December 2014).

## **2.7. Western blotting**

### **2.7.1. Background**

Western blotting is a fundamental technique used in cell and molecular biology to identify specific proteins from a crude protein extract. The extracted proteins are separated based on their molecular weight via gel electrophoresis and transferred to a membrane producing a band for each protein. The membrane is incubated for the relevant times with antibodies specific to the protein of interest. The next step involves incubation of the membrane with an enzyme-linked secondary antibody which allows visualisation of the blot following the addition of a chemiluminescent substrate.

### **2.7.2. Sample preparation**

HT-29 cells were treated with SF (5, 10 and 25 $\mu$ M, vehicle control for SF = < 0.1% (v/v) DMSO) in the presence or absence of 1ng/ml LPS (vehicle control for LPS = PBS) for 1 hour. Following treatment, the proteins were extracted from the cells using the Novagen ProteoExtract® Transmembrane Extraction kit (Cat. # 71772, Millipore) which enables the separation of the insoluble membrane fraction from the soluble cytoplasmic fraction to allow determination of the target protein level in both locations of the cell.

Briefly, HT-29 cells were washed with PBS and scraped into solution. Cells were centrifuged at 1000 x g for 5 minutes at 4°C before being resuspended in 1ml of extraction buffer 1 supplied in the kit. The solution was incubated for 10 minutes at 4°C and after repeating the centrifugation step, the soluble cytoplasmic fraction was collected. The remaining cell pellet was resuspended in 0.2ml of extraction buffer 2A (1:1 extraction buffer 2: reagent A supplied in the kit). The suspension was incubated at room temperature for 45 minutes with gentle agitation before centrifugation at 16000 x g for 15 minutes at 4°C yielding the membrane fraction.

The bicinchoninic acid (BCA) assay was used to determine the quantity of total protein within each sample (Cat. # BCA1-1KT, Sigma-Aldrich). The principle of the assay relies on the formation of a Cu<sup>2+</sup> protein complex under alkaline conditions followed by

the reduction of  $\text{Cu}^{2+}$  to  $\text{Cu}^{1+}$ . The extent of the reduction is proportional to the amount of protein present and can be analysed by measuring absorbance of the purple-blue complex formed between BCA and  $\text{Cu}^{1+}$  [204]. Each of the protein samples were diluted 1:5 with NaPi buffer (50mM NaPi, pH 6, containing 5mM EDTA) prior to quantification and a standard curve using BSA was produced ranging from 0-1000 $\mu\text{g}/\text{ml}$  by diluting the standards in NaPi buffer. The assay was performed in a 96 well plate in which 25 $\mu\text{l}$  of the standards and samples were added to each well in addition to 200 $\mu\text{l}$  of BCA working reagent (50:1 dilution between BCA and copper (II) sulphate solution) in duplicate. The plate was incubated at 37°C for 30 minutes and shielded from the light to allow the reduction to occur. The absorbance was measured at 550nm on the FLUOstar OPTIMA microplate reader (BMG Labtech) and the concentration of protein was calculated using the standard curve.

For gel electrophoresis, 35 $\mu\text{g}$  of protein was used for each sample. Protein samples were diluted appropriately with ultra-pure water to produce the final concentrations in a total volume of 18 $\mu\text{l}$ . 4.5 $\mu\text{l}$  of NuPAGE® LDS sample buffer (4X; Cat. # NP0008, Life Technologies) was added to each sample and samples were heated at 70°C for 10 minutes to denature tertiary and secondary protein structures. No dithiothreitol (DTT) was added as the samples required non-reducing conditions. The samples were centrifuged briefly to remove any air bubbles present before loading on to the gel.

### **2.7.3. Gel electrophoresis**

2 $\mu\text{l}$  of MagicMark™ XP Western Standard (Cat. # LC5602, Life Technologies) was used as the protein ladder to determine the size of the proteins. A total volume of 22.5 $\mu\text{l}$  of each protein sample was loaded in to the wells of a NuPAGE® 10 well 10% Bis-Tris SDS-PAGE gel (Cat. # NP0306, Life Technologies) for electrophoresis. Appropriately diluted NuPAGE® MOPS SDS running buffer (20X, Cat. # NP0001, Life Technologies) was used and the gel was run at 200V for 50 minutes at room temperature using the XCell SureLock™ Mini-Cell Electrophoresis system (Life Technologies).

### **2.7.4. Immunoblotting**

Once the gel electrophoresis was complete, the gel was separated from the plates and together with blotting paper, sponges and nitrocellulose membrane (Cat. # 162-0112, BioRad) that had been soaked in dilute NuPAGE® transfer buffer (20X, Cat. # NP006,

Life Technologies) containing 10% (v/v) methanol, were loaded into the XCell II™ Blot Module (Life Technologies). The blot module was then placed in the XCell SureLock™ Mini-Cell Electrophoresis system and the running chamber saturated with NuPAGE® transfer buffer while the outer chamber was filled with distilled water. The transfer was run at 30V for 1 hour to allow the proteins to transfer from the gel to the membrane.

Ponceau S staining (Sigma-Aldrich, Cat. # P7170) was used to determine successful transfer of the proteins from the gel to the membrane. The membrane was washed with Tris-buffered saline Tween-20 (TBST; 50mM Tris, pH 7.4; 200mM NaCl and 0.1% (v/v) Tween-20) three times for 5 minutes to ensure the Ponceau S stain was removed before the membrane was blocked with 5% (w/v) skimmed milk powder solution in TBST at room temperature for 1 hour with gentle agitation. Three washes with TBST were carried out after blocking to remove any residual milk powder solution before the membrane was probed with the primary antibodies. Anti-TLR4 (Cat. # ab22048, Abcam) at a concentration of 2µg/ml in 5% (w/v) BSA/TBST solution and the anti-Sodium-Potassium ATPase transporter used as the housekeeping protein for the membrane fractions (Cat. # ab76020, Abcam) at a 1:20000 dilution in 2% (w/v) BSA/TBST were incubated overnight at 4°C with gentle agitation. Anti-GAPDH (Cat. # AM4300, Life Technologies) was diluted 1:4000 in 5% (w/v) skimmed milk powder in TBST and incubated for 1 hour. Following incubation, the primary antibody was removed and the three washes with TBST were repeated to remove any unbound primary antibody. The enzyme-linked secondary antibody, either anti-Mouse (Cat. # A3682, Sigma-Aldrich) or anti-Rabbit HRP-linked IgG antibodies (Cat. # 70745, New England Biolabs) as appropriate were diluted 1:1000 with a 5% (w/v) skimmed milk powder solution in TBST and the blot was incubated at room temperature for 1 hour with gentle agitation. Three TBST washes were completed after the incubation to remove any unbound secondary antibody before adding the working reagent of SuperSignal West Pico Chemiluminescent Substrate (1:1 Luminol/Enhancer: Stable Peroxide buffer; Cat. # 34080, Thermo Scientific) according to manufacturer's instructions. The blot was protected from the light and incubated for 5 minutes to allow the enzyme linked to the secondary antibody to convert the substrate to a chemiluminescent product. The intensity of the chemiluminescence was measured using the BioRad Fluor-S MultiImager. To re-probe the membrane, the previous antibodies were stripped for 15 minutes at room temperature using Restore™ Western blot Stripping buffer (Cat. # 21059, Thermo Scientific) before re-blocking the membrane and repeating the process.

### **2.7.5. Data analysis and statistics**

In experiments carried out with ranging doses of treatments, one-way ANOVA was performed followed by Bonferroni multiple comparison tests.

## **2.8. Analysis of SF modifications on TLR4 using liquid chromatography-tandem mass spectroscopy (LC-MS/MS)**

### **2.8.1. Sample preparation**

#### **2.8.1.1. Recombinant TLR4 protein**

Purified extracellular domain of TLR4 (sourced from a mouse myeloma cell line, NS0-derived, Glu24-Lys631, with a C-terminal Ser and 10-His tag) was obtained from R&D systems (Cat. # 1478-TR-050). TLR4 (1 $\mu$ g) was incubated with SF (5-50 $\mu$ M; vehicle control for SF = < 0.1% (v/v) DMSO) for 1 hour at 37°C in a 100mM Tris-HCl (pH 7.8) and 10mM CaCl<sub>2</sub> digestion buffer. For reducing conditions, 1mM DTT was added for 15 minutes following SF treatment. Sequencing grade chymotrypsin (Cat. # 11418467001, Roche) was added for 7 hours, followed by trypsin digestion overnight after thermal denaturation of the chymotrypsin for 5 minutes at 95°C (both at 1:50 enzyme to substrate ratio). Protein digestion was quenched using formic acid at a final concentration of 5%. OMIX C18 pipette tips (Cat. # A57003100, Agilent Technologies) were used to concentrate the peptide fragments and remove undigested protein.

#### **2.8.1.2. Cytoplasmic and membrane protein extracts**

Duplicate membrane and cytoplasmic protein fractions were subjected to gel electrophoresis as explained in section 2.7.3.

#### **2.8.1.3. Immunoprecipitation of TLR4 protein**

In order to enrich the samples with TLR4, an immunoprecipitation (IP) method was used. The Pierce Classic IP Kit (Cat. # 26416, Thermo Scientific) was used according to manufacturer's instructions (**Figure 2.3**).

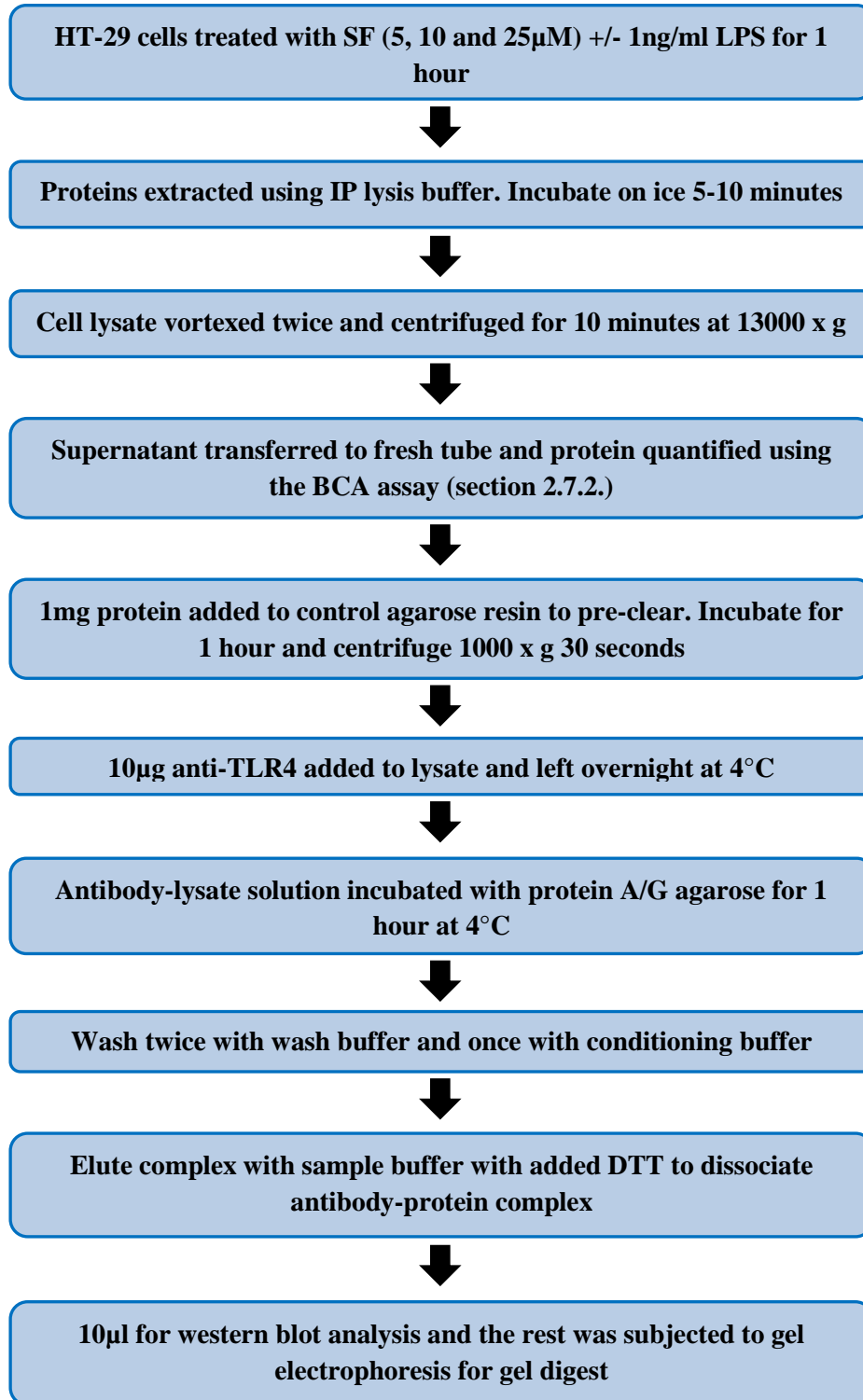


Figure 2.3. Protocol for immunoprecipitation of TLR4.

### **2.8.2. Gel digestion of protein bands**

Following gel electrophoresis, gels were fixed with a solution of 50% (v/v) methanol and 7% (v/v) acetic acid for 15 minutes to improve staining. The fixed gels were washed with distilled water three times to remove any remaining fixing agent. The gels were stained with GelCode Blue Stain Reagent, a coomassie blue protein stain (Cat. # 24590, Thermo Scientific) for 1 hour, followed by destaining with three washes of distilled water in order to reduce the background, resulting in only the proteins being stained. The gels were visualised using the GS800 Calibrated Densitometer (BioRad) using the Quantity One 4.6.1 software with Gel Coomassie setting and selected at 36.3 $\mu$ m.

The approximate band size of the expected TLR4 band is at 93kDa therefore from the gels where the cytoplasmic and membrane fractions were used, the area of gel excised was between the 80 and 100kDa markers. For the IP product, several bands were excised as described in further detail in Chapter 5, section 5.2.4. Once excised from the gel, as much unstained gel as possible was removed and the stained portion was cut finely into 1mm<sup>3</sup> with a razor blade. The samples were transferred in to 1.5ml eppendorfs and 400 $\mu$ l distilled water was added. The gel pieces were washed with 1ml of 0.2M ammonium bicarbonate (ABC) in 50% acetonitrile via vortexing briefly and leaving for 15 minutes to remove the GelCode Blue Stain Reagent. This step was repeated two-three times until the gel pieces were clear in colour. Once the stain was completely removed, the solution was aspirated. 1ml of acetonitrile was added for 10 minutes to remove aqueous solutions resulting in the gel pieces become white in colour and dry. The solution was aspirated and the tubes were left open to allow the remaining acetonitrile to evaporate.

For the enzyme digestion step, chymotrypsin was prepared in a solution of 20mM ABC/10mM CaCl<sub>2</sub>. A 25 $\mu$ g aliquot of chymotrypsin was dissolved in 500 $\mu$ l 20mM ABC/10mM CaCl<sub>2</sub> and 100 $\mu$ l of this solution was added to 150 $\mu$ l solvent to give a 20ng/ $\mu$ l working concentration and was kept on ice. A 5 $\mu$ g aliquot of trypsin was solubilised in 245 $\mu$ l 20mM ABC/10mM CaCl<sub>2</sub> to give a 20ng/ $\mu$ l working concentration and was left on ice. 10-20 $\mu$ l of each enzyme was added which was absorbed by the gel pieces, allowing the proteins within the gel pieces to be enzymatically digested. An appropriate volume of 20mM ABC/10mM CaCl<sub>2</sub> was subsequently added to each sample to ensure all gel pieces were in solution and samples were left overnight in a water bath at 37°C. To quench the enzyme reaction, the total volume of liquid added to

the gel pieces was calculated and this amount of 1% formic acid was added to each sample before they were left on dry ice for 10 minutes.

Samples were thawed and the digest solution was aspirated and transferred into fresh 1.5ml eppendorfs. The gel pieces were washed with 50% acetonitrile for 10 minutes before the solution was collected to increase the recovery of the digested proteins. The extracted digest samples were then dried down on the medium drying setting using the Speed Vac SC110 (Savant) fitted with a refrigerated condensation trap and a Vac V-500 (Buchi). The samples were then frozen at -80°C until ready for Orbitrap analysis.

### **2.8.3. LC-MS/MS analysis**

Samples were prepared in 50% acetonitrile and subjected to micro-LC-MS/MS analysis using the LTQ Orbitrap mass spectrometer (Thermo Electron) and a nanoflow-HPLC system (nanoACQUITY; Waters). Peptides were trapped on line to a Symmetry C18 Trap (5µm, 180µm x 20µm) held at 45°C. Peptides were eluted by a gradient of 0-80% acetonitrile in 0.1% formic acid over 50 minutes at a flow rate of 250nl/min. The mass spectrometer was operated in positive ion mode with a nano-spray source at a capillary temperature of 200°C.

The Orbitrap was run with a resolution of 60,000 over the mass range m/z 300-2000 and an MS target of 10<sup>6</sup> and 1 second maximum scan time. The MS/MS was triggered by a minimal signal of 2000 with an Automatic Gain Control target of 30000 ions and a maximum scan time of 150 milliseconds. For MS/MS events selection of 2+ and 3+ charge states selection were used. Dynamic exclusion was set to 1 count and 30 second exclusion time with an exclusion mass window of ± 20ppm.

### **2.8.4. Data analysis and statistics**

The protein levels of the bands from the IP product gel stained with coomassie blue were quantified using the Quantity One software. Adjusted % band volumes were used and for normalisation, the antibody band was used (Chapter 5, section 5.2.4).

For the LC-MS/MS data, the spectra were analysed using Mascot against the Uniprot protein database, restricted to taxonomy *Homo sapiens* of the SPTrEMBL database, chymotrypsin/trypsin digest which was permitted to have four missed cleavages and

oxidised methionine and cysteine-bound SF were selected as variable modifications. The peptide masses were monoisotopic and either 2+ or 3+ charged and the peptide error tolerance was  $\pm 1.5\text{Da}$  and MS/MS error tolerance was  $\pm 0.5\text{Da}$ . Data was also analysed using Peaks software to investigate the significance of the fragmentation pattern and Progenesis software to evaluate the dose-response relationship.

For investigating the relationship between SF treatment and the abundance of the modified cysteine-containing peptides, the abundance values were extracted from the Progenesis software and a one-way ANOVA was carried out followed by Bonferroni multiple comparison tests.

## **2.9. Measure of NF- $\kappa$ B activity using QUANTI-Blue™ assay**

### **2.9.1. Background**

QUANTI-Blue™ is a colorimetric enzyme assay which is able to determine the amount of alkaline phosphatase (AP) activity in cell culture supernatants via an enzymatic reaction resulting in the change of the QUANTI-Blue™ solution from a pink colour to a purple-blue colour in the presence of AP. SEAP, a truncated form of the GPI-anchored protein placental AP, is a commonly used reporter gene. It is secreted into the cell culture medium making this a quick assay that does not require disruption of the cells.

### **2.9.2. QUANTI-Blue™ assay**

HEK-Blue™ cells (described in section 2.2.2) were grown to 70% confluence in 384 well plates. Once treated for 24 hours with appropriate ligands in the presence or absence of SF (L-SF or DL-SF; 2, 5 and 10 $\mu\text{M}$ ; vehicle control for SF = < 0.1% (v/v) DMSO), the level of SEAP was measured. QUANTI-Blue™ powder (Cat. # rep-qb1, InvivoGen) was dissolved in distilled water and warmed to 37°C before use. 50 $\mu\text{l}$  of QUANTI-Blue™ was added to each well of a new 384 well plate before the addition of 5 $\mu\text{l}$  cell culture supernatant from each replicate. The plate was then incubated at room temperature (required between 10-60 minutes depending on which cells were used) and was shielded from the light to allow a colour change to occur from pink to purple-blue after which the absorbance was measured at 650nm using the MultiSkan Spectrum spectrophotometer (Thermo Scientific).

### **2.9.3. Statistics**

With ranging doses of treatments, one-way ANOVA was performed followed by Bonferroni multiple comparison tests.

## **2.10. Analysis of lipid accumulation and lipolysis in SGBS cells**

### **2.10.1. Background**

During adipogenesis, preadipocyte cells can be differentiated into mature adipocytes in response to a number of signals which results in the increased accumulation of lipids within the cells. This lipid accumulation can be used to quantify the level and progression of differentiation over time. In the present study, Oil Red O staining was performed.

Oil Red O is otherwise known as Sudan Red 5B and is a fat soluble diazo dye used for staining lipids. By using isopropanol as a solvent, the dye is able to enter the cells and stain the lipids bright red while the excess can be removed via washing with water. An advantage of this protocol is that the Oil Red O stain can be eluted from the cells using isopropanol without dissolving the lipids themselves and the level of staining can be quantified spectrophotometrically.

In terms of measuring lipolysis within the cells, a commonly used technique is measuring the glycerol release into the cell culture supernatant. Glycerol is the backbone of triglycerides and under a number of physiological conditions triglycerides can be hydrolysed, resulting in the release of glycerol and FFAs. Unlike the FFAs, glycerol is not reutilised by the adipocytes and is released by the cells. By measuring the levels of glycerol in the cell culture supernatant we can consider this to reflect the level of lipolysis. Kits are commercially available and involve an enzymatic reaction in which a coloured product is formed. The absorbance is proportional to the amount of glycerol released. **Figure 2.4** presents the reactions involved in measuring glycerol levels.

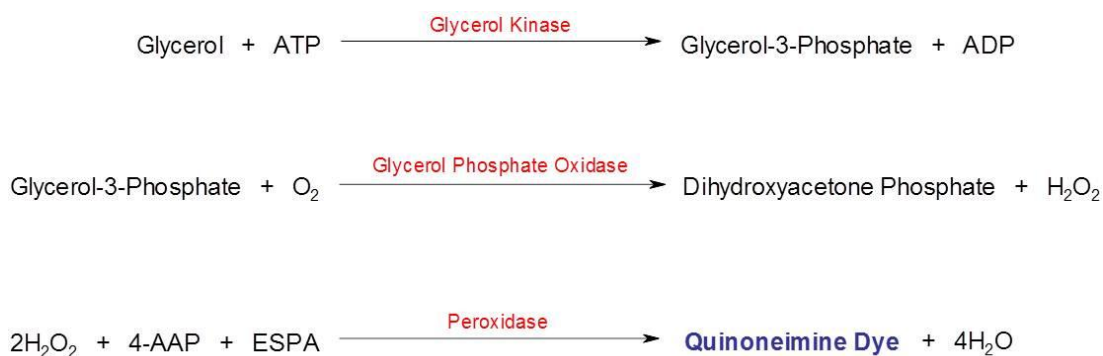


**Figure 2.4. Glycerol assay principle.**

Glycerol is phosphorylated by glycerol kinase to produce glycerol-3-phosphate and adenosine diphosphate (ADP). The glycerol-3-phosphate is oxidised by glycerol phosphate oxidase producing dihydroacetone phosphate and hydrogen peroxide (H<sub>2</sub>O<sub>2</sub>). Peroxidase catalyses the redox-coupled reaction of H<sub>2</sub>O<sub>2</sub> with 4-aminoantipyrine (4-AAP) and N-ethyl-N-(3-sulfopropyl)-*m*-anisidine (ESPA), producing a brilliant purple product with an absorbance maximum at 540nm. Figure adapted from the kit protocol.

**2.10.2. Oil Red O staining**

Oil Red O was obtained from Sigma-Aldrich (Cat. # O0625) and a stock solution of 3.4mM in isopropanol was produced. This was left on a stirrer plate overnight, filtered using a sterile 0.2µm pore size syringe filter and stored at 4°C. The working solution was produced using a 1.6-fold dilution in water to yield a working concentration of 2.1mM. The solution was mixed and left at room temperature for 20 minutes before being filtered again using a sterile 0.2µm pore size syringe filter. Details of the protocol are given in **Figure 2.5**.

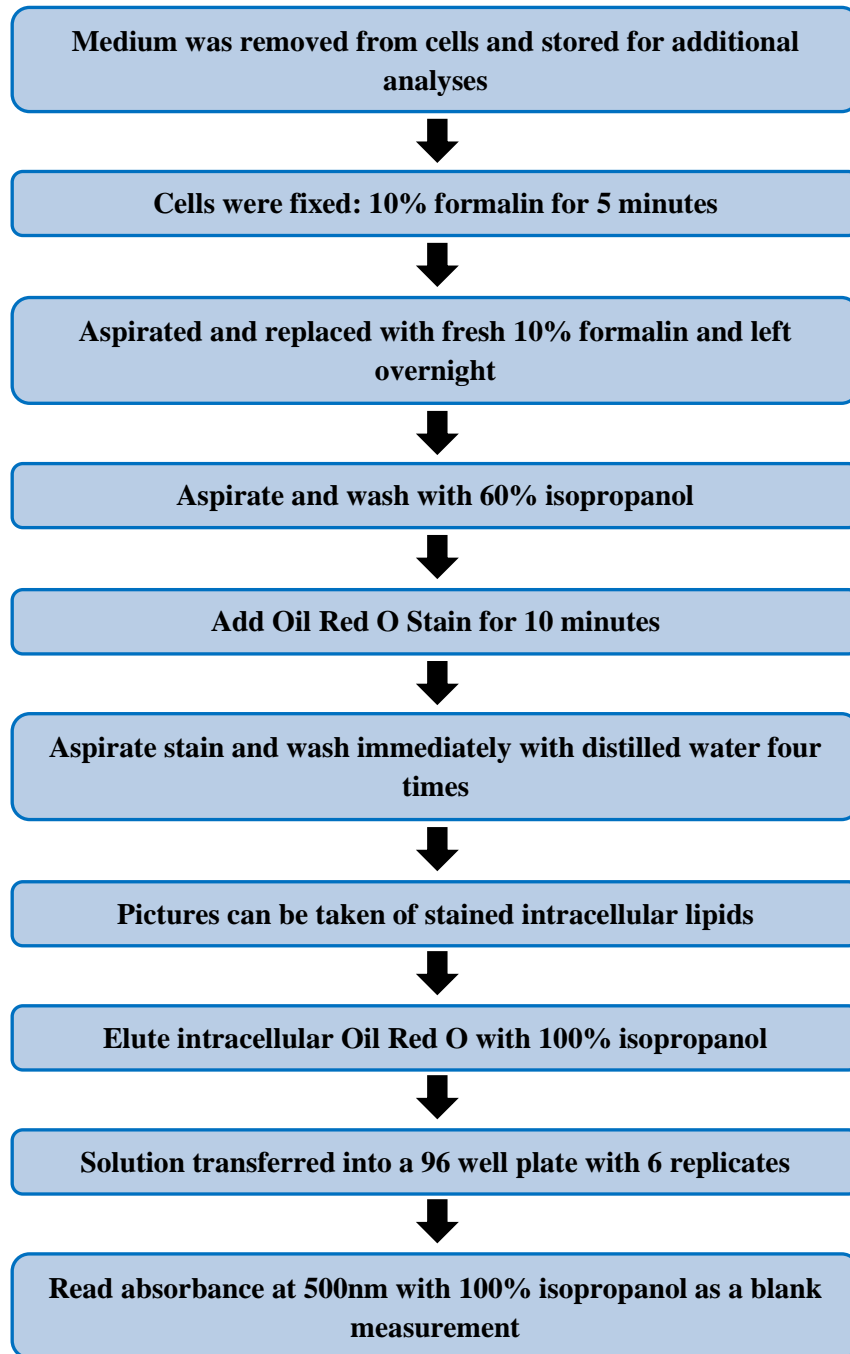


**Figure 2.5. Oil Red O staining protocol.**

### **2.10.3. Glycerol release analysis**

Prior to the Oil Red O staining, the cell culture supernatant was collected and cleared by centrifugation at 13000rpm for 20 minutes at 4°C before being stored at -20°C. For glycerol analysis, the Glycerol Colorimetric Assay Kit (Cat. # 10010755, Cambridge Biosciences) was used.

20µl of the Glycerol Standard was diluted with 980µl of the diluted Standard Diluent (all reagents were provided in the kit) to produce a stock solution of 20mg/l. From the stock solution, a standard curve was produced over the range of 0-20mg/l in order to allow the quantification of glycerol present in the samples. 10µl of standards and samples were added to the 96 well plate provided in the kit before the reaction was initiated via the addition of the diluted Enzyme Buffer solution to each well. The plate was shaken for a few seconds to mix before being covered and incubated for 15 minutes at room temperature. The absorbance was then measured at 550nm using the FLUOstar OPTIMA microplate reader. The concentration in each sample was determined by the use of the standard curve algorithm.

#### **2.10.4. Data analysis and statistics**

For the Oil Red O data, the OD values were corrected by subtracting the value found with isopropanol alone and these raw data values were used for analysis. For the glycerol release data, OD values were blank-corrected by subtracting the value found with 0mg/l of the glycerol standard curve and applying the standard curve equation to calculate the concentration of glycerol in each sample.

In experiments carried out with ranging doses of treatments, one-way ANOVA was performed followed by Bonferroni multiple comparison tests. In experiments with two variables (dose of treatment and time of exposure) two-way ANOVA was performed with Bonferroni multiple comparison tests.

### **2.11. Analysis of TCA intermediates in MaCM using LC-MS/MS analysis**

#### **2.11.1. Sample preparation**

MaCM was produced following the differentiation of monocytes into macrophages as described in section 2.3.2.

Both the DMEM/F12 + 10% (v/v) non-heat inactivated FCS (normal growth medium for the SGBS cells) and RPMI-1640 serum-free with and without 0.5% (w/v) BSA (differentiation medium for the monocytes to macrophages) were measured in combination with a number of doses (10, 20 and 50% MaCM). All were carried out in

two biological replicates and two technical replicates. Once prepared, all solutions were centrifuged at 1200 x g for 10 minutes at room temperature and the supernatant transferred to a fresh eppendorf. 100µl 3mM perchloric acid was added to all media samples to acidify the solution and samples were immediately placed on ice for 10 minutes. Samples were centrifuged at 12000 x g for 10 minutes at 4°C and the supernatant was collected. 100µl of each sample was added to amber 2ml HPLC vials with inserts.

A standard curve was produced with 1mg/ml concentration of a number of TCA intermediates, all purchased from Sigma-Aldrich; glutamic acid (Cat. # G1251), citric acid (Cat. # C0759), malic acid (Cat. # M0875), oxaloacetic acid (Cat. # O4216), succinic acid (Cat. # S3674), fumaric acid (Cat. # 47910), malonic acid (Cat. # M1296) and lactic acid (Cat. # L0625) were all solubilised in acidified medium (RPMI-1640 + 10% 3mM perchloric acid). 100µl of each of the standards were added together and made up to 1ml to give a solution of 100µg/ml of each standard. A separate standard curve was made up for isocitric acid (Cat. # I1252) and 100µl was taken and made up to 1ml in the same way as with the other intermediates. A five point standard curve is produced with a 10-fold serial dilution over the range of 10000ng/ml to 0ng/ml. 10µl of deuterated citrate is added to all samples as an internal standard (final concentration of 10µg/ml) to allow quantification based on the ratio of the internal standard to each intermediate peak.

### **2.11.2. LC-MS/MS analysis**

For LC-MS/MS analysis, the Agilent 1200 Series LC 6490 Triple Quad LC-MS mass spectrometer was used (Agilent). The HPLC column was a Kinetex C18 1.7µm (100 x 2.1mm) from Phenomenex. The flow rate was 0.4ml/min with a mobile phase of 0.2% formic acid. Electrospray ionisation (ESI) was used in the positive mode for glutamic acid and in the negative mode for the remaining intermediates investigated. 2µl was used for the injection volume and the autosampler was maintained at 4°C. **Table 2.2** summarises the monitored ions and the optimised MS operating parameters of the analytes.

**Table 2.2. LC-MS/MS parameters for analytes measured**

Analyte	Retention time (minutes)	Precursor Ion (m/z)	Product Ion (m/z)	Polarity
Glutamic Acid	0.6	148.1	129.9	Positive
Citric Acid	0.9	191.0	110.9	Negative
Iso-Citric Acid	0.7	191.0	154.9	Negative
$\alpha$ -Ketoglutaric acid	*	145.1	100.9	Negative
Malic Acid	0.7	133.1	114.8	Negative
Oxaloacetic Acid	*	131.0	87.1	Negative
Succinic Acid	1.2	117.0	98.9	Negative
Fumaric Acid	1.1	115.0	70.9	Negative
Malonic Acid	*	103.0	58.9	Negative
Lactic Acid	0.8	89.0	42.9	Negative

\* The retention time was unavailable as compounds were not found in samples

### 2.11.3. Data analysis and statistics

Data files were explored and analysed using MassHunter Workstation software (Agilent). The peak areas of the analytes were determined and using the peak area ratio (peak area of analyte/peak area of the internal standard) the concentration of the analyte was determined. In the present study, the treatment consisted of a number of doses thus requiring one-way ANOVA followed by Bonferroni multiple comparison tests.

# Chapter Three

---

Effect of SF on LPS-induced cytokine  
production in human monocytes

### **3.0. Introduction**

Chronic inflammation is a complex condition that has been described as the ‘common soil’ in the aetiology of a number of multifactorial diseases such as cancer, CVD and T2DM [205]. It is often characterised by the modulation of inflammatory mediators, e.g. cytokines, following a sustained response to an inflammatory stimulus. Cytokines are a large group of signalling molecules involved in cell communication and are often described as either pro- or anti-inflammatory [206]. However, many cytokines have a pleiotropic nature and can function as both pro- and anti-inflammatory, depending on the circumstances, which makes classification difficult. Of the cytokines found to be altered in chronic diseases, IL-6, IL-1 $\beta$  and TNF $\alpha$  are commonly investigated *in vitro* and *in vivo*, and most research classifies these as pro-inflammatory [33, 42, 43, 45, 206-213].

Chronic inflammation occurs when an acute inflammatory attack becomes dissociated from a specific stimulus. This stimulus may be a bacterial infection in which structural components of the bacteria elicit an inflammatory response. An example is LPS, a bacterial endotoxin found in the cell walls of Gram-negative bacteria. Endotoxin can be measured at detectable levels in circulation. In healthy individuals, it is present at a level in the low pg/ml range, however, in individuals suffering from chronic disease levels may be elevated at levels up to 0.9ng/ml [37, 45, 46]. LPS is a specific agonist for TLR4, a PRR which when activated by ligand binding, results in the stimulation of transcription factors including NF- $\kappa$ B and AP-1, which in turn control the expression of pro-inflammatory mediators [13]. Thus, elevation of LPS in circulation may be responsible for increased serum levels of cytokines seen in sufferers of chronic disease.

Monocytes are a fundamental cell type involved in both acute and chronic inflammation. They are found in circulation and are primed with the ability to rapidly invade tissues in response to an inflammatory stimulus [214]. In a low-grade inflammatory state, for example during atherosclerosis, monocytes are recruited as a result of increased LDL levels within the plasma. A positive correlation is seen between the number of monocytes in circulation and atherosclerotic plaque size in animal models and in humans, resulting in the level of circulating monocytes being described as an independent risk factor for CVD [215]. As a result, monocytes are commonly chosen as a model to study chronic inflammatory signalling pathways.

When investigating the role of dietary agents in human health, biological relevance is of critical importance. The fact that a state of low-grade systemic inflammation is common

to a number of chronic diseases makes the process a crucial target for dietary interventions. Diets rich in cruciferous vegetables have been associated with a decreased risk of developing cancer at a number of different sites and also with a lower risk of CVD mortality [115, 216-222]. ITCs, derived from GSLs present in cruciferous vegetables such as broccoli, are bioactive components that may mediate the observed beneficial health effects with increased cruciferous vegetable consumption. SF is the predominant ITC obtained from broccoli. Based on research by Gasper and colleagues, a peak concentration of  $2.4 \pm 0.4\mu\text{M}$  of total SF metabolites were found in the plasma of individuals 2 hours after consumption of standard broccoli, while consumption of high-GSL broccoli achieved a concentration of  $7.4 \pm 3.1\mu\text{M}$  [129]. This provides direct experimental evidence that consumption of broccoli results in the presence of biologically active SF in circulation.

SF has been previously shown to exert anti-inflammatory effects both *in vitro* and *in vivo* [181-187, 190-192, 195, 223, 224]. Taking into consideration the elevation of pro-inflammatory cytokines in sufferers of chronic disease, with the evidence that SF is able to exert anti-inflammatory effects, the hypothesis that SF was able to significantly suppress IL-6, IL-1 $\beta$  and TNF $\alpha$  expression and secretion in human monocytic cells in response to LPS was tested within this chapter.

### **3.1. Materials and Methods**

The cell models used were human PBMCs from healthy blood donors in order to optimise experimental design or from a commercial source, in addition to THP-1 monocytes. Details of these cell types are described in section 2.2.1. In order to measure the levels of cytokines secreted in response to LPS in the presence or absence of SF, an ELISA specific to each of the cytokines measured (IL-6, IL-1 $\beta$  and TNF $\alpha$ ) was performed and the technique is described in further detail in section 2.4. To determine the viability of the cells in response to SF a WST-1 cell viability assay was used (section 2.3). For investigations into the level of expression of each cytokine in the THP-1 monocytes, real-time RT-PCR was used (section 2.5).

## 3.2. Results

### 3.2.1. PBMCs

#### 3.2.1.1. Effect of SF on LPS-induced cytokine secretion

Human PBMCs were the chosen cell model in this experimental design due to their principle involvement in responding to pro-inflammatory signals. LPS is commonly used as an artificial inducer of inflammation but often at very high concentrations. The reason LPS was favoured in this experimental design as opposed to other inflammatory stimuli such as IL-1 $\beta$  and TNF $\alpha$ , was due to the presence of endotoxin circulating in different chronic conditions e.g. CVD and T2DM. Also, with choosing to measure IL-1 $\beta$  and TNF $\alpha$  as my endpoint biomarkers, using them as the inflammatory stimulus would have been inappropriate for the secretion studies and expression would have been potentially induced as a result of positive feedback. In the present study, concentrations of LPS were used in the range of 1-500ng/ml, with a level of 1ng/ml being relevant to the levels found circulating in sufferers of chronic disease [37, 45, 46]. When human PBMCs were treated with 1ng/ml LPS for 4 hours, a significant increase in the levels of IL-6 secretion was observed (**Figure 3.1**). Thus demonstrating that this physiologically relevant concentration was sufficient for induction of an inflammatory response and it was not necessary to further increase the concentration of LPS used.

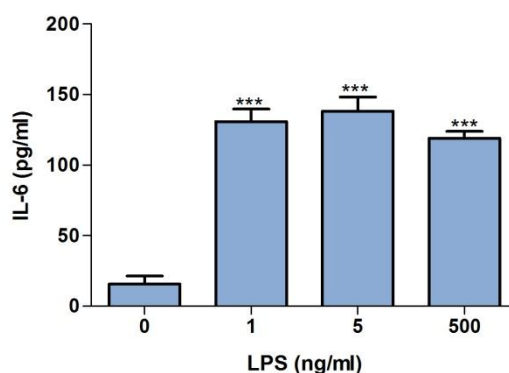


**Figure 3.1. Induction of IL-6 secretion with different LPS concentrations in human PBMCs.** Human PBMCs were treated with LPS at different concentrations (1, 5 and 500ng/ml; vehicle control for LPS = PBS) for 4 hours. The cell culture supernatant was collected and IL-6 was measured by ELISA. Data shown = mean  $\pm$  SD. Data was statistically analysed using one-way ANOVA followed by Bonferroni multiple comparison tests. \*\*\*p<0.001 vs. 0ng/ml.

The measurement of IL-6 secretion in response to LPS (1ng/ml) in human PBMCs was repeated over a 24 hour period to observe the secretion pattern. The secretion of IL-6 is

significantly induced at 4 hours initially (consistent with response seen in **Figure 3.1**) and continues to rise with increasing the time of exposure to LPS (**Figure 3.2**).

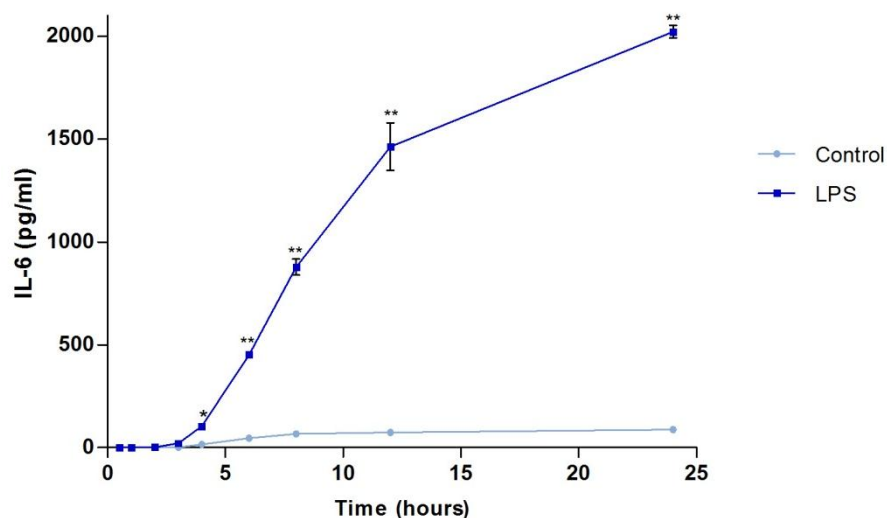


**Figure 3.2. LPS significantly induces IL-6 secretion in human PBMCs over 24 hours.** Human PBMCs were treated with 1ng/ml LPS (vehicle control for LPS = PBS) with varying times of exposure (0.5-24 hours). The cell culture supernatant was collected and IL-6 was measured by ELISA. Data shown = mean  $\pm$  SD. Data was statistically analysed using AUC followed by Student t tests for each time point comparing the cumulative AUC values. \* $p < 0.01$  and \*\* $p < 0.001$  vs. untreated controls at the same time point.

In order to investigate the effect of SF on LPS-induced IL-6 secretion, the time of SF exposure required determination. In previous experiments within the research group, human PBMCs were pre-treated with SF for 20 hours prior to LPS treatment for 4 hours. In terms of what was observed *in vivo*, Gasper and colleagues found that the concentration of SF peaks in the plasma 2 hours after ingestion of broccoli [129]. Based on those results, the effect of SF on LPS-induction with both a 2 hour and 20 hour pre-treatment of SF was compared. In both conditions, SF significantly suppressed LPS induction of IL-6 secretion (**Figure 3.3A and B**).

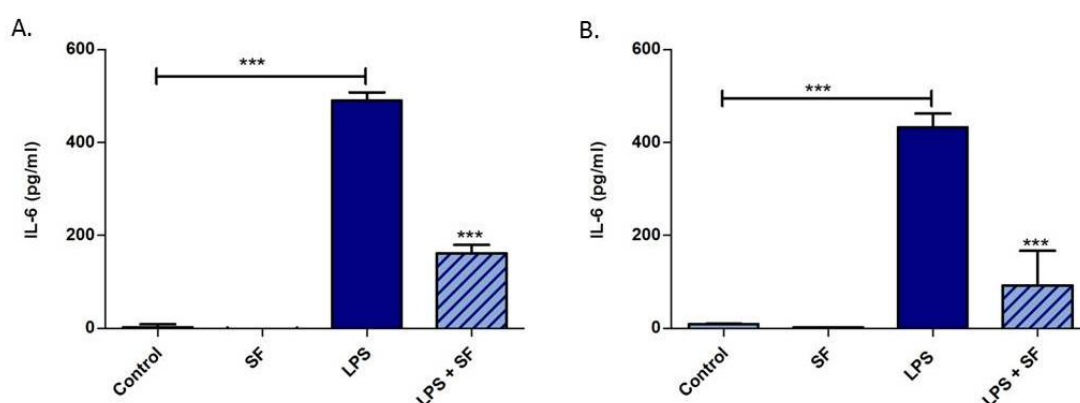


**Figure 3.3. SF suppresses LPS-induced IL-6 secretion in PBMCs with a 2 hour pre-treatment (A) and 20 hour pre-treatment (B).** PBMCs were treated with  $2\mu\text{M}$  SF (vehicle control for SF =  $< 0.1\%$  (v/v) DMSO) for 2 hours (A) or 20 hours (B) prior to treatment with  $1\text{ng/ml}$  LPS (vehicle control for LPS = PBS) for 4 hours. The cell culture supernatant was collected and IL-6 was measured by ELISA. Data shown = mean  $\pm$  SD. Data was statistically analysed using one-way ANOVA followed by Bonferroni multiple comparison tests. \*\*\* $p < 0.001$  against LPS or as annotated.

The suppression of LPS-induced IL-6 secretion by SF was explored further through measuring IL-6 secretion over 24 hours. Additional measurements of IL- $1\beta$  and TNF $\alpha$  secretion were also taken throughout a 24 hour period to determine the specificity of SF's effect. It was found that SF significantly reduced the level of LPS-induced secretion of all three cytokines throughout the 24 hours when PBMCs were pre-incubated with SF for 2 hours (**Figure 3.4**).

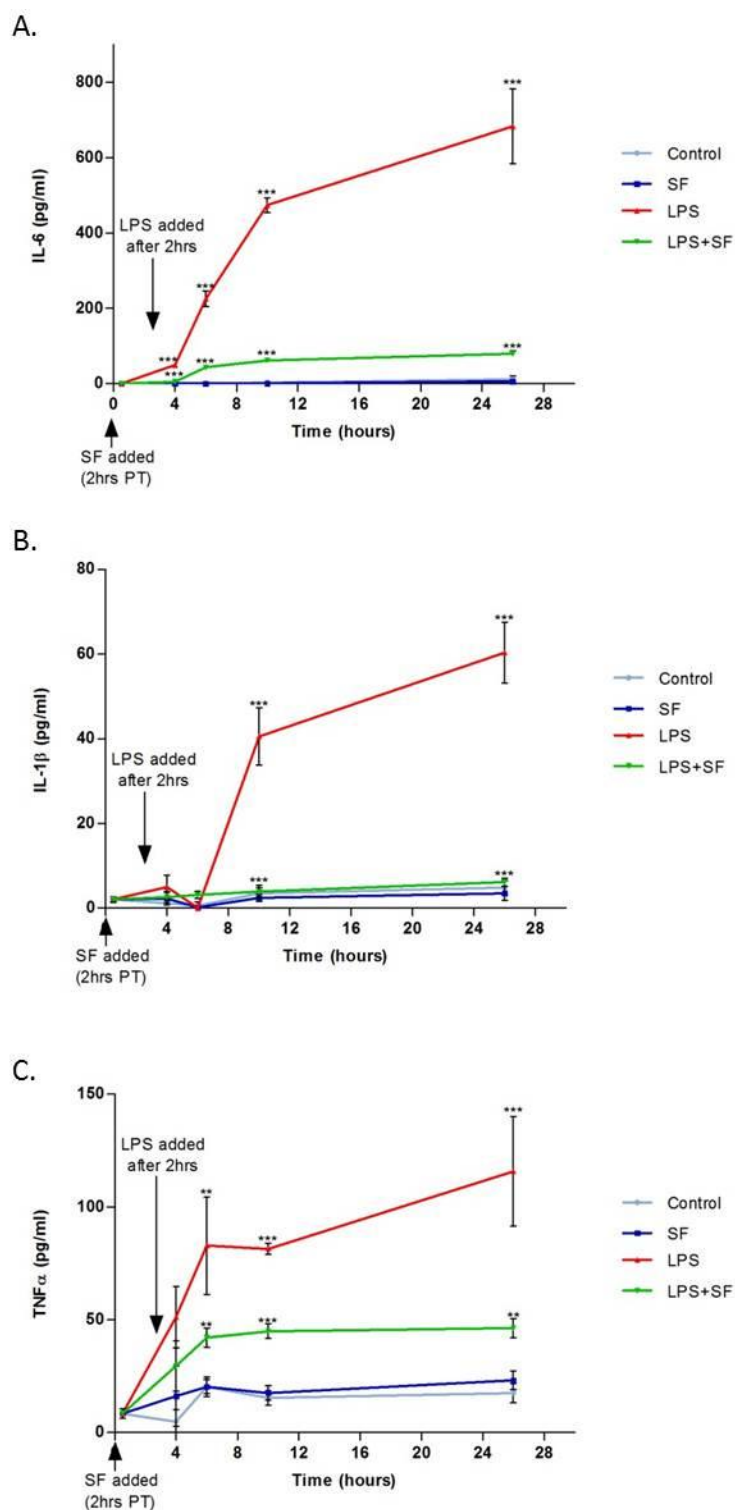


**Figure 3.4. SF significantly suppresses LPS-induced secretion of IL-6 (A), IL-1 $\beta$  (B) and TNF $\alpha$  (C) in PBMCs over time.** PBMCs were treated with 2 $\mu$ M SF (vehicle control for SF = < 0.1% (v/v) DMSO) at 0 hours. After 2 hours, 1 ng/ml of LPS (vehicle control for LPS = PBS) was added to the cells. The cell culture supernatant was collected after 4, 6, 10 and 26 hours and cytokines were measured by ELISA. Data shown = mean  $\pm$  SD. Data was statistically analysed using AUC followed by Student t tests for each time point comparing the cumulative AUC values. \*\*p<0.01 and \*\*\*p<0.001 LPS vs. untreated controls and LPS + SF vs. LPS only.

### 3.2.1.2 Effect of SF on PBMC cell viability

To ensure that the significant suppression observed with SF on LPS-induced cytokine secretion was not due to cytotoxic effects, a WST-1 viability assay (section 2.3) was carried out with a wide range of SF concentrations (0-200 $\mu$ M). SF was found to significantly reduce the viability of human PBMCs at concentrations of 10 $\mu$ M and above (**Figure 3.5**). The IC<sub>50</sub> was calculated at  $15.6 \pm 6.0\mu$ M. Importantly, no significant reduction was seen in cell viability as compared to the control with concentrations below 10 $\mu$ M. This confirms that 2 $\mu$ M SF used in the cytokine secretion experiments was not significantly reducing LPS-induced cytokine production as a result of cytotoxic effects.

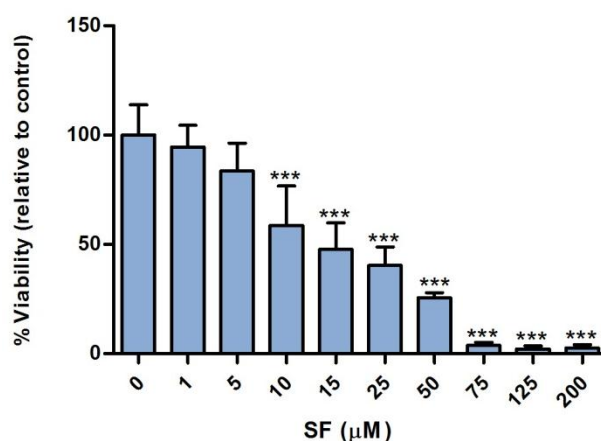


**Figure 3.5. Effect of SF on PBMC cell viability.** PBMCs were treated with SF (0-200 $\mu$ M) for 24 hours (vehicle control for SF = < 0.1% (v/v) DMSO). After treatment was complete, 10 $\mu$ l WST-1 reagent was added to each well. The plates were incubated at 37°C and measured using a spectrophotometer at 450nm every 15 minutes for 3 hours. Data shown is from the 2.5 hour measurement at which the levels of absorbance were all measurable and consistent. Data shown = mean  $\pm$  SD. Data was statistically analysed using one-way ANOVA followed by the Bonferroni multiple comparison test. \*\*\*p<0.001 vs. 0 $\mu$ M SF.

## 3.2.2 THP-1 monocytes

### 3.2.2.1 Effect of SF on LPS-induced cytokine secretion

The physiologically relevant concentration of 1ng/ml LPS was sufficient for inducing cytokine secretion in human PBMCs (**Figure 3.1**). Using a range of concentrations from 1-100ng/ml LPS, it was investigated whether human THP-1 monocytes, a cancerous cell line isolated from a sufferer of acute monocytic leukaemia [198], behaved in the same way. No induction in IL-6 secretion was observed following LPS treatment for 4 hours (data not shown) and subsequently LPS treatment for 24 hours was investigated with the THP-1 monocytes.

LPS at 1ng/ml was sufficient to significantly induce IL-6 secretion in THP-1 monocytes (**Figure 3.6**), replicating what was seen with PBMCs.

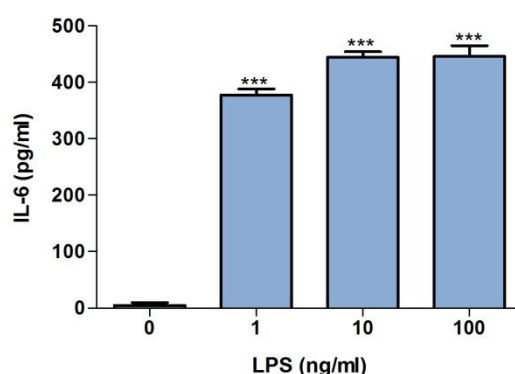


**Figure 3.6. Induction of IL-6 secretion with different LPS concentrations in THP-1 monocytes.** THP-1 monocytes were treated with LPS at different concentrations (1, 10 and 100ng/ml; vehicle control for LPS = PBS) for 24 hours. The cell culture supernatant was collected and IL-6 was measured by ELISA. Data shown = mean  $\pm$  SD. Data was statistically analysed using one-way ANOVA followed by Bonferroni multiple comparison tests. \*\*\* $p < 0.001$  vs. 0ng/ml.

LPS induction of IL-6 was further examined over a 24 hour period as was carried out with the PBMCs (**Figure 3.2**). IL-6 secretion was also found to be induced by LPS over time with the secretion beginning at 12 hours continuing linearly up to 24 hours (**Figure 3.7**).

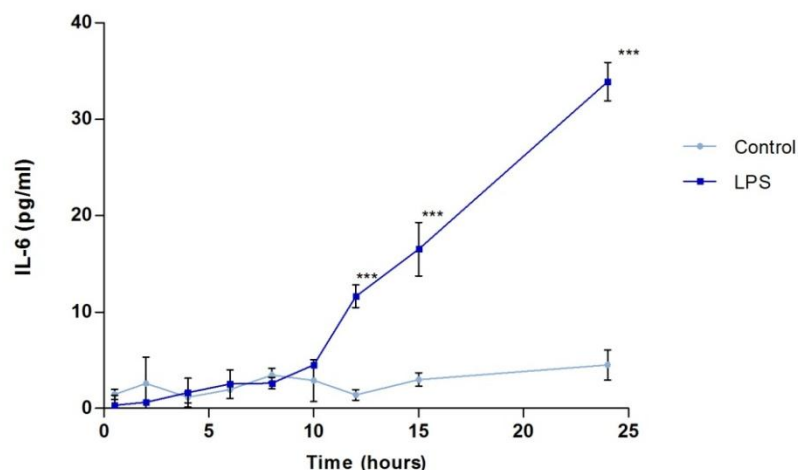


**Figure 3.7. LPS significantly induces IL-6 secretion in THP-1 monocytes over 24 hours.** THP-1 monocytes were treated with 1ng/ml LPS (vehicle control for LPS = PBS) with varying times of exposure (0.5-24 hours). The cell culture supernatant was collected and IL-6 was measured by ELISA. Data shown = mean  $\pm$  SD. AUC followed by Student t tests for each time point comparing the cumulative AUC values. \*\*\*p<0.001 vs. untreated controls at the same time point.

To investigate whether SF could suppress LPS-induced IL-6 secretion, THP-1 monocytes were treated with SF (2, 5 or 10 $\mu$ M) in combination with 1ng/ml LPS for 24 hours. Concentrations of 5 $\mu$ M and 10 $\mu$ M SF were able to significantly suppress the LPS induction of IL-6 secretion in THP-1 monocytes while 2 $\mu$ M, the concentration used with the PBMCs, shows a small but non-significant reduction (**Figure 3.8**).

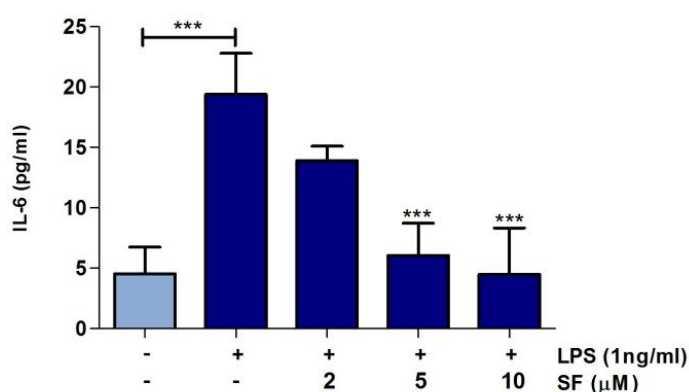


**Figure 3.8. SF suppresses LPS-induced IL-6 secretion in THP-1 monocytes.** THP-1 monocytes were treated with 1ng/ml LPS (vehicle control for LPS = PBS) for 24 hours in the presence or absence of SF (2, 5 and 10 $\mu$ M; vehicle control for SF = < 0.1% (v/v) DMSO). The cell culture supernatant was collected and IL-6 was measured by ELISA. Data shown = mean  $\pm$  SD. Data was statistically analysed using one-way ANOVA followed by Bonferroni multiple comparison tests. \*\*\*p<0.001 vs. LPS (1ng/ml) or as annotated.

The suppression of LPS-induced IL-6 secretion by SF was further investigated over time. 5 $\mu$ M SF completely suppressed LPS induction of IL-6 secretion for up to 72 hours with the levels of secretion remaining very close to those of the untreated controls (Figure 3.9). IL-6 was induced with LPS from 12 hours, which is consistent with what was previously shown (Figure 3.7).

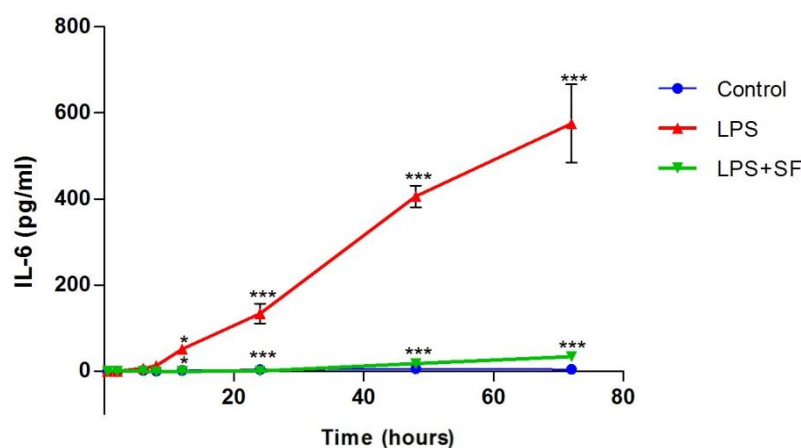


**Figure 3.9. SF significantly suppresses LPS-induced IL-6 secretion in THP-1 monocytes over time.** THP-1 monocytes were treated with 1ng/ml LPS (vehicle control for LPS = PBS) over a range of time points (0.5-72 hours) in the presence or absence of 5 $\mu$ M SF (vehicle control for SF = < 0.1% (v/v) DMSO). The cell culture supernatant was collected and IL-6 was measured by ELISA. Data shown = mean  $\pm$  SD. Data was statistically analysed using AUC followed by Student t tests for each time point comparing the cumulative AUC values. \*p<0.05 and \*\*\*p<0.001 LPS vs. untreated controls and LPS + SF vs. LPS only.

To ensure that the effect of SF was not limited to IL-6 alone, the effect of LPS and SF on the levels of IL-1 $\beta$  and TNF $\alpha$  secretion was also measured. THP-1 monocytes were co-treated with 1ng/ml LPS and 5 $\mu$ M SF for 12 hours before measuring the cytokine secretion. Both IL-1 $\beta$  and TNF $\alpha$  demonstrated a significant induction with 1ng/ml LPS, which was significantly suppressed in the presence of 5 $\mu$ M SF (Figure 3.10).

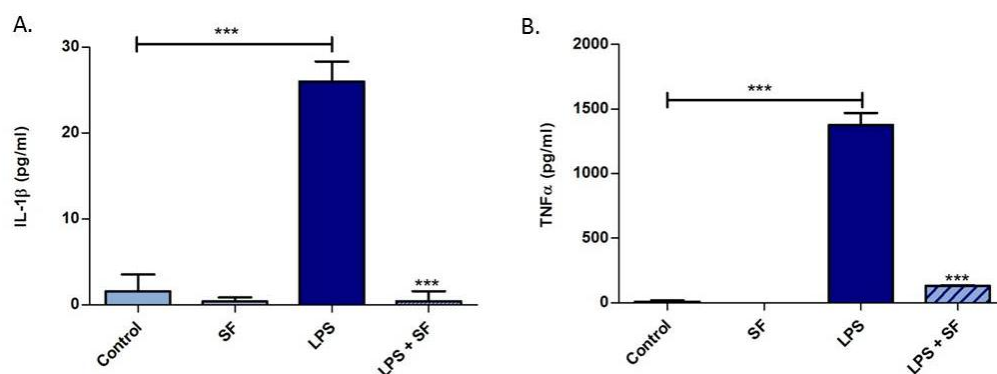


**Figure 3.10. SF significantly suppresses LPS-induced IL-1 $\beta$  (A) and TNF $\alpha$  (B) secretion in THP-1 monocytes.** THP-1 monocytes were treated with 1ng/ml LPS (vehicle control for LPS = PBS) in the presence or absence of 5 $\mu$ M SF (vehicle control for SF = < 0.1% (v/v) DMSO) for 12 hours. The cell culture supernatant was collected and IL-1 $\beta$  and TNF $\alpha$  was measured by ELISA. Data shown = mean  $\pm$  SD. Data was statistically analysed using one-way ANOVA followed by Bonferroni multiple comparison tests. \*\*\*p<0.001 vs. LPS or as annotated.

### 3.2.2.2. Effect of SF on THP-1 monocyte cell viability

Due to the significant reduction in LPS-induced IL-6, IL-1 $\beta$  and TNF $\alpha$  secretion in THP-1 monocytes, the effect of SF on THP-1 cell viability was investigated to ensure that this reduction was not simply due to a cytotoxic effect on the cells. THP-1 monocytes were treated with concentrations of SF from 0-200 $\mu$ M for 24 hours. Concentrations up to 15 $\mu$ M SF did not demonstrate any significant cytotoxic effects in THP-1 monocytes (**Figure 3.11**) with an IC<sub>50</sub> calculated at 36.4  $\pm$  5.9 $\mu$ M.

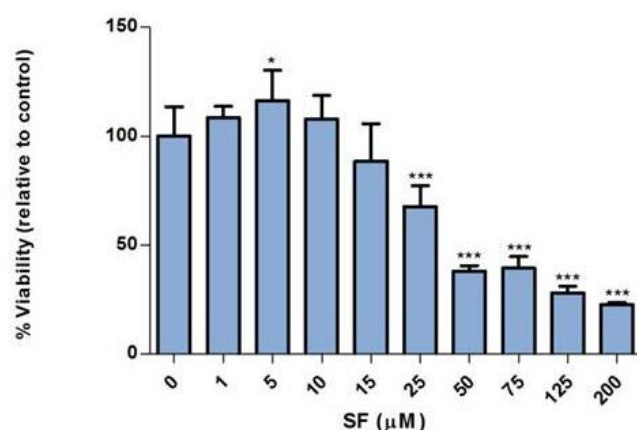


**Figure 3.11. Effect of SF on THP-1 monocyte cell viability.** THP-1 monocytes were treated with SF (0-200µM; vehicle control for SF = < 0.1% (v/v) DMSO) for 24 hours. After treatment was complete, 10µl WST-1 reagent was added to each well. The plates were incubated at 37°C and measured using a spectrophotometer at 450nm every 15 minutes for 3 hours. Data shown is from the 1 hour measurement at which the levels of absorbance were all measurable and consistent. Data shown = mean ± SD. Data was statistically analysed using one-way ANOVA followed by the Bonferroni multiple comparison test. \*p<0.05, \*\*\*p<0.001 vs. 0µM SF.

### 3.2.2.3. Effect of SF on LPS-induced cytokine expression

In order to evaluate which stage of cytokine production SF was targeting, cytokine expression was measured to see whether the induction by LPS and inhibition by SF was occurring at a transcriptional level in the THP-1 monocytes. Initially, a time course experiment was carried out with 1ng/ml LPS treatment measuring IL-6 expression. After 2 hours of LPS exposure, there was significant induction of IL-6 expression, with the peak level occurring after 12 and 24 hours (**Figure 3.12**).

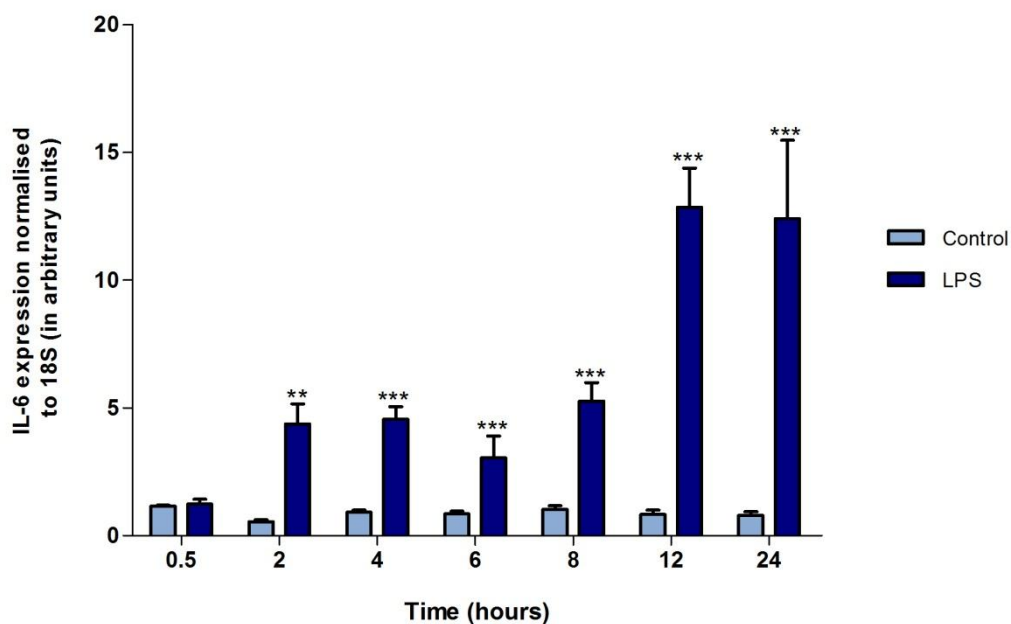


**Figure 3.12. LPS significantly induces IL-6 expression in THP-1 monocytes over time.** THP-1 monocytes were treated with 1ng/ml LPS for varying amounts of time (0.5-24 hours; vehicle control for LPS = PBS). The RNA was extracted, quantified and analysed by real-time RT-PCR. Data shown = mean  $\pm$  SD. Data was statistically analysed using AUC followed by Student t tests for each time point comparing the cumulative AUC values. LPS-treated conditions are compared to their own untreated control at each time point. \*\*p<0.01, \*\*\*p<0.001 vs. untreated controls.

Following these results, a co-treatment of 1ng/ml LPS and 5 $\mu$ M SF was carried out in order to monitor IL-6 expression over a 72 hour time period. It was demonstrated that at this physiologically relevant concentration of SF, a significant inhibition of IL-6 expression induced by LPS across all the time points measured was observed, with the levels of IL-6 expression being comparable to that found in the untreated controls (Figure 3.13).

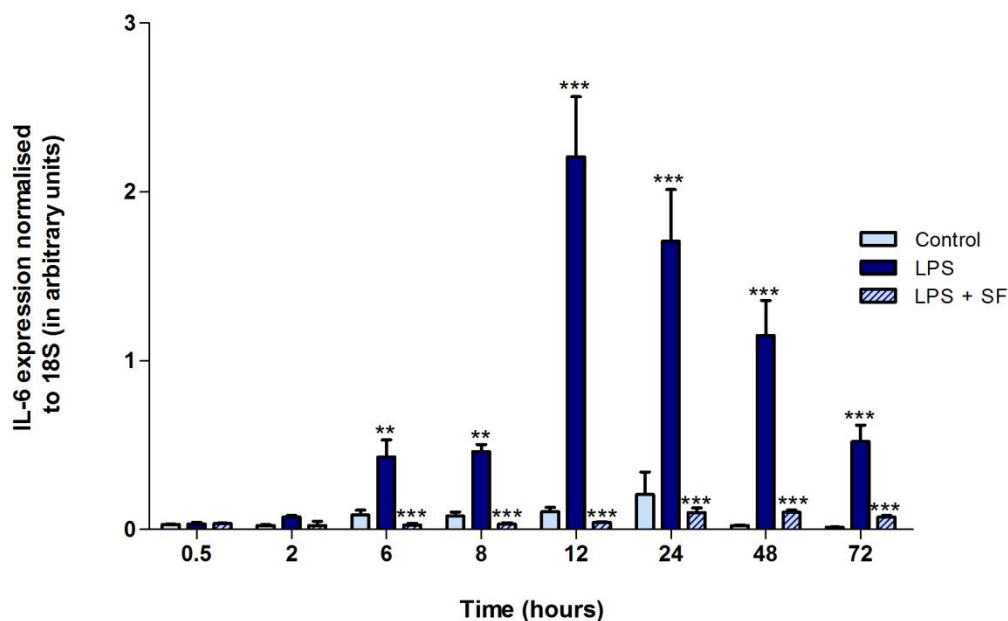


**Figure 3.13. SF significantly suppresses LPS-induced IL-6 expression in THP-1 monocytes over time.** THP-1 monocytes were treated with 1ng/ml LPS for varying amounts of time (0.5-72 hours; vehicle control for LPS = PBS) in the presence or absence of 5 $\mu$ M SF (vehicle control for SF = < 0.1% (v/v) DMSO). The RNA was extracted, quantified and IL-6 expression was analysed by real-time RT-PCR. Data shown = mean  $\pm$  SD. Data was statistically analysed using two-way ANOVA followed by Bonferroni multiple comparisons tests. \*\*\* $p$ <0.001 LPS vs. untreated controls and LPS + SF vs. LPS only.

To confirm SF can suppress the LPS-induced expression of both IL-1 $\beta$  and TNF $\alpha$ , real-time RT-PCR was carried out with the RNA from THP-1 monocytes treated for 12 hours with 1ng/ml LPS and 5 $\mu$ M SF. IL-1 $\beta$  and TNF $\alpha$  expression were both induced by LPS treatment (**Figure 3.14**). However, while IL-1 $\beta$  expression followed the same trend as IL-6 with 5 $\mu$ M SF treatment resulting in a significant suppression of LPS induction (**Figure 3.14A**), the suppression of LPS-induced TNF $\alpha$  expression by SF approached, but did not reach statistical significance (**Figure 3.14B**).

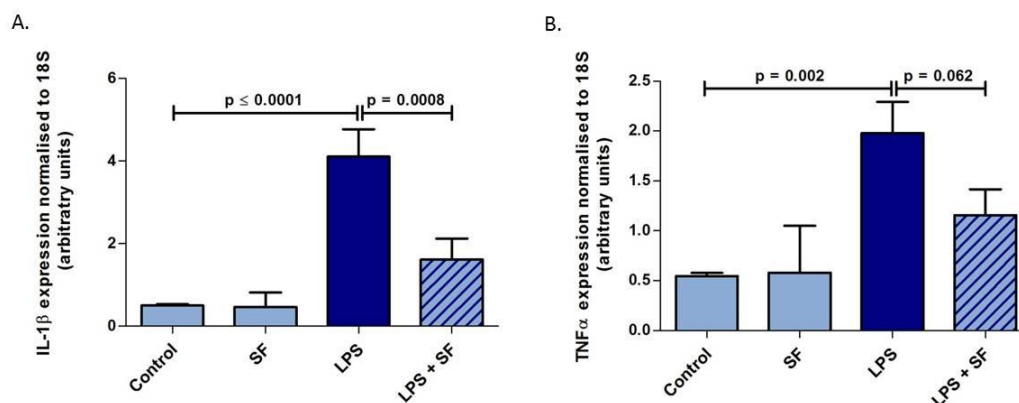


**Figure 3.14. SF significantly suppresses LPS-induced IL-1 $\beta$  expression (A) and shows a trend for suppression of TNF $\alpha$  expression (B) in THP-1 monocytes.** THP-1 monocytes were treated with 1ng/ml LPS (vehicle control for LPS = PBS) in the presence or absence of 5 $\mu$ M SF (vehicle control for SF = < 0.1% (v/v) DMSO) for 12 hours. The RNA was extracted, quantified and IL-1 $\beta$  and TNF $\alpha$  expression was analysed by real-time RT-PCR. Data shown = mean  $\pm$  SD. Data was statistically analysed using one-way ANOVA followed by Tukey multiple comparisons tests.

### 3.3. Discussion

Taking into account the elevated levels of endotoxin and pro-inflammatory cytokines in sufferers of chronic disease, this study aimed to establish a relevant cell model of chronic inflammation. LPS has been widely used *in vitro* as an artificial stimulant of inflammation. However, it is typically used at concentrations in the high ng/ml to low  $\mu$ g/ml range, a level that is higher than that found during acute inflammation such as sepsis [197]. The initial requirement of the model was to establish whether levels of LPS in the range of that observed in circulation of patients with chronic inflammatory diseases was sufficient to induce pro-inflammatory cytokine secretion.

Low-level endotoxin ( $\leq$  1ng/ml) has been shown to significantly induce levels of a number of pro-inflammatory mediators including the chemokines interleukin-8 (IL-8) and monocyte chemoattractant protein-1 (MCP-1), as well as the cell adhesion molecules VCAM-1 and ICAM-1 [197, 225-227]. Based on this data, it was investigated whether a physiologically relevant concentration of 1ng/ml LPS was sufficient to significantly induce the production of pro-inflammatory cytokines. The initial experiments were carried out investigating the effect of 1ng/ml LPS on IL-6 secretion, as this is the cytokine with the most consistent data supporting its involvement in chronic disease. *In vivo*, levels of IL-6 are commonly elevated in patients suffering from chronic diseases,

with the majority of studies find levels of IL-6 to be around 1-15pg/ml in both cases and controls [26, 27, 29, 34, 35, 39-41, 43].

PBMCs are an *ex vivo* model, making them a more suitable representation of what occurs *in vivo* as compared to established cell lines, and are a good candidate to use in a model of chronic inflammation. However, they do have their limitations. *In vivo*, monocytes would be subjected to hypoxic conditions and without the influence of the blood circulation, there will be a number of growth factors and signalling molecules the cells are not exposed to when in culture [228]. While cell lines are not directly from a patient and are therefore not as good a representation of what happens *in vivo*, they have distinct advantages for use. This includes their ability to be sub-cultured over a period of time in order for the same batch of cells to be used for a number of experiments, resulting in lower variation as compared to the use of primary cells from a number of individuals. Also, the use of cell lines does not require ethical approval, unlike primary cells.

The cell line chosen for comparison to primary PBMCs was the THP-1 monocytic cell line. THP-1 cells were derived from a one year old boy suffering from acute monocytic leukaemia in 1980, and following characterisation were confirmed as a leukaemic cell line with distinct monocytic markers [198]. THP-1 cells have often been used as a model of monocytes, and while there are evident differences, Qin and colleagues discuss how THP-1 cells behave in a similar way to monocytes from patients suffering from chronic disease [229]. One difference that was evident was the exposure time to LPS; while the PBMCs respond after around 4 hours of treatment THP-1 monocytes require at least 12 hours. This is possibly due to the fact that the PBMCs used were from a healthy individual, while the THP-1 monocytes are a cancerous cell line and may be more resistant to IL-6 induction by LPS. Differences in IL-6 secretion in response to LPS treatment in PBMCs and THP-1 monocytes was found previously by Schildberger and colleagues [230]. Nevertheless, from the data presented in this chapter, there is validation for the use of THP-1 monocytes as well as PBMCs to investigate chronic inflammation.

Once the response to LPS was confirmed, the next step was to investigate whether SF was able to exert an anti-inflammatory effect to reduce the level of LPS induction of cytokine production. SF has been previously shown to have the ability to significantly reduce the levels of pro-inflammatory cytokine production in a number of different cell

and animal models using varying concentrations [181-187, 190-192, 195, 223, 224]. This research led to the hypothesis that SF would reduce LPS-induced cytokine expression and secretion in THP-1 monocytes and PBMCs. Based on the study by Gasper and colleagues who demonstrate that the peak plasma concentration of SF was reached 2 hours following ingestion of broccoli [129], a 2 hour pre-treatment of PBMCs with SF was investigated and proved to significantly suppress LPS induction of IL-6 (**Figure 3.3A**), leading to a more physiologically relevant model. For the THP-1 monocytes, a co-treatment design was used with 1ng/ml LPS and 5 $\mu$ M SF, and LPS-induced IL-6, IL-1 $\beta$  and TNF $\alpha$  expression and secretion was suppressed. The reason for the increase in the SF concentration used as compared to the PBMCs was due to a lack of a statistically significant suppression with 2 $\mu$ M SF in THP-1 monocytes. For all subsequent experiments with the THP-1 cells (including in Chapter 4 and 8), 5 $\mu$ M SF was used.

It is important to note that in the experiments with LPS and the PBMCs there was evident variation in the absolute level of IL-6 secretion that was induced in response to LPS at the same concentration (1ng/ml) and for the same time of exposure. As these experiments were carried out with PBMCs from different donors, it is likely that these variable levels are as a result of individual differences in the donor. Also with the THP-1 monocytes the induction in response to 1ng/ml LPS was highly variable from observing an increase to 350pg/ml in **Figure 3.6** as compared to an increase to only 20pg/ml in **Figure 3.8** in response to the same concentration of LPS for the same length of time. As the THP-1 monocytes are a cell line, these results are not as result of individual differences and instead it is likely as a result of varying passage number. Following these results, it was ensured that experiments were carried out over a narrow passage number range to limit the level of variation.

While there was no significant suppression in cell viability for the chosen concentrations of SF used with the PBMCs (2 $\mu$ M) and the THP-1 monocytes (5 $\mu$ M), the IC<sub>50</sub>s from each cell type are significantly different ( $p < 0.001$ ; data not shown) and this could be due to several reasons. Being a primary cell type, the PBMCs are likely to be more sensitive to the SF treatment not only because they come from a healthy volunteer which will have no inherent inflammatory status, but also because they have a limited life span in culture before becoming senescent, due to a lack of growth factors and extracellular matrix components. The THP-1 monocytes on the other hand are an immortalised cell line, isolated from a sufferer of acute monocytic leukaemia and therefore as a cancerous

cell line may be able to withstand higher concentrations of the inflammatory stimulus LPS, and SF compared to human PBMCs.

Of the previous research investigating the effect of SF on LPS-induced cytokine production, a number of publications support the findings reported here. In murine macrophages, 5 $\mu$ M SF was found to significantly reduce LPS-induced IL-1 $\beta$  and TNF $\alpha$  secretion [185, 192] and in rat glial cells, 5 $\mu$ M SF was sufficient to suppress LPS-induced IL-1 $\beta$  and IL-6 secretion, while 15 $\mu$ M SF was required for TNF $\alpha$  secretion [187]. In all of these publications, LPS was used at a concentration of 0.1-1 $\mu$ g/ml, concentrations considerably higher than levels of endotoxin observed in chronic disease.

Research by Guo and colleagues using murine RAW 264.7 macrophage cells demonstrated that treatment with very low concentrations of SF (0.3 and 0.6 $\mu$ M) were able to suppress the capability of 1 $\mu$ g/ml LPS to induce both IL-1 $\beta$  expression and secretion, in addition to TNF $\alpha$  secretion [182]. In contrast, a publication by Cheung and colleagues found no significant reduction in LPS-induced IL-1 and TNF $\alpha$  secretion by 1 $\mu$ M SF when using 1 $\mu$ g/ml LPS [223]. This highlights that even with the use of the same experimental design with identical cell models, differing results can be observed.

In research published by Brandenburg and colleagues, a concentration of 1 $\mu$ M SF was able to significantly reduce the expression of IL-6, IL-1 $\beta$  and TNF $\alpha$  when induced with 100ng/ml LPS in primary mice microglia [184]. While the concentration of SF was lower than the 5 $\mu$ M used in the present study, the research was carried out in primary microglia isolated from rat and therefore species differences in addition to the fact that the cell model may have functional differences to the monocytes used in this chapter, may account for the differences observed in the SF response. This was supported by the fact that a different expression pattern was observed, with SF suppressing the LPS-induced cytokine expression at 6 hours followed by a much lower level of suppression at 12 hours before reverting back to almost complete suppression after 24 hours of exposure to LPS and SF [184]. Furthermore, it may be more appropriate in this experimental design with microglial cells to use a lower concentration of SF, because the level of SF that would be biologically available in the brain is not well established.

The publication most relevant to the research presented in this chapter is by Yehuda and colleagues who used THP-1 monocytes treated with 500ng/ml LPS and concentrations of SF of 1.13 $\mu$ M and 2.26 $\mu$ M, before measuring the expression of IL-1 $\beta$  and TNF $\alpha$ .

There were significant reductions in the LPS-induced expression of IL-1 $\beta$  with both concentrations of SF, and TNF $\alpha$  expression was suppressed by the higher concentration [181]. While the study by Yehuda used the same cell model as was used in this chapter, they use a different experimental design, using a concentration of LPS at 500ng/ml, rather than 1ng/ml used in this work, which is more representative of an acute inflammatory attack. Additionally, they measured the expression and secretion of the cytokines in response to LPS in differentiated THP-1 cells, which develop macrophage-like behaviours. They found that a concentration of 4.5 $\mu$ M was required to significantly reduce the levels of IL-6, IL-1 $\beta$  and TNF $\alpha$  expression, which supports my work with the monocytes and also lends some support to data shown in Chapter 8 (section 8.2.1) [181].

SF has also been shown to exert effects *in vivo* with the use of animal models. SF was able to significantly reduce the LPS-induced expression of TNF $\alpha$  and IL-6 in the hippocampus of mice [224] and the circulating levels of these cytokines in the serum of mice [195]. Most recently an epidemiological study was published demonstrating that consumption of diets rich in cruciferous vegetables was inversely correlated with a decreased level of circulating pro-inflammatory biomarkers [120]. This study provides evidence that the *in vitro* findings presented in this chapter are plausible for translation into humans.

All of the previously published data that has been mentioned has focused more on a cell model of acute inflammation based on excessive concentrations of LPS used however, most find significant anti-inflammatory effects with SF. The data from this chapter furthers these previous findings by demonstrating that SF, at concentrations that can be achieved via broccoli consumption, is able to significantly suppress LPS-induced expression and secretion of fundamental biomarkers in a model more comparable to chronic inflammation.

### **3.4. Conclusions**

It is apparent from the experiments performed that 1ng/ml LPS, a level relevant to that found in circulation of patients suffering from a prolonged low-grade state of inflammation, is sufficient to induce the expression and secretion of the pro-inflammatory cytokines, IL-6, IL-1 $\beta$  and TNF $\alpha$  in human monocyte cells. When the cells were treated with physiologically achievable concentrations of SF (2 $\mu$ M for

PBMCs and 5 $\mu$ M for THP-1 monocytes) there was a highly significant suppression of the LPS-induced cytokine production, without any effect on cell viability.

These data may help to explain the significant correlations found between consumption of a diet rich in cruciferous vegetables and an improved risk of cancer and CVD mortality via targeting a common factor in both of these chronic diseases. This study provides novel experimental evidence that SF at concentrations achievable by consumption of only 100-200g of standard broccoli or less than 100g of high-glucosinolate broccoli could mitigate chronic inflammation by targeting the response of monocytes to the elevated levels of circulating LPS found in sufferers of chronic diseases.

This chapter only focuses on a trio of important pro-inflammatory cytokines and so to further this research the next chapter will employ whole genome analysis of the THP-1 monocytes to investigate whether the effect of SF is restricted to a small selection of genes or if it is able to target the LPS signalling pathway on a global scale.

# Chapter Four

---

Effect of SF on global gene expression of  
THP-1 monocytes exposed to LPS

## **4.0. Introduction**

In the previous chapter, the hypothesis that 5 $\mu$ M SF would be able to significantly suppress LPS-induced expression and secretion in THP-1 monocytes was tested in a targeted approach with a selection of three specific cytokines, IL-6, IL-1 $\beta$  and TNF $\alpha$ . In this chapter, this work was expanded with the use of a non-targeted approach using Affymetrix GeneChip® Human Exon 1.0ST arrays to investigate the effect of 5 $\mu$ M SF on global gene expression in THP-1 monocytes treated with or without 1ng/ml LPS. Advantages for using this non-targeted approach are the removal of bias on the selection of biomarkers studied and also the vast amount of information that can be obtained from whole genome analysis. For example, the effect of SF can be investigated on all genes that are differentially expressed in response to LPS exposure in THP-1 monocytes to gain information on whether SF is able to target the TLR4 pathway as a whole. In addition, the genes differentially expressed in response to SF alone can be analysed.

As previously discussed, LPS is the specific agonist for the TLR4 molecule. It behaves to activate the receptor with the aid of a number of accessory proteins. LBP carries the LPS molecule to the GPI-anchored, N-glycosylated CD14 receptor which in turn, transfers LPS to the TLR4-MD2 complex [13]. MD2 is a membrane-associated receptor that has high binding affinity for TLR4, and is able to accentuate the ability of LPS to bind to TLR4 [13]. LPS binding to the TLR4-MD2 complex induces receptor dimerisation, which in turn initiates the downstream signalling cascade [13]. The TLR4 signalling pathway is summarised in **Figure 4.1**. Upon stimulation of the TLR4-MD2 receptor complex, either MyD88-dependent or MyD88-independent pathways can be stimulated. Activation of the MyD88-dependent pathway results in rapid activation of the transcription factor NF- $\kappa$ B, which subsequently induces the expression of pro-inflammatory cytokines including IL-6, IL-1 $\beta$ , TNF $\alpha$  and chemokines such as IL-8. Activation of MyD88-independent pathway results in the swift activation of IRF3, followed later by activation of NF- $\kappa$ B, leading to the release of type 1 IFNs e.g. IFN $\beta$ . IFN $\beta$  activates STAT1 leading to the production of chemokines such IP-10 and many other IFN-induced genes [14].

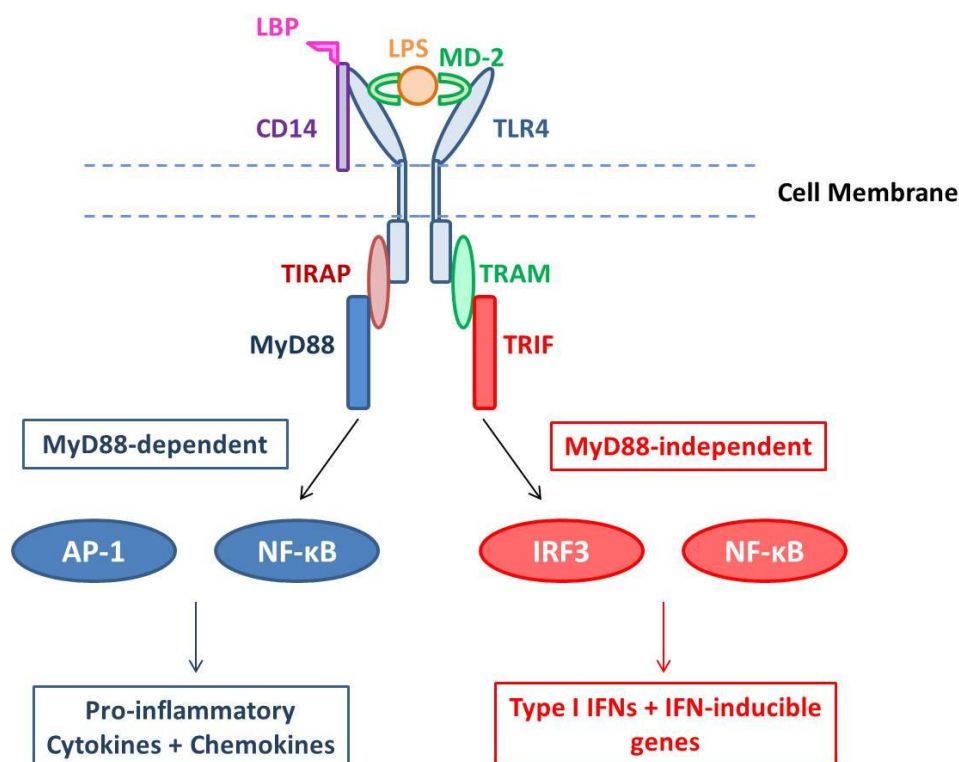


**Figure 4.1. Overview of the TLR4 signalling pathway.** LPS is bound to the TLR4-MD2 complex via the aid of LBP and CD14 accessory proteins. The binding of LPS to the TLR4-MD2 complex results in homodimerisation and activation of an intracellular signalling cascade. This can be MyD88-dependent or independent. The MyD88-dependent pathway activates NF-κB and AP-1 resulting in pro-inflammatory cytokine and chemokine expression, while the MyD88-independent pathway results in activation of predominantly IRF3 followed later by NF-κB, leading to the expression of type I IFNs and IFN-inducible genes [13, 14].

It was hypothesised that THP-1 monocytes will have a number of differentially expressed genes in response to 5µM SF alone. SF has been studied previously *in vitro* at a range of concentrations in a number of different cell models and global gene expression patterns have commonly highlighted an induction in genes encoding phase 2 enzymes and enzymes involved in xenobiotic metabolism [145, 147, 160, 231, 232]. The induction of these genes by SF is controlled by AREs found to be present in their gene promoter region. These AREs are recognised by Nrf2, which is sequestered within the cytoplasm by Keap1 in unstimulated conditions by directly binding to the Nrf2 transcription factor and targeting it for proteasomal degradation [154]. When cells are exposed to SF, Nrf2 is able to dissociate from Keap1 allowing it to translocate into the nucleus where it is able to recognise and bind to AREs to activate the expression of its target genes.

SF behaves as an electrophile and is able to bind to free cysteine thiol groups within a number of proteins to form a thioacyl adduct. Keap1 has 27 cysteines within its structure that are readily available to react with electrophiles. SF is able to form thioacyl adducts with cysteine residues within the Keap1 protein [156-158] and it is predicted that these modifications are responsible for the mechanism by which Keap1 is no longer able to target Nrf2 for proteasomal degradation. This results in Nrf2 accumulation within the nucleus and subsequent induction of the transcription of its target genes. However, this has yet to be shown in cells due to the thioacyl adduct formation being reversible and sensitive to hydrolysis and alkylation [157-159]. By investigating the constitutive effect of 5 $\mu$ M SF on THP-1 monocytes, it will provide an indication as to whether SF is behaving with these cells in agreement with previous literature i.e. a number of the phase 2 enzymes and those involved in xenobiotic metabolism would be expected to demonstrate up-regulated expression levels [145, 147, 160, 231, 232].

The main aim of this chapter was to investigate whether 5 $\mu$ M SF is able to affect all genes differentially expressed in response to 1ng/ml LPS using Affymetrix GeneChip® Human Exon 1.0ST arrays to expand the previous studies of investigating the effect on selected biomarkers.

## **4.1. Materials and Methods**

Within this chapter, the THP-1 monocytes have been treated for 12 hours with SF (5 $\mu$ M) and LPS (1ng/ml) both alone and as a co-treatment to determine the effects on global gene expression. RNA was extracted from treated THP-1 monocytes and subjected to whole genome expression analysis using the Affymetrix GeneChip® Human Exon 1.0ST microarrays (section 2.6).

## **4.2. Results**

### **4.2.1. Effect of SF on THP-1 monocytes**

To establish the effect of SF on global gene expression in the absence of any inflammatory stimulus, the THP-1 monocytes were treated with 5 $\mu$ M SF for 12 hours before RNA was extracted and subjected to an Affymetrix GeneChip® Human Exon 1.0ST array. An initial pairwise comparison was carried out between 5 $\mu$ M SF and untreated controls to determine the numbers of genes changed at different adjusted p

values (**Table 4.1**).

**Table 4.1. Number of genes differentially expressed in response to SF**

	Fold change in Gene Expression			Total Gene Number
	<1.5	1.5-2.0	2.0-4.0	
<u>CTRL v SF*</u>				
< 0.05	<b>699</b> (335,364)	<b>95</b> (46,49)	<b>38</b> (27,11)	<b>832</b>
< 0.01	<b>284</b> (152,132)	<b>85</b> (46,39)	<b>38</b> (27,11)	<b>407</b>
< 0.001	<b>76</b> (43,33)	<b>59</b> (38,21)	<b>34</b> (27,7)	<b>169</b>

The number in bold gives the total number of transcripts changed. In brackets, the number of up-regulated transcripts is followed by the number of down-regulated transcripts.

\* P values are adjusted for false discovery rates using the Benjamini-Hochberg correction

A total of 407 genes were differentially expressed in response to 5µM SF compared to untreated controls (adjusted  $p < 0.01$ ). Of these 407 genes, 284 had less than a 1.5-fold change with a relatively even number of genes being increased (152 genes) and decreased in expression (132 genes). Only 38 of the 407 genes that were differentially expressed in response to 5µM SF (adjusted  $p < 0.01$ ) demonstrated more than a 2-fold change in expression with 27 genes being up-regulated by SF and 11 genes being down-regulated (**Table 4.1**).

The next question addressed was whether there were common functions to the genes that were altered in THP-1 monocytes in response to 5µM SF. Based on a large body of previous research, it was expected that a number of phase 2 enzymes and xenobiotic metabolism genes would be differentially expressed [145, 147, 160, 231, 232]. However, very few groups have investigated a concentration of SF as low as the physiologically relevant 5µM used in this study. To carry out analysis of the genes differentially regulated by SF in terms of the pathways affected, DAVID software was used (**Table 4.2**) [202, 203]. Glutathione metabolism had the highest fold enrichment level of 4, signifying that four times the amount of genes expected by chance were identified. Inflammatory signalling and cancer pathways were also highlighted, in addition to carbohydrate metabolism. However, while each of these pathways demonstrated significant p values, when adjusted using the Benjamini and Hochberg algorithm used to account for the rate of false discoveries, the only pathway that remained significant was cytokine-cytokine receptor interactions (**Table 4.2**).

**Table 4.2. Pathway analysis of genes differentially expressed in response to SF**

Term	Count	%	P Value	Fold Enrichment	Benjamini p value*
Cytokine-cytokine receptor interaction	21	5.30	9.7 x 10 <sup>-5</sup>	2.638	0.0136
Chemokine signalling pathway	14	3.54	0.0039	2.466	0.2414
p53 signalling pathway	7	1.77	0.0194	3.246	0.3265
Toll-like receptor signalling pathway	9	2.27	0.0115	2.896	0.3358
Glutathione metabolism	6	1.52	0.0154	4.025	0.3536
Glycolysis / Gluconeogenesis	6	1.52	0.0372	3.207	0.3846
Pathways in cancer	16	4.04	0.0772	1.577	0.5301

The list of genes used for analysis was SF v CTRL p<0.01.

\*While the initial p values are significant for these pathways, only the cytokine-cytokine receptor interaction pathway remained significant after correction with Benjamini-Hochberg.

Out of the 407 genes found to be differentially expressed with 5µM SF at p < 0.01, only 79 were significantly classified into common pathways. For this reason, the data was interrogated further to identify related groups of genes. **Table 4.3** presents the genes encoding phase 2, phase 3 and xenobiotic metabolising enzymes differentially expressed in response to 5µM SF. Moreover, a number of genes involved in carbohydrate metabolism were identified (**Table 4.4**).

**Table 4.3. Genes differentially expressed in response to SF involved in detoxification pathways**

Affymetrix Transcript Cluster ID	Gene Symbol	Gene	SF Fold Change vs. Control*
<u>Xenobiotic metabolising enzymes</u>			
3232979	<i>AKRIC1</i>	Aldo-keto reductase family 1, member C1	2.68 <sup>3</sup>
3274758	<i>AKRIC2</i>	Aldo-keto reductase family 1, member C2	2.27 <sup>3</sup>
3692701	<i>CES1</i>	Carboxylesterase 1	1.76 <sup>3</sup>
2382970	<i>EPHX1</i>	Epoxide hydrolase 1, microsomal (xenobiotic)	1.72 <sup>3</sup>
3233049	<i>AKRIC3</i>	Aldo-keto reductase family 1, member C3	1.53 <sup>2</sup>
<u>Phase 2 enzymes</u>			
3894322	<i>SRXN1</i>	Sulfiredoxin 1	3.15 <sup>3</sup>
3130161	<i>GSR</i>	Glutathione reductase	2.58 <sup>3</sup>
3696666	<i>NQO1</i>	NAD(P)H dehydrogenase, quinone 1	2.57 <sup>3</sup>
2423625	<i>GCLM</i>	Glutamate-cysteine ligase, modifier subunit	2.48 <sup>3</sup>
3429460	<i>TXNRD1</i>	Thioredoxin reductase 1	2.42 <sup>3</sup>
3944129	<i>HMOX1</i>	Hemeoxygenase (decycling) 1	2.08 <sup>3</sup>
3406589	<i>MGST1</i>	Microsomal glutathione S-transferase 1	1.35 <sup>1</sup>
2892277	<i>NQO2</i>	NAD(P)H dehydrogenase, quinone 2	1.31 <sup>1</sup>
3220156	<i>TXN</i>	Thioredoxin	1.29 <sup>1</sup>
3917851	<i>SOD1</i>	Superoxide Dismutase 1, soluble	1.28 <sup>1</sup>
<u>Phase 3 enzymes</u>			
3649890	<i>ABCC1</i>	ATP-binding cassette, sub-family C (CFTR/MRP), member 1	2.03 <sup>3</sup>
3726691	<i>ABCC3</i>	ATP-binding cassette, sub-family C (CFTR/MRP), member 3	1.86 <sup>3</sup>

Adjusted p values of fold change: <sup>1</sup> p<0.01; <sup>2</sup> p<0.001; <sup>3</sup> p<0.0001

\* Data taken from the list SF v CTRL p<0.01

**Table 4.4. Genes differentially expressed in response to SF involved in carbohydrate cell metabolism**

Affymetrix Transcript Cluster ID	Gene Symbol	Gene	SF Fold Change vs. Control*
2962820	<i>ME1</i>	Malic enzyme 1, NADP(+)-dependent, cytosolic	2.11 <sup>3</sup>
4027416	<i>G6PD</i>	Glucose-6-phosphate dehydrogenase	1.81 <sup>3</sup>
2319802	<i>PGD</i>	Phosphogluconate Dehydrogenase	1.80 <sup>3</sup>
3316208	<i>TALDO1</i>	Transaldolase 1	1.48 <sup>3</sup>
2676671	<i>TKT</i>	Transketolase	1.46 <sup>2</sup>
3233605	<i>PFKFB3</i>	6-Phosphofructo-2-kinase/Fructose-2,6-biphosphatase 3	1.27 <sup>1</sup>
3631964	<i>PKM2</i>	Pyruvate kinase, muscle	1.18 <sup>1</sup>
3215570	<i>FBP1</i>	Fructose-1,6-bisphosphatase 1	-1.32 <sup>1</sup>

Adjusted p values of fold change: <sup>1</sup>p<0.01; <sup>2</sup>p<0.001; <sup>3</sup>p<0.0001

\* Data taken from the list SF v CTRL p<0.01

All of the genes highlighted as being involved in carbohydrate metabolism encoded enzymes involved in important steps of glycolysis and the pentose phosphate pathway (**Figure 4.2**). Several genes did not reach a 1.5-fold change in expression in response to SF, nevertheless they remained statistically significant, and due to the fact that these 8 genes were linked by function they were still included in **Figure 4.2**.

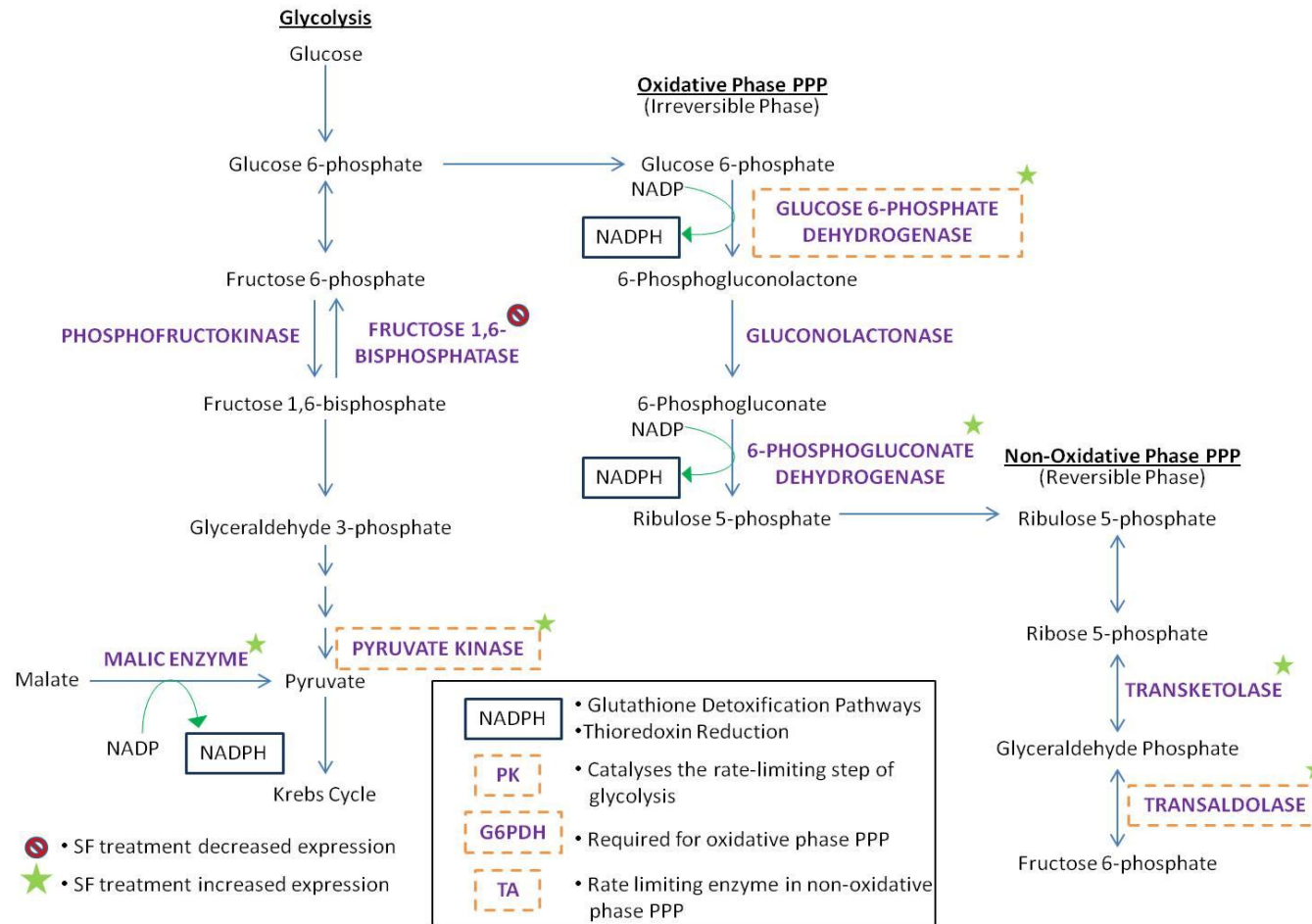


**Figure 4.2. Effect of SF on expression of genes encoding enzymes involved in glycolysis and the pentose phosphate pathway.** Glycolysis is a fundamental process in aerobic respiration which is responsible for producing the necessary intermediate, pyruvate, for the TCA cycle in order to produce ATP. The pentose phosphate pathway behaves to produce the universal electron donor NADPH and ribose phosphates required for nucleic acid formation. These two pathways are linked by the glucose 6-phosphate intermediate which is utilised by each pathway depending on the requirements of the cells. SF increased the expression of enzymes involved in the forward reactions, and decreased one of the enzymes involved in the reverse reactions.

As previously mentioned, THP-1 cells are a cancerous, leukaemic cell line. This means they are a suitable model for human monocytes in a chronic inflammatory state, but also can be considered as a cancer cell model. Of the 407 genes altered by SF in the THP-1 monocytes (adjusted  $p < 0.01$ ), a number of genes were found to be specifically associated with pathways involved in cancer and demonstrated more than 1.5-fold increase or decrease in expression (**Table 4.5**).

**Table 4.5. Genes differentially expressed in response to SF involved in pathways in cancer**

Affymetrix Transcript Cluster ID	Gene Symbol	Gene	SF Fold Change vs. Control*
3464747	<i>KITLG</i>	KIT ligand	1.92 <sup>2</sup>
3790704	<i>PMAIP1</i>	Phorbol-12-myristate-13-acetate-induced protein 1	1.71 <sup>3</sup>
2539821	<i>ADAM17</i>	ADAM metalloproteinase 17	1.65 <sup>2</sup>
3389077	<i>PDGFD</i>	Platelet derived growth factor D	-1.52 <sup>2</sup>
3059464	<i>SEMA3A</i>	Sema domain, immunoglobulin domain (Ig), short basic domain, secreted, (semaphorin) 3A	-1.64 <sup>1</sup>
3058944	<i>HGF</i>	Hepatocyte growth factor	-1.75 <sup>1</sup>
2720584	<i>SLIT2</i>	Slit homolog 2 (Drosophila)	-1.92 <sup>2</sup>

Adjusted p values of fold change: <sup>1</sup>  $p < 0.01$ ; <sup>2</sup>  $p < 0.001$ ; <sup>3</sup>  $p < 0.0001$

\* Data taken from the list SF v CTRL  $p < 0.01$

There were also a number of genes differentially expressed in response to SF in THP-1 monocytes that were found to be associated with inflammatory signalling pathways, in particular, a selection of chemokine ligands and receptors (**Table 4.6**).

**Table 4.6. Genes differentially expressed in response to SF involved in inflammatory signalling pathways**

Affymetrix Transcript Cluster ID	Gene Symbol	Gene	SF Fold Change vs. Control*
<u>Toll-like receptor and cytokine signalling molecules</u>			
2766262	<i>TLR6</i>	Toll-like receptor 6	1.64 <sup>1</sup>
2853102	<i>PRLR</i>	Prolactin receptor	-1.56 <sup>2</sup>
<u>Chemokine signalling molecules</u>			
2731332	<i>IL-8</i>	Interleukin-8	2.36 <sup>3</sup>
2669979	<i>CX3CR1</i>	Chemokine (C-X3-C motif) receptor 1	-1.59 <sup>1</sup>
4040063	<i>CCL4</i>	**Chemokine (C-C motif) ligand 4	-2.00 <sup>1</sup>
2732508	<i>CXCL13</i>	Chemokine (C-X-C motif) ligand 13	-2.08 <sup>1</sup>
3718977	<i>CCL4</i>	**Chemokine (C-C motif) ligand 4	-2.38 <sup>2</sup>
3719020	<i>CCL4</i>	**Chemokine (C-C motif) ligand 4	-2.38 <sup>1</sup>
2773972	<i>CXCL11</i>	Chemokine (C-X-C motif) ligand 11	-2.44 <sup>2</sup>
2876608	<i>CXCL14</i>	Chemokine (C-X-C motif) ligand 14	-2.56 <sup>3</sup>
2773958	<i>CXCL10</i>	Chemokine (C-X-C motif) ligand 10	-2.63 <sup>2</sup>

Adjusted p values of fold change: <sup>1</sup> p<0.01; <sup>2</sup> p<0.001; <sup>3</sup> p<0.0001

\* Data taken from the list SF v CTRL p<0.01

\*\* Multiple transcript cluster IDs identify alternative transcripts of the same gene and cannot distinguish between them

#### 4.2.2. Effect of LPS on THP-1 monocytes

For analysis of global gene expression changes induced by LPS, THP-1 monocytes were treated with 1ng/ml LPS for 12 hours. As with the data for the SF treatment (**Table 4.1**), pairwise comparison tests were carried out to identify the number of differentially expressed genes in response to LPS at varying adjusted p values (**Table 4.7**).

**Table 4.7. Number of genes differentially expressed in response to LPS**

	Fold change in Gene Expression				Total Gene Number
	<1.5	1.5-2.0	2.0-4.0	>4	
<b>CTRL v LPS*</b>					
< 0.05	<b>1695</b> (595,1100)	<b>247</b> (179,68)	<b>116</b> (109,7)	<b>48</b> (48,0)	<b>2106</b>
< 0.01	<b>814</b> (343,471)	<b>233</b> (174,59)	<b>115</b> (109,6)	<b>48</b> (48,0)	<b>1210</b>
< 0.001	<b>264</b> (153,111)	<b>202</b> (154,48)	<b>114</b> (108,6)	<b>48</b> (48,0)	<b>628</b>

The number in bold gives the total number of transcripts changed. In brackets, the number of up-regulated transcripts is followed by the number of down-regulated transcripts.

\* P values are adjusted for false discovery rates using the Benjamini-Hochberg correction

Compared to the 407 genes that were differentially expressed in response to SF (**Table 4.1**), 1210 genes were differentially expressed in response to 1ng/ml LPS (adjusted  $p < 0.01$ ). Interestingly, of those that demonstrate more than a 1.5-fold increase, 84% of the genes were up-regulated by LPS (**Table 4.7**). Pathway analysis was carried out on the 1210 genes altered in response to 1ng/ml LPS and 20 different pathways were identified as being affected, not all of which were significant (data not shown). Nevertheless, there was a statistically significant association of genes after the Benjamini-Hochberg multiple testing correction with inflammatory signalling pathways including cytokine-cytokine receptor interaction, TLR signalling pathway, chemokine signalling pathway and NOD signalling pathways (**Table 4.8**).

**Table 4.8. Pathway analysis of genes differentially expressed in response to LPS**

Term	Count	%	P-Value	Fold Enrichment	Benjamini p value*
Cytokine-cytokine receptor interaction	51	4.28	$5.33 \times 10^{-8}$	2.213	$9.22 \times 10^{-6}$
TLR signalling pathway	25	2.10	$4.8 \times 10^{-6}$	2.779	$4.21 \times 10^{-4}$
Chemokine signalling pathway	35	2.94	$2.39 \times 10^{-5}$	2.123	0.0013
Cell adhesion molecules (CAMs)	24	2.02	$4.42 \times 10^{-4}$	2.179	0.0189
RIG-I-like receptor signalling pathway	16	1.34	$8.35 \times 10^{-4}$	2.601	0.0285
NOD-like receptor signalling pathway	15	1.26	$9.53 \times 10^{-4}$	2.679	0.0271
Cytosolic DNA-sensing pathway	13	1.09	0.00144	2.832	0.0350

The list of genes used for analysis was LPS v CTRL  $p < 0.01$ .

\*The adjusted p-values for all of the pathways listed are significant  $p < 0.05$ .

### 4.2.3. Effect of SF on LPS-treated THP-1 monocytes

Following the findings that many genes were differentially expressed in response to 1ng/ml LPS, the next major research question was whether 5µM SF was able to target all of the LPS-affected genes, or if the effect of SF was specific to particular genes. The combined treatment of 1ng/ml LPS and 5µM SF for 12 hours was found to significantly alter the expression of 1081 genes when a pairwise comparison was carried out with the co-treatment versus LPS alone (adjusted  $p < 0.01$ ) (**Table 4.9**). In contrast to the LPS treatment alone where the majority of genes with a fold change of more than 1.5-fold were up-regulated (**Table 4.7**), 71% of genes changed by LPS and SF together demonstrate a down-regulation compared to the LPS alone (**Table 4.9**).

**Table 4.9. Number of differentially expressed genes in response to LPS and SF co-treatment**

	Fold change in Gene Expression				Total Gene Number
	<1.5	1.5-2.0	2.0-4.0	>4	
<b>LPS v LPS+SF*</b>					
< 0.05	<b>1502</b> (945,557)	<b>241</b> (85,156)	<b>141</b> (35,106)	<b>25</b> (0,25)	<b>1909</b>
< 0.01	<b>688</b> (393,295)	<b>227</b> (78,149)	<b>141</b> (35,106)	<b>25</b> (0,25)	<b>1081</b>
< 0.001	<b>200</b> (107,93)	<b>191</b> (68,123)	<b>138</b> (34,104)	<b>25</b> (0,25)	<b>554</b>

The number in bold gives the total number of transcripts changed. In brackets, the number of up-regulated transcripts is followed by the number of down-regulated transcripts.

\* P values are adjusted for false discovery rates using the Benjamini-Hochberg correction

While the majority of genes differentially expressed in response to LPS were up-regulated (**Table 4.7**) and the genes changed in response to a co-treatment of LPS and SF compared to LPS alone were down-regulated, it was not known whether there was a commonality between the genes affected. A venn diagram was constructed to investigate the overlap between these two pairwise comparisons and 562 genes were found to be common to both gene lists (**Figure 4.3**). Furthermore, of these 562 genes that were significantly affected by SF in the presence of LPS, 467 of these genes were specifically affected only in the presence of LPS (105/562 genes were affected in CTRL v SF treatment, data not shown).

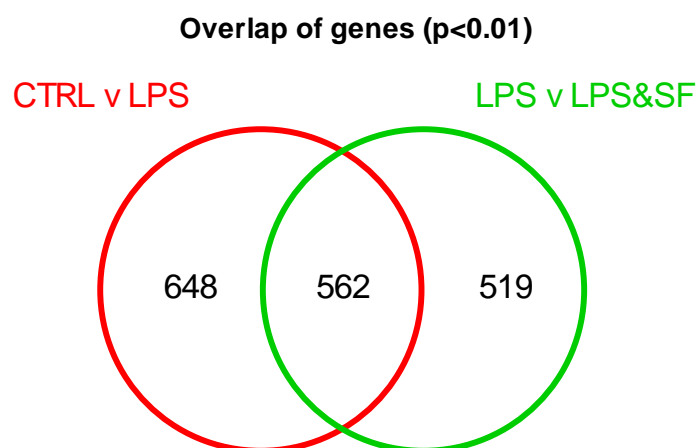


**Figure 4.3. Effect of LPS in the presence or absence of SF on gene expression.** 562 genes were found to be affected by 1ng/ml LPS alone and in the presence of 5 $\mu$ M SF (Genes affected by LPS only = 1210; genes affected by LPS and SF co-treatment = 1081).

To get an idea of the relationship between the genes affected by LPS alone and in combination with SF, a regression analysis was conducted with all 1210 genes altered by LPS plotted against the effect of SF presence. 5 $\mu$ M SF was able to significantly oppose the effect of LPS on all genes differentially expressed in response to 1ng/ml LPS alone with a clear inverse relationship seen (**Figure 4.3**). The gradient of the line of regression was -1.068 meaning the overall change seen with LPS is almost identical to the extent the gene is oppositely affected by LPS and SF in combination. Because the effects of LPS and SF have already been characterised on IL-6, IL-1 $\beta$  and TNF $\alpha$  expression (see Chapter 3), these have been annotated on **Figure 4.4** to demonstrate that the suppressive effect of SF was not selective to these genes alone and many genes were affected to a much larger extent than the three cytokines previously studied.

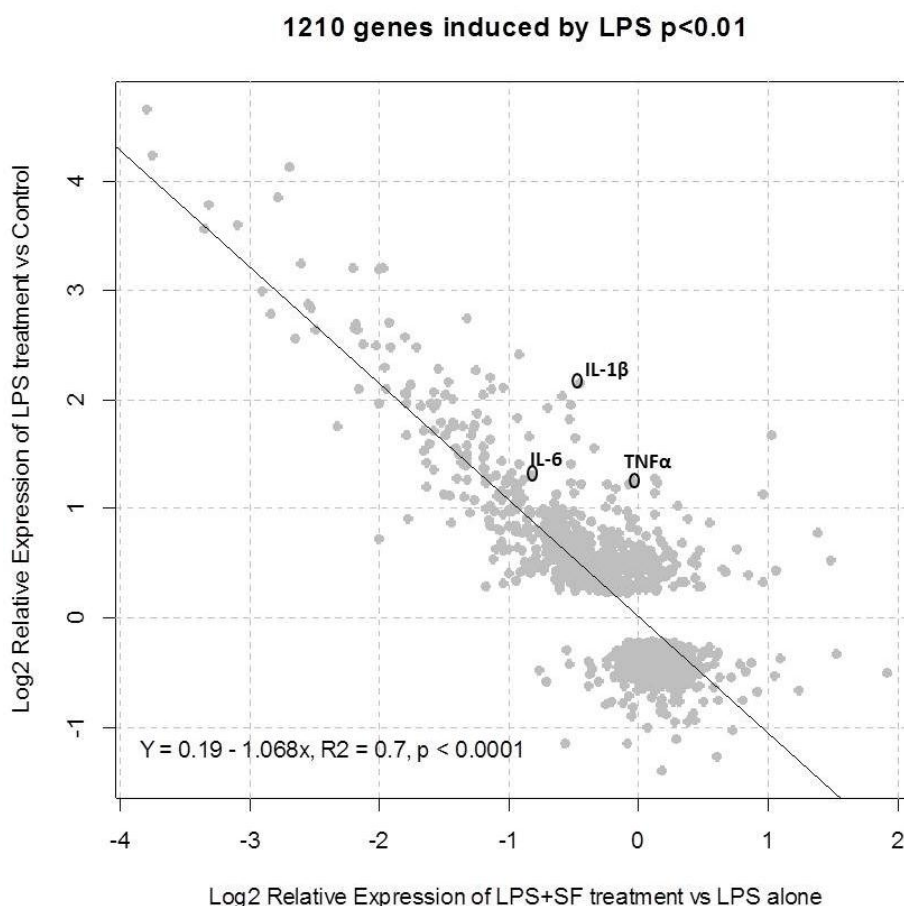


**Figure 4.4. 5 $\mu$ M SF suppresses all changes induced by 1ng/ml LPS.** 1210 genes differentially expressed in response to 1ng/ml LPS were plotted with the LPS effect relative to the control (y) against the effect of LPS+SF co-treatment compared to LPS alone (x). The regression analysis demonstrates a statistically significant association ( $p < 0.0001$ ) with a regression coefficient of -1.07 and an  $R^2$  value of 0.7. IL-6, IL-1 $\beta$  and TNF $\alpha$  are circled to highlight where these previously investigated genes lie within the regression (biomarkers chosen for targeted approach in Chapter 3).

The genes altered by more than 2-fold in response to LPS alone were selected for further analysis to investigate the extent of the effect of SF on these LPS-affected genes. Genes were characterised into groups according to their associated inflammatory signalling pathways (**Table 4.10**). In addition, many genes identified had miscellaneous functions which were not associated with inflammatory pathways (**Tables 4.11**).

**Table 4.10. Effect of SF on genes differentially expressed in response to LPS (with > 2-fold change) with functions in inflammatory signalling pathways**

Affymetrix Transcript Cluster ID	Gene Symbol	Gene	LPS Fold Change vs. Control†	LPS + SF Fold Change vs. LPS alone††
<u>Toll like receptor and cytokine signalling pathways</u>				
3275690	<i>IL15RA</i>	Interleukin 15 receptor, alpha	2.00 <sup>3</sup>	-1.56 <sup>1</sup>
3645626	<i>IL32</i>	Interleukin 32	2.01 <sup>3</sup>	-1.50 <sup>1</sup>
2617563	<i>MYD88</i>	Myeloid differentiation primary response gene (88)	2.09 <sup>3</sup>	-1.95 <sup>3</sup>
3351166	<i>IL10RA</i>	Interleukin 10 receptor, alpha	2.23 <sup>3</sup>	-1.94 <sup>3</sup>
2690900	<i>CD80</i>	CD80 molecule	2.25 <sup>3</sup>	-1.89 <sup>3</sup>
2905404	<i>PIM1</i>	Pim-1 oncogene	2.34 <sup>3</sup>	-1.19*
3887302	<i>CD40</i>	CD40 molecule, TNF receptor superfamily member 5	2.35 <sup>3</sup>	-1.36 <sup>1</sup>
2902416	<i>TNF</i>	Tumor necrosis factor	2.40 <sup>3</sup>	> 0.01
3500787	<i>TNFSF13B</i>	Tumor necrosis factor (ligand) superfamily, member 13B	2.44 <sup>3</sup>	-2.21 <sup>3</sup>
2992576	<i>IL-6</i>	Interleukin 6 (interferon, beta 2)	2.49 <sup>3</sup>	-1.77 <sup>2</sup>
2497161	<i>IL18RAP</i>	Interleukin 18 receptor accessory protein	2.59 <sup>3</sup>	-2.28 <sup>3</sup>
2884301	<i>IL12B</i>	Interleukin 12B (natural killer cell stimulatory factor 2, cytotoxic lymphocyte maturation factor 2, p40)	2.90 <sup>3</sup>	-3.15 <sup>3</sup>
2501204	<i>IL1RN</i>	Interleukin 1 receptor antagonist	2.96 <sup>3</sup>	-2.66 <sup>3</sup>
2395146	<i>TNFRSF9</i>	Tumor necrosis factor receptor superfamily, member 9	3.16 <sup>3</sup>	-1.79 <sup>2</sup>
2806468	<i>IL7R</i>	Interleukin 7 receptor	3.90 <sup>3</sup>	-2.95 <sup>3</sup>
2510464	<i>TNFAIP6</i>	Tumor necrosis factor, alpha-induced protein 6	4.11 <sup>3</sup>	-1.51*
2705706	<i>TNFSF10</i>	Tumor necrosis factor (ligand) superfamily, member 10	4.28 <sup>3</sup>	-4.45 <sup>3</sup>
2571510	<i>IL1B</i>	Interleukin 1, beta	4.45 <sup>3</sup>	-1.38*
2783916	<i>TNIP3</i>	TNFAIP3 interacting protein 3	5.35 <sup>3</sup>	-1.89 <sup>1</sup>
<u>Chemokine signalling</u>				
2731332	<i>IL8</i>	Interleukin-8	3.19 <sup>3</sup>	2.04 <sup>2</sup>
3457752	<i>STAT2</i>	Signal transducer and activator of transcription 2, 113kDa	3.36 <sup>3</sup>	-2.75 <sup>3</sup>

<u>Chemokine signalling (continued)</u>				
2732508	<i>CXCL13</i>	Chemokine (C-X-C motif) ligand 13	3.39 <sup>3</sup>	-5.03 <sup>3</sup>
2592268	<i>STAT1</i>	Signal transducer and activator of transcription 1, 91kDa	3.41 <sup>3</sup>	-2.41 <sup>3</sup>
2773947	<i>CXCL9</i>	Chemokine (C-X-C motif) ligand 9	3.90 <sup>3</sup>	-4.02 <sup>3</sup>
3754133	<i>CCL3L1</i>	Chemokine (C-C motif) ligand 3-like 1	4.13 <sup>3</sup>	-2.29 <sup>3</sup>
3754070	<i>CCL3L1</i>	Chemokine (C-C motif) ligand 3-like 1	4.29 <sup>3</sup>	-2.20 <sup>3</sup>
4040932	<i>CCL3L1</i>	Chemokine (C-C motif) ligand 3-like 1	4.32 <sup>3</sup>	-2.07 <sup>3</sup>
3754009	<i>CCL3</i>	Chemokine (C-C motif) ligand 3	4.63 <sup>3</sup>	-2.20 <sup>3</sup>
3756319	<i>CCR7</i>	Chemokine (C-C motif) receptor 7	6.53 <sup>3</sup>	-3.79 <sup>3</sup>
7385547	<i>CCL2</i>	Chemokine (C-C motif) ligand 2	6.70 <sup>3</sup>	-2.50 <sup>3</sup>
4040063	<i>CCL4L1</i>	Chemokine (C-C motif) ligand 4-like 1	9.12 <sup>3</sup>	-4.01 <sup>3</sup>
3718930	<i>CCL4</i>	Chemokine (C-C motif) ligand 4	5.60 <sup>3</sup>	-3.29 <sup>3</sup>
3718977	<i>CCL4</i>	Chemokine (C-C motif) ligand 4	9.22 <sup>3</sup>	-3.93 <sup>3</sup>
3719020	<i>CCL4</i>	Chemokine (C-C motif) ligand 4	9.25 <sup>3</sup>	-4.61 <sup>3</sup>
2773958	<i>CXCL10</i>	Chemokine (C-X-C motif) ligand 10	13.82 <sup>3</sup>	-9.95 <sup>3</sup>
2773972	<i>CXCL11</i>	Chemokine (C-X-C motif) ligand 11	18.83 <sup>3</sup>	-13.53 <sup>3</sup>
3718191	<i>CCL8</i>	Chemokine (C-C motif) ligand 8	25.33 <sup>3</sup>	-13.93 <sup>3</sup>
<u>Interferon-induced genes</u>				
4053534	<i>ISG15</i>	ISG15 ubiquitin-like modifier	2.14 <sup>2</sup>	-1.88 <sup>2</sup>
3357840	<i>IFITM3</i>	Interferon induced transmembrane protein 3 (1-8U)	2.15 <sup>3</sup>	-1.86 <sup>3</sup>
3579546	<i>WARS</i>	Tryptophanyl-tRNA synthetase	2.17 <sup>3</sup>	-2.55 <sup>3</sup>
3774906	<i>SECTM1</i>	Secreted and transmembrane 1	2.19 <sup>3</sup>	-2.75 <sup>3</sup>
2421925	<i>GBP7</i>	Guanylate binding protein 7	2.36 <sup>3</sup>	-2.27 <sup>3</sup>
2403261	<i>IFI6</i>	Interferon, alpha-inducible protein 6	2.38 <sup>3</sup>	-1.98 <sup>3</sup>
2875348	<i>IRF1</i>	Interferon regulatory factor 1	2.68 <sup>3</sup>	-1.89 <sup>3</sup>
3722338	<i>IFI35</i>	Interferon-induced protein 35	2.82 <sup>3</sup>	-2.29 <sup>3</sup>
2584207	<i>IFIH1</i>	Interferon induced with helicase C domain 1	3.29 <sup>3</sup>	-2.99 <sup>3</sup>
3315675	<i>IFITM1</i>	Interferon induced transmembrane protein 1 (9-27)	3.39 <sup>3</sup>	-2.56 <sup>3</sup>
2439554	<i>AIM2</i>	Absent in melanoma 2	3.47 <sup>3</sup>	-2.88 <sup>3</sup>
3474831	<i>OASL</i>	2'-5'-oligoadenylate synthetase-like	3.81 <sup>3</sup>	-2.99 <sup>3</sup>
2603051	<i>SP110</i>	SP110 nuclear body protein	3.91 <sup>3</sup>	-3.46 <sup>3</sup>
3432467	<i>OAS3</i>	2'-5'-oligoadenylate synthetase 3, 100kDa	4.01 <sup>3</sup>	-2.71 <sup>3</sup>
3432514	<i>OAS2</i>	2'-5'-oligoadenylate synthetase 2, 69/71kDa	4.12 <sup>3</sup>	-2.82 <sup>3</sup>

Interferon-induced genes (continued)

2362394	<i>IFI16</i>	Interferon, gamma-inducible protein 16	4.12 <sup>3</sup>	-3.47 <sup>3</sup>
2735409	<i>HERC5</i>	Hect domain and RLD 5	4.18 <sup>3</sup>	-3.48 <sup>3</sup>
2468351	<i>RSAD2</i>	Radical S-adenosyl methionine domain containing 2	4.28 <sup>3</sup>	-3.85 <sup>3</sup>
3922037	<i>MX2</i>	Myxovirus (influenza virus) resistance 2 (mouse)	4.40 <sup>3</sup>	-3.38 <sup>3</sup>
3432438	<i>OAS1</i>	2',5'-oligoadenylate synthetase 1, 40/46kDa	4.47 <sup>3</sup>	-2.76 <sup>3</sup>
3257268	<i>IFIT5</i>	Interferon-induced protein with tetratricopeptide repeats 5	5.59 <sup>3</sup>	-3.78 <sup>3</sup>
3257192	<i>IFIT2</i>	Interferon-induced protein with tetratricopeptide repeats 2	5.65 <sup>3</sup>	-4.06 <sup>3</sup>
2421995	<i>GBP4</i>	Guanylate binding protein 4	5.92 <sup>3</sup>	-6.30 <sup>3</sup>
3549575	<i>IFI27</i>	Interferon, alpha-inducible protein 27	6.25 <sup>3</sup>	-5.63 <sup>3</sup>
3318443	<i>TRIM22</i>	Tripartite motif-containing 22	6.26 <sup>3</sup>	-4.50 <sup>3</sup>
3922100	<i>MX1</i>	Myxovirus (influenza virus) resistance 1, interferon-inducible protein p78 (mouse)	6.29 <sup>3</sup>	-4.57 <sup>3</sup>
3203086	<i>DDX58</i>	DEAD (Asp-Glu-Ala-Asp) box polypeptide 58	6.49 <sup>3</sup>	-4.54 <sup>3</sup>
2421883	<i>GBP1</i>	Guanylate binding protein 1, interferon-inducible, 67kDa	7.94 <sup>3</sup>	-7.50 <sup>3</sup>
2343511	<i>IFI44</i>	Interferon-induced protein 44	9.53 <sup>3</sup>	-6.10 <sup>3</sup>
2343473	<i>IFI44L</i>	Interferon-induced protein 44-like	11.86 <sup>3</sup>	-10.18 <sup>3</sup>
3257246	<i>IFIT1</i>	Interferon-induced protein with tetratricopeptide repeats 1	12.18 <sup>3</sup>	-8.54 <sup>3</sup>
3257204	<i>IFIT3</i>	Interferon-induced protein with tetratricopeptide repeats 3	14.50 <sup>3</sup>	-6.87 <sup>3</sup>

Adjusted p values of fold change: <sup>1</sup> p<0.01 <sup>2</sup> p<0.001; <sup>3</sup> p<0.0001.

\*These fold changes were not found to be significant at p<0.01 but remain significant at p<0.05.

† The list of genes used for analysis was LPS v CTRL p<0.01.

†† The list of genes used for analysis was LPS+SF v LPS p<0.01.

**Table 4.11. Effect of SF on genes differentially expressed in response to LPS (with > 2-fold change) with miscellaneous functions**

Affymetrix Transcript Cluster ID	Gene Symbol	Gene	LPS Fold Change vs. Control†	LPS + SF Fold Change vs. LPS alone††
<u>Miscellaneous Function</u>				
3791935	<i>SERPINB2</i>	Serpin peptidase inhibitor, clade B (ovalbumin), member 2	-2.63 <sup>3</sup>	1.13**
3387259	<i>SESN3</i>	Sestrin 3	-2.40 <sup>3</sup>	1.51 <sup>2</sup>
2428796	<i>PTPN22</i>	Protein tyrosine phosphatase, non-receptor type 22 (lymphoid)	-2.22 <sup>3</sup>	-1.06**
3791958	<i>SERPINB10</i>	Serpin peptidase inhibitor, clade B (ovalbumin), member 10	-2.20 <sup>3</sup>	-1.48 <sup>1</sup>
3466687	<i>HAL</i>	Histidine ammonia-lyase	-2.13 <sup>3</sup>	1.22*
3466687	<i>VLDLR</i>	Very low density lipoprotein receptor	-2.04 <sup>3</sup>	1.65 <sup>3</sup>
3068587	<i>GPR85</i>	G protein-coupled receptor 85	2.01 <sup>2</sup>	-2.27 <sup>3</sup>
3489481	<i>PHF11</i>	PHD finger protein 11	2.01 <sup>3</sup>	-1.67 <sup>2</sup>
2777333	<i>PPM1K</i>	Protein phosphatase, Mg2+/Mn2+ dependent, 1K	2.01 <sup>3</sup>	-1.98 <sup>3</sup>
2698738	<i>XRN1</i>	5'-3' exoribonuclease 1	2.02 <sup>3</sup>	-1.92 <sup>2</sup>
2709778	<i>BCL6</i>	B-cell CLL/lymphoma 6	2.02 <sup>3</sup>	-1.19**
2951859	<i>ETV7</i>	Ets variant 7	2.04 <sup>3</sup>	-2.21 <sup>3</sup>
3464860	<i>DUSP6</i>	Dual specificity phosphatase 6	2.05 <sup>3</sup>	1.23*
3442854	<i>SLC2A3</i>	Solute carrier family 2 (facilitated glucose transporter), member 3	2.06 <sup>3</sup>	-1.90 <sup>3</sup>
3581404	<i>GPR132</i>	G protein-coupled receptor 132	2.09 <sup>3</sup>	-1.58 <sup>3</sup>
2343231	<i>NEXN</i>	Nexilin (F actin binding protein)	2.11 <sup>3</sup>	-2.42 <sup>2</sup>
3388807	<i>MMP1</i>	Matrix metalloproteinase 1 (interstitial collagenase)	2.11 <sup>3</sup>	-2.08 <sup>3</sup>
2919669	<i>PRDM1</i>	PR domain containing 1, with ZNF domain	2.14 <sup>3</sup>	-1.15**
3601387	<i>PML</i>	Promyelocytic leukemia	2.17 <sup>3</sup>	-2.14 <sup>3</sup>
3346548	<i>BIRC3</i>	Baculoviral IAP repeat-containing 3	2.19 <sup>3</sup>	-1.55 <sup>1</sup>
2897172	<i>RNF144B</i>	Ring finger protein 144B	2.19 <sup>3</sup>	-1.88 <sup>3</sup>
3806211	<i>PSTPIP2</i>	Proline-serine-threonine phosphatase interacting protein 2	2.20 <sup>3</sup>	-2.84 <sup>3</sup>
3140213	<i>MSC</i>	Musculin	2.20 <sup>3</sup>	1.95 <sup>3</sup>
2720145	<i>LAP3</i>	Leucine aminopeptidase 3	2.20 <sup>3</sup>	-2.04 <sup>3</sup>

<i>Miscellaneous Function (continued)</i>				
3638188	<i>HAPLN3</i>	Hyaluronan and proteoglycan link protein 3	2.21 <sup>3</sup>	-2.12 <sup>3</sup>
2362746	<i>SLAMF8</i>	SLAM family member 8	2.22 <sup>3</sup>	-1.41 <sup>1</sup>
2553970	<i>PNPT1</i>	Polyribonucleotide nucleotidyltransferase 1	2.23 <sup>3</sup>	-2.09 <sup>3</sup>
3150579	<i>ENPP2</i>	Ectonucleotide pyrophosphatase/phosphodiesterase 2	2.23 <sup>3</sup>	-2.07 <sup>3</sup>
3971806	<i>SATI</i>	Spermidine/spermine N1- acetyltransferase 1	2.28 <sup>3</sup>	-1.14**
2720584	<i>SLIT2</i>	Slit homolog 2 (Drosophila)	2.30 <sup>3</sup>	-3.12 <sup>3</sup>
2955827	<i>PLA2G7</i>	Phospholipase A2, group VII (platelet- activating factor acetylhydrolase, plasma)	2.34 <sup>3</sup>	-1.05**
2729667	<i>STAP1</i>	Signal transducing adaptor family member 1	2.36 <sup>1</sup>	-1.89 <sup>1</sup>
2796553	<i>ACSL1</i>	Acyl-CoA synthetase long-chain family member 1	2.36 <sup>3</sup>	-1.43 <sup>1</sup>
3075932	<i>PARP12</i>	Poly (ADP-ribose) polymerase family, member 12	2.36 <sup>3</sup>	-2.03 <sup>3</sup>
3066818	<i>NAMPT</i>	Nicotinamide phosphoribosyltransferase	2.37 <sup>3</sup>	-1.94 <sup>2</sup>
3049292	<i>IGFBP3</i>	Insulin-like growth factor binding protein 3	2.38 <sup>3</sup>	1.11**
3299469	<i>ANKRD22</i>	Ankyrin repeat domain 22	2.41 <sup>3</sup>	-1.85 <sup>2</sup>
2677902	<i>HESX1</i>	HESX homeobox 1	2.42 <sup>3</sup>	-2.50 <sup>3</sup>
3944129	<i>HMOX1</i>	Hemeoxygenase (decycling) 1	2.42 <sup>3</sup>	1.09**
3087703	<i>PDGFRL</i>	Platelet-derived growth factor receptor- like	2.44 <sup>3</sup>	-2.65 <sup>3</sup>
3618736	<i>RASGRP1</i>	RAS guanyl releasing protein 1 (calcium and DAG-regulated)	2.44 <sup>3</sup>	-2.01 <sup>3</sup>
3205293	<i>PAX5</i>	Paired box 5	2.44 <sup>3</sup>	-2.27 <sup>3</sup>
3185498	<i>SLC3IA2</i>	Solute carrier family 31 (copper transporters), member 2	2.47 <sup>3</sup>	-2.15 <sup>3</sup>
2548402	<i>EIF2AK2</i>	Eukaryotic translation initiation factor 2-alpha kinase 2	2.53 <sup>3</sup>	-1.97 <sup>2</sup>
3818596	<i>EMR1</i>	EGF-like module containing, mucin- like, hormone receptor-like 1	2.56 <sup>3</sup>	-2.99 <sup>3</sup>
3944243	<i>APOL6</i>	Apolipoprotein L, 6	2.59 <sup>3</sup>	-2.31 <sup>3</sup>

<u>Miscellaneous Function (continued)</u>				
3161082	<i>CD274</i>	CD274 molecule	2.64 <sup>2</sup>	-2.53 <sup>2</sup>
3835726	<i>BCL3</i>	B-cell CLL/lymphoma 3	2.66 <sup>3</sup>	-1.43 <sup>3</sup>
3757602	<i>DHX58</i>	DEXH (Asp-Glu-X-His) box polypeptide 58	2.66 <sup>3</sup>	-2.50 <sup>3</sup>
2421843	<i>GBP3</i>	Guanylate binding protein 3	2.67 <sup>3</sup>	-2.52 <sup>3</sup>
2403446	<i>PTAFR</i>	Platelet-activating factor receptor	2.68 <sup>3</sup>	-2.57 <sup>3</sup>
3403754	<i>CLEC6A</i>	C-type lectin domain family 6, member A	2.68 <sup>2</sup>	-3.11 <sup>3</sup>
2699726	<i>PLSCR1</i>	Phospholipid scramblase 1	2.72 <sup>3</sup>	-2.08 <sup>3</sup>
3331355	<i>SERPING1</i>	Serpin peptidase inhibitor, clade G (C1 inhibitor), member 1	2.76 <sup>3</sup>	-2.51 <sup>3</sup>
2638962	<i>DTX3L</i>	Deltex 3-like (Drosophila)	2.77 <sup>3</sup>	-2.29 <sup>3</sup>
2950214	<i>TAP1</i>	Transporter 1, ATP-binding cassette, sub-family B (MDR/TAP)	2.84 <sup>3</sup>	-2.51 <sup>3</sup>
2896545	<i>GMPR</i>	Guanosine monophosphate reductase	2.85 <sup>3</sup>	-2.62 <sup>3</sup>
3895614	<i>SIGLEC1</i>	Sialic acid binding Ig-like lectin 1, sialoadhesin	2.92 <sup>3</sup>	-2.64 <sup>3</sup>
3905875	<i>MAFB</i>	v-maf musculoaponeurotic fibrosarcoma oncogene homolog B (avian)	2.96 <sup>3</sup>	-1.27 <sup>1</sup>
2991860	<i>ITGB8</i>	Integrin, beta 8	2.98 <sup>3</sup>	-2.29 <sup>3</sup>
2539125	<i>CMPK2</i>	Cytidine monophosphate (UMP-CMP) kinase 2, mitochondrial	3.01 <sup>3</sup>	-2.50 <sup>3</sup>
3360622	<i>TRIM5</i>	Tripartite motif-containing 5	3.02 <sup>3</sup>	-3.06 <sup>3</sup>
3737274	<i>RNF213</i>	Ring finger protein 213	3.11 <sup>3</sup>	-2.22 <sup>3</sup>
3737338	<i>RNF213</i>	Ring finger protein 213	3.19 <sup>3</sup>	-2.45 <sup>3</sup>
2975014	<i>SGK1</i>	Serum/glucocorticoid regulated kinase 1	3.15 <sup>3</sup>	-1.40*
2440354	<i>CD48</i>	CD48 molecule	3.20 <sup>3</sup>	-2.80 <sup>3</sup>
3442941	<i>C3AR1</i>	Complement component 3a receptor 1	3.21 <sup>3</sup>	-3.46 <sup>3</sup>
2945741	<i>FAM65B</i>	Family with sequence similarity 65, member B	3.30 <sup>3</sup>	-3.16 <sup>3</sup>
2792800	<i>DDX60</i>	DEAD (Asp-Glu-Ala-Asp) box polypeptide 60	3.33 <sup>3</sup>	-2.43 <sup>3</sup>
3373962	<i>UBE2L6</i>	Ubiquitin-conjugating enzyme E2L 6	3.38 <sup>3</sup>	-2.69 <sup>3</sup>
3119339	<i>LY6E</i>	Lymphocyte antigen 6 complex, locus E	3.47 <sup>3</sup>	-2.70 <sup>3</sup>
3635198	<i>BCL2A1</i>	BCL2-related protein A1	3.52 <sup>3</sup>	-2.25 <sup>3</sup>

<i>Miscellaneous Function (continued)</i>				
3820443	<i>ICAM1</i>	Intercellular adhesion molecule 1	3.55 <sup>3</sup>	-1.45 <sup>2</sup>
3817380	<i>EBI3</i>	Epstein-Barr virus induced 3	3.59 <sup>3</sup>	-1.91 <sup>3</sup>
2422035	<i>GBP5</i>	Guanylate binding protein 5	3.66 <sup>3</sup>	-2.37 <sup>3</sup>
3733275	<i>KCNJ2</i>	Potassium inwardly-rectifying channel, subfamily J, member 2	3.80 <sup>3</sup>	-1.62 <sup>1</sup>
3061438	<i>SAMD9</i>	Sterile alpha motif domain containing 9	3.86 <sup>3</sup>	-3.20 <sup>3</sup>
2982319	<i>SOD2</i>	Superoxide dismutase 2, mitochondrial	3.89 <sup>3</sup>	-1.44 <sup>1</sup>
2639054	<i>PARP14</i>	Poly (ADP-ribose) polymerase family, member 14	3.90 <sup>3</sup>	-3.04 <sup>3</sup>
2371346	<i>RGL1</i>	Ral guanine nucleotide dissociation stimulator-like 1	4.08 <sup>3</sup>	-1.51 <sup>2</sup>
2692060	<i>PARP9</i>	Poly (ADP-ribose) polymerase family, member 9	4.19 <sup>3</sup>	-2.99 <sup>3</sup>
3061456	<i>SAMD9L</i>	Sterile alpha motif domain containing 9-like	4.19 <sup>3</sup>	-3.46 <sup>3</sup>
3060332	<i>STEAP4</i>	STEAP family member 4	4.81 <sup>3</sup>	-2.39 <sup>3</sup>
2735362	<i>HERC6</i>	Hect domain and RLD 6	4.88 <sup>3</sup>	-2.91 <sup>3</sup>
2707876	<i>LAMP3</i>	Lysosomal-associated membrane protein 3	4.92 <sup>3</sup>	-3.88 <sup>3</sup>
2363202	<i>SLAMF7</i>	SLAM family member 7	5.68 <sup>3</sup>	-4.37 <sup>3</sup>
3511698	<i>EPSTI1</i>	Epithelial stromal interaction 1 (breast)	5.97 <sup>3</sup>	-3.50 <sup>3</sup>
2348992	<i>VCAM1</i>	Vascular cell adhesion molecule 1	6.89 <sup>3</sup>	-7.16 <sup>3</sup>
3095223	<i>IDO1</i>	Indoleamine 2,3-dioxygenase 1	7.18 <sup>3</sup>	-5.78 <sup>3</sup>
3936550	<i>USP18</i>	Ubiquitin specific peptidase 18	7.35 <sup>3</sup>	-5.88 <sup>3</sup>
2749011	<i>TDO2</i>	Tryptophan 2,3-dioxygenase	17.59 <sup>3</sup>	-6.46 <sup>3</sup>

Adjusted p values of fold change: <sup>1</sup> p<0.01; <sup>2</sup> p<0.001; <sup>3</sup> p<0.0001.

\*These fold changes were not found to be significant at p<0.01 but remain significant at p<0.05.

\*\*These fold changes are not found to be statistically significant (p>0.05).

† The list of genes used for analysis was LPS v CTRL p<0.01.

†† The list of genes used for analysis was LPS+SF v LPS p<0.01.

### 4.3. Discussion

In order to expand on the research presented in Chapter 3, a systematic investigation was carried out to address the question of whether SF was able to significantly alter the expression of all LPS-affected genes, and in addition whether SF was able to induce significant changes in global gene expression constitutively.

407 gene expression patterns were found to be significantly changed in response to 5 $\mu$ M SF as compared to untreated controls. Of these genes, associations were identified with xenobiotic and carbohydrate metabolism, cancer and inflammatory signalling pathways. One mechanism which is consistently associated with SF is the induction of Nrf2. Under normal conditions, Nrf2 is sequestered in the cytoplasm by its negative regulator, Keap1, which behaves to target the transcription factor for proteasomal degradation [154]. In the presence of SF, the electrophilic nature of the ITC results in it binding to free cysteine residues to form thioacyl adducts with Keap1, providing a potential mechanism for the up-regulation of Nrf2-controlled gene expression [156-159].

Global gene expression changes in response to SF have been previously investigated in a number of different cell models. Caco-2 cells, a colon adenocarcinoma cell line, were exposed to 1, 5, 25 and 50 $\mu$ M SF for 24 hours and a number of significant gene changes were found [147]. When exposed to 5 $\mu$ M SF, only 4 gene changes were induced in Caco-2 cells with more than a 2-fold change as compared to 38 found in the microarray analysis in this study with the THP-1 monocytes. While the concentrations necessary to induce the changes were much higher in the Caco-2 study, the genes affected were comparable with the results in this chapter [147].

In data from non-cancerous primary prostate epithelial and stromal cells treated with 15 $\mu$ M SF for 24 hours, 196 genes were found to be altered by more than 1.5-fold in epithelial cells, while only 42 genes were altered by more than 1.5-fold in stromal cells (adjusted p value < 0.001) [146]. In cancerous LNCaP prostate cells, 2579 transcripts were altered in response to 25 $\mu$ M SF and 3061 transcripts were differentially expressed in response to 10 $\mu$ M SF compared to controls (p < 0.05) [231]. There are many more transcripts changed in the LNCaP cells compared to the previously described data, which may be as a result of different arrays and alternative methods of analysis. However, of the genes that were differentially expressed in LNCaP cells in response to SF, genes that encoded enzymes involved in xenobiotic metabolism and detoxification such as NQO1, TXNRD1, MGST1 and SOD1 were altered to the greatest extent [231]. Similar results were also recorded in human hepatocytes and normal breast epithelial cells [160, 232]. All of these genes were also significantly changed in this chapter with THP-1 monocytes (**Table 4.3**).

When microarray analysis of the human lens epithelial cell line FHL124 was carried out following treatment with 1 and 2 $\mu$ M SF for 24 hours, both NQO1 and TXNRD1 were

up-regulated [145], consistent with previously reported findings. These results also demonstrate that concentrations of SF easily achievable from the diet (1 and 2 $\mu$ M) are able to induce phase 2 enzymes and cause differential gene expression. The effectiveness of lower concentrations in this cell line may reflect the likelihood that concentrations found in systemic circulation may be difficult to achieve within lens cells [145].

In addition, a number of genes associated with carbohydrate metabolism in glycolysis and the pentose phosphate pathway were also identified. The pentose phosphate pathway consists of two distinct branches; an oxidative irreversible pathway that is responsible for the production of NADPH and a ribose 5-phosphate molecule, and a non-oxidative pathway made up of a number of reversible reactions that interconverts between ribose phosphates and glycolytic intermediates depending on the cell's requirements for NADPH, ribose phosphates or ATP (**Figure 4.2**) [233]. The pentose phosphate pathway is able to provide an alternative pathway for glucose oxidation and contributes between 10-20% of all glucose oxidation while glycolysis is responsible for the remaining 80-90%. This pathway, unlike glycolysis does not require oxygen and does not produce ATP. The production of NADPH from the pentose phosphate pathway is of particular importance due to its function as the universal electron donor, behaving as a reducing agent in a number of biosynthetic pathways. **Table 4.4** shows how SF was able to significantly induce the expression of the genes responsible for encoding a number of enzymes involved in both glycolysis and the pentose phosphate pathway while **Figure 4.2** depicts the linked pathways and those enzymes that were differentially expressed in response to 5 $\mu$ M SF. These results were supported by the previously mentioned results from non-cancerous human breast epithelial MCF10A cells [160]. After treatment with 15 $\mu$ M SF for 24 hours, a significant increase of at least 1.2-fold in the expression of PGD, G6PD, TALDO1 and TKT was seen in response to SF [160].

The importance of potentially increasing NADPH production in response to SF is related to the involvement of NADPH in xenobiotic metabolism and the reduction of oxidative stress by behaving as a universal electron donor. SF behaves to increase GST activity, allowing conjugation of xenobiotics to GSH to allow detoxification enabling safe excretion. This is in addition to NADPH donating electrons to reactive oxygen species, alleviating oxidative stress. The increase seen in GST activity is likely due to an increase in the expression of the GCLM, an enzyme responsible for catalysing the rate-limiting step in GSH synthesis and this is supported by SF's ability to increase intracellular GSH

[234]. Once safe excretion of xenobiotics is complete, in order for GSH and TXN to continue to conjugate to other xenobiotics they require reduction. This reduction reaction uses NADPH as an electron donor. While there are a number of logical hypotheses for the importance of increasing NADPH production, it is important not to over-interpret the data from the global gene expression analysis. In order to confirm that the glycolysis and pentose phosphate pathways are up-regulated, the activity of the differentially expressed enzymes should also be measured.

In response to LPS, 1210 genes were found to be significantly differentially expressed, with 396 demonstrating more than a 1.5-fold change (adjusted p value < 0.01). The genes that were altered in expression were mainly involved inflammatory signalling pathways such as TLR signalling, cytokines and chemokines and many induced by IFNs. This work is completely novel as there are no previously documented microarray studies investigating the effect of physiologically relevant concentration of LPS (1ng/ml) on THP-1 monocytic cells. Concentrations in the range of 1ng/ml LPS have only been used in studies using bone marrow-derived macrophages from mice (Accession Numbers: E-GEOD-53810 and E-GEOD-19941, ArrayExpress) and in both of these studies a different strain of LPS (*Salmonella minnesota*) has been used to that used in my study (*E.coli* 055:B5). This *Salmonella* strain has been previously found to behave to an extent that was significantly different to that seen with LPS from the *E.coli* 055:B5 strain in its ability to induce TNF $\alpha$  and MCP-1 [14], so it is likely the results from these studies would not be comparable to the present study with THP-1 monocytes. Ellertsen and colleagues used THP-1 monocytes and treated them with 10 $\mu$ g/ml LPS (*E.coli* 026:B6) for 24 hours only around 15% of their reported changes were consistent with the data presented in this chapter presumably due to the large difference in LPS concentration used [235].

SF was able to significantly affect 562 genes induced by LPS, with only 105 of those changes also being recorded in the absence of LPS. When exploring the effect of SF on a global scale including all 1210 genes induced by LPS the regression analysis demonstrated a significantly inverse linear relationship between the effect of LPS alone and the co-treatment of LPS and SF on gene expression with a gradient of the regression line calculated as -1.068. Annotated on **Figure 4.3** are IL-6, IL-1 $\beta$  and TNF $\alpha$ , the three cytokines that were focused on in Chapter 3. While IL-6 is fairly close to the line of best fit, IL-1 $\beta$  and TNF $\alpha$  demonstrate a lesser change with the co-treatment of LPS and SF compared to LPS alone, as demonstrated with real-time RT-PCR (**Figure 3.13** and

**3.14).** This highlights that there are many more genes that are particularly sensitive to LPS and to the presence of SF than the biomarkers previously used. It is important to note that while some gene expression changes demonstrate a 2-fold change in expression and others demonstrate 25-fold changes, the conclusion that should be made from these results is the magnitude of the number of changes seen. If SF is able to suppress low-grade inflammation induced as a result of circulating endotoxin levels in individuals with chronic disease, the reduction in the production of pro-inflammatory biomarkers that are associated with increased risk of CVD and cancer for example, means there is potential to prevent adverse inflammatory effects by consuming 1-2 portions of high-glucosinolate broccoli, which is achievable within a normal diet.

The results in this chapter provide the first evidence that a physiologically relevant concentration of 5 $\mu$ M SF is able to affect the gene expression of all genes induced by 1ng/ml LPS. Thus, evidence is provided that SF targets the TLR4 pathway as a whole and is not restricted to particular genes as investigated in Chapter 3. The next chapter will investigate a potential mechanism of direct interaction between SF and the TLR4 receptor to provide potential insights into how SF, at a concentration of 5 $\mu$ M is able to significantly suppress LPS-induced expression on a global scale.

#### **4.4. Conclusions**

In summary, the physiologically relevant concentration of 5 $\mu$ M SF was able to exert profound effects on global gene expression in THP-1 monocytes. Constitutively, SF was able to induce enzymes involved in xenobiotic metabolism and phase 2 enzymes, as has been previously shown.

LPS at a concentration of 1ng/ml, relevant to levels found in circulation of sufferers of chronic disease, significantly induced the expression of 1210 genes (adjusted p value < 0.01) and in the presence of 5 $\mu$ M SF, all of these genes were significantly suppressed (regression analysis:  $p < 0.001$ ,  $R^2 = 0.7$ ,  $Y = 0.19 - 1.068x$ ).

These results demonstrate that the anti-inflammatory effects seen with SF in Chapter 3 can be extended to all genes affected by LPS. The next chapter will aim to address a potential mechanism of SF, by investigating direct interactions with the TLR4 receptor.

# Chapter Five

---

Investigations into the mechanism of SF on  
TLR4 signalling

## **5.0. Introduction**

The results presented in Chapter 4 demonstrate the ability of SF, at a physiologically relevant concentration of 5µM, to reverse the global effects of LPS at a low concentration achieved *in vivo* during a state of chronic inflammation, in THP-1 monocytes. Based on these findings, it was hypothesised that SF was able to target the TLR4 signalling pathway at an early point within the cascade. Activation of the TLR4 receptor by the binding of its ligand LPS, results in the downstream activation of not only NF-κB and AP-1 responsible for the transcription of pro-inflammatory cytokines, but also the IRF3 transcription factor which controls the expression of IFNs and IFN-inducible genes

A widely recognised function of SF is its inhibitory effects on the activity of the transcription factor NF-κB by either targeting its transcriptional activity directly or by promoting inhibition or degradation of the inhibitor of NF-κB, which maintains the transcription factor in its inactive form within the cytoplasm [184, 189, 191-194]. This mechanism of SF is thought to be responsible for the suppression of pro-inflammatory cytokine expression. However, in Chapter 4 the effect of SF was not restricted to LPS-induced genes controlled by the NF-κB transcription factor, but also included many IFN-induced genes, whose transcription is controlled by IRF3. This would suggest that the global effect of SF on LPS signalling is greater than the mechanism of targeting only NF-κB.

A paper by Youn and colleagues suggested an alternative function for SF on LPS signalling which involved direct targeting of cysteine residues within the TLR4 receptor [195]. The publication describes the ability of SF to covalently bind to specific cysteine residues within the extracellular domain of the TLR4 and it hypothesised that this modification prevented the dimerisation of the receptor required for downstream signalling and subsequent activation of transcription factors to occur. However, limitations of this research include the use of a recombinant form of the protein, likely under reducing conditions and as a result the effects may not be representative of what happens with SF *in vitro* and *in vivo*. In addition, a concentration of 100µM SF was used, which is far in excess of the achievable concentrations following consumption of broccoli within the diet.

The structure of SF means it is able to behave as an electrophile and where available, has the ability to covalently bind to free thiol groups of cysteine residues. This function has

been recognised previously with a number of different proteins including the Keap1 protein, fundamental in the function of SF on Nrf2 signalling. The known protein targets of SF have been summarised by Melchini and colleagues [236].

In order to progress from this previous research, the objectives of this chapter was to investigate whether SF was able to bind cysteine residues within a recombinant form of the TLR4 extracellular domain using physiologically relevant concentrations of SF under non-reducing conditions. In addition, this aim was extended by investigating whether these SF-thiol adducts were able to form *in vitro* using cells exposed to SF in the presence or absence of LPS to determine whether cysteine modification was a plausible mechanism for the effect of SF on global LPS-induced gene expression at physiologically relevant concentrations (Chapter 4).

## **5.1. Materials and Methods**

Within this chapter, the recombinant TLR4 protein was treated with varying doses of SF and subjected to enzyme digestion to yield peptide fragments (section 2.8.1). In addition, proteins were extracted from HT-29 cells subjected to SF treatments (0-25 $\mu$ M) in the presence or absence 1ng/ml LPS for 1 hour, using an extraction kit designed to separate the soluble and the membrane fractions. To improve the specificity of the proteins present within the sample, IP was carried out on the whole protein extract from cells subjected to the same treatments. Both the soluble and membrane fraction samples and the IP samples were subjected to gel electrophoresis and immunoblotting with an anti-TLR4 antibody to identify protein bands for gel digestion. All of the recombinant peptides and the gel digest products were subjected to LC-MS/MS analysis to identify potential cysteine modifications within the TLR4 (see sections 2.7 and 2.8 for more details of the methods used).

## **5.2. Results**

### **5.2.1. Modification of TLR4 cysteine residues by SF under reducing and non-reducing conditions**

In the study by Youn and colleagues, 2 $\mu$ g of the purified extracellular domain of TLR4 was incubated with SF at a concentration of 100 $\mu$ M for 1 hour. The protein was

subjected to in-solution digestion with chymotrypsin, followed by trypsin before being quenched by the addition of formic acid.

A common step in proteomic analysis with enzymatic digestion is a step to reduce the protein of interest with DTT and alkylate the thiol groups the disulphide bonds to allow the enzymes to reach the interior of the protein structure and to prevent any disulphide bonds reforming. If the disulphide bridges of the TLR4 extracellular domain were reduced, the thiol groups of the cysteine residues would be free and able to be readily bound by SF, due to its electrophilic nature, and thus any binding could potentially be an artefact. In this experiment, 2µg of recombinant extracellular TLR4 was treated with 100µM SF for 1 hour in the same way as in the study by Youn. This treatment was followed by the addition of 1mM DTT (or Tris-HCl buffer as the vehicle control) for 15 minutes to compare the extent of SF-cysteine adducts formed under reducing or non-reducing conditions.

**Table 5.1** presents the cysteine residues which were bound by SF with and without DTT treatment. A clear increase was found in the amount of cysteines bound by SF with the reducing agent treatment. In addition, most of the cysteines identified as SF bound with DTT treatment were consistent with those found in the article by Youn and colleagues [195].

**Table 5.1. Cysteine residues bound by SF with and without DTT treatment**

Non-reducing conditions	Reducing conditions
Cys246	Cys192
Cys609	Cys246
	Cys390
	Cys391
	Cys506
	Cys542
	Cys583
	Cys585
	Cys609

### **5.2.2. Effect of SF at lower concentrations on TLR4 modification**

The next step was to establish whether this SF-cysteine adduct formation was able to occur with concentrations of SF that were more relevant to that physiologically

achievable following consumption of broccoli, under non-reducing conditions. Concentrations were chosen ranging from 5 $\mu$ M, which was used in my previous *in vitro* experiments with THP-1 monocytes (Chapters 3 and 4), up to 50 $\mu$ M.

As before, Cys609 and Cys246 were consistently found to be modified by SF (**Figure 5.1**). For each peptide fragment identified, the amount of detected b and y ions of the fragment were recorded. The b ions contain the N-terminus of the amino acid, while the y ions contain the C-terminus. Identification of more b and y ions increased the confidence that this modification was not as a result of a false discovery. Interestingly, the abundance of the SF-modified peptides containing the Cys246 and Cys609 residues increased dose-dependently (**Figure 5.2**). A small amount of modified Cys609-containing peptide was detected at 5 $\mu$ M, and while the abundance increased following a steady pattern until 25 $\mu$ M, a larger increase in abundance was observed when treated with 50 $\mu$ M SF (**Figure 5.2A**). For the modification of the peptide containing Cys246, the intensity of the peak was much lower than that measured for the peptide containing Cys609. There was also a level of modified peptide identified in the control-treated conditions suggesting that there was a higher level of background noise (**Figure 5.2B**). However, consistent with the pattern seen with the Cys609-containing peptide, there was a much larger level of SF modification of the Cys246 when subjected to 50 $\mu$ M SF (**Figure 5.2B**).

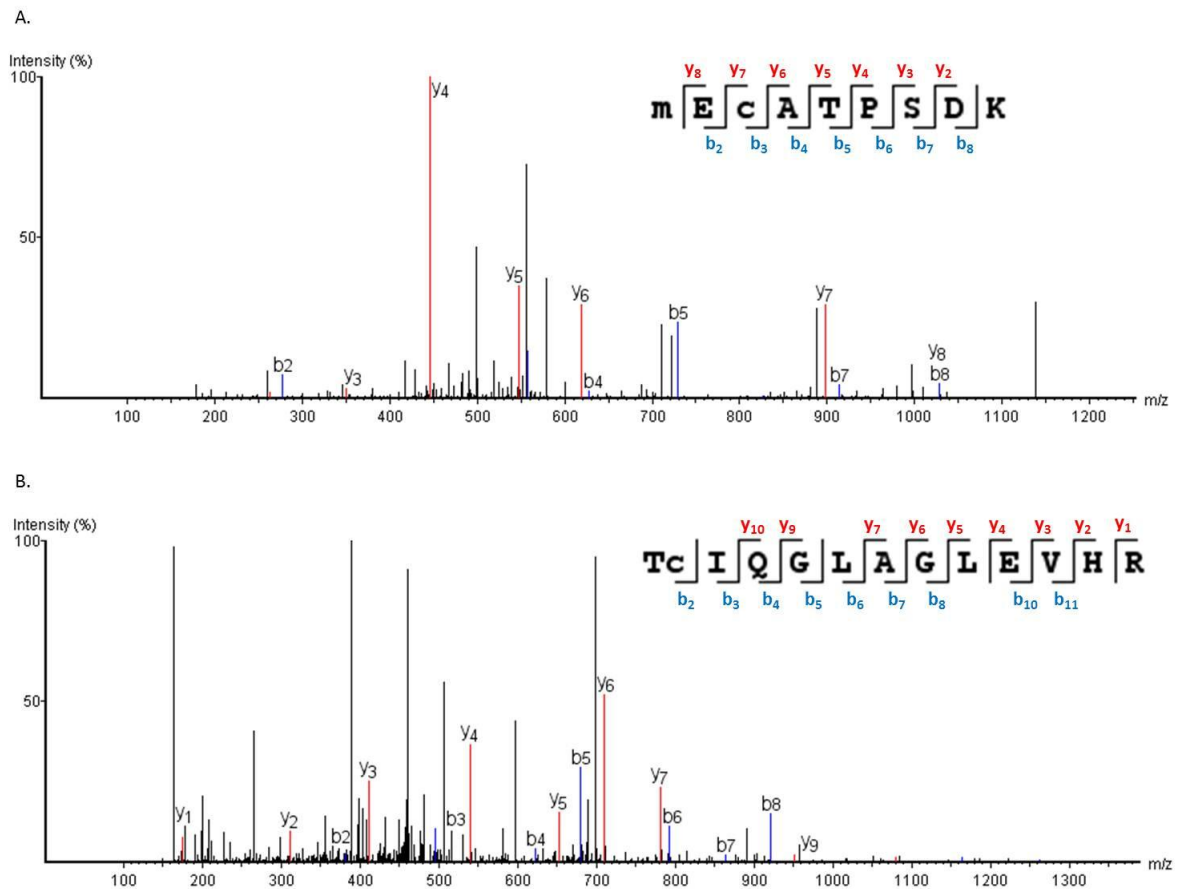


**Figure 5.1. SF directly modifies Cys609 (A) and Cys246 (B) within the extracellular domain of TLR4 under non-reducing conditions.** Recombinant extracellular domain of TLR4 (24-631 residues) was treated with SF (5-50 $\mu$ M; vehicle control for SF = < 0.1% (v/v) DMSO) for 1 hour at 37 $^{\circ}$ C prior to enzymatic digestion and micro-LC-MS/MS analysis using the LTQ Orbitrap. Data was analysed using Mascot against the Uniprot protein database to identify cysteine-bound SF modifications and oxidised methionine. Following analysis of the fragments using Peaks software the modified fragments were analysed. Sequences Met607-Lys615 (A) and Thr245-Arg257 (B) were identified as containing a SF-modified cysteine and b (blue) and y (red) fragment ions were assigned. Lower case m indicates oxidised methionine modification and lower case c represents SF-modified cysteine residue. The b and y ions are annotated in the spectra.

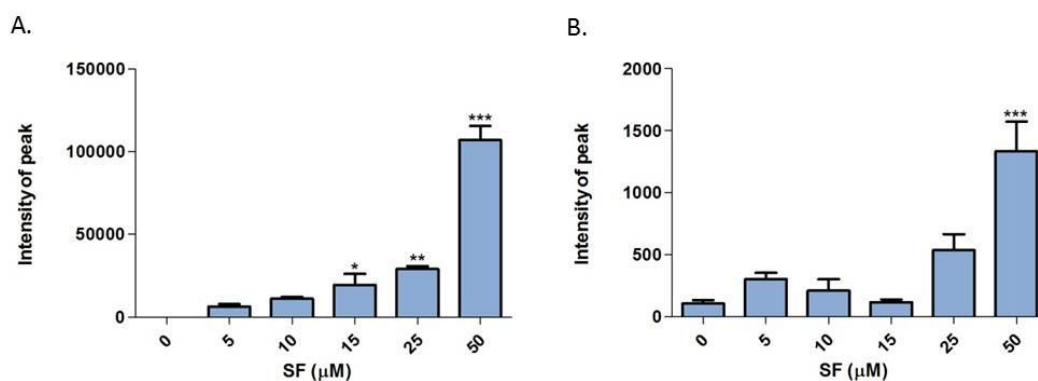


**Figure 5.2. Intensity of SF-modified peptides containing Cys609 (A) or Cys246 (B) in response to varying SF concentrations under non-reducing conditions.** Recombinant extracellular domain of TLR4 (24-631 residues) was treated with SF (5-50 μM; vehicle control for SF = < 0.1% (v/v) DMSO) for 1 hour at 37°C prior to enzymatic digestion and micro-LC-MS/MS analysis using the LTQ Orbitrap. Data was analysed using Mascot against the Uniprot protein database to identify cysteine-bound SF modifications and oxidised methionine. Data was then subjected to analysis with Progenesis software to determine the intensity of the SF-modified peptides at each SF concentrations. Data shown = mean ± SD, data representative of three independent experiments. Data was statistically analysed using one-way ANOVA followed by the Bonferroni multiple comparison test. \*p<0.05, \*\*p<0.01 and \*\*\*p<0.001 vs. 0 μM SF.

### 5.2.3. Quantification of TLR4 protein *in vitro*

To further progress with this research, the ability of SF to modify cysteine residues within the TLR4 was investigated as a plausible mechanism for the results seen with SF suppression of LPS-induced transcription on global scale and cytokine secretion in human monocyte cells (Chapters 3 and 4).

In the initial stages of optimisation, a western blot analysis was completed with protein extracts from THP-1 monocytes, as this was the cell model used in the previous experiments in this thesis. However, even after a number of optimisation steps only a very faint band for TLR4 was detected from THP-1 monocyte protein extracts and this was not reproducible (data not shown). As a result of these difficulties, the HT-29 colon cancer cell line was chosen for use. Intestinal cells were used as the positive control for the TLR4 antibody utilised in these experiments, and therefore it was suggested that the HT-29 cells may be more appropriate. As only a very small band was achieved with the THP-1 monocytes using a whole protein extract, a kit was used which was able to separate the insoluble membrane fraction from the soluble cytosolic protein fractions. TLR4 is anchored at the membrane when it binds to LPS but is also present in the cytosol, so by using this more complex protein extraction method, the level of protein

expression in both locations can be compared, but also the isolated samples can be used for separate subsequent analysis steps.

As with the THP-1 monocytes previously, it was initially difficult to achieve reproducible results. However, when the extracts were stored as a number of separate aliquots the data was consistently reproducible. For the TLR4 protein, it appeared more than one freeze-thaw cycle resulted in the denaturation of the structure so it was no longer recognised by the antibody, which explained the non-reproducibility.

HT-29 cells were treated with 5, 10 and 25 $\mu$ M SF for 1 hour in the presence or absence of 1ng/ml LPS. These concentrations were chosen based on the results in **Figure 5.2**, where SF-modified TLR4 peptides were identified, and excluding 50 $\mu$ M due to being far in excess of physiologically relevant levels. **Figure 5.3** displays the western blot analysis for TLR4 from both the cytosolic and the membrane protein fractions. A band at 93kDa was identified, which was the recommended molecular weight for TLR4 with this antibody. A number of additional bands were seen in the blots and were possibly due to fragmentation of the receptor during the protein extraction method.

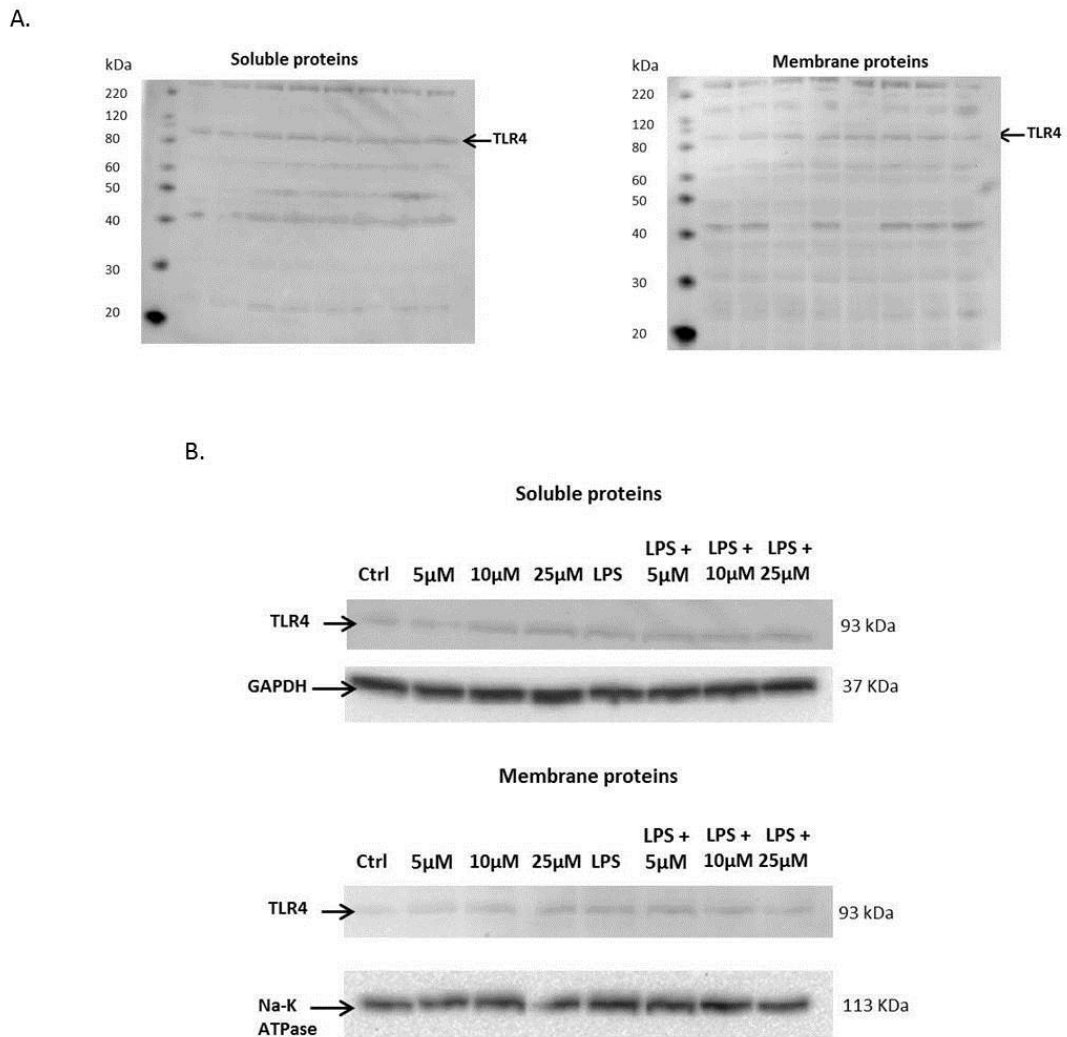


**Figure 5.3. TLR4 is expressed as a soluble and membrane bound protein.** (A) HT-29 cells were treated with SF (5, 10 and 25 $\mu$ M; vehicle control for SF = < 0.1% (v/v) DMSO) in the presence or absence of 1ng/ml LPS (vehicle control for LPS = PBS) for 1 hour. Proteins were extracted using a two-step kit that involved isolating the soluble protein fractions from the insoluble membrane protein fraction. The proteins were then separated using gel electrophoresis on a NuPage® 10% Bis-tris gel with NuPage® MOPS running buffer under non-reducing conditions. The proteins were transferred to a nitrocellulose membrane before being probed with anti-TLR4 at 2 $\mu$ g/ml in 2% (w/v) BSA/TBST followed by anti-mouse HRP-linked secondary antibody. Following the addition of a chemiluminescent substrate the blots were visualised. Representative of four blots from three independent protein extractions. (B). The 93kDa bands from the blots in (A) are represented here against the appropriate loading controls for soluble proteins (GAPDH) and for membrane proteins (Na-K ATPase).

#### **5.2.4. Investigations into SF modifications of TLR4 from HT-29 cells treated with SF in the presence or absence of LPS**

The next step was to carry out a gel digestion of the protein fragment around 93kDa (highlighted in **Figure 5.3**) followed by LC-MS/MS analysis to aim to identify potential SF modifications of cysteine residues within the TLR4, as with the cell-free recombinant protein studies.

HT-29 cells were treated with SF (5, 10 and 25 $\mu$ M) for 1 hour in the presence or absence of 1ng/ml LPS before proteins were extracted in the same way as in section 5.2.3. A duplicate of each protein sample was run on a gel. A duplicate was used to maximise the total amount of protein yield and hence give an increased likelihood of identifying TLR4 in both the membrane and the cytosolic fraction. The gels were stained with a coomassie blue stain to allow visualisation of all of the proteins present in the sample. As seen in **Figure 5.3**, the TLR4 band was identified at approximately 93kDa and so for enzymatic digestion, the area of the gel that was selected was between the 80 and 100kDa marker bands (**Figure 5.4**).

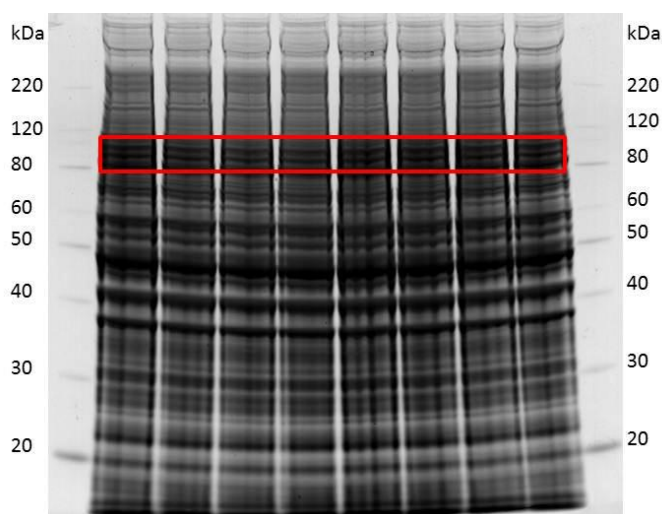


**Figure 5.4. Densitometry blots of the gels for digestion.** HT-29 cells were treated with SF (5, 10 and 25 $\mu$ M; vehicle control for SF = < 0.1% (v/v) DMSO) in the presence or absence of 1ng/ml LPS (vehicle control for LPS = PBS) for 1 hour. Proteins were extracted using a two-step kit that involves isolating the soluble protein fractions from the membrane protein fraction (section 2.7.2). The proteins were then separated using gel electrophoresis on a NuPage® 10% Bis-tris gel with NuPage® MOPS running buffer under non-reducing conditions and each sample was run in duplicate. The gels were stained and digested according to details in section 2.8.2. Data shown is representative of the four gels produced (two from the cytosolic samples and 2 from the membrane fractions). The red box surrounds the area of the gel excised for analysis via LC-MS/MS.

Following enzymatic digestion of the peptides within the gel pieces, the samples were subjected to LC-MS/MS analysis to aim to identify TLR4 peptide fragments with or without SF modifications. When data was analysed using Mascot software, TLR4 was not identified. **Table 5.2** lists the 12 most highly scored proteins identified within the membrane fraction from HT-29 cells treated with 10 $\mu$ M SF with 1ng/ml LPS. The results from this sample demonstrated the most representative results for all the membrane and cytosolic fraction samples. Across the different treatments, the findings were fairly consistent with the most highly scored proteins identified in all samples. Based on the majority of proteins identified being within the 80-110kDa molecular weight, this data confirms that the positioning of the gel digest for identifying a 93kDa TLR4 protein was correct.

**Table 5.2. Proteins identified by LC-MS/MS from gel digestion samples\***

Family**	Member	Accession	Name of Gene	Score	Mass (Da)	# of peptide matches	# of significant peptide matches	# of sequences	# of significant sequences
1	1	O43707	Alpha-actinin-4	1309	105245	66	43	45	31
1	2	B7Z565	cDNA FLJ54739, highly similar to Alpha-actinin-1	515	95237	35	19	26	15
1	3	B2RCS5	Alpha-actinin-2	319	104425	18	9	14	7
2	1	P55072	Transitional endoplasmic reticulum ATPase	942	89950	38	25	29	21
3	1	P08238	Heat Shock Protein 90-beta	909	83554	54	34	37	23
3	2	K9JA46	Epididymis luminal secretory protein 52	694	85006	39	23	29	19
3	3	P14625	Endoplasmin	169	92696	10	4	9	3
4	1	Q1KLZ0	HCG15971, isoform CRA_a	861	42052	33	28	19	18
4	2	A8K3K1	cDNA FLJ78096, highly similar to Homo Sapiens actin, alpha, cardiac muscle (ACTC), mRNA	525	42362	23	20	13	13
5	1	P19338	Nucleolin	716	76625	41	25	27	18
6	1	P13639	Elongation factor 2	665	96246	38	27	28	20
7	1	Q14444	Caprin-1	518	78489	21	14	16	11

\*This list of proteins is from the samples of HT-29 membrane proteins subjected to 10 $\mu$ M SF and LPS treatment with a peptide mass tolerance of 5ppm. This is representative of all samples measured, both membrane and cytosolic fractions.

\*\*Proteins are categorised into families when a high level of shared peptide matches are identified.

## **5.2.5. Identification of potential SF-modified TLR4 using immunoprecipitation**

### **5.2.5.1. Immunoprecipitation and gel electrophoresis**

In an attempt to identify SF-modified TLR4 fragments, the work from the gel digest was followed with the use of an IP method prior to gel electrophoresis. This method was advantageous compared to the previous gel digest method due to the fact that with IP, the TLR4 will be isolated from the crude protein extract and therefore will not compete with the large amount of proteins present in the sample at the same molecular weight in terms of abundance.

HT-29 cells were treated as before for 1 hour with SF (5, 10 and 25 $\mu$ M) in the presence or absence of 1ng/ml LPS. Total proteins were extracted using the lysis buffer provided in the Pierce Classic IP kit, therefore combining those proteins present within the membrane of the cells but also within the cytosol, unlike in previous experiments where these localised pools of protein were separated. It was deemed unnecessary to separate the membrane and cytosolic fractions due to the comparable findings of both fractions when analysed by LC-MS/MS (**Table 5.2**).

In order to isolate TLR4 from the total protein extract, an immune complex was prepared. This involved combining the protein lysate with the anti-TLR4 antibody, before adding this to the protein A/G agarose to capture the antibody-bound TLR4 protein. This antibody-protein complex was then eluted into sample buffer under reducing conditions to subject directly to gel electrophoresis. Following gel electrophoresis, the gels were stained with a coomassie blue stain to identify proteins present within the samples. In addition, a western blot analysis was carried out to compare with the coomassie blue stained gel. The densitometry blot of the coomassie blue stained gel and the visualised western blot are presented in **Figure 5.5**. Five bands were annotated as being of interest in **Figure 5.5** and were subjected to gel digestion. The reasons for this were that bands 2-5 appeared to vary with the treatment of the cells while band 1 appeared to be fairly consistently present in all the samples. In order to determine whether there was any indication of an effect of the treatments, the band volumes were quantified. To give some level of normalisation, the band at around 25kDa which is attributed to the anti-TLR4 antibody, was used.

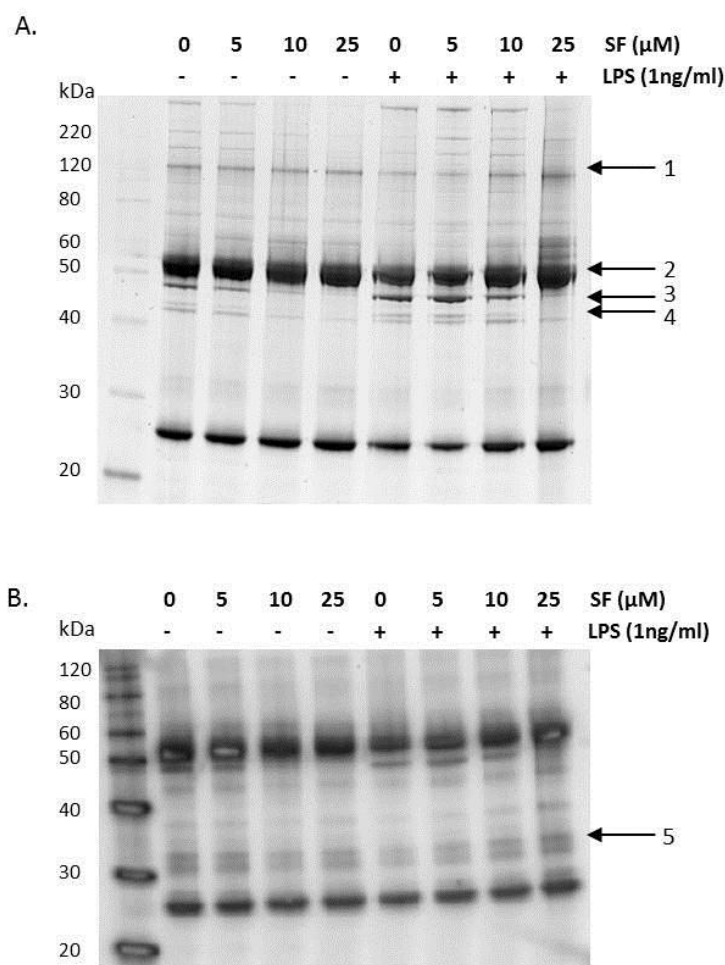


**Figure 5.5. Analysis of immunoprecipitation product by gel electrophoresis with coomassie blue stain (A) and western blot analysis (B) for TLR4.** HT-29 cells were treated with SF (5, 10 and 25 $\mu$ M; vehicle control for SF = < 0.1% (v/v) DMSO) in the presence or absence of LPS (1ng/ml; vehicle control for LPS = PBS) for 1 hour. Proteins were extracted from the cells and immunoprecipitated using the Pierce Classic IP kit following manufacturer's instructions. In order to immunoprecipitate the TLR4 protein, the mouse monoclonal anti-TLR4 antibody was used. The antigen-antibody complex was eluted in sample buffer under reducing conditions and subjected to gel electrophoresis. One gel was stained with GelCode Blue Stain overnight (A) and densitometry measured using the GS800 Calibrated Densitometer. The other gel was subjected to western blot analysis with the same anti-TLR4 antibody and chemiluminescence was measured using anti-mouse HRP-linked secondary antibody and a chemiluminescent substrate (B). Annotations 1-5 are the bands that were identified for gel digestion and analysis via LC-MS/MS.

The bands highlighted in **Figure 5.5** were quantified using the Quantity One software to get some indications as to whether treatment effects were observed.

In **Figure 5.6**, the data presented demonstrates varying effects of SF and LPS on the highlighted bands. While band 1 appears to have no consistent pattern in response to SF or LPS, band 2 demonstrates a slight reduction in the levels with increasing doses of SF (**Figure 5.6A-B**). Of particular interest are bands 3 and 4 which demonstrate similar patterns with a reduction at higher concentrations of SF relative to the control, while both are induced by LPS. When subjected to a combined treatment of LPS and SF, 10 and 25 $\mu$ M SF treatment results in a large reduction of the levels of bands 3 and 4 (**Figure 5.6C-D**). Band 5 follows a different pattern where SF reduces the levels in the absence of LPS and when treated with LPS alone, a reduction in the levels relative to the control was observed. When treated in combination with LPS and SF, there is a dose-dependent restoration of the level of the protein present to that measured in the control condition (**Figure 5.6E**).

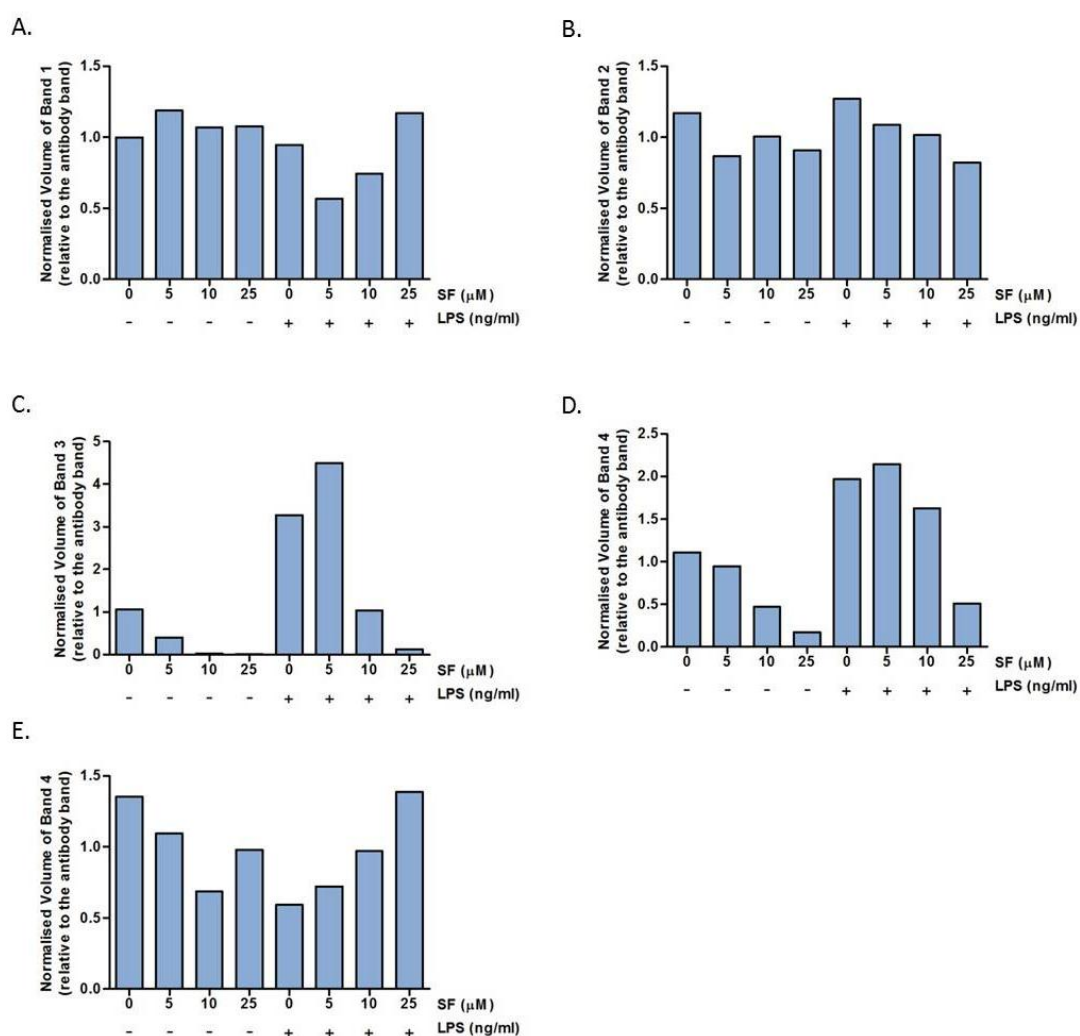


**Figure 5.6. Quantification of the bands of interest from the IP product.** Using the Quantity One software necessary to visualise both the coomassie blue stained gel and the western blot, the individual bands annotated in **Figure 5.5** were quantified based on their volume and were normalised using the volume of the antibody band for each corresponding lane.

#### **5.2.5.2. LC-MS/MS analysis of gel digestion fragments**

From the five digested protein bands subjected to gel digestion (**Figure 5.5**), TLR4 was not identified in any of the samples. High levels of keratin was found within the samples suggesting a technical contamination during the procedure for preparing samples from the stained gel through until the samples were ready for LC-MS/MS analysis. Following the staining of the gel, there was a period where the gel had semi-dried and it is possible it was at this point that keratins were able to penetrate the gel and following reconstitution the keratins remained present within the gel. In order to confirm the identity of the proteins present in the bands highlighted in **Figures 5.5** and **5.6**, this experiment would need to be repeated.

### **5.3. Discussion**

In experiments with the recombinant TLR4 receptor, SF at 100 $\mu$ M was able to modify Cys246 and Cys609 of the TLR4 molecule under non-reducing conditions, and when carried out under reducing conditions, results were comparable with Youn and colleagues with many cysteine residues demonstration thiol modification [195]. The modification of Cys609 was also detected with SF at low concentrations with a dose-dependent increase with concentrations of 5 $\mu$ M to 25 $\mu$ M, with a large increase when subjected to treatment with 50 $\mu$ M SF (**Figure 5.1A**). With Cys246, there were slightly different findings however a significant increase was seen in the levels of modified protein at 50 $\mu$ M (**Figure 5.1B**). These results demonstrated that Cys609 was most sensitive to modification by SF even at the lower, physiologically relevant concentrations. These novel findings suggest that Cys246 and Cys609 are potentially most important for the suppression of LPS-induced gene expression, but this hypothesis requires more investigation.

Interestingly, when investigating the Cys609 residue, it was found that it is attributed to a disulphide bridge with Cys583 according to the Uniprot database (Accession Number: O00206) [8, 237, 238]. While Cys609 was found to be modified under both non-reducing and reducing conditions, the other reported cysteine within the disulphide bond, Cys583, was only modified by SF following a reduction step using DTT (**Table 5.1**). To investigate the existence of this particular disulphide bond, the literature that was referred to in the Uniprot database was reviewed and no evidence of support for the presence of this disulphide bridge was found in any of the articles cited [8, 237, 238]. The combination of the lack of literature findings with my observations that Cys609 was bound by SF in the absence

of a reduction treatment (**Table 5.1** and **Figure 5.1**), does not corroborate the presence of the disulphide bonds in the experimental design presented in this chapter.

The mechanism of cysteine modification by SF was not a novel concept [236]. With relevance to the ability of SF to significantly suppress LPS-induced gene expression, SF has also been identified as being able to modify the Cys133 residue within the mouse MD2 protein, the co-receptor of TLR4 required for LPS-induced signalling. This modification prevents LPS binding to MD2 [196]. Cys133 is freely available while other cysteines present within the structure of MD2 are involved in disulphide bonds. Those involved in disulphide bonds were not modified by SF, suggesting that in order for SF to covalently modify cysteine residues, the thiol group must be free. In combination with the identified TLR4 modification by SF, this evidence in a cell-free system may support the hypothesis that SF is able to significantly suppress LPS-induced gene expression on a global scale as a result of targeting the receptor and its interaction with its specific ligand, LPS.

Additionally, modification of cysteine residues by SF has been described as a plausible explanation for additional functions of SF such as its role in Nrf2 activation. During a basal state, Nrf2 is sequestered within the cytoplasm of the cell via its inhibitory co-factor, Keap1, which behaves to target the Nrf2 transcription factor for proteosomal degradation [154]. When activated by the presence of an Nrf2 inducer for example SF, Keap1 is no longer able to sequester the Nrf2 to the cytoplasm, leaving Nrf2 free to translocate to the nucleus and activate the transcription of ARE-controlled genes [155]. SF was identified as being able to directly interact with the thiol group of the Cys151 residue within the Keap1 protein, a residue essential for the activity of the protein [156-159].

All evidence of direct binding of SF to thiol groups of cysteine residues within target proteins has come from LC-MS/MS analysis utilising recombinant forms of the proteins and subjecting them to SF treatment, often at concentrations that cannot be achieved *in vivo* following the consumption of broccoli. While a lack of Nrf2 activation was seen in cells exposed to SF when Cys151 within the Keap1 protein was substituted with a serine residue, this experimental design has not been undertaken with TLR4 or MD2, making it difficult to justify the importance of the cysteine modification and the relevance to the anti-inflammatory effects of SF *in vitro* and *in vivo*. For this reason, investigations were carried out into whether the modified cysteine residues could be identified within the TLR4 in a cell model following exposure to SF.

To investigate whether it was possible to demonstrate SF thiol modification of TLR4 *in vitro* HT-29 cells with SF (5, 10 and 25 $\mu$ M) in the presence or absence of 1ng/ml LPS for 1 hour prior to extracting the cytosolic and membrane protein pools. These samples were subjected to gel electrophoresis and following coomassie blue staining, a band was excised from gels covering the region between 80-100kDa, the area at which the TLR4 protein with a molecular weight of 93kDa should potentially be found. The proteins present within the band were subjected to a chymotrypsin/trypsin double enzyme digestion to yield peptides that were subjected to LC-MS/MS analysis. When analysed, the data did not identify the TLR4 protein as present within the band. Reasons for the lack of identifying TLR4 within these samples include the fact that the TLR4 is likely to be expressed at very low levels compared to actin proteins found within the samples (**Table 5.2**) and therefore the TLR4 would have to compete for identification. When exposed to the enzymes during digestion, TLR4 would also have to contest with the other proteins present within the band to be digested and in addition, when analysed via LC-MS/MS there would be competition between the peptides for ionisation and subsequent identification. If the experiment was to be repeated, a band over a more narrow range could be excised to try and increase the probability of TLR4 identification.

IP techniques were subsequently used with the cell lysate to try and improve the probability of identifying SF-modified TLR4 and when a western blot was carried out a number of interesting bands were discovered that appeared to change with LPS and SF treatment. However, whether these results were a true effect of SF and LPS remain to be determined as LC-MS/MS analysis did not identify the TLR4 protein within any of the samples analysed and instead the highest scoring proteins were keratins (data not shown). This was thought to be due to contamination following the drying of the gel which occurred after the staining procedure. While the gel remained intact following rehydration, it is possible keratins from the environment were able to penetrate the gel and hence were present within the digested peptides. However, due to the identification of protein bands within the IP product which were thought to be specific interactions with the TLR4 molecule, in combination with bands that demonstrated differing effects with SF and LPS treatments in some cases, it is important that this experiment be repeated in future work, ensuring stricter experimental procedures are used.

While there were a fairly large number of treatments used with the IP experimental design which may result in difficulties when trying to further the work, it would be necessary to repeat these experiments with the same conditions as it is important to investigate the effect

of SF both with and without LPS. In the absence of LPS, the potential modifications between TLR4 and SF in a resting state can be investigated, while in the presence of LPS, investigation can be carried out into whether SF is able to modify the TLR4 and prevent LPS binding in addition to addressing the question of whether SF is able to bind to TLR4 and prevent downstream activation following ligand binding.

Within Chapters 3 to 5, all the research focused on the TLR4 signalling pathway. In the next chapter, the scope of the research was broadened to investigate whether the effect of SF was restricted to TLR4 signalling or whether SF was also able to target TLR2 and NOD2 pathways, which are also of fundamental importance in chronic inflammatory signalling.

## **5.4 Conclusion**

To summarise, it was demonstrated that physiologically relevant concentrations of SF, as low as 5µM, were able to modify Cys609 and Cys246 present in the extracellular domain of recombinant TLR4. These residues remained modified under non-reducing conditions, suggesting these may be of larger importance to a potential mechanism.

To investigate whether this was a plausible mechanism to explain the global effects on the TLR4 pathway seen *in vitro*, a gel digest was carried out from both a crude total protein sample and an IP product with the aim to enrich the presence of TLR4. In both experimental designs, there was no identification of TLR4. This is likely as a result of technical drawbacks and while indications of proteins dependent on both LPS and SF treatments were identified from the IP product, the lack of LC-MS/MS confirmation means this experiment would need to be repeated with an optimised protocol.

Thus far, the TLR4 signalling pathway has been the sole focus of this thesis. The next chapter will aim to address whether SF has the ability to target other inflammatory signalling pathways, namely TLR2 and NOD2, and whether common polymorphisms in the TLR4 and NOD2 receptors implicated in Crohn's disease, affect the response to their ligands or SF.

# Chapter Six

---

Effect of SF on NF- $\kappa$ B in PRR-expressing cell  
models

## 6.0. Introduction

In the previous chapter, evidence was provided to demonstrate that SF at physiologically relevant concentrations could directly target and modify cysteine residues within the TLR4 (Chapter 5). Furthermore, this mechanism may be able to explain the global effect SF can exert on LPS signalling (Chapter 4). However, until this point only the TLR4 pathway has been focused on. This chapter aimed to address whether the suppressive effect of SF was specific to TLR4 signalling, or whether SF was able to target other important signalling pathways involved in chronic inflammation. Additionally, investigations were carried out into whether any differences were observed in the effect of SF when comparing L-SF and DL-SF forms.

### 6.0.1. L-SF versus DL-SF

Both L-SF and DL-SF compounds have been widely investigated *in vitro*, and throughout this thesis, the DL-SF form was used. L-SF is isolated from broccoli and is known to be biologically active. SF is a chiral molecule meaning it has two non-superimposable mirror-image compounds, L-SF and the stereoisomer D-SF. DL-SF is the racemic mixture and is available commercially as a synthetic analogue of the naturally occurring L-SF [239]. Its synthetic nature has advantages e.g. it is cheaper to produce and is potentially a more consistent product, whereas L-SF is derived from broccoli which is advantageous due to being the biologically active breakdown product found in circulation following broccoli consumption [239]. The stereoisomer of L-SF, D-SF is also commercially available, however due to the low natural abundance in broccoli, no research has been carried out investigating the biological activity of this form. The hypothesis was that no significant differences in the biological activity of the naturally occurring L-SF and the synthetic DL-SF will be observed. Support for this hypothesis includes a study by Zhang and colleagues who found equipotent levels of quinone reductase induction when comparing L-SF and DL-SF *in vitro* [239].

### 6.0.2. Chronic inflammatory signalling pathways

In recent years it has become more widely accepted that a state of low-grade inflammation is a contributing common factor to many chronic diseases such as cancer, atherosclerosis and IBDs [205]. The importance in trying to prevent the development of these chronic diseases, the leading causes of mortality throughout the world, and improving potential treatment

options, is crucial. With chronic inflammation as a mutual factor in these diseases, this has become an increasingly attractive target for dietary and pharmaceutical interventions.

Inflammatory signalling in chronic diseases is controlled by an array of PRRs which behave to recognise specific PAMPs, resulting in the activation of their associated signalling pathways [240]. The main classes of PRRs are the TLRs, NLRs and RLRs [241] and within this chapter TLR4, TLR2 and NOD2 have been investigated. The TLR4, TLR2 and NOD2 pathways are individually activated in response to their specific ligands but ultimately, these pathways converge with NF- $\kappa$ B activation common to all (**Figure 6.1**). As mentioned in previous chapters, TLR4 responds specifically to LPS and can follow one of two different pathways: a MyD88-independent pathway which results in the activation of the transcription factor IRF3 followed by NF- $\kappa$ B, or a MyD88-dependent pathway that results in the activation of NF- $\kappa$ B and AP-1. This MyD88-dependent pathway is also common to the TLR2 signalling pathway, which is activated in response to lipopeptides. NOD2 signalling is triggered in response to MDP binding and also results in the activation of NF- $\kappa$ B and AP-1. While NOD2 signalling doesn't involve MyD88, adaptors common to the TLR4, TLR2 and NOD2 pathways prior to NF- $\kappa$ B transcription factor activation, including RIP1 and MAPKs, are necessary for signalling to occur [240].

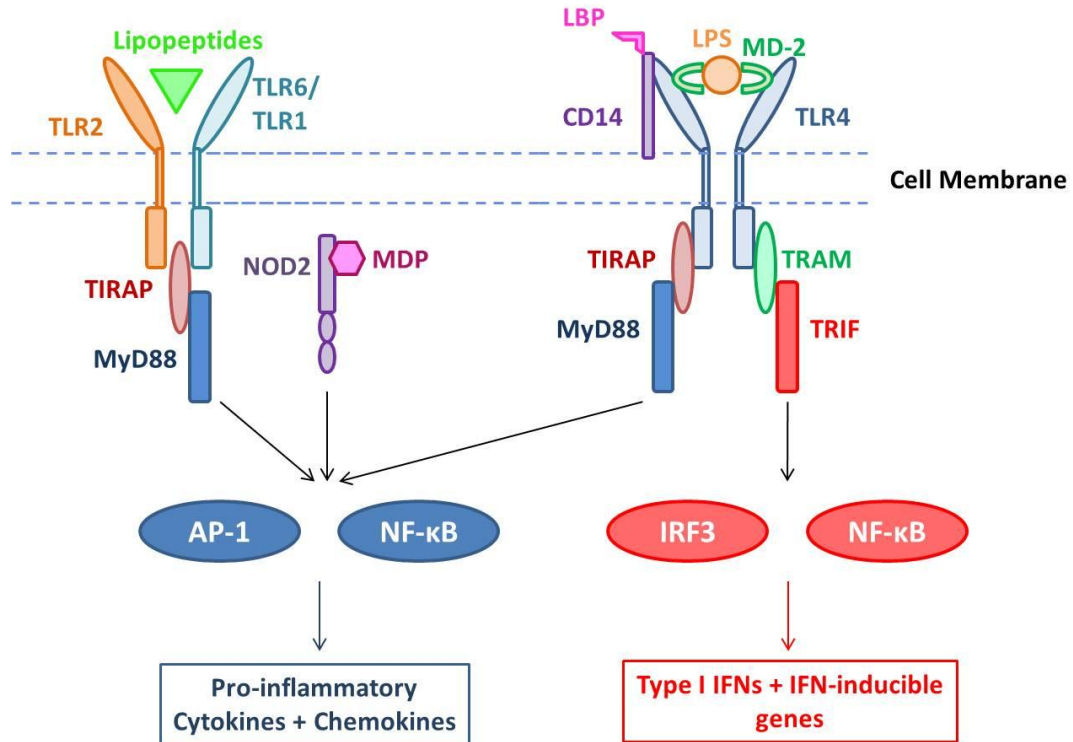


**Figure 6.1. Overview of the TLR4, TLR2 and NOD2 signalling pathways.** In the TLR4 signalling pathway, LPS binds to the TLR4-MD2 complex via the aid of LBP and CD14 accessory proteins. The binding of LPS to the TLR4-MD2 complex results in homodimerisation and activation of an intracellular signalling cascade. This can be MyD88-independent or dependent. The MyD88-independent pathway results in the activation of IRF3 followed later by NF- $\kappa$ B. This leads to the expression of type I IFNs and IFN-inducible genes. The MyD88-dependent pathway stimulates NF- $\kappa$ B and AP-1 resulting in pro-inflammatory cytokine and chemokine expression [13, 14]. The MyD88-dependent pathway is also activated as a result of lipopeptides binding to TLR2. In addition, adaptor proteins downstream of MyD88 can be activated by MDP binding to the intracellular NOD2 receptor, again resulting in the activation of NF- $\kappa$ B and AP-1 [240].

The reason for focusing on the TLR4, TLR2 and NOD2 signalling pathways is due to identified associations with chronic inflammatory pathologies. Increased TLR4 and TLR2 expression levels have been linked to chronic diseases including IBDs [48-50], cancer [30], metabolic syndrome [242, 243], atherosclerosis [36], obesity [44] and T2DM [44]. Identified polymorphisms within TLR4, namely D299G where an aspartate residue at position 299 has been substituted with a glycine and T399I where a threonine at position 399 has been replaced with an isoleucine residue, have also been investigated in patients with IBDs with contradictory results reported [54-62]. Conversely, these polymorphisms have been associated with a protective function against T2DM [244].

NOD2 has been widely studied in Crohn's disease and three SNPs have been commonly associated with IBDs. One SNP results in a frameshift mutation within the NOD2 receptor sequence, which leads to the introduction of an early stop codon. As a result, a truncated NOD2 protein is produced with the final 33 amino acids of the protein missing [53]. The other two commonly associated SNPs are missense mutations, G908R where a glycine residue at position 908 has been replaced with an arginine residue and R702W, where an arginine residue at position 702 is replaced with a tryptophan [245]. Approximately 15% of Crohn's disease patients are found to have at least one of these mutations in the NOD2 receptor and these three polymorphisms described account for 82% of the mutations in NOD2 found in patients suffering from Crohn's disease or UC [51, 52]. These NOD2 polymorphisms have also been found at higher prevalence in patients with coronary artery disease [246] and some cancers [247], however, further research needs to be carried out to firmly establish a link as seen with Crohn's disease.

Based on previously published data and the results from earlier chapters, the hypothesis within this chapter was that both the L-SF and DL-SF compounds would significantly suppress NF- $\kappa$ B activity induced in response to appropriate TLR4, TLR2 and NOD2 ligands, with the same extent of suppression observed with each form, was tested. In addition, mutations within these receptors that are commonly associated with IBDs were studied to determine if they affected the response to either the ligand or SF treatments.

## **6.1. Materials and Methods**

For the experiments within this chapter HEK-Blue<sup>TM</sup> cells or HEK cells transfected in-house, either stably or transiently transfected, were used (section 2.2.2). These cell lines were subjected to various treatments with their appropriate ligands in the presence or absence of SF (2, 5 and 10 $\mu$ M) for 24 hours before the cell culture supernatant was used to determine the level of NF- $\kappa$ B activity indirectly via the use of a QUANTI-Blue<sup>TM</sup> assay that measures the level of AP enzyme activity (section 2.9). To investigate the effect of SF on the viability of these HEK cells, a WST-1 cell viability assay was used (section 2.3).

## 6.2. Results

### 6.2.1. Effect of SF on cell viability of HEK293 cells

To determine which concentration of L-SF and DL-SF to use for the experiments to test the effect of SF on NF- $\kappa$ B activity, HEK-Blue<sup>TM</sup> TLR4, TLR2, NOD2 (wildtype and G908R mutant) cells were treated with L-SF or DL-SF (0-200 $\mu$ M) for 24 hours and a WST-1 cell viability assay was carried out. The data was analysed collectively because HEK293 cells were used consistently, with only the receptor they were transfected with changing. L-SF caused a significant reduction in cell viability at concentrations of 15 $\mu$ M and above (**Figure 6.2A**) while with DL-SF, concentrations of 10 $\mu$ M and above resulted in significant reductions in cell viability (**Figure 6.2B**).

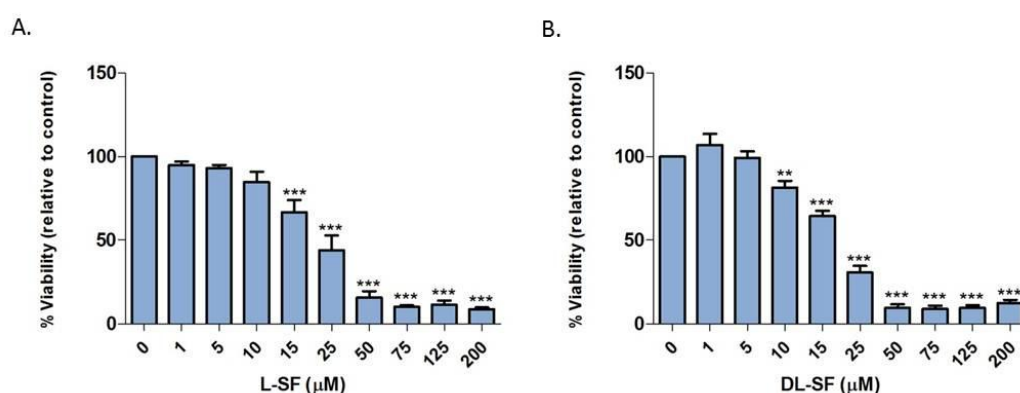


**Figure 6.2. Effect of SF on viability of HEK293 cells.** HEK-Blue<sup>TM</sup> cells were treated with A) L-SF or B) DL-SF (0-200 $\mu$ M; vehicle control for L-SF and DL-SF = < 0.1% (v/v) DMSO) for 24 hours. After treatment was complete, 10 $\mu$ l WST-1 reagent was added to each well. The plates were incubated at 37 $^{\circ}$ C and measured using a spectrophotometer at 450nm every 30 minutes for 3 hours. Data shown is from the 1.5 hour measurement at which the levels of absorbance were all measurable and consistent. Data shown = mean  $\pm$  SEM, n = 4. Data was statistically analysed using one-way ANOVA followed by the Bonferroni multiple comparison test. \*\*p<0.01 and \*\*\*p<0.001 vs. 0 $\mu$ M.

To determine whether there were any differences in the level of cytotoxicity between the L-SF and DL-SF compounds, the IC<sub>50</sub> for each compound was calculated. Using a t-test, no significant difference was found in the levels of cytotoxicity with L-SF and DL-SF (**Table 6.1**).

**Table 6.1. IC<sub>50</sub> for L-SF and DL-SF on HEK293 cells**

	IC <sub>50</sub> ( $\mu$ M)	SEM	P value
<b>L-SF</b>	23.92	3.94	0.148
<b>DL-SF</b>	17.01	1.35	

The IC<sub>50</sub> values were compared using the Student's T-test,  $p > 0.05$  = non-significant.

### 6.2.2. Effect of SF on NF- $\kappa$ B activity in TLR4-expressing cells

To determine whether 1ng/ml LPS (the concentration used in previous chapters) was sufficient to induce NF- $\kappa$ B activity in TLR4-expressing cells, HEK-Blue<sup>TM</sup>-hTLR4 cells were treated with 1, 5 and 10ng/ml LPS for 24 hours and level of SEAP was analysed as a measure of NF- $\kappa$ B activity. A significant induction of NF- $\kappa$ B activity was seen in response to 1, 5 and 10ng/ml LPS (**Figure 6.3**).

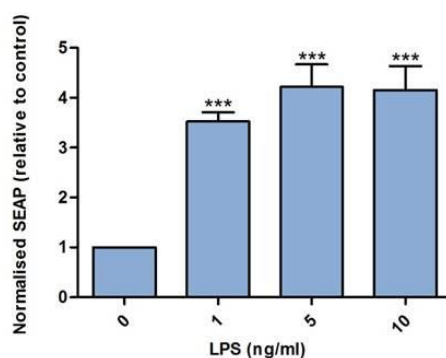


**Figure 6.3. LPS significantly induces NF- $\kappa$ B activity in HEK-Blue<sup>TM</sup>-hTLR4 cells.** HEK-Blue<sup>TM</sup>-hTLR4 cells were treated with LPS (1, 5 and 10ng/ml; vehicle control for LPS = PBS) for 24 hours. Cell culture supernatant was added to QUANTI-Blue<sup>TM</sup> solution until colour change was evident (pink to purple blue, caused by the activity of SEAP). The colour change induced by SEAP was analysed as a measure of NF- $\kappa$ B activity at 650nm using a spectrophotometer. Data shown = mean  $\pm$  SEM,  $n = 4$ . Data was statistically analysed using one-way ANOVA followed by the Bonferroni multiple comparison test. \*\*\* $p < 0.001$  vs. 0ng/ml.

Based on the findings in **Figure 6.2**, concentrations of both L-SF and DL-SF up to 10 $\mu$ M were chosen for use in further experiments, where cell viability would be maintained at above 80%. This was to ensure that any effects observed on NF- $\kappa$ B activity were not as a result of cytotoxic effects induced by SF. Both L-SF and DL-SF at concentrations of 5 and 10 $\mu$ M were able to significantly suppress NF- $\kappa$ B induction seen in response to 1ng/ml LPS (**Figure 6.4**).

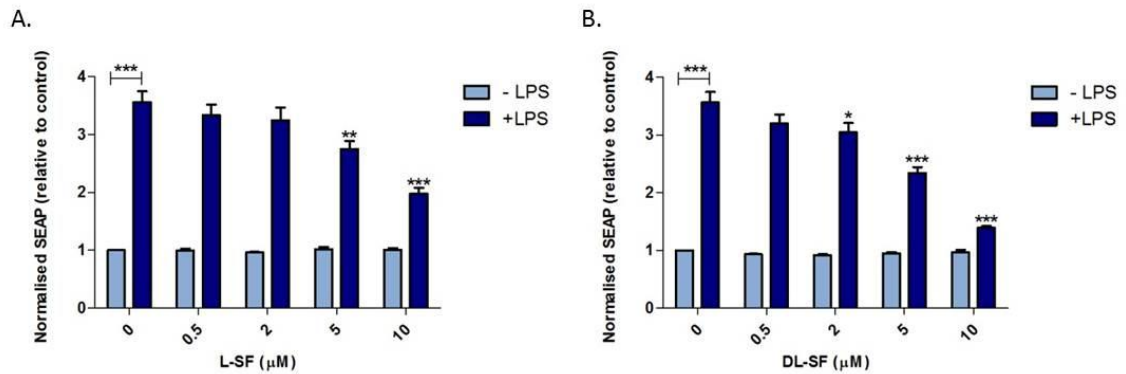


**Figure 6.4. L-SF and DL-SF significantly suppress LPS-induced NF- $\kappa$ B activity in HEK-Blue<sup>TM</sup>-hTLR4 cells.** HEK-Blue<sup>TM</sup>-hTLR4 cells were treated with A) L-SF or B) DL-SF (0.5, 2, 5 or 10 $\mu$ M; vehicle control for L-SF and DL-SF = < 0.1% (v/v) DMSO) in the presence or absence of LPS (1ng/ml; vehicle control for LPS = PBS) for 24 hours. Cell culture supernatant was added to QUANTI-Blue<sup>TM</sup> solution until colour change was evident (pink to purple blue, caused by the activity of SEAP). The colour change induced by SEAP was analysed as a measure of NF- $\kappa$ B activity at 650nm using a spectrophotometer. Data shown = mean  $\pm$  SEM, n = 4. \*p<0.05, \*\*p<0.01 and \*\*\*p<0.001, comparison to 0 $\mu$ M + LPS.

### 6.2.3. Effect of SF on NF- $\kappa$ B activity in transiently transfected TLR4 cells

In Crohn's disease, a higher prevalence of two SNPs within the TLR4 receptor, D299G and T399I, have been reported, though it is controversial [54-62]. These TLR4 variants were investigated to determine if the mutations resulted in a different response to either their ligand LPS, or to SF. HEK293 cells were transiently transfected with either the wildtype or mutant TLR4 receptors in addition to the NF- $\kappa$ B-controlled SEAP reporter gene. Cells were treated with LPS (1, 5 and 10ng/ml) for 24 hours before NF- $\kappa$ B activity was measured to determine whether the transiently transfected TLR4 cells responded to the same extent to LPS as the stably transfected cells previously used (section 6.2.2). A concentration of 1ng/ml LPS was sufficient to significantly induce NF- $\kappa$ B activity in cells expressing the wildtype TLR4 receptor (**Figure 6.5A**) and the mutant receptors, D299G and T399I (**Figure 6.5B-C**). The extent of the response to LPS was compared across cells expressing the wildtype and the mutant TLR4 receptors and no significant differences were seen in the level of NF- $\kappa$ B activity induced in response to LPS (**Figure 6.5D**).

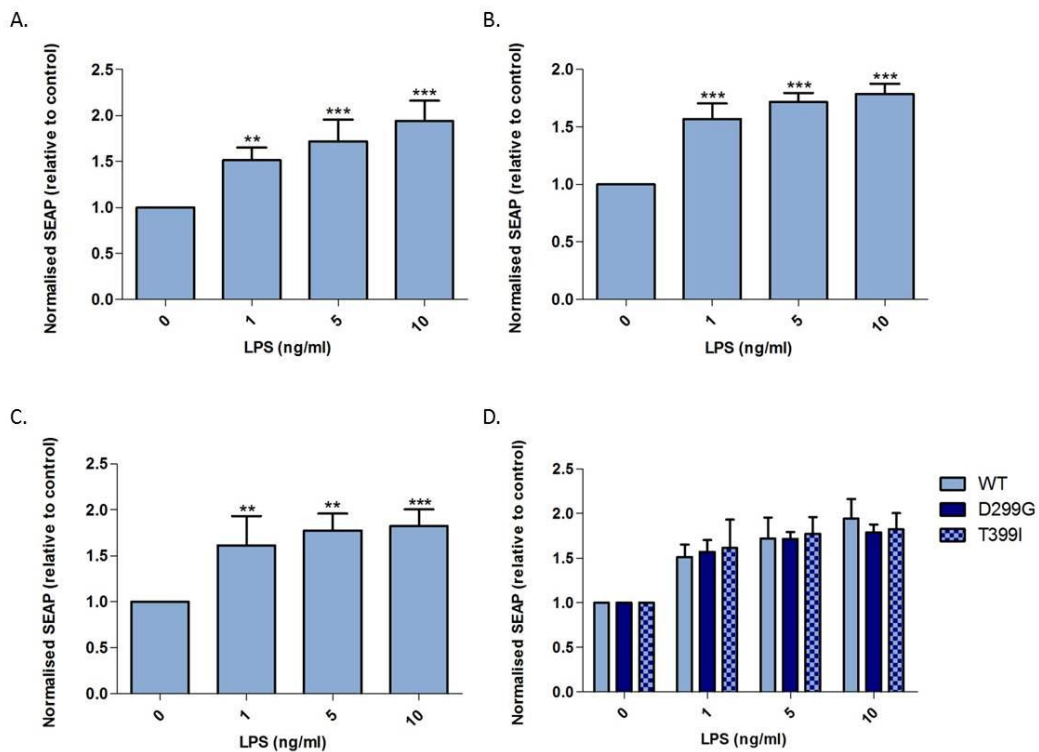


**Figure 6.5. LPS significantly induces NF- $\kappa$ B activity in cells transiently transfected with wildtype or mutant TLR4.** 293-hMD2-CD14 cells transiently transfected with either the wildtype or mutant TLR4 receptor (A. wildtype, B. D299G and C. T399I) were treated with LPS (1, 5 and 10ng/ml; vehicle control for LPS = PBS) for 24 hours. Cell culture supernatant was added to QUANTI-Blue™ solution until colour change was evident (pink to purple blue, caused by the activity of SEAP). The colour change induced by SEAP was analysed as a measure of NF- $\kappa$ B activity at 650nm using a spectrophotometer. D) shows the response of wildtype, D299G and T399I cells collectively. Data shown = mean  $\pm$  SEM, n = 4. Data was statistically analysed using one-way ANOVA followed by the Bonferroni multiple comparison test. \*\*p<0.01 and \*\*\*p<0.001 vs. 0ng/ml.

The effect of L-SF and DL-SF on LPS induction of NF- $\kappa$ B activity was investigated. At concentrations of both 5 and 10 $\mu$ M, L-SF and DL-SF were able to demonstrate a significant suppression of LPS-induced NF- $\kappa$ B activity in cells expressing either the wildtype or mutant TLR4 receptors (**Figure 6.6**).

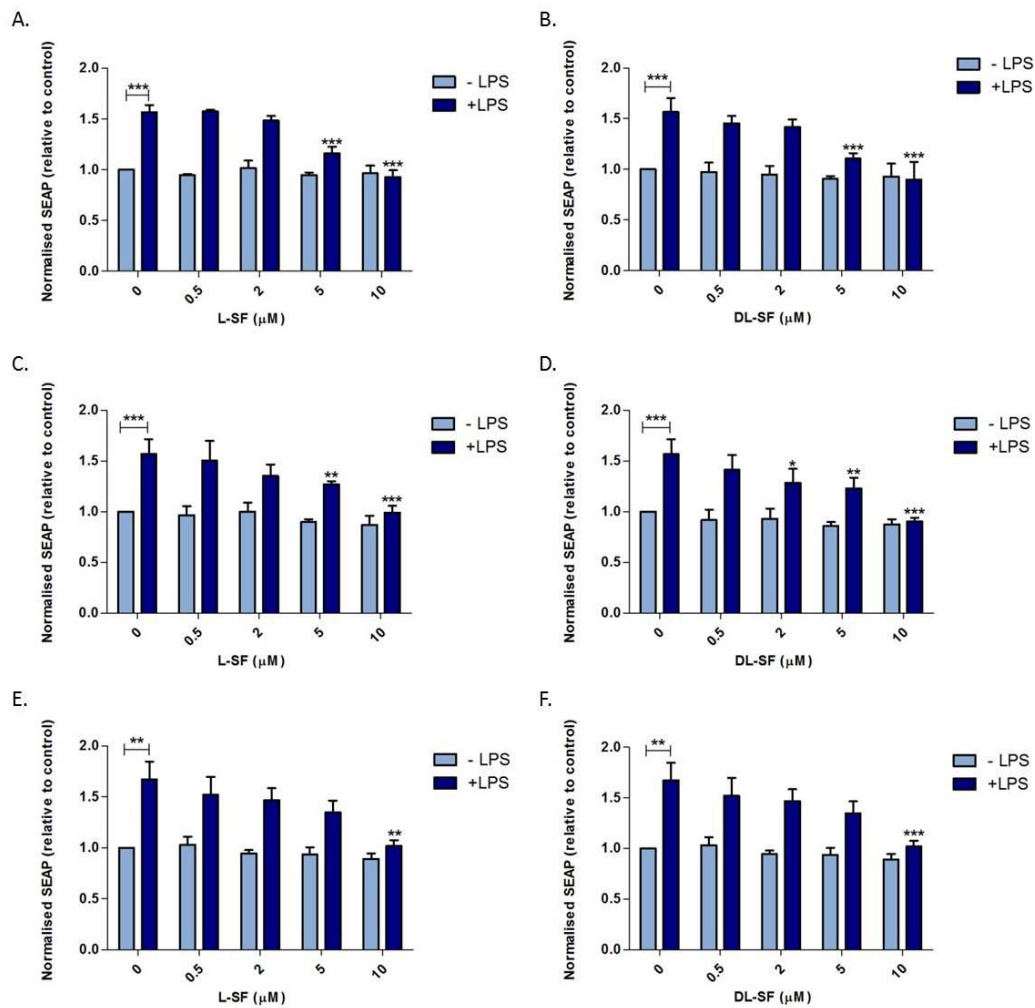


**Figure 6.6. L-SF and DL-SF significantly suppress LPS-induced NF- $\kappa$ B activity in cells transiently transfected with wildtype or mutant TLR4.** 293-hMD2-CD14 cells transiently transfected with either the wildtype or mutant TLR4 receptor (A + B. wildtype, C + D. D299G and E + F. T399I) were treated with L-SF (A, C + E) or DL-SF (B, D + F) at concentrations of 0.5, 2, 5 and 10  $\mu$ M (vehicle control for L-SF and DL-SF = < 0.1% (v/v) DMSO) in the presence or absence of LPS (1ng/ml; vehicle control for LPS = PBS) for 24 hours. Cell culture supernatant was added to QUANTI-Blue™ solution until colour change was evident (pink to purple blue, caused by the activity of SEAP). The colour change induced by SEAP was analysed as a measure of NF- $\kappa$ B activity at 650nm using a spectrophotometer. Data shown = mean  $\pm$  SEM, n = 4. \*p<0.05, \*\*p<0.01 and \*\*\*p<0.001, comparison to 0  $\mu$ M + LPS.

To determine whether the D299G or T399I mutations caused differential responses to SF, a comparison was carried out between the cells expressing the three TLR4 variants. No significant differences were seen in the level of suppression of NF- $\kappa$ B activity induced by LPS in response to either L-SF (**Figure 6.7A**) or DL-SF (**Figure 6.7B**).

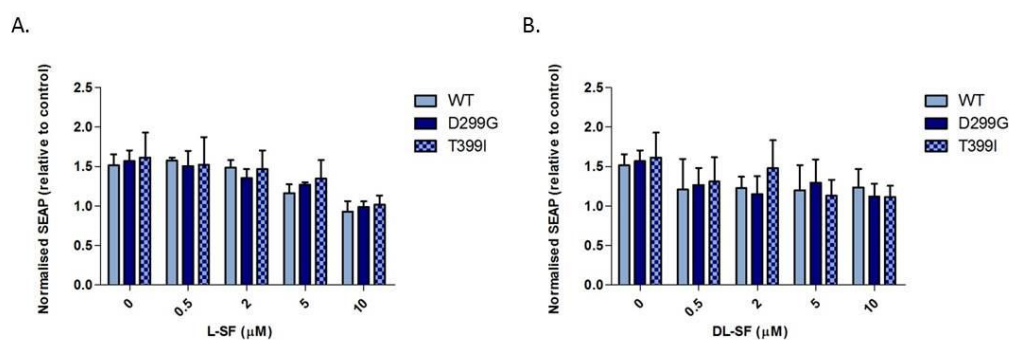


**Figure 6.7. No significant differences were seen in the response to L-SF (A) or DL-SF (B) by cells transiently transfected with either wildtype or mutant TLR4.** 293-hMD2-CD14 cells transiently transfected with either the wildtype or mutant TLR4 receptor (D299G and T399I) were compared in terms of their responses to LPS (1ng/ml; vehicle control for LPS = PBS) in the presence or absence of A) L-SF or B) DL-SF (0.5, 2, 5 and 10 $\mu$ M SF; vehicle control for L-SF and DL-SF = < 0.1% (v/v) DMSO) after 24 hours of treatment. Cell culture supernatant was added to QUANTI-Blue™ solution until colour change was evident (pink to purple blue, caused by the activity of SEAP). The colour change induced by SEAP was analysed as a measure of NF- $\kappa$ B activity at 650nm using a spectrophotometer. Data shown = mean  $\pm$  SEM, n = 4. Data was statistically analysed using two-way ANOVA followed by the Bonferroni multiple comparison test.

#### 6.2.4. Effect of SF on NF- $\kappa$ B in TLR2-expressing cells

Until now, investigations had only been carried out with a focus on the effect of SF in response to LPS and thus, specifically, on the TLR4 pathway. As previously mentioned, TLR2 is fundamental in chronic inflammatory signalling where it can respond to bacterial or mycoplasma lipopeptides [4, 5]. TLR2, unlike TLR4, undergoes heterodimerisation forming complexes with either TLR1 or TLR6. These dimers have different ligand specificities; the TLR2/TLR1 complex specifically binds triacylated lipopeptides and the TLR2/TLR6 complex recognises diacylated lipopeptides [4, 5].

In Chapter 5, TLR2 was also studied as a direct target for SF modification however practical implications meant that no direct interactions with thiol groups of cysteine residues were observed (data not shown). In this chapter, TLR2-expressing cells were utilised to address whether the effect of SF was specific to TLR4 signalling or whether SF was able to target additional receptors involved in chronic inflammatory signalling.

In order to measure NF- $\kappa$ B activity in TLR2-expressing cells, activation of both the TLR2/TLR1 and TLR2/TLR6 dimeric complexes required investigation. Firstly, activation

of NF- $\kappa$ B via the TLR2/TLR1 pathway was explored using a synthetic ligand for the TLR2 receptor complex, Pam3CSK4, a triacylated lipopeptide that behaves to mimic bacterial lipoproteins. To determine the necessary concentration to significantly induce NF- $\kappa$ B activity, TLR2-expressing cells were treated with concentrations of Pam3CSK4 (5, 15 and 50pg/ml) for 24 hours and SEAP levels were analysed as a measure of NF- $\kappa$ B activity. A concentration of 50pg/ml Pam3CSK4 significantly induced NF- $\kappa$ B activity (**Figure 6.8**).

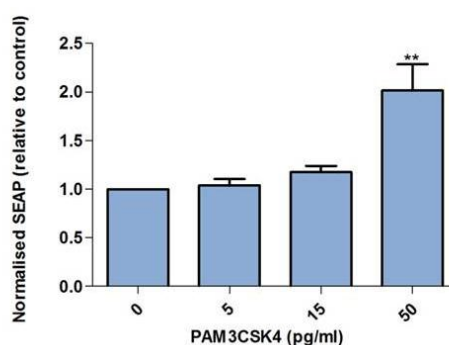


**Figure 6.8. Pam3CSK4 significantly induces NF- $\kappa$ B activity in HEK-Blue<sup>TM</sup>-hTLR2 cells.** HEK-Blue<sup>TM</sup>-hTLR2 cells were treated with Pam3CSK4 (5, 15 and 50pg/ml; vehicle control for Pam3CSK4 = endotoxin-free water) for 24 hours. Cell culture supernatant was added to QUANTI-Blue<sup>TM</sup> solution until colour change was evident (pink to purple blue, caused by the activity of SEAP). The colour change induced by SEAP was analysed as a measure of NF- $\kappa$ B activity at 650nm using a spectrophotometer. Data shown = mean  $\pm$  SEM, n = 3. Data was statistically analysed using one-way ANOVA followed by the Bonferroni multiple comparison test. \*\*p<0.01 vs. 0pg/ml.

To determine the effect of L-SF and DL-SF on Pam3CSK4-induced NF- $\kappa$ B activity, TLR2-expressing cells were treated with L-SF and DL-SF (0.5, 2, 5 and 10 $\mu$ M) in the presence or absence of 50pg/ml Pam3CSK4 for 24 hours. Both L-SF and DL-SF were able to significantly suppress levels of NF- $\kappa$ B activity induced in response to Pam3CSK4 consistently at concentrations of 5 and 10 $\mu$ M (**Figure 6.9**).

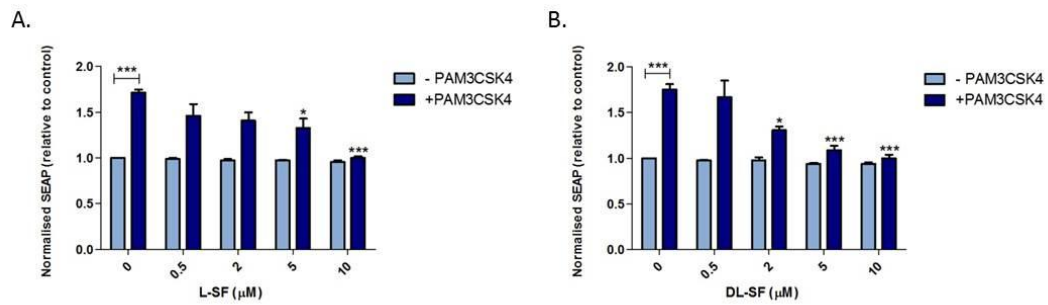


**Figure 6.9. L-SF and DL-SF are able to significantly suppress Pam3CSK4-induced NF- $\kappa$ B activity in HEK-Blue<sup>TM</sup>-hTLR2 cells.** HEK-Blue<sup>TM</sup>-hTLR2 cells were treated with Pam3CSK4 (50pg/ml; vehicle control for Pam3CSK4 = endotoxin-free water) in the presence or absence of A) L-SF or B) DL-SF (0.5, 2, 5 or 10 $\mu$ M; vehicle control for L-SF and DL-SF = < 0.1% (v/v) DMSO) for 24 hours. Cell culture supernatant was added to QUANTI-Blue<sup>TM</sup> solution until colour change was evident (pink to purple blue, caused by the activity of SEAP). The colour change induced by SEAP was analysed as a measure of NF- $\kappa$ B activity at 650nm using a spectrophotometer. Data shown = mean  $\pm$  SEM, n = 3. \*p<0.05, and \*\*\*p<0.001, comparison to 0pg/ml for -Pam3CSK4 and +Pam3CSK4 conditions separately or as annotated.

FSL-1, a diacylated lipopeptide derived from mycoplasma, is specifically recognised by the TLR2/TLR6 dimer. The same experimental design used with Pam3CSK4 was repeated with FSL-1 in the TLR2-expressing cells to investigate the levels of NF- $\kappa$ B activity as a result of activating the TLR2/TLR6 dimer. HEK-Blue<sup>TM</sup>-hTLR2 cells were treated with FSL-1 at concentrations of 5, 15 and 50pg/ml and the level of induction of NF- $\kappa$ B activity was measured. Levels of 15 and 50pg/ml FSL-1 significantly induced NF- $\kappa$ B activity in HEK-Blue<sup>TM</sup>-hTLR2 cells (**Figure 6.10**).

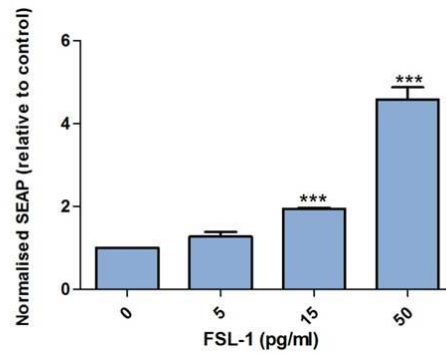


**Figure 6.10. FSL-1 significantly induces NF- $\kappa$ B activity in HEK-Blue<sup>TM</sup>-hTLR2 cells.** HEK-Blue<sup>TM</sup>-hTLR2 cells were treated with FSL-1 (5, 15 and 50pg/ml; vehicle control for FSL-1 = endotoxin-free water) for 24 hours. Cell culture supernatant was added to QUANTI-Blue<sup>TM</sup> solution until colour change was evident (pink to purple blue, caused by the activity of SEAP). The colour change induced by SEAP was analysed as a measure of NF- $\kappa$ B activity at 650nm using a spectrophotometer. Data shown = mean  $\pm$  SEM, n = 3. Data was statistically analysed using one-way ANOVA followed by the Bonferroni multiple comparison test. \*\*\*p<0.001 vs. 0pg/ml.

The effect of both L-SF and DL-SF on FSL-1-mediated NF- $\kappa$ B induction was investigated using 15pg/ml FSL-1, the minimum concentration sufficient to significantly induce NF- $\kappa$ B activity (**Figure 6.10**). TLR2-expressing cells were treated with L-SF and DL-SF (0.5, 2, 5 and 10 $\mu$ M) in the presence or absence of 15pg/ml FSL-1 for 24 hours. Both 5 and 10 $\mu$ M L-SF and DL-SF consistently demonstrated a significant suppression of NF- $\kappa$ B activity induced in response to 15pg/ml FSL-1 (**Figure 6.11**).

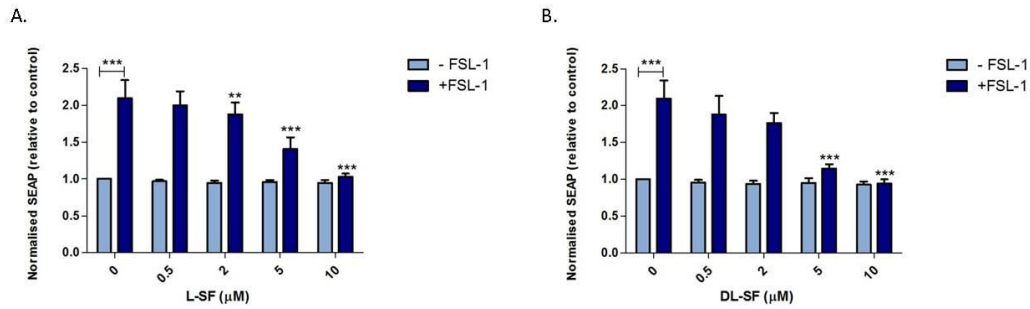


**Figure 6.11. L-SF and DL-SF are able to significantly suppress FSL-1-induced NF- $\kappa$ B activity in HEK-Blue<sup>TM</sup>-hTLR2 cells.** HEK-Blue<sup>TM</sup>-hTLR2 cells were treated with FSL-1 (15pg/ml; vehicle control for FSL-1 = endotoxin-free water) in the presence or absence of A) L-SF or B) DL-SF (0.5, 2, 5 or 10 $\mu$ M; vehicle control for L-SF and DL-SF = < 0.1% (v/v) DMSO) for 24 hours. Cell culture supernatant was added to QUANTI-Blue<sup>TM</sup> solution until colour change was evident (pink to purple blue, caused by the activity of SEAP). The colour change induced by SEAP was analysed as a measure of NF- $\kappa$ B activity at 650nm using a spectrophotometer. Data shown = mean  $\pm$  SEM, n = 3. \*\*p<0.01, and \*\*\*p<0.001, comparison to 0pg/ml for -FSL-1 and +FSL-1 conditions separately or as annotated.

### 6.2.5. Effect of SF on NF- $\kappa$ B activity in NOD2 wildtype and mutant G908R cells

As explained previously, NOD2 is another example of a PRR like TLR2 and TLR4, but differs in terms of its location. While the TLRs are anchored to the cell membrane and are bound by their specific ligands extracellularly, the NOD2 receptor is found intracellularly [19]. NOD2 has been commonly implicated in Crohn's disease and one of the mutants commonly found in higher prevalence in patients suffering from the chronic inflammatory disease is characterised by the SNP, G908R [51, 53, 54].

The ligand for the NOD2 receptor is MDP, a breakdown product of PGN which is found in the cell walls of both Gram-positive and Gram-negative bacteria [19]. MDP is the minimum structure required to activate the NOD2 receptor [19]. To determine the concentrations of MDP sufficient to induce NF- $\kappa$ B activity via NOD2 signalling, cells expressing either the wildtype NOD2 or mutant G908R NOD2 were treated with MDP (0.2, 1 and 4 $\mu$ g/ml) for 24 hours before measuring NF- $\kappa$ B activity. A concentration of 0.2 $\mu$ g/ml MDP was sufficient to induce NF- $\kappa$ B activity in cells expressing the wildtype NOD2 receptor (**Figure 6.12A**) and in cells expressing the mutant G908R NOD2 receptor (**Figure 6.12B**).

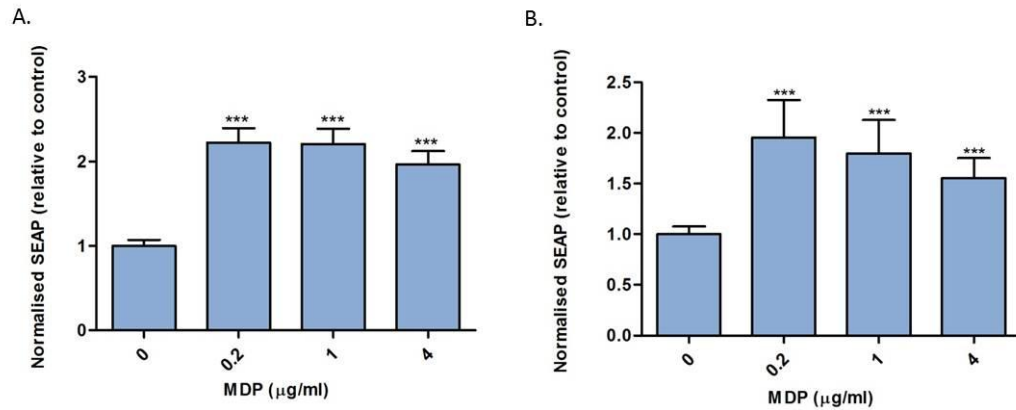


**Figure 6.12. MDP significantly induces NF- $\kappa$ B activity in cells expressing wildtype (A) and mutant G908R (B) NOD2.** HEK-Blue™-hNOD2 wildtype cells (A) or HEK293 cells stably transfected with NOD2 G908R (B) were treated with MDP (0.2, 1 and 4µg/ml; vehicle control for MDP = endotoxin-free water) for 24 hours. Cell culture supernatant was added to QUANTI-Blue™ solution (until colour change was evident (pink to purple blue, caused by the activity of SEAP). The colour change induced by SEAP was analysed as a measure of NF- $\kappa$ B activity at 650nm using a spectrophotometer. Data shown = mean  $\pm$  SEM, n = 3. Data was statistically analysed using one-way ANOVA followed by the Bonferroni multiple comparison test. \*p<0.05 and \*\*\*p<0.001 vs. 0µg/ml.

To establish whether the G908R mutation within the NOD2 receptor had an effect on the extent of NF- $\kappa$ B activation in response to MDP, levels of NF- $\kappa$ B activity were compared between cells expressing the wildtype NOD2 receptor and the mutant G908R receptor. At concentrations of 1 and 4µg/ml, cells expressing the wildtype NOD2 receptor demonstrated significantly higher levels of NF- $\kappa$ B activity in response to MDP than in cells expressing the mutant G908R receptor (**Figure 6.13**).

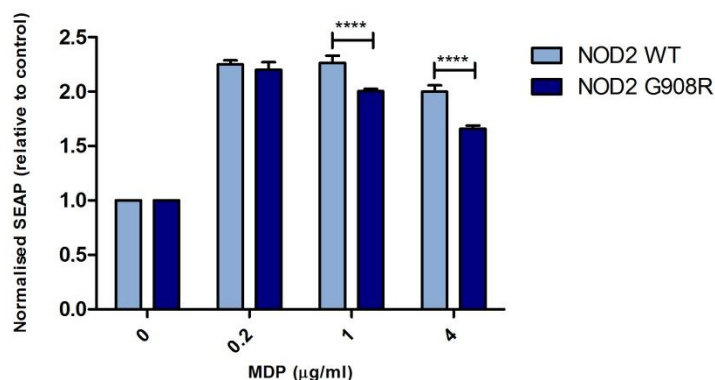


**Figure 6.13. Mutant G908R NOD2 cells are less responsive to MDP induction of NF- $\kappa$ B activity.** HEK-Blue<sup>TM</sup>-hNOD2 wildtype cells or HEK293 cells stably transfected with NOD2 G908R were treated with MDP (0.2, 1 and 4µg/ml; vehicle control for MDP = endotoxin-free water) for 24 hours. Cell culture supernatant was added to QUANTI-Blue<sup>TM</sup> solution until colour change was evident (pink to purple blue, caused by the activity of SEAP). The colour change induced by SEAP was analysed as a measure of NF- $\kappa$ B activity at 650nm using a spectrophotometer. Data shown = mean  $\pm$  SEM, n = 4. Data was statistically analysed using two-way ANOVA followed by the Bonferroni multiple comparison test. \*\*\*\*p<0.001 G908R vs. wildtype for 1 and 4µg/ml MDP

To establish the effect of L-SF and DL-SF on NOD2 signalling, cells expressing the wildtype NOD2 receptor were treated with L-SF or DL-SF (0.5, 2, 5 and 10µM) in the presence or absence of 0.2µg/ml MDP for 24 hours. Concentrations of 5 and 10µM of both L-SF and DL-SF significantly suppressed MDP-induced NF- $\kappa$ B activity (**Figure 6.14**). In HEK-Blue<sup>TM</sup>-hNOD2 wildtype and G908R cells, 2 and 5µM SF consistently induced a significant increase in the constitutive levels of NF- $\kappa$ B activity in cells expressing the wildtype NOD2 receptor (**Figure 6.14**). The absolute change observed with these concentrations of SF in the absence of MDP is small and while these changes are statistically significant, they are unlikely to be biologically relevant.

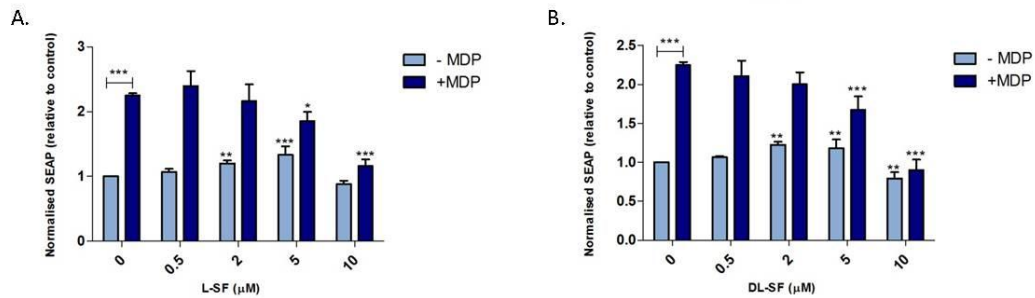


**Figure 6.14. L-SF and DL-SF are able to significantly suppress MDP-induced NF- $\kappa$ B activity in HEK-Blue™-hNOD2 wildtype cells.** HEK-Blue™-hNOD2 wildtype cells were treated with MDP (0.2 $\mu$ g/ml; vehicle control for MDP: endotoxin-free water) in the presence or absence of A) L-SF or B) DL-SF (0.5, 2, 5 or 10 $\mu$ M; vehicle control for L-SF and DL-SF = < 0.1% (v/v) DMSO) for 24 hours. Cell culture supernatant was added to QUANTI-Blue™ solution until colour change was evident (pink to purple blue, caused by the activity of SEAP). The colour change induced by SEAP was analysed as a measure of NF- $\kappa$ B activity at 650nm using a spectrophotometer. Data shown = mean  $\pm$  SD, representative of three independent experiments. Data was statistically analysed using one-way ANOVA followed by the Bonferroni multiple comparison test with –MDP and +MDP analysed separately. \*p<0.05, \*\* p<0.01, \*\*\*p<0.001 comparison to 0 $\mu$ M for –MDP and +MDP conditions or as annotated.

The effect of L-SF and DL-SF was further investigated in cells expressing the mutant G908R NOD2 receptor. G908R-expressing cells were treated with either L-SF or DL-SF (0.5, 2, 5 and 10 $\mu$ M) in the presence or absence of 0.2 $\mu$ g/ml MDP for 24 hours. Concentrations from 2 $\mu$ M of both L-SF and DL-SF demonstrate consistent significant suppressions of MDP-induced NF- $\kappa$ B activity (**Figure 6.15**). 10 $\mu$ M of L-SF and DL-SF also induced a significant decrease in the constitutive levels of NF- $\kappa$ B activity in cells expressing the mutant G908R NOD2 receptor (**Figure 6.15**).

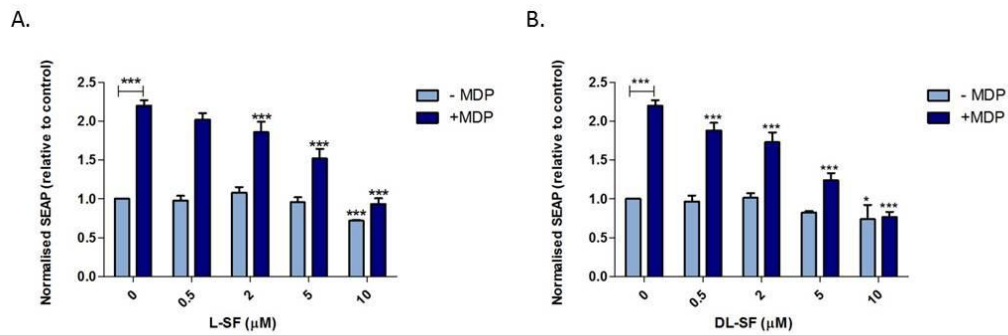


**Figure 6.15. L-SF and DL-SF are able to significantly suppress MDP-induced NF- $\kappa$ B activity in NOD2 G908R cells.** HEK293 cells stably transfected with NOD2 G908R were treated with MDP (0.2 $\mu$ g/ml; vehicle control for MDP: endotoxin-free water) in the presence or absence of A) L-SF or B) DL-SF (0.5, 2, 5 or 10 $\mu$ M; vehicle control for L-SF and DL-SF = < 0.1% (v/v) DMSO) for 24 hours. Cell culture supernatant was added to QUANTI-Blue<sup>TM</sup> solution until colour change was evident (pink to purple blue, caused by the activity of SEAP). The colour change induced by SEAP was analysed as a measure of NF- $\kappa$ B activity at 650nm using a spectrophotometer. Data shown = mean  $\pm$  SD, representative of three independent experiments. Data was statistically analysed using one-way ANOVA followed by the Bonferroni multiple comparison test with -MDP and +MDP analysed separately. \*\*\* $p$ <0.001 comparison to 0 $\mu$ M for -MDP and +MDP conditions separately or as annotated.

Finally, the level of NF- $\kappa$ B activity suppression seen with L-SF and DL-SF was compared in cells expressing the wildtype and mutant G908R NOD2 receptor. The comparison identified a greater suppression of NF- $\kappa$ B activity in cells expressing the G908R NOD2 receptor with both L-SF and DL-SF, compared to the levels of suppression observed in cells expressing the NOD2 wildtype receptor (**Figure 6.16**).

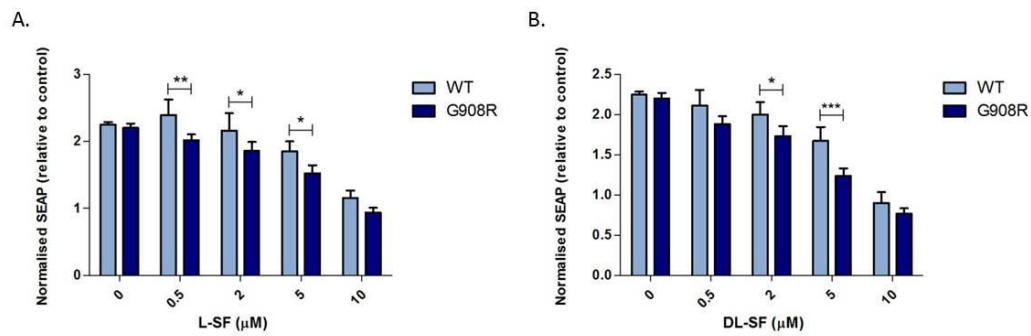


**Figure 6.16. Significant differences were seen in the response L-SF (A) and DL-SF (B) by cells expressing either the wildtype or mutant G908R NOD2 receptor.** HEK-Blue<sup>TM</sup>-hNOD2 wildtype cells or HEK293 cells stably transfected with NOD2 G908R were compared in terms of their responses to A) L-SF or B) DL-SF (0.5, 2, 5 and 10 $\mu$ M SF; vehicle control for L-SF and DL-SF = < 0.1% (v/v) DMSO) in the presence of 0.2 $\mu$ g/ml MDP (vehicle control for MDP = endotoxin-free receptor) for 24 hours. Cell culture supernatant was added to QUANTI-Blue<sup>TM</sup> solution until colour change was evident (pink to purple blue, caused by the presence of SEAP). The colour change induced by SEAP was analysed as a measure of NF- $\kappa$ B activity at 650nm using a spectrophotometer. Data shown = mean  $\pm$  SD, representative of three independent experiments. Data was statistically analysed using two-way ANOVA followed by the Bonferroni multiple comparison test. \*p<0.05, \*\*p<0.01 and \*\*\*p<0.001 as annotated.

### 6.2.6. Comparison of the effects of L-SF and DL-SF on NF- $\kappa$ B activity

An additional aim for this chapter was to determine whether there were any significant differences in the extent of effects seen with the naturally occurring L-SF isomer from broccoli and the synthetic analogue, DL-SF. For each of the cell lines, both the L-SF and DL-SF forms were able to suppress NF- $\kappa$ B activity induced as a result of ligand treatment. When L-SF and DL-SF were compared for all experiments, no significant differences were seen in the level of suppression. **Figure 6.17** shows a representative example of the comparative analysis.

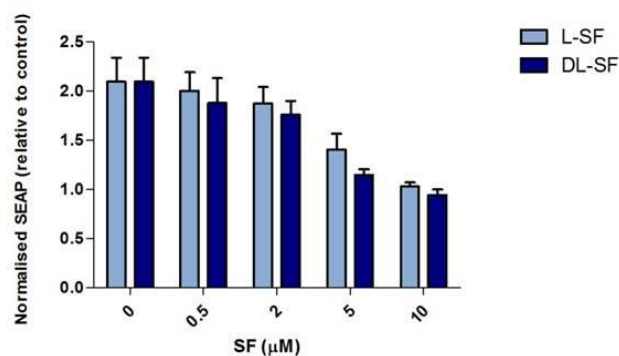


**Figure 6.17. L-SF and DL-SF show no significant differences between their effects on ligand-induced NF- $\kappa$ B activity.** Cells were treated with the appropriate ligand in the presence or absence of L-SF or DL-SF (0.5, 2, 5 or 10 $\mu$ M; vehicle control for L-SF and DL-SF = < 0.1% (v/v) DMSO) for 24 hours. Cell culture supernatant was added to QUANTI-Blue™ solution until colour change was evident (pink to purple blue, caused by the activity of SEAP). The colour change induced by SEAP was analysed as a measure of NF- $\kappa$ B activity at 650nm using a spectrophotometer. Data shown = mean  $\pm$  SEM, n = 3. Data is from an experiment with HEK-Blue™-hTLR2 cells treated with FSL-1 and is representative of all comparative analyses in all cell types. Data was statistically analysed using two-way ANOVA followed by the Bonferroni multiple comparison test.

### 6.3. Discussion

Within this chapter, the effect of L-SF and DL-SF was investigated on the TLR4, TLR2 and NOD2 signalling pathways (**Figure 6.1**). The reason for focusing on the TLR4, TLR2 and NOD2 signalling pathways is due to identified associations with chronic inflammatory pathologies such as the IBDs Crohn's disease and UC, CVD, obesity, T2DM, metabolic syndrome and cancer [36, 44, 48-50, 54-62, 242-244, 246-249].

With the use of a cell model that specifically expressed the TLR4 receptor, more information about the effect of SF on TLR4 signalling can be obtained. In Chapters 3 and 4, the effect of SF on LPS-induced cytokine production and global gene expression was investigated. In the previous chapters, the physiologically relevant concentration of 1ng/ml LPS was used to induce cytokine secretion and expression. However, in Chapters 3 and 4, the human monocytic THP-1 cell model was used and as this cell type is fundamentally important in the rapid response to an inflammatory attack, it was expected that there would be a high level of sensitivity to PAMPs such as LPS. Less was known about the HEK293 cells and their ability to respond to LPS.

Both L-SF and DL-SF were able to significantly suppress LPS-induced NF- $\kappa$ B activity in TLR4-expressing cells. In Chapter 3, SF suppressed LPS-induced cytokine production in

THP-1 monocytes to a much greater extent, by almost 100% in some cases. This variability in the level of suppression seen with SF may be due to the measurements that were taken e.g. NF- $\kappa$ B activity versus ELISA for specific cytokines, the different cell types e.g. HEK-Blue™ transfected cells versus THP-1 monocytes which endogenously express the PRRs, as well as the associated sensitivity levels of the cells. The production of cytokines is controlled by NF- $\kappa$ B and AP-1 activity. In this chapter, the activity of NF- $\kappa$ B has been studied alone, thus the lesser suppression seen with SF on NF- $\kappa$ B activity compared to in Chapters 3 and 4 on cytokine expression and secretion, is potentially due to the lack of consideration for potential suppression of AP-1 activity. The results from this chapter do however provide further support for the hypothesis that SF is able to directly target the TLR4 signalling pathway.

As previously mentioned, TLR4 polymorphisms, D299G and T399I have been associated with IBDs [54-62], but conversely, there is an indication that these polymorphisms may confer protection against T2DM [244]. In HEK293 cells transiently transfected with the wildtype or mutant (D299G and T399I) TLR4 receptors, NF- $\kappa$ B activity was significantly induced by 1.5-fold in response to 1ng/ml LPS (**Figure 6.5**). When HEK293 cells were stably transfected with TLR4, the response to LPS was greater with around a 3.5-fold increase in NF- $\kappa$ B activity (**Figure 6.3**). This large difference in LPS response is likely a result of lower transfection efficiency with the transient transfection method as opposed to stable transfection. During transient transfection, the foreign DNA is not integrated into the host genome and after several days, expression of the foreign DNA is eliminated from the cells through cell division. When cells are stably transfected, the foreign DNA is integrated into the host genome meaning the cells can be sub-cultured over time with the transfected gene being expressed as an endogenous gene [250]. Thus, cells that are stably transfected with TLR4 will demonstrate higher levels of TLR4 expression than the transiently transfected TLR4 cells and thus demonstrate a larger induction of NF- $\kappa$ B activity in response to LPS (**Figures 6.3 and 6.5**).

No significant differences were observed in the level of NF- $\kappa$ B induction in response to LPS in cells transiently transfected with the D299G and T399I mutants compared to the wildtype TLR4 receptor. This disagrees with previous data by Arbour and colleagues who demonstrated hypo-responsiveness to LPS inhalation in subjects carrying the D299G and T399I mutations and the same was seen with a significantly lower LPS response in THP-1 cells transfected with the D299G mutant [248]. However, the inconsistency between the results in those two experiments and the results presented in this chapter may be due to using

a concentration of LPS 100 times lower than in the study by Arbour [248]. In addition, no differences were observed in the level of suppression induced by L-SF or DL-SF in cells expressing the D299G and T399I TLR4 mutants. This is in support of data shown in Chapter 5. When a recombinant form of the TLR4 receptor was subjected to SF treatment under non-reducing conditions, SF was able to target cysteine residues within the receptor at positions 246 and 609. The D299G and T399I mutations do not involve these cysteine residues and the positions of these mutations within the TLR4 receptor are not in close proximity to the specific cysteine targets of SF.

To extend the findings from the investigations of SF with the TLR4 signalling pathway, the hypothesis that SF was able to additionally exert anti-inflammatory effects on the TLR2 signalling pathway was tested. As with the TLR4-expressing cells, L-SF and DL-SF were able to significantly suppress NF- $\kappa$ B activity induced by Pam3CSK4 (the ligand for TLR2/TLR1) and FSL-1 (the ligand for TLR2/TLR6). While in Chapter 5, some evidence that SF was able to modify cysteine residues within the extracellular domain of TLR4 was produced, similar findings with TLR2 were not observed, likely due to practical implications. When the peptide coverage was analysed following LC-MS/MS analysis of the enzyme digested TLR2, no cysteines were found within the identified fragments. However, based on the data within this chapter, there may be reason for further exploring potential interactions between SF and TLR2, which is also supported by previous research [195]. It is nevertheless important to note that while the data in this chapter demonstrates a significant reduction in NF- $\kappa$ B activity following ligand induction, the suppression could be as a result not only of direct interaction of SF with the receptor, but also by SF targeting NF- $\kappa$ B as previously reported [184, 189, 191-194], to produce the level of suppression observed.

Finally, the PRR NOD2 was also investigated. In previously published data, HEK293 cells transfected with G908R NOD2 receptors have demonstrated a significantly reduced response to ligands when compared to cells expressing the wildtype NOD2 receptor [251, 252]. However, the reduced response to MDP in G908R cells seen in this study is more modest than the large reductions seen previously [251, 253]. Another study that monitored the NF- $\kappa$ B activity in response to MDP treatment in cells expressing the wildtype or G908R mutant receptor by Lecine and colleagues presented more comparable data to the results shown in this chapter. Only a small reduction was observed in the response to MDP at a concentration of 50ng/ml, a concentration four times smaller than the lowest concentration used in the studies presented in this chapter [254].

As reported with TLR4 and TLR2-expressing cells, L-SF and DL-SF were also able to suppress MDP-induced NF- $\kappa$ B activity in the wildtype and G908R mutant NOD2 cells, with a larger suppression observed in the G908R cells. These differences in the level of suppression may be due to the positions of the SNP G908R mutation reducing the affinity of a potentially direct interaction with the SF as a result of the large difference in the properties of the amino acids involved in the substitution if the mechanism seen with the TLR4 is consistent with NOD2 (Chapter 5, [195]).

From a practical standpoint, the results within this chapter have confirmed that it is not necessary to use the natural L-SF from broccoli in preference to the synthetic analogue DL-SF. In all cell models studied, no significant differences were seen in the level of suppression of ligand-induced NF- $\kappa$ B activity with the two SF forms tested (**Figure 6.17**). While these results confirm they behave in the same way functionally, there are advantages for using each form. While the L-SF is directly relevant to the form found in human systemic circulation following the consumption of broccoli, the synthetic DL-SF is substantially less expensive to use.

Based on the results presented in this chapter, it can be concluded that SF has the ability to target a number of different inflammatory signalling pathways. This chapter has confirmed that SF's ability to significantly suppress the effect of ligand induction on cytokine production, global gene expression or NF- $\kappa$ B activity is not restricted to the TLR4 pathway. These findings are of critical importance to provide support for the use of SF as a suppressor of chronic inflammation due to its breadth of targets which are able to respond to many different stimuli.

## **6.4. Conclusions**

In summary, the use of physiologically relevant concentrations of either L-SF or DL-SF was able to cause significant suppression of ligand-induced NF- $\kappa$ B activity. This function of SF was not restricted to TLR4 signalling, but was also observed with TLR2 and NOD2 signalling, two additional pathways that are associated with chronic inflammatory pathologies such as IBDs, CVD and T2DM. Common TLR4 variants, D299G and T399I, which have been identified at a higher prevalence in patients with IBD were not found to vary in their response to LPS or SF as compared to cells expressing the wildtype form of TLR4.

SF was also able to suppress NF- $\kappa$ B activity induced in response to the specific ligands in TLR2-expressing cells and NOD2 wildtype or G908R-expressing cells. In cells expressing the G908R NOD2 receptor, lower levels of NF- $\kappa$ B activity induction was observed in response to higher concentrations of MDP and these cells were significantly more sensitive to SF as compared to cells expressing the wildtype NOD2. These results suggest that SF would be able to target the inflammatory signalling important in subjects with and without mutations within their PRRs, but may be able to selectively target patients with the G908R mutation to a greater extent to act as a suppressor of pro-inflammatory signalling associated with Crohn's disease.

In order to further this work, the next chapter investigates the effect of SF in a translational *in vitro* model involving human SGBS adipocyte cells, firstly in terms of the effects SF can exert on lipid metabolism in adipocytes (Chapter 7) followed by investigations into the effect of SF in response to MaCM treatment of these human adipocytes, a model which provides a good representation of the chronic adipose tissue inflammation in individuals suffering from obesity (Chapter 8).

# Chapter Seven

---

Effect of SF on human SGBS adipocyte lipid  
metabolism

## **7.0. Introduction**

In the research presented so far, it has been demonstrated that SF can behave as an anti-inflammatory agent by targeting a number of inflammatory signalling pathways e.g. TLR4, TLR2 and NOD2 in order to suppress NF- $\kappa$ B activity, pro-inflammatory gene expression and cytokine secretion. In the final two chapters, this research was translated into a more complex model of chronic inflammation with relevance to obesity.

Obesity is characterised by an increase in fat mass as a result of the enlargement and hyperplasia of adipocytes within the adipose tissue. In particular, an increase in abdominal obesity and visceral fat is significantly associated with an increased risk of developing chronic disorders [255, 256]. The enlargement of adipocytes is as a result of an elevation in the levels of accumulated triglycerides following increased dietary consumption. In the adipose tissue of a lean individual, triglyceride stores within the adipocytes are released into circulation where they are transported to organs with increased energy demands. Triglycerides are utilised as an energy source, with breakdown resulting in metabolism through  $\beta$ -oxidation to produce intermediates for the TCA cycle and electron transport chain [84]. In an obese individual, the large increase in accumulation of triglycerides outweighs the rate of  $\beta$ -oxidation, which results in the lipolysis of triglycerides and an increase in FFAs in circulation [88]. Elevated levels of FFAs have been consistently identified in patients suffering from obesity and insulin resistance [85, 86, 257].

To date, there is no commercially available human adipocyte cell line and in much of the literature investigating adipose tissue biology, the murine 3T3-L1 cell line is used. In this thesis so far, only cell lines of human origin have been studied and thus the aim was to continue with the use of human adipocytes, due to the known inconsistencies in the behaviours of cells from murine and human origin [258]. Primary human preadipocytes are either commercially available or obtained from human subjects if ethical approval is given, however there are disadvantages associated: high levels of variability between individuals would potentially be observed; primary human preadipocytes have a low differentiation capacity after sub-culturing several times; there may be a limited supply of material and large costs would be incurred.

In recent studies into adipocyte biology, a human preadipocyte cell line developed by Wabitsch and colleagues has become more commonly used [200]. The cells were isolated from an infant suffering from Simpson-Golabi-Behmel Syndrome, a condition characterised by increased levels of pre- and postnatal growth, and patients often demonstrate large

adipose tissue depots [200]. When preadipocytes were isolated, these cells were able to be sub-cultured many times and maintained their capacity to differentiate up to generation 50. Once fully differentiated, via an insulin-dependent process, (see section 2.2.4), mature fat cells that were biochemically and functionally similar to primary human adipocytes were obtained [200].

One particular research question investigated in this chapter was the effect of SF on the differentiation of human SGBS preadipocytes. During the differentiation process of preadipocytes, there is a distinct increase in the levels of accumulated lipids within the cells. SF has been previously shown to reduce the level of lipid accumulation within murine 3T3-L1 cells at concentrations of 10 $\mu$ M SF and above [162, 164, 259-261]. As yet, no studies have been carried out investigating the effect of SF on adipocytes of human origin. One study hypothesised that the reduction in lipid accumulation with SF in 3T3-L1 cells was as a result of inducing lipolysis [163] and thus in this chapter the aim was to investigate whether SF was able to suppress lipid accumulation within adipocytes by inducing lipolysis. It was thought that this research question could provide potential support for how supplementation with high concentrations of SF was able to suppress weight gain, adipogenesis and liver triglyceride accumulation in mice subjected to a high-fat diet [161], but with the use of more physiologically relevant concentrations of SF.

## **7.1. Materials and Methods**

The human SGBS adipocyte cells were used throughout this chapter (section 2.2.4). SGBS preadipocytes were differentiated in the presence of SF (2, 5 and 10 $\mu$ M) and Oil Red O staining and an assay to determine the glycerol concentration within the media was carried out to investigate effects on lipid accumulation and lipolysis within the cells (section 2.10). Additionally, RNA was extracted at days 10 and 14 of the differentiation process to monitor the expression level of CPT1A to investigate if SF had any effects on the metabolism of lipids (section 2.5).

## 7.2. Results

### 7.2.1. Effect of SF on human SGBS cells

#### 7.2.1.1. Effect of SF on SGBS preadipocyte and adipocyte cell viability

To determine the concentrations of SF that were appropriate for use with the SGBS cell line as preadipocytes and differentiated adipocytes, a WST-1 cell viability assay was carried out. SGBS cells were subjected to SF treatment over a wide range of concentrations (0-200 $\mu$ M) for 24 hours before determining the level of cell viability. Concentrations of SF from 15 $\mu$ M significantly reduced SGBS preadipocyte cell viability (**Figure 7.1A**). SGBS adipocytes behaved very differently in response to SF with concentrations up to 10 $\mu$ M dramatically increasing cell viability in adipocytes relative to the untreated cells. A significant decrease in cell viability was not seen until concentrations of SF reached 125 $\mu$ M and above (**Figure 7.1B**). The IC<sub>50</sub> for the preadipocytes was calculated at  $24.4 \pm 5.4\mu$ M while for the mature adipocytes this was much higher at  $92.8 \pm 15.4\mu$ M.

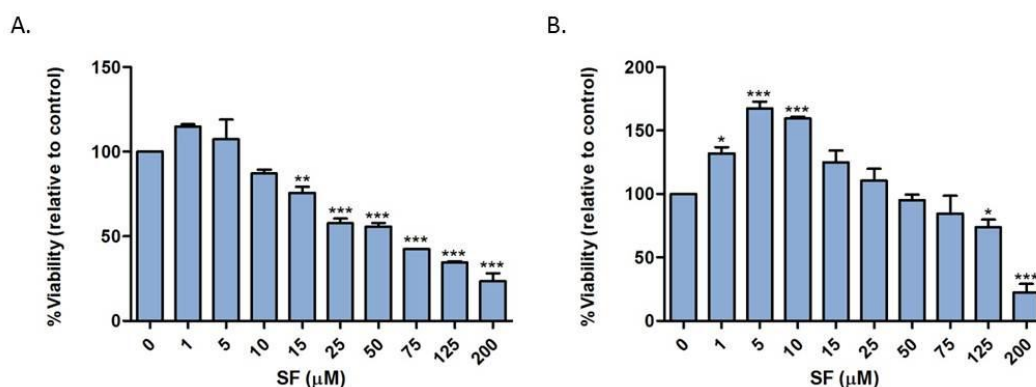


**Figure 7.1. Effect of SF on SGBS cell viability.** A) SGBS preadipocytes were treated with SF (0-200 $\mu$ M; vehicle control for SF = < 0.1% (v/v) DMSO) for 24 hours. B) SGBS preadipocytes were chemically differentiated over 14 days resulting in mature adipocytes (see section 2.2.4). On day 14, mature SGBS adipocytes were treated with SF (0-200 $\mu$ M; vehicle control for SF = < 0.1% (v/v) DMSO) for 24 hours. Once treatment was complete, 10 $\mu$ l WST-1 reagent was added to each well (see section 2.3). The plates were incubated at 37°C and measured using a spectrophotometer every 15 minutes. Data shown is from the 1.5 hour measurement at which the levels of absorbance were all measurable and consistent. Data shown = mean  $\pm$  SD and is representative of two independent experiments. Data was statistically analysed using one-way ANOVA followed by Bonferroni multiple comparison tests. \* $p$ <0.05, \*\* $p$ <0.01 and \*\*\* $p$ <0.001 vs. 0 $\mu$ M SF.

#### 7.2.1.2. Effect of SF on lipid accumulation in SGBS cells

When SGBS preadipocytes were chemically differentiated, the cells gradually accumulated intracellular lipid droplets. This level of lipid accumulation was measured using Oil Red O, a dye which is able to enter the cells and stain the intracellular lipids (**Figure 7.2**). The

advantage with using Oil Red O staining is not only that lipid accumulation can be clearly seen visually as shown in **Figure 7.2**, but the stain can be eluted from inside the cells and quantified using an absorbance-based assay. Throughout the 14 day differentiation period, there was a significant increase in the level of lipid accumulation, demonstrated by an increasing level of Oil Red O staining, an observation that is indicative of successful differentiation (**Figure 7.3**).

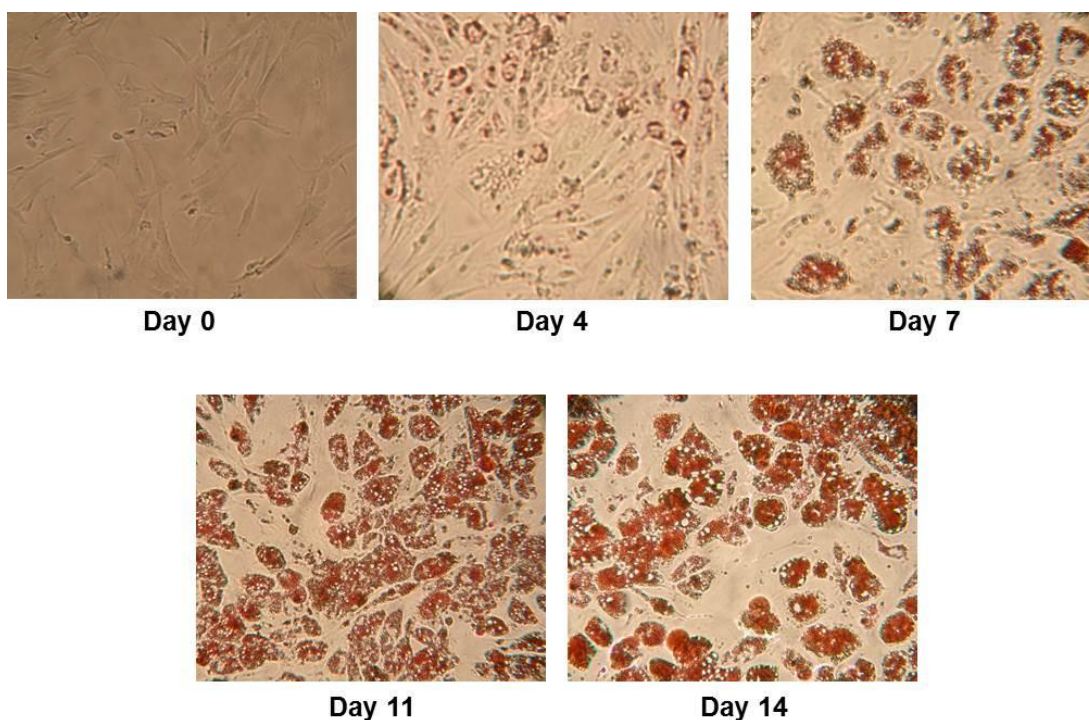


**Figure 7.2. Intracellular lipids accumulate within SGBS cells during differentiation.** SGBS preadipocytes were chemically differentiated as described in section 2.2.4 and on days 0, 4, 7, 11 and 14, cells were fixed with 10% formalin and stained with Oil Red O. Photographs were taken using a light microscope following staining at a magnification of 10X.

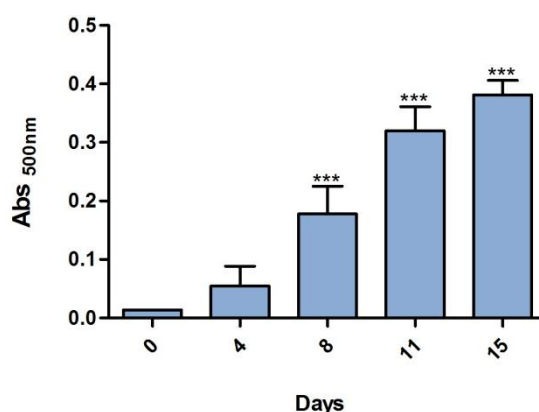


**Figure 7.3. Intracellular lipid accumulation increased over the differentiation process of SGBS cells.** SGBS preadipocytes were chemically differentiated as described in section 2.2.4 and on days 0, 4, 8, 11 and 15, cells were fixed with 10% formalin and stained with Oil Red O. After excess dye was removed, the stain was eluted from the cells with 100% isopropanol and absorbance was measured at 500nm. Absorbance was corrected against 100% isopropanol from an unstained well. Data shown = mean  $\pm$  SEM; n = 2. Data was statistically analysed using a one-way ANOVA followed by Bonferroni multiple comparison tests. \*\*p<0.01 and \*\*\*p<0.001 vs. Day 0.

During the differentiation process, SGBS preadipocytes were treated with SF (2, 5 and 10 $\mu$ M) and the level of lipid accumulation was measured at day 0, 4, 7, 11 and 14, to investigate whether SF could affect adipogenesis. 10 $\mu$ M SF significantly suppressed the level of lipid accumulation in SGBS cells from day 11 onwards (**Figure 7.4**). This significant reduction could be seen visually from microscope photographs at days 11 and 14 (**Figure 7.5**).

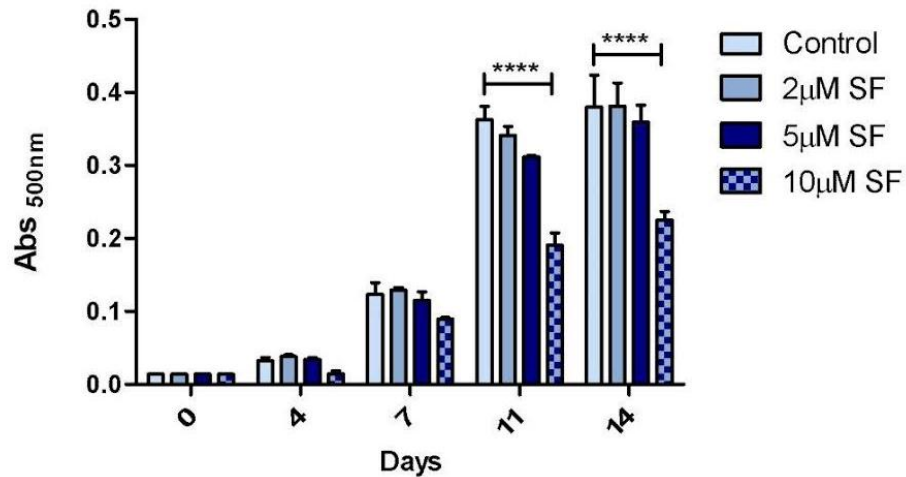


**Figure 7.4. 10µM SF significantly suppresses lipid accumulation of SGBS cells.** SGBS preadipocytes were chemically differentiated in the presence or absence of SF (2, 5 and 10µM; vehicle control for SF = < 0.1% (v/v) DMSO). At days 0, 4, 7, 11 and 14, cells were fixed with 10% formalin and stained with Oil Red O. After excess dye was removed, the stain was eluted from the cells with 100% isopropanol and absorbance was measured at 500nm. Absorbance was corrected against 100% isopropanol from an unstained well. Data shown = mean  $\pm$  SD and is representative of two independent experiments. Data was statistically analysed using a two way ANOVA followed by Bonferroni multiple comparison tests. \*\*\*\*  $p < 0.0001$  for 10µM SF compared to the control on each day as annotated.

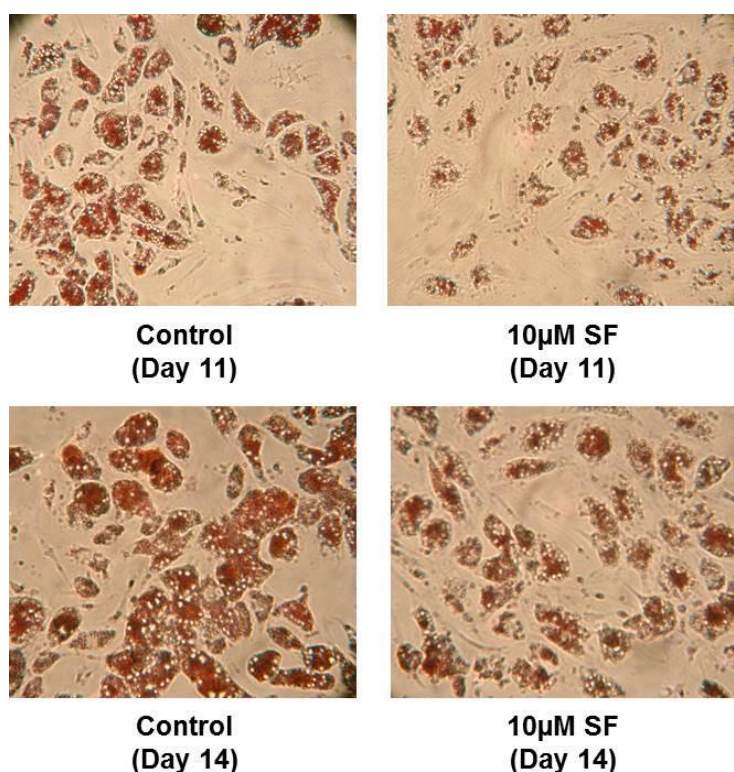


**Figure 7.5. Lipid accumulation was reduced in SGBS adipocytes differentiated in the presence of 10µM SF.** SGBS preadipocytes were chemically differentiated in the presence or absence of SF (2, 5 and 10µM; vehicle control for SF = < 0.1% (v/v) DMSO). At days 0, 4, 7, 11 and 14, cells were fixed with 10% formalin and stained with Oil Red O. Photographs were taken using a light microscope following staining at a magnification of 10X. Data shown from Control and 10µM SF only at days 11 and 14.

### 7.2.1.3. Effect of SF on CPT1A expression

The decrease in lipid accumulation induced by 10µM SF at days 11 and 14 of differentiation (**Figure 7.4** and **7.5**) could be due to an increase in lipolysis of the fat droplets that increase within the adipocytes during the differentiation process (**Figure 7.2** and **7.3**). Lipolysis has previously been highlighted as a potential mechanism for SF, and if so this would result in an increase in the levels of FFAs within the cells [163]. It was hypothesised that in order to prevent the FFAs behaving as a pro-inflammatory stimulus within the cells, the SGBS cells would metabolise them and use as an energy source. An enzyme fundamental to the fatty acid  $\beta$ -oxidation process is CPT1A, which behaves to transfer the long-chain fatty acyl group to carnitine allowing the fatty acids to be shuttled into the mitochondria [88, 89].

SGBS preadipocytes were treated with SF (2, 5 and 10µM) over the 14 day differentiation period and RNA was extracted from the cells at days 10 and 14 in order to quantify the

levels of CPT1A expression by real-time RT-PCR. 10 $\mu$ M SF significantly induced CPT1A expression at both days 10 and 14 (**Figure 7.6**).

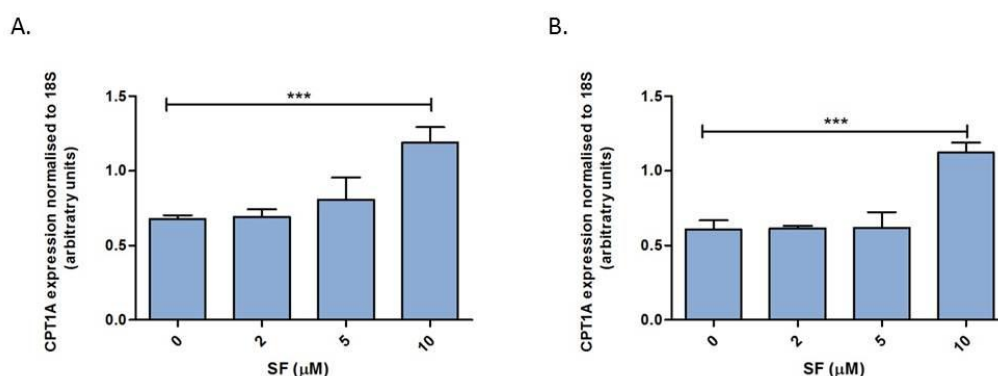


**Figure 7.6. 10 $\mu$ M SF significantly induces CPT1A expression in SGBS cells.** SGBS preadipocytes were chemically differentiated in the presence or absence of SF (2, 5 and 10 $\mu$ M; vehicle control for SF = < 0.1% (v/v) DMSO). At days 10 (A) and 14 (B), RNA was extracted, quantified and analysed by real time RT-PCR. Data shown = mean  $\pm$  SD. Data was statistically analysed using one-way ANOVA followed by Bonferroni multiple comparison tests. \*\*\*  $p < 0.001$  as annotated.

#### 7.2.1.4. Effect of SF on glycerol release

As a result of lipolysis, the glycerol backbone of a triglyceride molecule is secreted by the cells and can be measured free in cell culture supernatants [163]. The hypothesis was that glycerol would be found at increased levels in the cell culture supernatant from cells treated with 10 $\mu$ M SF at days 10 and 14, consistent with SF inducing lipolysis. However, when the levels of glycerol were measured, no significant differences were seen with SF treatment at days 10 or 14 (**Figure 7.7**).

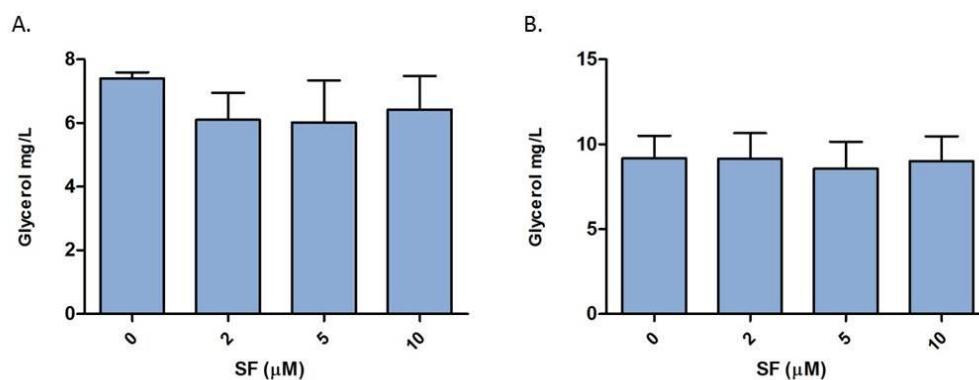


**Figure 7.7. SF caused no significant changes in the levels of glycerol released by SGBS cells.** SGBS preadipocytes were chemically differentiated in the presence or absence of SF (2, 5 and 10 $\mu\text{M}$ ; vehicle control for SF = < 0.1% (v/v) DMSO). At days 10 (A) and 14 (B), cell culture supernatant was collected and cleared by centrifugation before analysis with a Glycerol Assay Kit (Cambridge Bioscience Limited, Cat. # 10010755). Data shown = mean  $\pm$  SD and is representative of two independent experiments. Data was analysed using one-way ANOVA followed by Bonferroni multiple comparison tests.

### 7.3. Discussion

In order to translate results observed in the previous chapters into a translational model of chronic inflammation, human SGBS adipocytes were investigated. In this chapter, the effect of SF alone on differentiation of the preadipocytes was investigated with measurements involved in lipid accumulation.

When the mature SGBS adipocytes were monitored in terms of their response to SF, there were very different results. Concentrations up to 10 $\mu\text{M}$  were able to induce large significant increases in cell viability, with concentrations of 5 and 10 $\mu\text{M}$  SF demonstrating a 50% increase. Potential reasons for this could be due to the high level of accumulated lipids within these cells, which could potentially interfere with absorbance readings. Visually, it did not appear that low concentrations of SF led to a larger population of cells relative to the control which could increase the cell viability reading, however, absolute cell numbers were not measured. It is important to note that the WST-1 assay is not a direct measurement of viability even though it is widely used as a representation. It behaves to measure the conversion of a tetrazolium salt to a coloured formazan compound (**Figure 2.1**, see section 2.3 for more details). This is controlled by mitochondrial dehydrogenase enzymes and results in the formation of NADPH. SF has been previously shown to have roles in NADPH flux (Chapter 4, **Figure 4.2**), and therefore, the mature SGBS adipocyte cells may be highly sensitive to SF altering NADPH production resulting in an inaccurate reading of metabolic

activity. For these reasons it may be more appropriate to use a different assay or method e.g. flow cytometry in order to determine the cell viability of the mature adipocyte SGBS population in response to SF.

When the SGBS preadipocytes were exposed to SF (2, 5 and 10 $\mu$ M) throughout the differentiation period, there was a significant reduction in intracellular lipid accumulation by over 40% with 10 $\mu$ M SF at days 11 and 14 (**Figure 7.4**) and no significant effect on glycerol release, a measure of lipolysis (**Figure 7.7**), but a significant increase in CPT1A expression was observed in response to 10 $\mu$ M SF (**Figure 7.5**). A decrease in Oil Red O staining was previously found in research using the mouse fibroblast 3T3-L1 cell line, where concentrations of 10 $\mu$ M SF and above are able to significantly suppress differentiation of the cells [162, 164, 259-261]. The findings of no effect on glycerol release was in contrast to findings in murine 3T3-L1 cells in which an increase in glycerol levels in response to SF at concentrations of 5 $\mu$ M and above was demonstrated, however this previous study did demonstrate a significant induction in CPT1A expression [163]. These results provide support for utilisation of lipids in order to prevent the induction of an inflammatory response.

In order to continue investigations into the mechanism of SF an additional method that could be used is the measure of intracellular triglycerides, not via Oil Red O staining but with a more direct and quantitative method by extracting the intracellular lipids from the cells. SF was found to significantly reduce the levels of triglyceride accumulation in murine 3T3-L1 cells [162, 164, 259-261]. Additionally, similar findings were observed *in vivo* within the livers of CYP2E1 knock-in mice [262] and C57BL/6N mice subjected to a high-fat diet in the presence or absence of SF [161].

The subsequent hypothesis was that 10 $\mu$ M SF reduced the level of adipocyte differentiation as a result of suppressing lipid accumulation. Previous literature supports this hypothesis, for example in the study by Choi and colleagues, there was little effect of SF on lipid accumulation if cells were exposed to SF at later stages of adipogenesis, whereas at earlier stages, SF completely blocked the differentiation process [164]. The group expanded this work with a more recent *in vivo* study in mice, in which they investigated the effect of SF in combination with a high-fat diet over 6 weeks. SF (1g/kg body weight) significantly suppressed body weight gain, decreased perirenal and epididymal adipose tissue weight, liver weight and fat accumulation in the liver, in addition to total cholesterol, serum glucose and leptin when compared to the mice subjected to the high-fat diet alone [161]. While this

study provides a convincing argument for the use of SF as an anti-obesity agent, the concentration of SF used here is far higher than could be achieved following the consumption of broccoli. A previous study by Souza and colleagues used a concentration of SF at 1mg/kg body weight, 1000 times lower than the study by Choi and colleagues, and found that SF accentuated blood glucose impairments induced by a highly palatable diets in Wistar rats [263]. Nevertheless, it is important to remember that it is very difficult to directly compare the concentrations of SF administered in rodent models with relevance to broccoli consumption in humans. While Souza and colleagues found no significant changes in adipogenesis in rats [263], there is a distinct lack of similar studies for comparison, and there is no evidence to suggest that lower concentrations could not achieve comparable results to those seen in the study by Choi and colleagues. However, it is thought that these findings may be largely under-reported, with the hypothesis that the large reductions seen in the study by Choi and colleagues may be due to potential toxicity effects.

In terms of the mechanism for how SF may affect adipogenesis, previous research indicated a link with the Nrf2 pathway [259-262, 264, 265]. The results in this chapter suggest that Nrf2 is an inhibitor of adipogenesis. The discussion of the role of Nrf2 was based on a number of studies with largely contradictory arguments [264]. In a study by Pi and colleagues, knockdown of Nrf2 in mice fed a high-fat diet resulted in a decrease in adipose tissue depots and protected against obesity. With an overexpression of Nrf2 by knockdown of Keap1, there was an accelerated response to hormone-induced adipocyte differentiation, suggesting that Nrf2 augmented adipocyte differentiation [266]. Conversely, in a study by Shin and colleagues there was a significantly accelerated rate of differentiation in immortalised mouse embryonic fibroblasts (MEFs) isolated from mice with a knockdown of Nrf2. Additionally, a significantly slower rate of differentiation was observed in MEFs isolated from mice with a knockdown of Keap1 and hence an increased level of Nrf2 activity [267]. The differing findings in this area of research may be as a result of using variations in the study models, e.g. primary cultures as opposed to immortalised cells, murine versus human cultures, and different methods of activating or inactivating Nrf2 activity.

While the evidence is contradictory, several studies have been discovered to support the findings within this chapter however, little of the previous research carried out investigated the effect of SF on adipogenesis in cell models of human origin. Based on the research published until now, no previous studies have been carried out monitoring the effect of SF on lipid accumulation in human adipocytes as presented in this chapter, either with a cell line or primary cells. More research should be carried out in this area to determine whether

species differences play a role in determining the effect of Nrf2 activation in response to SF on adipogenesis and more endpoints studied to try and ascertain the mechanistic details involved.

In the final chapter, the ability of SF to target the increased pro-inflammatory state observed in obese individuals, was investigated. The effect of SF was investigated on cytokine production induced in a model of human adipose tissue inflammation.

#### **7.4. Conclusion**

It is apparent from the results in this chapter that 10 $\mu$ M SF was able to suppress adipogenesis by reducing the level of lipid accumulation within the SGBS cells during differentiation. An elevation in the levels of CPT1A expression, an important enzyme in  $\beta$ -oxidation was observed and it was hypothesised to be as a result of increased levels of FFA release due to an induction of lipolysis. Measurements of free glycerol demonstrated no changes in response to SF, suggesting that SF is not inducing lipolysis. A potential mechanism for this function of SF is the activation of Nrf2, which in turn controls a number of enzymes involved in lipid metabolism.

In the next chapter, the effect of SF will be investigated on cytokine production in a model of human adipose tissue inflammation, a condition commonly observed in individuals that are obese, using the human SGBS adipocytes exposed to MaCM from the human THP-1 macrophages.

# Chapter Eight

---

Effect of SF on adipose tissue inflammation

## 8.0. Introduction

In the previous chapter, the suppression of lipid accumulation by SF at the concentration of 10 $\mu$ M in SGBS adipocytes has been described. This effect could be potentially related to the up-regulation of Nrf2 signalling and subsequent increase in expression of genes encoding enzymes involved in lipid metabolism, such as CPT1A. Obesity is characterised by an increased level of lipid accumulation and an elevated pro-inflammatory status. In this chapter, the research question investigated was whether SF could exert anti-inflammatory effects to target cytokine production in SGBS adipocytes in response to MaCM from human THP-1 macrophages, an *in vitro* model described as the closest representation of human adipose tissue inflammation [258, 268-271].

The low-grade inflammatory state observed in obese individuals is likely as a result of a number of factors. There is a large body of scientific evidence reporting that obese subjects present with circulating monocytes in a pro-inflammatory status, higher levels of circulating pro-inflammatory cytokines and an increased level of macrophage infiltration within the adipose tissue [83, 100-102, 272, 273]. As a result of these factors, it is unsurprising that obesity is described as an independent risk factor for a number of chronic diseases such as cancer [63-65], CVD [66-70] and T2DM [71]. With the incidence of obesity increasing worldwide, its association with the listed chronic pathologies provides support for the strong need to prevent or treat obesity and its associated comorbidities. Evidence supporting the hypothesis that preventing or treating obesity can reduce the risks of developing more severe consequences such as cancer and CVD, comes from studies where the inflammatory status of obese individuals has been significantly suppressed in response to weight loss [104-108, 272]. With these findings and the widely accepted notion that a state of low-grade inflammation is the common soil to these chronic diseases, chronic inflammatory signalling has become a crucial target for dietary, lifestyle and pharmaceutical interventions [205].

The effects of SF on chronic inflammatory diseases has been previously investigated *in vivo* using mouse models of osteoarthritis [179], cancer [274, 275] and obesity induced in response to a high-fat diet [161]. SF demonstrated significant suppressions of a low-grade inflammatory state and a reduction in the progression of these conditions. When SF was administered in mice following exposure to LPS to mimic an inflammatory response, it was able to reduce the level of circulating pro-inflammatory cytokines [195]. These studies do however have disadvantages. Firstly, the very high concentrations of SF that were administered were not relevant to the potential levels of SF that could be achieved through diet [161, 195, 274, 275]. Secondly, several studies administer SF via intraperitoneal

injection instead of supplementing diets with pure SF or broccoli as a source, which is a poor representation of how SF would be encountered following broccoli consumption within the diet [195, 275]. This literature demonstrates the necessity for further *in vivo* studies, utilising physiologically relevant concentrations of SF, both in mouse models and human studies.

Following a review of the current literature it was ascertained that the effect of physiologically relevant concentrations of SF on a model of human adipose tissue inflammation had not been previously investigated *in vivo* or *in vitro*. The effect of SF on adipocyte biology has been primarily investigated using concentrations of 10 $\mu$ M and above in murine cell models [162, 164, 259-261]. Therefore, the aim of this chapter was to investigate the effect of physiologically relevant concentrations of SF on adipocyte pro-inflammatory gene expression in a model of human adipose tissue inflammation and SF's potential mechanistic targets. The dietary bioactives investigated on adipose tissue inflammation to date are only grape seed extracts and other polyphenol compounds [269-271, 276]. Thus, investigating the effect of SF at physiologically relevant concentrations on human SGBS adipocytes pro-inflammatory gene expression induced by human THP-1 MaCM is a novel concept.

## 8.1. Materials and Methods

For the experiments within these chapters the differentiated THP-1 macrophages and the human SGBS cells were used (sections 2.2.1 and 2.2.4). For measurement of cytokine secretion, an ELISA was carried out for the specific cytokine (section 2.4) and for the expression level, real-time RT-PCR was used with the specific primers and probes for each target gene (section 2.5). For assessment of cell viability in response to SF or the MaCM, a WST-1 cell viability assay was used (section 2.3). To determine the effect of MaCM on lipid accumulation with SGBS cells, Oil Red O staining was used (section 2.10). Determination of the TCA intermediates within the MaCM was carried out using LC-MS/MS (section 2.11).

## 8.2. Results

### 8.2.1. Characterisation of THP-1 macrophages

#### 8.2.1.1. Effect of SF on LPS-induced cytokine secretion

Before beginning experiments using MaCM, the THP-1 macrophages themselves were characterised due to potential differences in the behaviours of macrophages compared to the

previously used monocytes (Chapters 3 and 4). To induce differentiation, THP-1 monocytes were treated with 125ng/ml PMA for 48 hours in serum-free conditions. Differentiation was confirmed by monitoring the change in characteristics of the cells; the monocytes are a suspension cell line, while the differentiated macrophages are able to adhere to the plastic of the culture vessel (**Figure 8.1**).

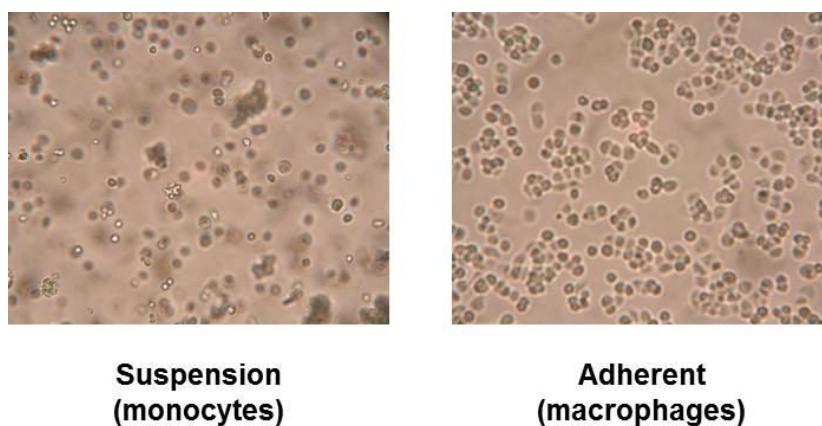


**Figure 8.1. THP-1 cell morphology.** When cultured in the monocytic form, THP-1 cells exist as a suspension. When differentiated with 125ng/ml PMA for 48 hours in serum-free conditions, the monocytes differentiate into macrophages and they become adherent to the culture vessel.

To determine whether THP-1 macrophages were able to respond to LPS in the same way as THP-1 monocytes (Chapter 3), macrophages were treated with 1ng/ml LPS in the presence or absence of 5 $\mu$ M SF. The cell culture supernatant was collected for measuring cytokine secretion. 5 $\mu$ M SF significantly suppressed LPS induction of IL-6, IL-1 $\beta$  and TNF $\alpha$  secretion with 12 or 24 hours of exposure (**Figure 8.2**).

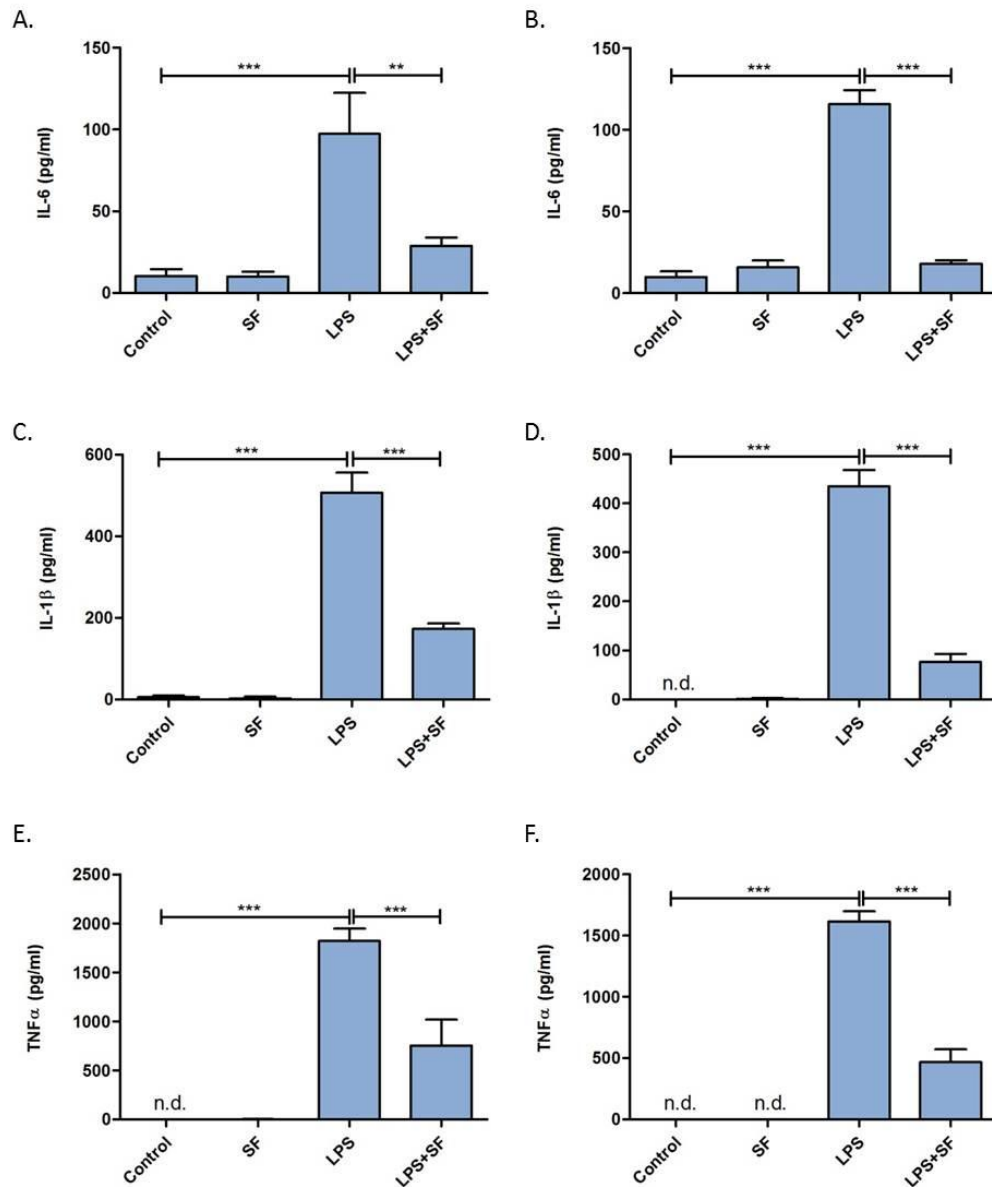


**Figure 8.2. SF significantly suppresses LPS-induced IL-6 (A + B), IL-1 $\beta$  (C + D) and TNF $\alpha$  (E + F) secretion in THP-1 macrophages.** THP-1 monocytes were treated with 125ng/ml PMA for 48 hours to allow differentiation to macrophages. THP-1 macrophages were treated with 1ng/ml LPS (vehicle control for LPS = PBS) for 12 hours (A, C and E) or 24 hours (B, D and F) in the presence or absence of 5 $\mu$ M SF (vehicle control for SF = < 0.1% (v/v) DMSO). The cell culture supernatant was collected and cytokines were measured by ELISA. Data shown = mean  $\pm$  SD. Data was statistically analysed using one-way ANOVA followed by Bonferroni multiple comparisons tests. \*\* p<0.01 and \*\*\*p<0.001 as annotated; n.d. not detected.

### 8.2.1.2. Effect of SF on THP-1 macrophage cell viability

To ensure that the significant suppression observed with SF on LPS-induced cytokine secretion was not due to cytotoxic effects, THP-1 macrophages were treated with concentrations of SF from 0-200 $\mu$ M for 24 hours before determining cell viability using a WST-1 assay. SF was found to significantly reduce cell viability at concentrations of 10 $\mu$ M and above (**Figure 8.3**). The IC<sub>50</sub> was calculated at  $26.9 \pm 5.5\mu$ M.

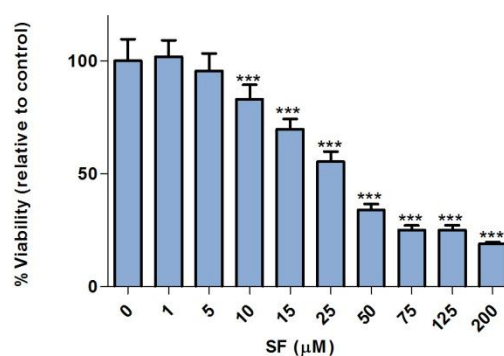


**Figure 8.3. Effect of SF on cell viability of THP-1 macrophages.** THP-1 macrophages were treated SF (0-200 $\mu$ M; vehicle control for SF = < 0.1% (v/v) DMSO) for 24 hours. After treatment was complete, 10 $\mu$ l WST-1 reagent was added to each well (see section 2.3). The plates were incubated at 37 $^{\circ}$ C and measured using a spectrophotometer every 15 minutes. Data shown is from the 45 minute measurement at which levels of absorbance were all measurable and consistent. Data shown = mean  $\pm$  SD and is representative of two independent experiments. Data was statistically analysed using one-way ANOVA followed by Bonferroni multiple comparison tests. \*\*\*p<0.001 vs. 0 $\mu$ M SF.

### 8.2.1.3. Effect of SF on LPS-induced cytokine expression

In order to determine whether SF was able to act at a transcriptional level, cytokine expression was measured. THP-1 macrophages were treated with 1ng/ml LPS in the presence or absence of 5 $\mu$ M SF for 12 or 24 hours before IL-6, IL-1 $\beta$  and TNF $\alpha$  expression levels were determined. SF significantly suppressed LPS induction of IL-6, IL-1 $\beta$  and TNF $\alpha$  expression (**Figure 8.4**).

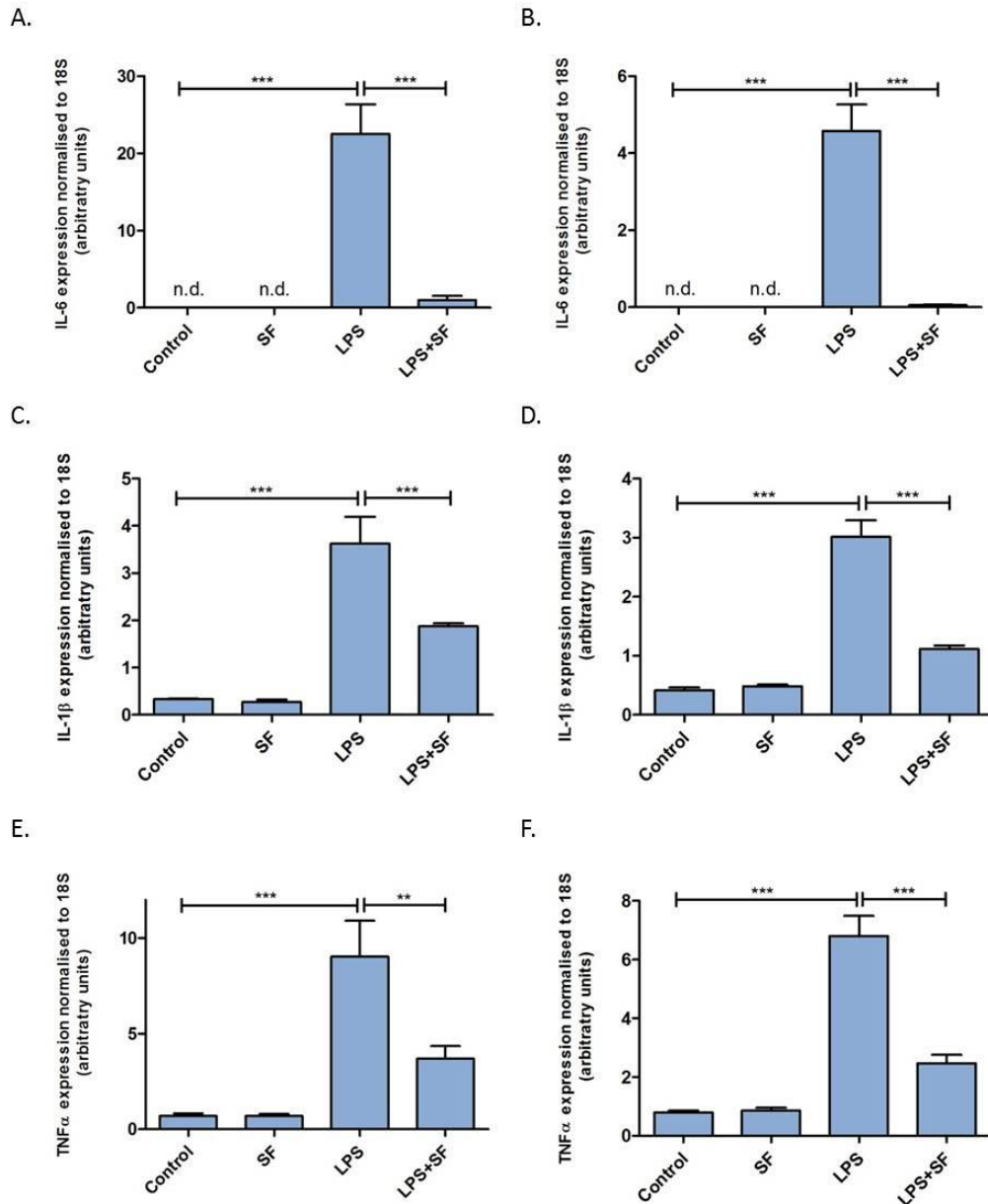


**Figure 8.4. SF significantly suppresses LPS-induced IL-6 (A + B), IL-1 $\beta$  (C + D) and TNF $\alpha$  (E + F) expression in THP-1 macrophages.** THP-1 macrophages were treated with 1ng/ml LPS (vehicle control for LPS = PBS) for 12 hours (A, C and E) or 24 hours (B, D and F) in the presence or absence of 5 $\mu$ M SF (vehicle control for SF = < 0.1% (v/v) DMSO). RNA was extracted, quantified and analysed by real-time RT-PCR. Data shown = mean  $\pm$  SD. Data was statistically analysed using one-way ANOVA followed by Bonferroni multiple comparison tests. \*\* $p$ <0.01 and \*\*\*  $p$ <0.001 as annotated; n.d. not detected.

## 8.2.2. Effect of MaCM in the presence or absence of SF on SGBS cells

### 8.2.2.1. Effect of MaCM on SGBS adipocyte cell viability

To ensure that treating the SGBS adipocytes with MaCM would not result in any cytotoxic effects, a WST-1 cell viability assay was carried out. THP-1 monocytes were differentiated with 125ng/ml PMA treatment for 48 hours. The medium was replaced after 48 hours with serum-free RPMI medium supplemented with 0.5% (w/v) BSA, in order to stabilise macrophage-secreted factors and cells were incubated for a further 48 hours. The cell culture supernatant was collected and cleared from cell debris with centrifugation and this is the MaCM used for subsequent experiments. When SGBS adipocytes were treated with MaCM from the THP-1 macrophages, concentrations of 10 and 20% did not induce any significant reduction in cell viability, whereas 50% caused a significant reduction with the percentage of viable cells remaining at approximately 70% (Figure 8.5).

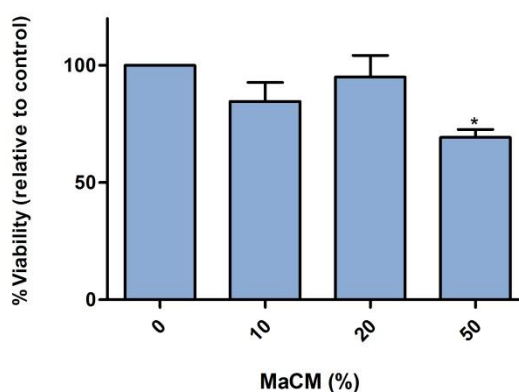


**Figure 8.5. 50% MaCM significantly reduces cell viability of SGBS adipocytes.** SGBS preadipocytes were chemically differentiated over 14 days (see section 2.2.4) to produce mature adipocytes. On day 14 after complete differentiation, SGBS adipocytes were treated with MaCM (10, 20 and 50%; vehicle control for MaCM = serum-free RPMI + 0.5% (w/v) BSA) for 24 hours. Once treatment was complete, 10 $\mu$ l WST-1 reagent was added to each well. The plates were incubated at 37°C and measured using a spectrophotometer every 15 minutes. Data shown is from the 1.5 hour measurement at which levels of absorbance were all measurable and consistent. Data shown = mean  $\pm$  SEM, n = 2. Data was statistically analysed using one-way ANOVA followed by Bonferroni multiple comparison tests. \*p<0.05 compared to 0% MaCM.

### 8.2.2.2 Effect of MaCM on differentiation of SGBS cells

In previous literature, MaCM has been found to prevent differentiation of preadipocytes to mature adipocytes in a number of murine and human adipocyte cells with MaCM from various murine and human macrophages cells [258, 268, 277-281]. To confirm that during the differentiation process my experimental model is behaving in the same way as previously used models, SGBS preadipocytes were treated with doses of MaCM (10, 20 and

50%) and the level of lipid accumulation was measured. At all doses of MaCM, after day 7 there was a significant reduction in the level of lipid accumulation and this is maintained up to day 14 (**Figure 8.6**).

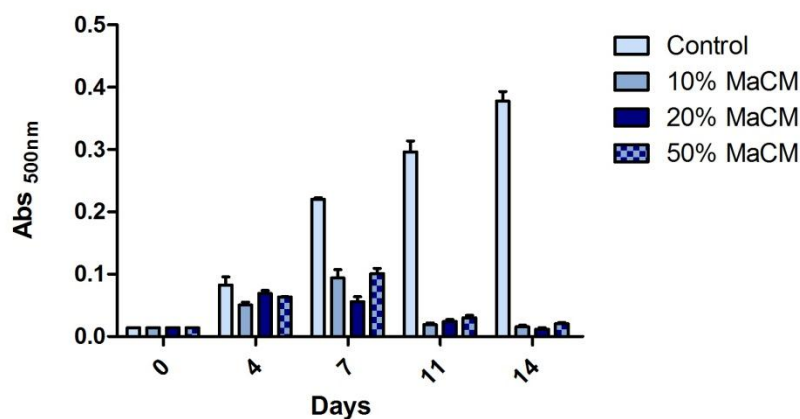


**Figure 8.6. MaCM significantly suppresses differentiation of SGBS cells.** SGBS preadipocytes were chemically differentiated in the presence or absence of MaCM (10, 20 and 50%; vehicle control for MaCM = serum-free RPMI + 0.5% (w/v) BSA). At days 0, 4, 7, 11 and 14, cells were fixed with 10% formalin and stained with Oil Red O. After the excess dye was removed, the stain was eluted and absorbance was measured at 500nm. Data shown = mean  $\pm$  SD and is representative of two independent experiments. 10%, 20% and 50% MaCM at days 7, 11 and 14 are all significantly different compared to their appropriate control for each day (\*\*\*)  $p < 0.001$ .

### 8.2.2.3. Effect of MaCM in the presence or absence of SF on SGBS cytokine expression

In obese subjects, there is a higher level of macrophage infiltration within the adipose tissue [83, 100, 101, 272, 282]. In a recent article, THP-1 macrophages and SGBS cells were described as the optimum model of human adipose tissue inflammation observed in obesity [258]. Using these cell models, the hypothesis was that MaCM from THP-1 macrophages was able to significantly induce the expression of pro-inflammatory cytokines e.g. IL-6, IL-1 $\beta$  and TNF $\alpha$ , and additionally, that SF could target this induction and cause a significant suppression. Firstly, when SGBS adipocytes were treated with MaCM (10, 20 and 50%) for 24 hours, a significant induction in IL-1 $\beta$  expression was observed. SF was able to significantly suppress the induction in IL-1 $\beta$  seen with MaCM in a dose-dependent manner (**Figure 8.7**). The same response to MaCM and SF was not seen with SGBS adipocyte IL-6 expression (**Figure 8.8**). While an induction in IL-6 expression was seen in response to MaCM, in the presence of SF, there was an additional significant increase in IL-6 expression when compared to MaCM alone in SGBS adipocytes (**Figure 8.8**). In addition, TNF $\alpha$  expression was measured and found to be below the detection capability in all samples (data not shown).

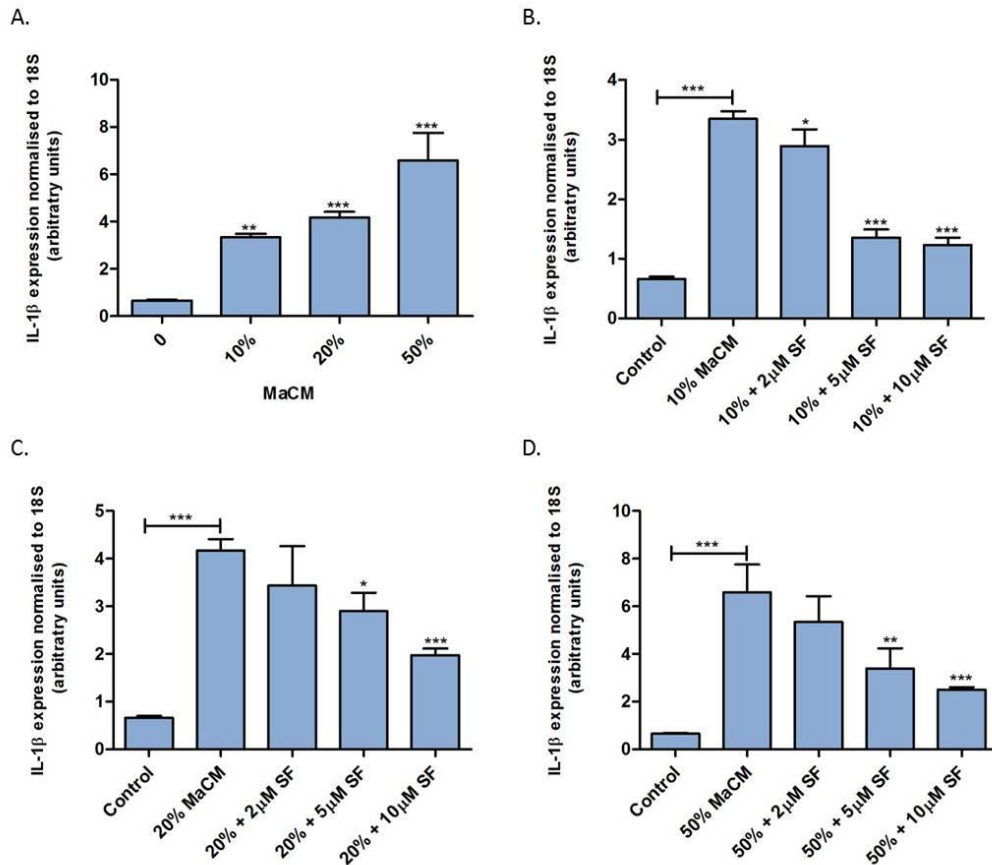


**Figure 8.7. SF significantly suppresses MaCM-induced IL-1 $\beta$  expression in SGBS adipocytes.** SGBS preadipocytes were chemically differentiated over 14 days (section 2.2.4) to produce mature adipocytes. SGBS adipocytes were treated with MaCM (10, 20 and 50%; vehicle control for MaCM = serum-free RPMI + 0.5% (w/v) BSA) for 24 hours in the presence or absence of SF (2, 5 and 10  $\mu$ M; vehicle control for SF = < 0.1% (v/v) DMSO). Following treatment, RNA was extracted and IL-1 $\beta$  expression was analysed using real-time RT-PCR. Data shown = mean  $\pm$  SD. Data was analysed using one-way ANOVA followed by Bonferroni multiple comparison tests. \*p<0.05, \*\*p<0.01 and \*\*\*p<0.001 compared against 0% MaCM (A), MaCM alone or as annotated (B-D).

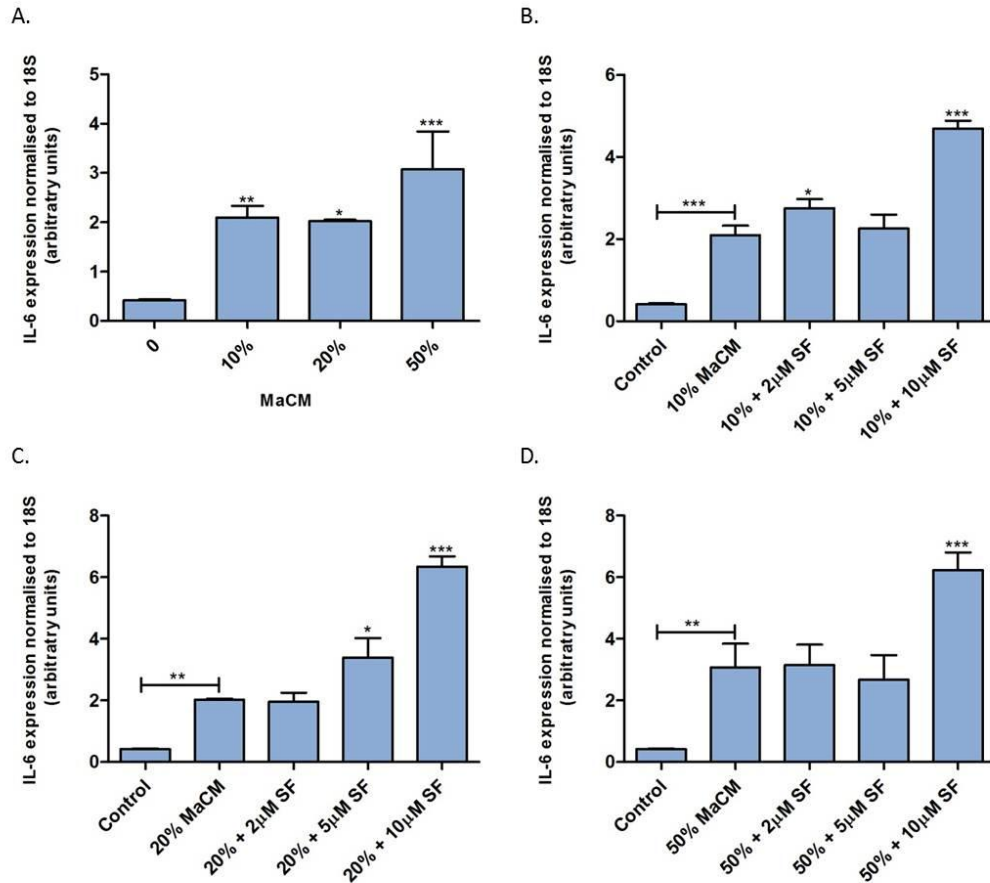


**Figure 8.8. SF significantly suppresses MaCM-induced IL-6 expression in SGBS adipocytes.** SGBS preadipocytes were chemically differentiated over 14 days (section 2.2.4) to produce mature adipocytes. SGBS adipocytes were treated with MaCM (10, 20 and 50%; vehicle control for MaCM = serum-free RPMI + 0.5% (w/v) BSA) for 24 hours in the presence or absence of SF (2, 5 and 10μM; vehicle control for SF = < 0.1% (v/v) DMSO). Following treatment, RNA was extracted and IL-6 expression was analysed using real-time RT-PCR. Data shown = mean ± SD. Data was analysed using one-way ANOVA followed by Bonferroni multiple comparison tests. \* $p < 0.05$ , \*\* $p < 0.01$  and \*\*\* $p < 0.001$  compared against 0% MaCM (A), MaCM alone or as annotated (B-D).

### 8.2.3. Analysis of MaCM

#### 8.2.3.1. LC-MS/MS for TCA intermediate analysis

Due to a lack of TNF $\alpha$  expression by SGBS adipocytes, it was hypothesised that the production of IL-1 $\beta$  and IL-6 expression was controlled by the IL-1 $\beta$  signalling pathway. Several of the TCA cycle intermediates have been associated with enhancing the IL-1 $\beta$  signalling pathway [283]. It has been hypothesised that the TCA intermediates are able to influence pro-inflammatory biomarker production as a result of the activation of the hypoxia inducible factor (HIF)-1 $\alpha$  pathway [283]. When macrophages are in an inflammatory state,

they switch their core metabolism to glycolysis and as a result a number of TCA intermediates may be induced which behave to stabilise the HIF-1 $\alpha$ , resulting in activation of its target genes of which IL-1 $\beta$  is an example [283]. Based on this research, MaCM was analysed for a number of TCA cycle intermediates to determine whether these were the components of the MaCM were responsible for the effect on IL-1 $\beta$  and IL-6 gene expression.

Citrate, succinate, lactate and malate were all identified at measurable concentrations in MaCM while the other intermediates described in **Table 2.2** were below the limit of detection. The levels of citrate, succinate, lactate and malate increased dose-dependently as would be expected (**Figure 8.9**).

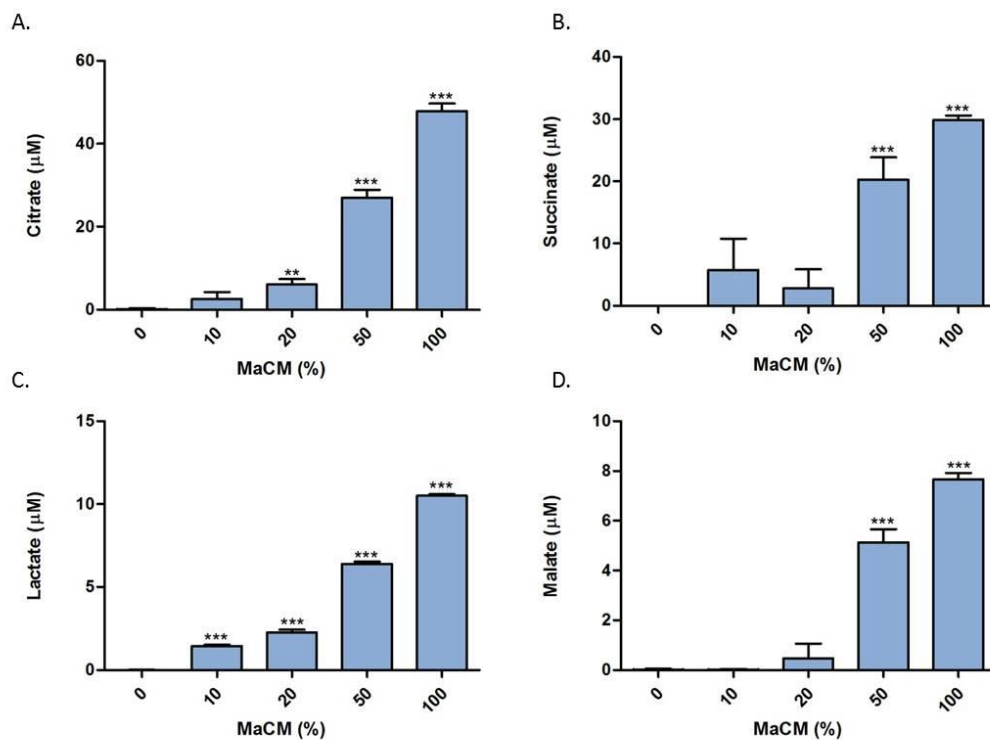


**Figure 8.9. TCA intermediate levels increase dose-dependently in MaCM from THP-1 macrophages.** THP-1 monocytes were differentiated to macrophages with a 48 hour treatment of 125ng/ml PMA. The macrophage-secreted factors were stabilised by culturing the cells with serum-free media + 0.5% (w/v) BSA for a further 48 hours. The MaCM doses were produced by diluting in DMEM/F12 + 10% (v/v) FCS (the control media of SGBS cells). The 0% MaCM condition is RPMI + 0.5% (w/v) BSA. The samples were measured for TCA intermediates using LC-MS/MS and data was analysed using Masshunter software (see section 2.11 for more details). Data shown = mean  $\pm$  SD and is representative of 2 independent experiments. \*\* $p < 0.01$  and \*\*\* $p < 0.001$  compared to 0% MaCM.

### 8.2.3.2. Effect of TCA intermediates on SGBS cytokine expression in the presence or absence of SF

Based on the high levels of several TCA intermediates measured in the MaCM, SGBS adipocytes were treated with the average levels (from two independent experiments) of the pure TCA intermediates found in 50% MaCM, to investigate whether these were responsible for the induction in IL-1 $\beta$  and IL-6 expression.

Differentiated SGBS adipocytes were treated with citrate, succinate, lactate and malate alone and in combination, however no significant changes were seen in IL-6 except for in response to lactate alone and the combination, as a result of the lactate presence (**Figure 8.10**). This significant reduction is likely due to the high millimolar concentration of lactate used and visually it could be seen to cause a high level cell death, as determined by detachment of cells from the culture vessel and changes in morphology. IL-1 $\beta$  expression was very low in the samples, resulting in poor amplification efficiency, preventing extrapolation of the relative amounts of IL-1 $\beta$  expression (data not shown).

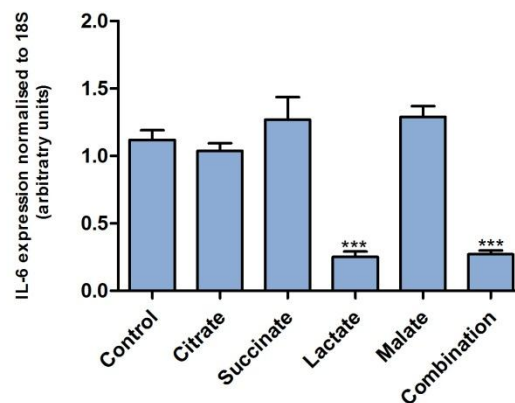


**Figure 8.10. TCA intermediates are not responsible for the induction in IL-6 expression seen in response to MaCM.** SGBS preadipocytes were chemically differentiated into mature adipocytes (see section 2.2.4). Once differentiation was complete, cells were treated with 20 $\mu$ M citrate, 15 $\mu$ M succinate, 5mM lactate and 10 $\mu$ M malate alone or in combination (all solubilised in DMEM/F12 medium) for 24 hours. RNA was extracted and IL-6 expression was analysed using real-time RT-PCR. Data shown = mean  $\pm$  SD. Data was analysed using one-way ANOVA followed by Bonferroni multiple comparison tests. \*\*\*p<0.001 vs. control.

### 8.2.3.3. Quantification of cytokines in MaCM

During the differentiation process, the morphological changes from monocytes to macrophages are accompanied by a number of functional changes such as the level of cytokine expression, which would affect the level available for secretion [268]. A number of

independent THP-1 monocyte differentiation experiments were carried out and MaCM from four independent experiments were analysed. Levels of IL-6, IL-1 $\beta$  and TNF $\alpha$  were quantified by ELISA. TNF $\alpha$  was present at levels almost three times higher than either IL-6 or IL-1 $\beta$  (**Table 8.1**).

**Table 8.1. Levels of cytokines quantified in MaCM**

<u>Cytokine</u>	<u>Concentration</u> (ng/ml; mean $\pm$ SEM*)
IL-6	8.2 $\pm$ 0.6
IL-1 $\beta$	6.7 $\pm$ 1.7
TNF $\alpha$	21.3 $\pm$ 1.7

\*Data from four independent experiments

#### **8.2.3.4. Effect of TNF $\alpha$ on SGBS cytokine expression in the presence or absence of SF**

Prior to the analysis of MaCM described in **Table 8.1**, an individual batch of MaCM was analysed to give an indication as to the levels of TNF $\alpha$ . A level of around 1ng/ml was found which was significantly lower than the levels calculated in **Table 8.1** with the larger sample group. However, this lower concentration was used to establish an experimental design where SGBS adipocytes were treated with pure TNF $\alpha$  (0.1, 0.2 and 0.5ng/ml) which was thought to be representative for 10, 20 and 50% MaCM in the presence or absence of SF (2, 5 and 10 $\mu$ M) prior to measuring IL-1 $\beta$  and IL-6 gene expression. TNF $\alpha$  treatment significantly induced IL-1 $\beta$  gene expression in a dose-dependent manner (**Figure 8.11A**). SF however was unable to suppress this induction with no effect seen at 2 and 5 $\mu$ M, but a further significant induction was seen when the SGBS adipocytes were co-treated with 10 $\mu$ M SF and TNF $\alpha$  (**Figure 8.11B-D**). The same response to TNF $\alpha$  and SF treatment was not observed with IL-6 expression. While TNF $\alpha$  treatment significantly induced IL-6 expression in a dose-dependent manner, there were no significant effects seen with SF treatment (**Figure 8.12**).

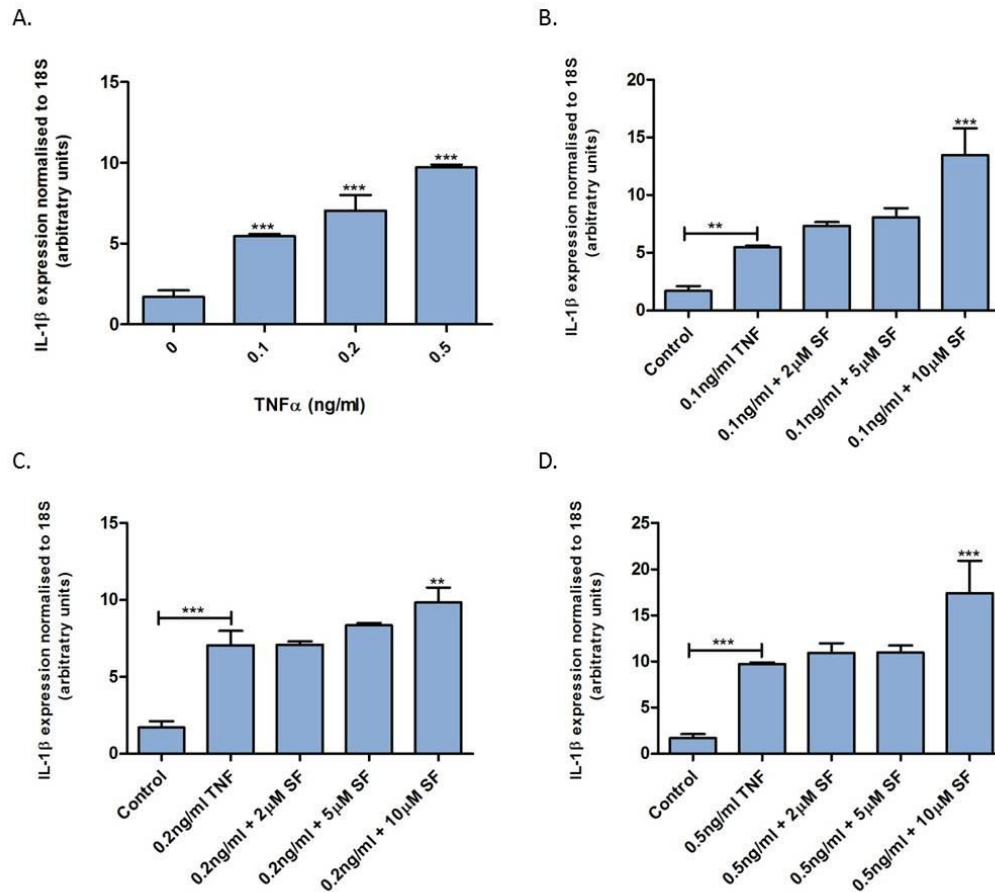


**Figure 8.11. TNF $\alpha$  induces IL-1 $\beta$  expression in SGBS adipocytes and when co-treated with 10 $\mu$ M SF, there is an additional induction.** SGBS preadipocytes were differentiated for 14 days (section 2.2.4) to produce mature adipocytes. SGBS adipocytes were treated for 24 hours with TNF $\alpha$  (0.1, 0.2 and 0.5ng/ml; vehicle control for TNF $\alpha$  = PBS) in the presence or absence of SF (2, 5 and 10 $\mu$ M; vehicle control for SF = < 0.1% (v/v) DMSO). Following treatment, RNA was extracted and IL-1 $\beta$  expression was analysed using real-time RT-PCR. Data shown = mean  $\pm$  SD. Data was analysed using one-way ANOVA followed by Bonferroni multiple comparison tests. \*\*p<0.01 and \*\*\*p<0.001 compared against 0ng/ml TNF $\alpha$  (A), TNF $\alpha$  alone or as annotated (B-D).

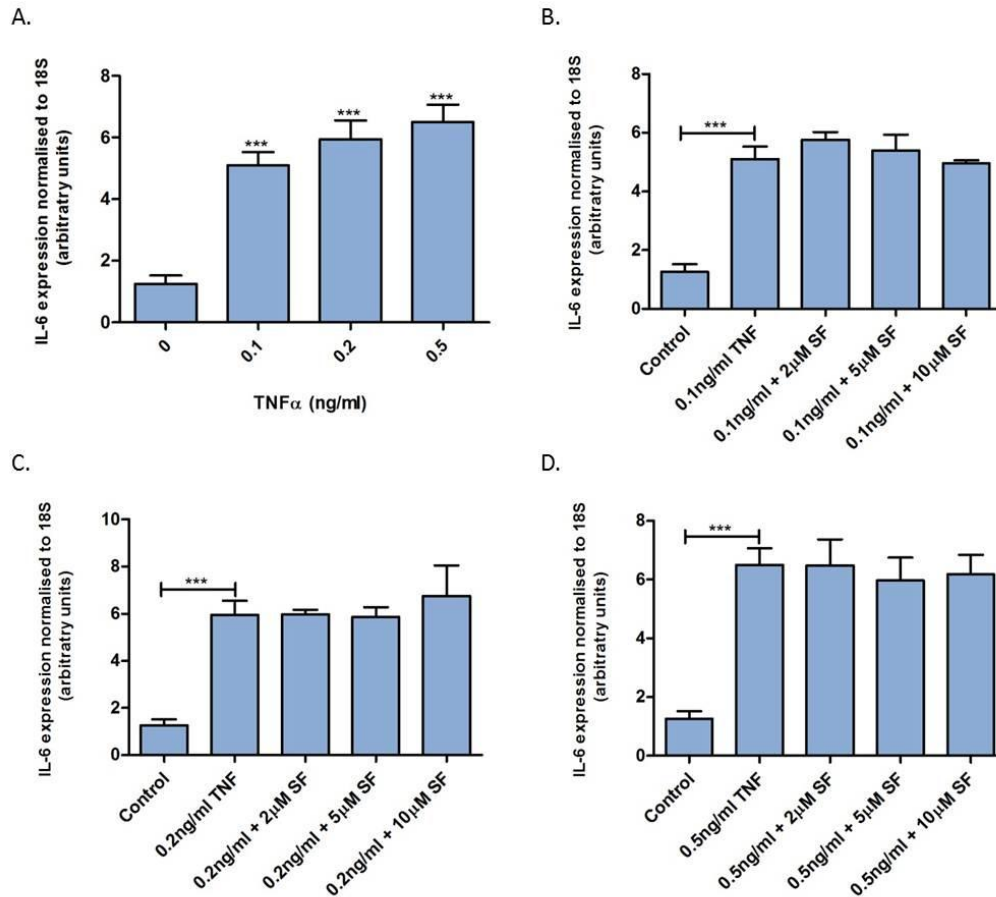


**Figure 8.12. TNF $\alpha$  induces IL-6 expression in SGBS adipocytes while SF has no significant effect.** SGBS preadipocytes were differentiated for 14 days (section 2.2.4) to produce mature adipocytes. SGBS adipocytes were treated for 24 hours with TNF $\alpha$  (0.1, 0.2 and 0.5ng/ml; vehicle control for TNF $\alpha$  = PBS) in the presence or absence of SF (2, 5 and 10 $\mu$ M; vehicle control for SF = < 0.1% (v/v) DMSO). Following treatment, RNA was extracted and IL-6 expression was analysed using real-time RT-PCR. Data shown = mean  $\pm$  SD. Data was analysed using one-way ANOVA followed by Bonferroni multiple comparison tests. \*\*\*p<0.001 compared against 0ng/ml TNF $\alpha$  (A) or as annotated (B-D).

#### 8.2.4. Effect of pre-treating SGBS adipocytes with SF on MaCM-induced cytokine expression

To further characterise the main targets by which SF could exert its anti-inflammatory effects, SGBS adipocytes were pre-treated with SF (2, 5 and 10 $\mu$ M) for 24 hours prior to being exposed to MaCM. The aim was to investigate whether a different effect was seen with IL-1 $\beta$  and IL-6 gene expression using a SF pre-treatment as compared to the previous experimental design based on SF co-treatment with MaCM (**Figures 8.7** and **8.8**). MaCM significantly induced IL-1 $\beta$  expression and SF significantly suppressed MaCM induction of IL-1 $\beta$  expression seen with 20 and 50% MaCM (**Figure 8.13**).

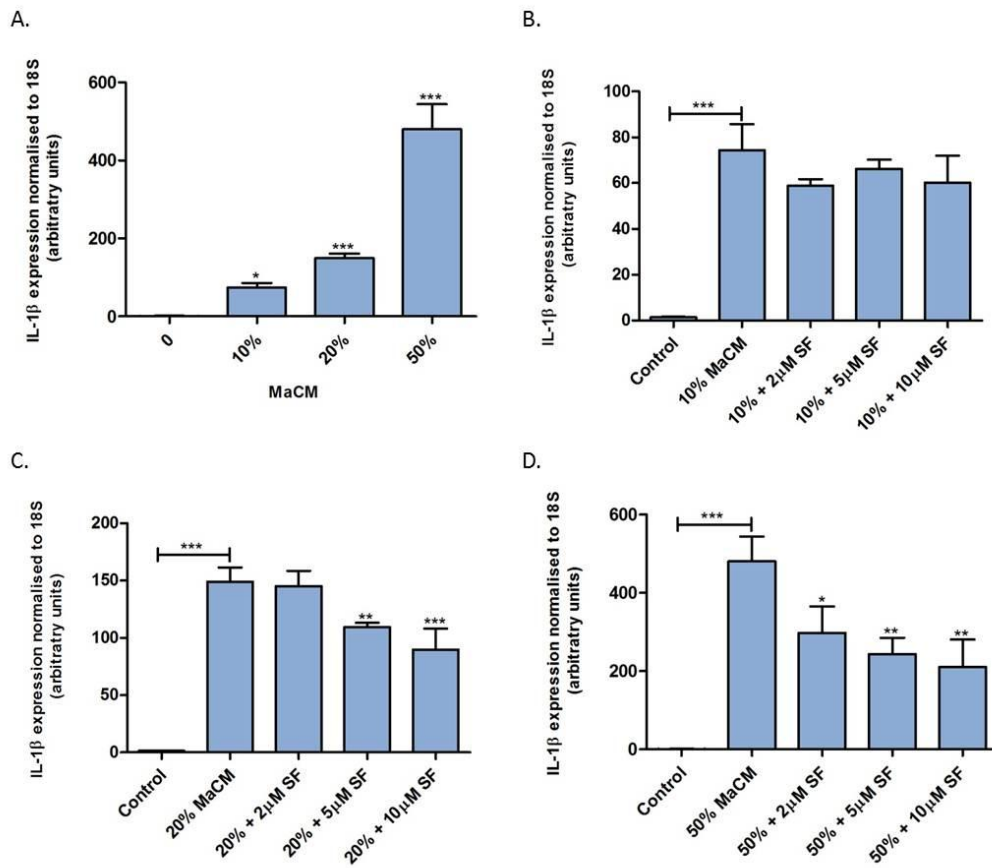


**Figure 8.13. SF significantly suppresses MaCM-induced IL-1 $\beta$  expression in SGBS adipocytes when used as a pre-treatment.** SGBS preadipocytes were differentiated for 14 days (section 2.2.4) to produce mature adipocytes. SGBS adipocytes were treated for 24 hours with SF (2, 5 and 10 $\mu$ M; vehicle control for SF = < 0.1% (v/v) DMSO) before being exposed to MaCM (10, 20 and 50%; vehicle control for MaCM = serum-free RPMI + 0.5% (w/v) BSA) for a further 24 hours. Following treatment, RNA was extracted and IL-1 $\beta$  expression was analysed using real-time RT-PCR. Data shown = mean  $\pm$  SD. Data was analysed using one-way ANOVA followed by Bonferroni multiple comparison tests. \* $p$ <0.05, \*\* $p$ <0.01 and \*\*\* $p$ <0.001 compared against 0% MaCM (A), MaCM alone or as annotated (B-D).

A significant induction in IL-6 gene expression with MaCM treatment was observed. However, SF at 10 $\mu$ M was able to further increase IL-6 expression with 10% MaCM (Figure 8.14).

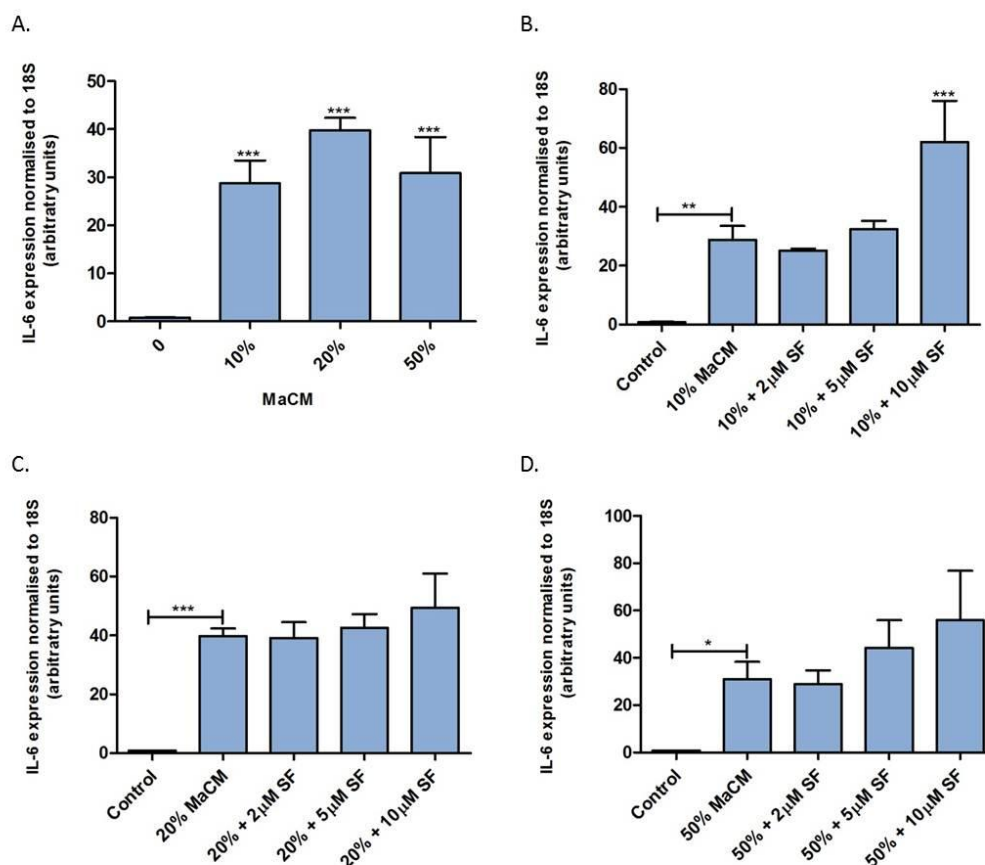


**Figure 8.14. SF had no consistent significant effects on MaCM-induced IL-6 expression in SGBS adipocytes when used as a pre-treatment.** SGBS preadipocytes were differentiated for 14 days (section 2.2.4) to produce mature adipocytes. SGBS adipocytes were treated for 24 hours with SF (2, 5 and 10 µM; vehicle control for SF = < 0.1% (v/v) DMSO) before being exposed to MaCM (10, 20 and 50%; vehicle control for MaCM = serum-free RPMI + 0.5% (w/v) BSA) for a further 24 hours. Following treatment, RNA was extracted and IL-6 expression was analysed using real-time RT-PCR. Data shown = mean ± SD. Data was analysed using one-way ANOVA followed by Bonferroni multiple comparison tests. \* $p < 0.05$ , \*\* $p < 0.01$  and \*\*\* $p < 0.001$  compared against 0% MaCM (A), MaCM alone or as annotated (B-D).

## 8.2.5. Effect of targeting macrophages with SF prior to challenging SGBS adipocytes with MaCM

### 8.2.5.1. Effect of MaCM from SF pre-treated macrophages on cytokine expression in SGBS adipocytes

To establish whether SF was able to target the macrophages with anti-inflammatory effects, THP-1 macrophages were treated with SF (2, 5 and 10 µM) for 48 hours when medium was replaced with RPMI supplemented with 0.5% (w/v) BSA. MaCM from SF-treated and

untreated macrophages was collected and SGBS adipocytes were exposed to MaCM for 24 hours before IL-1 $\beta$  and IL-6 gene expression was measured.

Treatment with MaCM from SF-treated macrophages resulted in a significantly reduced level of IL-1 $\beta$  and IL-6 gene expression induction compared to the levels seen in response to MaCM from untreated macrophages (**Figure 8.15** and **8.16**).

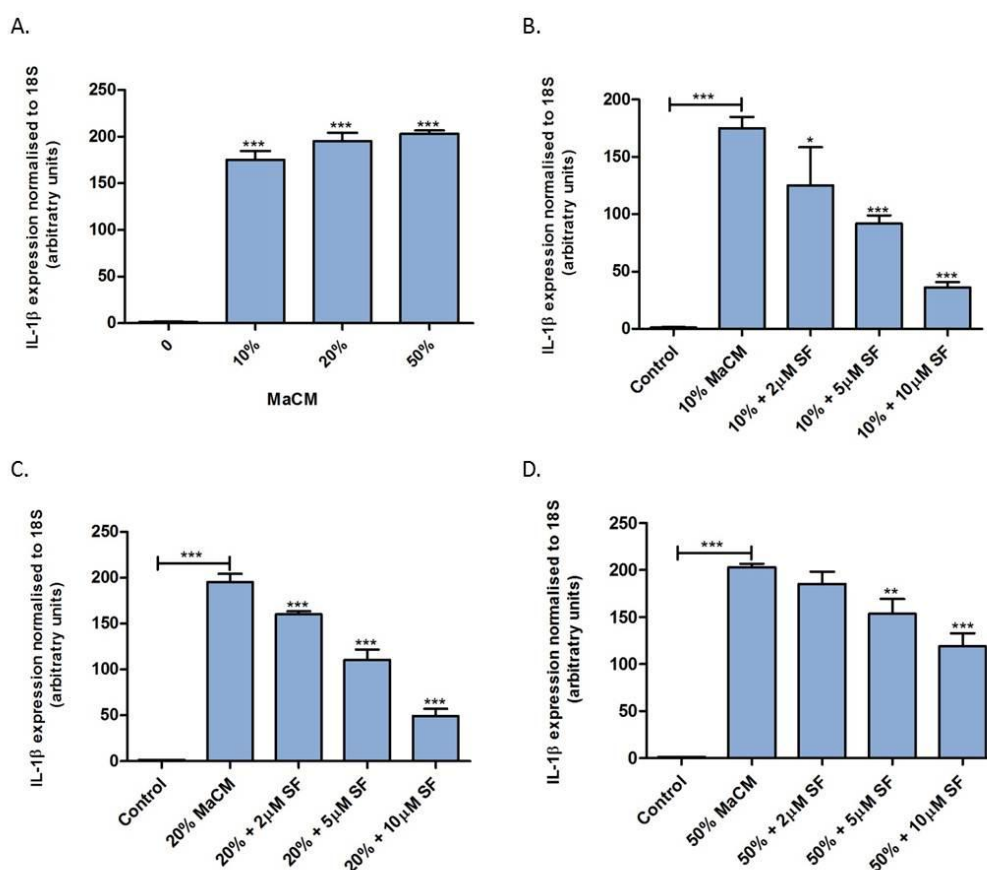


**Figure 8.15. MaCM from SF-treated macrophages demonstrates significantly reduced levels of IL-1 $\beta$  gene expression induction.** THP-1 monocytes were differentiated into macrophages with 125ng/ml PMA treatment for 48 hours. The macrophages were then incubated with RPMI + 0.5% (w/v) BSA in the presence or absence of SF (2, 5 and 10 $\mu$ M; vehicle control for SF = < 0.1% (v/v) DMSO) for a further 48 hours. SGBS preadipocytes were chemically differentiated for 14 days (section 2.2.4) to produce mature adipocytes. SGBS adipocytes were treated for 24 hours with MaCM (10, 20 and 50%; vehicle control for MaCM = serum-free RPMI + 0.5% (w/v) BSA) from either SF-treated or control-treated macrophages. RNA was extracted and IL-1 $\beta$  expression was analysed using real-time RT-PCR. Data shown = mean  $\pm$  SD. Data was analysed using one-way ANOVA followed by Bonferroni multiple comparison tests. \* $p$ <0.05, \*\* $p$ <0.01 and \*\*\* $p$ <0.001 compared against 0% MaCM (A), MaCM alone or as annotated (B-D).

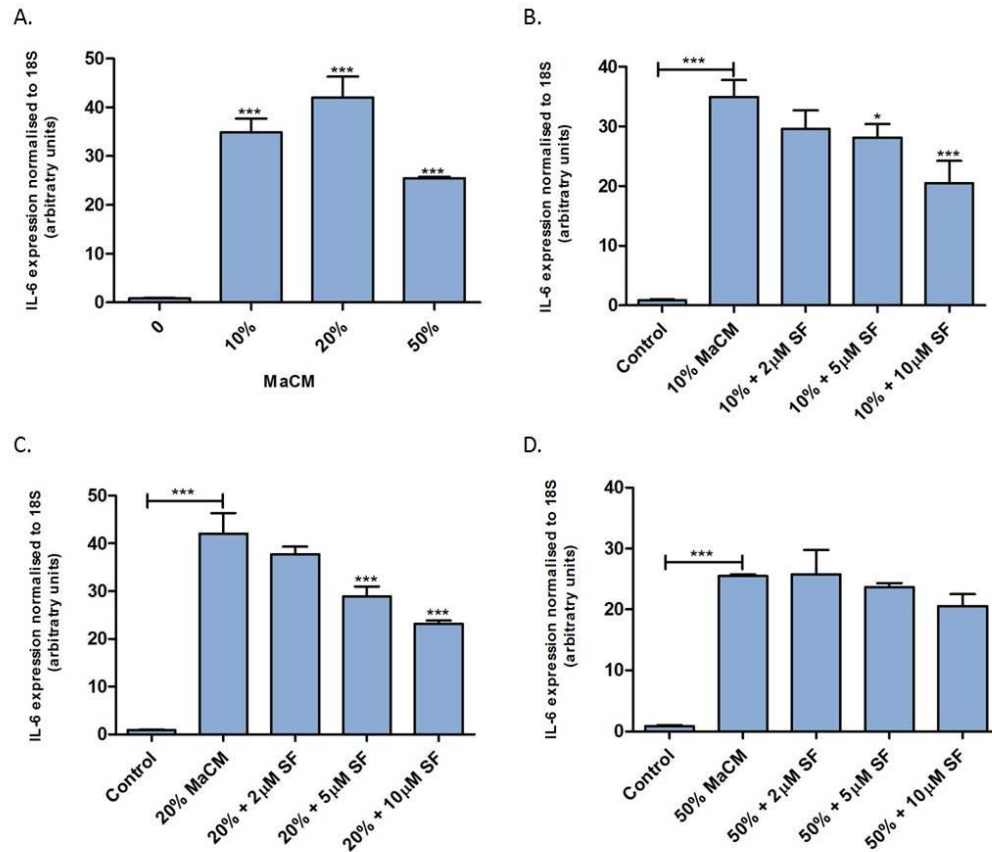


**Figure 8.16. MaCM from SF-treated macrophages demonstrates significantly reduced levels of IL-6 gene expression induction.** THP-1 monocytes were differentiated into macrophages with 125ng/ml PMA treatment for 48 hours. The macrophages were then incubated with RPMI + 0.5% (w/v) BSA in the presence or absence of SF (2, 5 and 10 µM; vehicle control for SF = < 0.1% (v/v) DMSO) for a further 48 hours. SGBS preadipocytes were chemically differentiated for 14 days (section 2.2.4) to produce mature adipocytes. SGBS adipocytes were treated for 24 hours with MaCM (10, 20 and 50%; vehicle control for MaCM = serum-free RPMI + 0.5% (w/v) BSA) from either SF-treated or control-treated macrophages. RNA was extracted and IL-6 expression was analysed using real-time RT-PCR. Data shown = mean ± SD. Data was analysed using one-way ANOVA followed by Bonferroni multiple comparison tests. \* $p < 0.05$  and \*\*\* $p < 0.001$  compared against 0% MaCM (A), MaCM alone or as annotated (B-D).

### 8.2.5.2. Quantification of cytokine levels in MaCM from SF-treated macrophages

To gain more information about how the pre-treatment of macrophages with SF resulted in a significant reduction of both IL-1 $\beta$  and IL-6 gene expression in SGBS adipocytes, the levels of IL-1 $\beta$ , IL-6 and TNF $\alpha$  were quantified in the MaCM from SF-treated or control-treated macrophages in the same way as described for **Table 8.1**. SF treatment significantly reduced the levels of IL-1 $\beta$ , IL-6 and TNF $\alpha$  secreted by the macrophages dose-dependently (**Figure 8.17**).

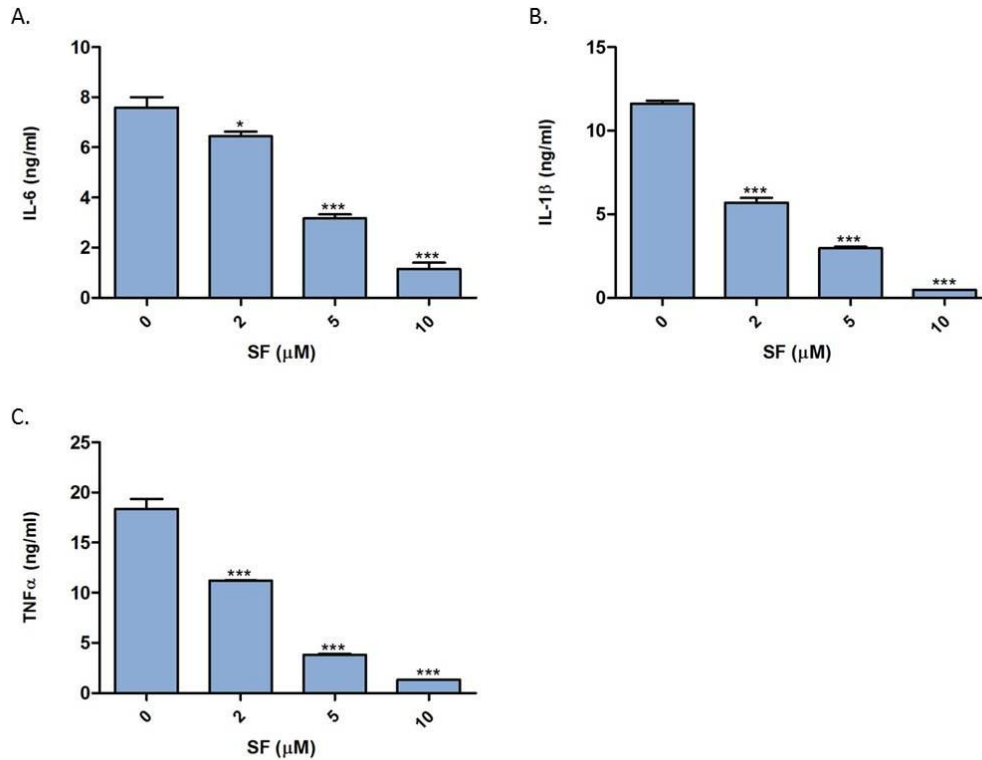


**Figure 8.17. SF significantly suppresses cytokine secretion of macrophages.** THP-1 monocytes were treated with 125ng/ml PMA for 48 hours to allow differentiation to macrophages. THP-1 macrophages were then treated with SF (2, 5 and 10 $\mu\text{M}$ ; vehicle control for SF = < 0.1% (v/v) DMSO) in RPMI + 0.5% (w/v) BSA to stabilise macrophage-secreted factors for a further 48 hours. The MaCM was collected and cytokines were measured by ELISA. Data shown = mean  $\pm$  SD. Data was statistically analysed using one-way ANOVA followed by Bonferroni multiple comparisons tests. \*  $p < 0.05$  and \*\*\* $p < 0.001$  compared to 0 $\mu\text{M}$  SF.

### 8.3. Discussion

In the previous chapters, it was reported that SF was able to exert anti-inflammatory effects at physiologically relevant concentrations by targeting not only the TLR4 signalling pathway, but also TLR2 and NOD2 inflammatory signalling pathways. This led to the conclusion that SF was able to exert its anti-inflammatory effects as a result of a multi-targeted approach. Obesity is often characterised by a state of chronic inflammation and is an independent risk factor for cancers at several sites [63-65], CVD [66-70] and T2DM [71]. Adipose tissue inflammation is common in obese subjects and contributes to the increased risk of morbidities associated with obesity. For this reason, the hypothesis of whether SF was able to suppress pro-inflammatory cytokine expression in response to macrophage-secreted factors was explored.

SF at a concentration of 5 $\mu$ M was able to suppress LPS-induced cytokine expression and secretion in differentiated THP-1 macrophages in a similar way to the results seen in Chapter 3 with THP-1 monocytes and previous results from Lin and colleagues [185]. These findings support the use of THP-1 macrophages for treatment of SGBS cells with MaCM as a highly reproducible and inexpensive *in vitro* model of adipose tissue inflammation based on the research by Keuper and colleagues [258].

The MaCM from THP-1 macrophages was found to significantly prevent preadipocyte differentiation at concentrations as low as 10% MaCM. These findings were found to be specific to this *in vitro* model of adipose tissue inflammation [268]. A number of alternative models have been used and the most commonly described combination was murine 3T3-L1 cells and the murine RAW 264.7 macrophages. These murine cell lines have been observed to behave differently to similar cell types of human origin [258]. This was demonstrated when murine 3T3-L1 cells were subjected to treatment with MaCM from murine J774 macrophages, where differentiation was only completely suppressed in the presence of 80-100% MaCM [277-280].

Based on previous findings [258, 281, 284, 285], the hypothesis that SF was able to suppress pro-inflammatory gene expression potentially increased in response to THP-1 MaCM in human SGBS adipocytes was investigated. Mature SGBS adipocytes that were exposed to a co-treatment of SF (2, 5 and 10 $\mu$ M) and MaCM (10, 20 and 50%) demonstrate a significant suppression of MaCM-induced IL-1 $\beta$  expression with concentrations from 5 $\mu$ M SF, but a further increase in IL-6 expression at the highest SF concentration (**Figure 8.7** and **8.8**). Unlike IL-1 $\beta$  which is widely accepted as a pro-inflammatory cytokine, IL-6 is more controversial with reports demonstrating its pleiotropic nature. For example, in reference to obesity, which is often associated with insulin resistance, IL-6 can have beneficial effects in some cases [286, 287]. Therefore, the additional increase in response to SF may be beneficial to consequences of adipose tissue inflammation. Furthermore, this experimental design is focusing on the effect SF exerts directly on the SGBS adipocytes due to SF being administered as a co-treatment with MaCM.

In addition to IL-1 $\beta$  and IL-6, the levels of TNF $\alpha$  expression was also measured as had been carried out in previous chapters. However, no detectable expression was found. In previous reports with SGBS cells, a significant increase in IL-6 and IL-1 $\beta$  in response to MaCM has been observed, however in the same studies there was no mention of the effect on TNF $\alpha$  expression [258, 281, 284, 285]. In this *in vitro* context where the expression of the

adipocytes alone is measured, there may be little relevance in measuring TNF $\alpha$  and this may support findings that the majority of TNF $\alpha$  expression within adipose tissue is as a result of the SVF and in particular, ATMs [83, 96, 100, 281, 288] as opposed to the adipocytes themselves.

It was hypothesised that the induction in IL-1 $\beta$  and IL-6 in response to MaCM could be through the IL-1 $\beta$  pathway. This pathway has been recently investigated in terms of its link with TCA intermediates, succinate and malonate which can behave to accentuate the inflammatory signalling through this pathway [283]. While levels of citrate, succinate, lactate and malate were detected in the MaCM, these compounds were not found to be responsible for the induction. This led to the investigations of the cytokines produced by the macrophages [281, 284, 285, 289-291]. Non-fat cells within the adipose tissue are described as being predominantly responsible for production of these pro-inflammatory mediators [83, 96, 100, 281, 288]. TNF $\alpha$  was found at the highest level with between 2.5 and 3-fold higher than the levels of IL-6 and IL-1 $\beta$  within the MaCM. Gagnon and colleagues presented data that measured IL-1 $\beta$  in MaCM also from THP-1 macrophages at a level of 500pg/ml, significantly lower than the levels reported in this chapter [289]. This could be as a result of Gagnon and colleagues collecting the media after only 24 hours culture (48 hours after differentiation in the present study), a lack of BSA presence to stabilise the macrophage-secreted factors (0.5% (w/v) BSA added to serum-free RPMI in this chapter) and also could be affected by the passage number of the THP-1 monocytes used for differentiation

Both IL-1 $\beta$  and IL-6 expression levels were significantly induced in response to all TNF $\alpha$  concentrations (**Figure 8.11A** and **8.12A**). This is consistent with previous findings where TNF $\alpha$  was able to significantly induce pro-inflammatory gene expression, of which IL-6 was consistently an example, in human adipocytes [100, 292, 293]. IL-1 $\beta$  expression was further induced when exposed to TNF $\alpha$  in combination with 10 $\mu$ M SF (**Figure 8.11B-D**), while IL-6 expression induced by TNF $\alpha$  was unaffected by SF presence (**Figure 8.12B-D**). Surprisingly, these results are completely the opposite to those observed in SGBS adipocytes exposed to the co-treatment of MaCM and SF, where IL-1 $\beta$  expression induced in response to MaCM was significantly reduced by SF and the IL-6 expression was further induced in response to SF (**Figure 8.7** and **Figure 8.8**). Based on these contradictory findings, it was concluded that while TNF $\alpha$  present within the MaCM may be partly responsible for the significant induction of IL-1 $\beta$  and IL-6 expression levels seen in response to MaCM treatment, SF was unable to suppress IL-1 $\beta$  expression and further induce IL-6 expression in response to MaCM via targeting of the TNF $\alpha$  signalling pathway.

Following these results, the experimental design that was used to answer the research question of whether SF was able to target adipose tissue inflammation was re-evaluated. As previously stated, the ATMs are derived from circulating monocytes [83, 281, 282], which would be in a pro-inflammatory state [273]. Following the consumption of broccoli, these pro-inflammatory circulating monocytes would be subjected to free SF at a similar concentration to that used in the experiments within this chapter, and would be able to significantly reduce the levels of pro-inflammatory gene expression of the circulating monocytes. These SF-suppressed monocytes would then extravasate from circulation and enter the tissue resulting in differentiation into ATMs. Due to their suppressed inflammatory status, the ATMs have the potential to be unable to express or secrete such high levels of pro-inflammatory mediators as seen without broccoli consumption and therefore reduce the level of adipose tissue inflammation. In further support, SF has been shown to accumulate in cells and tissues [294-298] and thus may be able to target the macrophages directly.

Induction of both IL-1 $\beta$  and IL-6 expression was suppressed when SGBS adipocytes were exposed to MaCM from SF-treated macrophages compared to MaCM from control-treated macrophages (**Figure 8.15A** and **8.16B**). This was presumably as a result of the observed significant suppression of IL-6, IL-1 $\beta$  and TNF $\alpha$  when subjected to SF treatment prior to collection of MaCM. This provides evidence that the response of adipocytes to MaCM is not as a result of individual compounds, but instead is as a result of a collection of molecules, a concept that has been previously suggested [279, 299]. To further address the research question that SF would primarily target the inflammatory cells rather than the adipocytes to suppress adipose tissue inflammation, an additional experimental design could be used. Prior to differentiation, the THP-1 monocytes could be exposed to SF at 2, 5 and 10 $\mu$ M before continuing with differentiation to macrophages. The SGBS adipocytes would then be exposed to MaCM from SF-treated monocytes and it could be investigated whether this is sufficient to suppress SGBS pro-inflammatory gene expression as a representation of exposure to SF following the consumption of broccoli.

Following a review of relevant literature, only one published study was identified where this experimental design of pre-treating macrophages prior to collection of MaCM for human adipocyte treatment was used in order to test a grape powder extract, known to be high in the polyphenol quercetin [270]. Quercetin was able to suppress pro-inflammatory basal gene expression in the macrophages and when human adipocytes were treated with MaCM from quercetin-treated macrophages, there was a significantly lower capacity for inducing inflammation in the adipocytes [270]. The disadvantage of this study is that quercetin in

humans is not readily biologically available unlike SF, but nevertheless these results demonstrate an additional dietary factor that may target adipose tissue inflammation. Another study carried out investigating the effect of polyphenols on adipose tissue inflammation investigated the effect of resveratrol on plasminogen activator inhibitor-1, a protein involved in obesity [269]. In that study, they used the same experimental design as seen with the results shown in **Figures 8.7** and **8.8**, where the SGBS adipocytes were co-treated with THP-1 MaCM (prepared in the same way as in the experiments within this chapter) and resveratrol, with the only difference being a 48 hour treatment [269].

From an experimental viewpoint, there was an inconsistency in the method used for the production of MaCM in this chapter compared to many other studies. Within this chapter, MaCM from human THP-1 cells was prepared by differentiating monocytes with PMA (125ng/ml) for 48 hours, followed by replacement of the media with serum-free RPMI supplemented with 0.5% (w/v) BSA in order to stabilise the macrophage-secreted factors for a further 48 hours, before collecting and using as MaCM. This is in accordance to the method used in previous studies [258, 268, 269]. In the study by Bassols and colleagues, MaCM was derived from THP-1 cells in a different way by differentiating the monocytes for only 24 hours followed by replacement of the medium, without BSA addition, before collecting the supernatant as MaCM after a further 24 hours. In addition, this study used LPS treatment at a low concentration of 10ng/ml to activate the macrophages and following monocyte differentiation, the next 24 hour treatment was supplemented with LPS and medium was collected and known as activated MaCM (AcMaCM) [284]. MaCM alone was able to induce pro-inflammatory gene expression in primary human adipocytes e.g. IL-6, and AcMaCM was able to induce the gene expression at comparable levels [284]. This was in disagreement with the study findings from Lacasa and colleagues, who employed the use of human primary adipocytes and human primary monocytes that were differentiated to yield MaCM. In the same way as Bassols and colleagues, there was a comparison with MaCM with no activation of the macrophages and MaCM from macrophages activated with LPS (100ng/ml) for 24 hours. Lacasa and colleagues found no induction in IL-6 and IL-1 $\beta$  expression in preadipocytes that were treated with MaCM from unactivated macrophages, and only saw an induction when cultured with AcMaCM [284]. This study does however make use of a very different experimental design in which the preadipocytes are differentiated in the presence of MaCM before measuring the inflammatory gene expression signature, whereas in the experiments presented in this chapter and previously reported studies, it was carried out in mature differentiated adipocytes. Nevertheless, comparable results to those found in this study were seen with a significant induction in IL-6 expression

in preadipocytes cultured in the presence of MaCM from ATMs [284]. This may further support the use of the SGBS adipocytes and THP-1 macrophages as the most advantageous *in vitro* model of adipose tissue inflammation as suggested by [258].

The data within this chapter has provided some evidence for how SF, at a physiological concentration, could exert beneficial effects on an *in vitro* model of adipose tissue inflammation with a multi-targeted approach. At a physiologically relevant concentration, SF was able to significantly suppress adipogenesis and the adipocyte inflammatory response by targeting the adipocytes directly and also macrophages prior to SGBS adipocytes being exposed to the macrophage-secreted factors. While the recent *in vivo* study with a rodent model by Choi and colleagues was able to demonstrate a significant reduction in weight gain with SF, as a result of a reduction in the amount of epididymal tissue depots via specifically targeting the important PPAR $\gamma$  and C/EBP $\alpha$  transcription factors and adipokines, the concentration used was supraphysiological. For this reason and based on the promising results seen with the *in vitro* work in this chapter, this hypothesis could be further investigated by designing *in vivo* studies in rodents using a concentration that is physiologically relevant to the consumption of broccoli. To further translate the results, a human dietary intervention study could be designed to monitor the effect of broccoli consumption on the low-grade inflammatory status commonly found in obese subjects.

## 8.4. Conclusions

It is apparent from the results in this chapter that SF was able to exert its anti-inflammatory effects via a multi-targeted approach, not limited to individually activated signalling pathways (Chapters 3-6). Human SGBS adipocytes were subjected to treatment with THP-1 MaCM in combination with SF. SF was able to significantly suppress the pro-inflammatory IL-1 $\beta$  cytokine expression but increase the pleiotropic IL-6 expression. It was discovered that although macrophages are responsible for large levels of TNF $\alpha$  production, TNF $\alpha$  alone was not solely responsible for the induction seen in IL-1 $\beta$  and IL-6 in response to MaCM and in addition, SF does not target the TNF $\alpha$  signalling pathway. It is likely that the induction seen with MaCM and the suppression with SF is due to a combination of molecules produced by the macrophages.

By targeting the macrophages directly in an improved experimental design representing a model of adipose tissue inflammation following consumption of broccoli, there was a significant reduction in the levels of IL-1 $\beta$  and IL-6 expression by the SGBS adipocytes

presumably as a result of a reduction in the levels of IL-1 $\beta$ , IL-6 and TNF $\alpha$  present within the MaCM.

This provides support for continuing this work *in vivo*, first in a rodent model using a physiologically relevant amount of SF which could be further translated into a human intervention study where obese subjects with a state of low-grade inflammation could consume a diet supplemented with broccoli, before measuring whether this dietary intervention resulted in an improvement in their systemic inflammatory status.

# Chapter Nine

---

General discussion

## 9.1. Summary of findings

The overall aim of this study was to establish whether SF, the dietary ITC from broccoli, was able to significantly suppress pro-inflammatory signalling in an *in vitro* model of chronic inflammation at a physiologically relevant concentration. It has been well-documented that SF can behave to induce phase 2 enzymes, halt the cell cycle, alter cell metabolism and also affect inflammation [300]. The work in this thesis aimed to shed light on whether the effect of SF was targeted to several pro-inflammatory mediators or whether it was able to target signalling pathways on a global scale, in addition to investigating potential mechanistic explanations before translating the findings into an *in vitro* model of adipose tissue inflammation.

In Chapter 3, the aim was to develop an *in vitro* model of chronic inflammation. Human monocytes (PBMCs and THP-1 monocytes) were the cell models of choice due to their importance in the inflammatory response. It was established that very low concentrations of LPS could be used with these sensitive cell types, with 1ng/ml being sufficient to induce the production of commonly studied pro-inflammatory cytokines IL-6, IL-1 $\beta$  and TNF $\alpha$ . While the *ex vivo* model of PBMCs have their advantages, the THP-1 monocyte cell line was able to mimic their response to LPS. At physiological concentrations of SF, a significant reduction was seen in the levels of cytokine secretion and expression in both PBMCs and THP-1 monocytes induced in response to LPS.

Chapter 4 aimed to determine whether the results seen in Chapter 3 were a specific response or whether SF was able to affect the global expression pattern of THP-1 monocytes exposed to LPS using Affymetrix GeneChip® Human Exon 1.0ST arrays. In the absence of LPS, SF at only 5 $\mu$ M was able to demonstrate a significant induction in genes encoding phase 2 enzymes and enzymes involved in cell metabolism, findings which were comparable to previously published data. A concentration of 5 $\mu$ M SF was able to significantly oppose all gene expression changes induced in response to LPS, allowing the conclusion that SF can target the TLR4-LPS signalling pathway on a global scale.

As a result of SF demonstrating the ability to target all genes induced by LPS, it was hypothesised in Chapter 5 that SF was able to target the TLR4 receptor directly, which had also been suggested by previously published research [195]. Experiments were initially carried out using a recombinant form of the extracellular domain of TLR4 with varying concentrations of SF. Concentrations as low as 5 $\mu$ M were able to modify thiol groups of cysteine residues within the TLR4 receptor. While investigations were carried out into

whether SF was able to modify the TLR4 *in vitro*, technical difficulties resulted in this not being ascertained.

With all of the experiments thus far being dependent on TLR4 signalling, in Chapter 6 the aim was to establish whether the anti-inflammatory effects seen were limited to this particular pathway, or if the same suppression could be seen when other important pro-inflammatory signalling pathways were activated. With the use of HEK293 cells that were stably transfected with the TLR4, TLR2 and NOD2 PRRs, in combination with an SEAP reporter gene under the control of NF- $\kappa$ B, the effect of SF was investigated with both the L-SF form derived from broccoli and DL-SF, the synthetic analogue. SF was able to significantly suppress ligand-induced NF- $\kappa$ B activity at physiologically relevant concentrations in response to the TLR4, TLR2 and NOD2 agonists. In addition, polymorphisms within the TLR4 and the NOD2 receptors were investigated which have been implicated in the IBD, Crohn's disease. While the SNPs in TLR4 had no impact on the level of response to either LPS or SF, the G908R NOD2 mutant demonstrated a significantly lower response to the NOD2 agonist MDP, at higher concentrations. The G908R-expressing cells also demonstrated a significantly larger reduction in NF- $\kappa$ B activity in response to SF, compared to the response seen in cells expressing the NOD2 wildtype receptor. This provides some evidence that SF may be able to have anti-inflammatory effects, to varying extents, depending on the genotype, displayed in Crohn's disease sufferers.

Based on the compiled results thus far, the next step was to translate these findings into a more complex *in vitro* model designed to mimic human adipose tissue inflammation. Initially, the effects of SF alone on adipogenesis were explored in human SGBS cells (Chapter 7). SF was able to significantly suppress the level of lipid accumulation at a concentration of 10 $\mu$ M and concomitantly, induce the level of CPT1A gene expression, a fundamental enzyme in fatty acid  $\beta$ -oxidation. With no change seen in glycerol release, it was suggested that the reduced level of lipid accumulation was not as a result of an induction in lipolysis.

In the final chapter, the ability of SF to suppress cytokine production by human SGBS adipocytes in response to MaCM from THP-1 macrophages was tested in an *in vitro* model, aimed to simulate adipose tissue inflammation in humans. While SF was able to significantly suppress the levels of IL-1 $\beta$  expression induced in response to MaCM in an experimental design where SF was targeting the adipocytes directly, IL-6 expression was further increased in response to MaCM and 10 $\mu$ M SF. Following optimisation of the

experimental design, both IL-1 $\beta$  and IL-6 expression was significantly suppressed following treatment with MaCM from SF-treated macrophages. Investigations were carried out to try and conclude the particular targets of SF in the MaCM response, and while the TNF $\alpha$  pathway was ruled out, no definitive evidence was determined, with the hypothesis being that SF was exerting anti-inflammatory effects in a multi-targeted fashion to suppress chronic inflammation.

Much of the work described in this thesis is summarised in **Figure 9.1**.

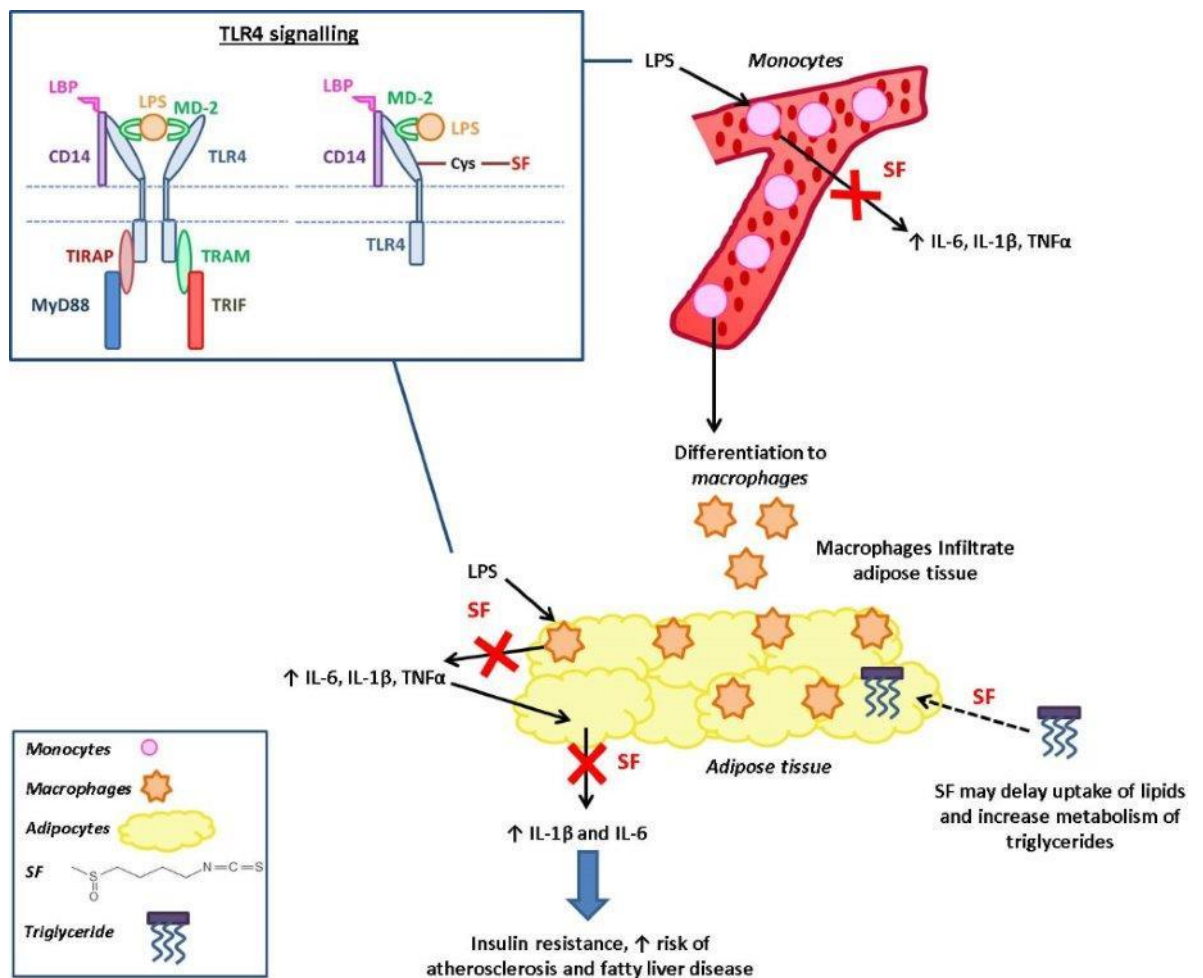


**Figure 9.1. Targets of SF for suppression of chronic inflammation.** SF is able to target circulating monocytes that may be exposed to levels of LPS at around 1ng/ml and suppress the levels of pro-inflammatory cytokines produced by interacting with the TLR4 directly or by suppressing NF- $\kappa$ B activity. Monocytes differentiate into macrophages and infiltrate the adipose tissue. SF can target the macrophages directly and lower their inflammatory potential, subsequently preventing induction of pro-inflammatory cytokine expression in the adipocytes. SF is able to suppress lipid accumulation within adipocytes, a process that occurs during obesity and increase triglyceride metabolism.

## 9.2. How do these results compare with previous literature?

The effect of SF on inflammatory signalling has been investigated previously with variations in the experimental designs. In Chapter 3, the experiments initially began with the use of an *ex vivo* model of PBMCs from healthy donors to optimise the appropriate concentration of LPS to use in order to simulate an inflammatory response. While the *ex vivo* models have distinct advantages due to their increased relevance to *in vivo* conditions, experimentally they have disadvantages. For this reason, the use of an *in vitro* monocytic cell line was used namely the THP-1 cell line, which had been previously described as a good model for human monocytes [229]. Both cell models were able to significantly respond to concentrations of 1ng/ml LPS, in terms of cytokine expression and secretion, and these levels were significantly suppressed with physiologically relevant concentrations of SF. In comparison to other studies, the importance of this data comes from the use of a very low concentration of LPS. A concentration approaching 1ng/ml is physiologically relevant to the levels of endotoxin that can be achieved in circulation in individuals that are suffering from a chronic inflammatory disorder [37, 45, 46], and even when the concentrations of LPS were further increased, there was little difference in the level of induction. In many studies, concentrations in the  $\mu\text{g/ml}$  range have been used which is not representative of the levels achieved in circulation following an acute inflammatory attack such as septic shock [197]. An additional finding in the comparison with other studies is that many are carried out with cell lines of murine origin or with cells from different locations within the body e.g. microglial cells and mouse macrophages. This therefore makes comparisons of the results difficult due to potential species differences and variations in response to LPS.

When investigated on a global scale (Chapter 4), SF alone was able to significantly affect expression of THP-1 monocytes, with a number of phase 2 enzymes being up-regulated in addition to a number of genes encoding enzymes involved in carbohydrate cell metabolism. The effect of SF on phase 2 enzyme expression has been widely documented at varying concentrations. The expression of genes such as NQO1 and TXNRD1 were commonly up-regulated in cells from a wide range of locations with concentrations as low as 1-2 $\mu\text{M}$  demonstrating an induction in both global scale microarray analyses and RT-PCR, however in some studies concentration as high as 50 $\mu\text{M}$  SF were used [140-153, 160, 231, 232, 301].

The investigations with SF and LPS, found that SF was able to oppose the effects of LPS on a global scale as demonstrated by a significant linear regression analysis ( $p < 0.001$ ). To the best of my knowledge, the global effect of SF on LPS signalling has not been previously investigated. These results demonstrate the importance of untargeted approaches to gain

more information about the extent of the effect rather than targeting a selection of specific biomarkers.

Based on previous literature and the findings describing the ability of SF to target the whole TLR4 pathway, Chapter 5 aimed to investigate potential mechanisms of SF. Youn and colleagues demonstrated that SF at a concentration of 100 $\mu$ M was able to directly modify cysteine residues within the extracellular domain of the TLR4 [195]. Similar changes were found in the investigations in Chapter 5 when the recombinant receptor was exposed to SF at the same concentration under reducing conditions. However, to make it more comparable to the *in vitro* and *in vivo* environment, the experiments were carried out under non-reducing conditions and found that Cys609 and Cys246 were modified by much lower concentrations of SF. The concept of direct binding of SF to proteins has been previously described with SF being able to bind directly to cysteine residues in proteins such as the Keap1 and MD2. This function has also been described with other ITC compounds due to the common electrophilic nature and was reviewed by Brown and colleagues [302]. In order to determine whether thiol modification by SF was a plausible mechanism for the results seen in Chapters 3 and 4, it was important to try and model these findings *in vitro*. While investigations were carried out, due to technical difficulties, conclusions could not be made. This is a general difficulty in the area of investigating the thiol adduct mechanism, as to the best of my knowledge, direct interactions with any proteins by SF via thiol modification has not been demonstrated *in vitro*.

The findings in Chapter 6 which demonstrated that SF was able to target additional inflammatory signalling pathways namely TLR2 and NOD2, led to the hypothesis that SF was able to suppress inflammatory signalling via multiple targets. In these experiments, levels of NF- $\kappa$ B activity were determined by measuring the levels of reporter gene SEAP activity. Both L-SF and DL-SF, at physiologically relevant concentrations, were able to significantly suppress NF- $\kappa$ B activity in response to agonists specific to the TLR4, TLR2 and NOD2 receptors. While polymorphisms within the TLR4 receptor had no effect on the response to either LPS or SF, the G908R polymorphism resulted in a significantly lower response to higher concentrations of MDP and also demonstrated a larger reduction in response to SF. This was possibly as a result of the change in amino acid properties, where a small aliphatic glycine was replaced with a longer chain, positively charged arginine residue, which could potentially alter interactions. In comparison with other studies that have investigated the effect of the G908R mutant, there were contrasting views. Much larger reductions in the response to MDP have been observed previously [251, 253], however the

results in the present study were more comparable to those presented by Lecine and colleagues [254].

SF has previously been shown to exert an inhibitory effect on NF- $\kappa$ B activity targeting the DNA binding activity of NF- $\kappa$ B or by directly targeting the inhibitor and subsequently affecting the translocation of the transcription factor to the nucleus, where it can actively affect the transcription of its associated genes. In terms of aiming to suppress chronic inflammation, this may be a favoured target due to the fact that a large number of other phytochemicals have demonstrated significant suppression on the activity including curcumin and resveratrol [240].

In Chapters 7 and 8, the aim was to translate the findings of the previous chapters into a more complex model of chronic inflammation via the use of human SGBS adipocytes, to model adipose tissue inflammation. In Chapter 7, it was established that SF at a concentration of 10 $\mu$ M was able to significantly reduce the levels of lipid accumulation within the cells. During obesity, the levels of lipid accumulation within adipocytes are elevated and due to an imbalance between the rate of accumulation and the rate of  $\beta$ -oxidation, FFAs are released in to systemic circulation. When triglycerides are metabolised, the glycerol backbone is released and can be measured as a marker of lipolysis. In the present study, no change in the level of glycerol released was observed but a significant increase in the level of CPT1A expression was demonstrated. The hypothesis was that there would be a reduction in the levels of lipids with SF as a result of an induction in lipolysis as previously suggested, but this was not the case [163]. The increase in the level of CPT1A expression was however in accordance with the suggestion that SF has an effect on  $\beta$ -oxidation, a hypothesis also suggested based on findings from a human intervention study with high-GSL broccoli [166]. While the effect of lipid accumulation has been previously published, the effect has only been determined in 3T3-L1 cells, a mouse fibroblast cell line that demonstrates behaviours similar to adipocytes [162, 164, 259]. Therefore, these results confirm the importance of investigating the effect of SF on human adipocytes at concentrations in a physiologically achievable range.

Finally, the level of pro-inflammatory cytokine production by SGBS adipocytes was monitored following treatment with MaCM from THP-1 macrophages. This combination of cell models has been previously described as the most representative model for human adipose tissue inflammation [258]. When treating the SGBS cells with the MaCM and SF as a co-treatment, contrasting results were seen in terms of the effect on IL-1 $\beta$  expression

compared to IL-6 expression. Optimisation of the experimental design led to the treatment of macrophages with SF prior to collection of the MaCM, in order to produce a more relevant *in vitro* model representing the effect of consuming broccoli on adipose tissue inflammation. When SGBS adipocytes were then exposed to MaCM from SF-treated macrophages, there was a dose-dependent decrease in the levels of both IL-1 $\beta$  and IL-6 expression.

While these cell models have been used in other studies, only polyphenol compounds have been investigated in terms of their effects on inflammatory cytokine production. In particular, only one article that used the same experimental design was identified, where macrophages were pre-treated with quercetin [270]. Treatment of SGBS adipocytes with MaCM from quercetin-treated macrophages demonstrated a significant reduction in the expression of pro-inflammatory mediators. However, quercetin is considerably less bioactive than SF and therefore the results seen in the present study with SF may be of increased biological relevance for investigating the effects of phytochemicals on pro-inflammatory signalling.

### **9.3. Limitations of the research**

The major limitation of this research is that all experiments presented are from *in vitro* cell models or cell-free systems. Results from *in vitro* studies are difficult to translate to *in vivo* situations for a number of reasons. These include the fact that the cells are isolated in culture and do not experience the same conditions as encountered *in vivo* such as the hypoxic nature and without existing in circulation a number of growth factors may not be experienced. However, when investigating mechanistic details of the effects of SF, it would be more difficult to investigate in an *in vivo* model. Hence, without these *in vitro* studies there would be less basis for subsequent animal and human studies.

A limitation of Chapter 3 was the varying levels of cytokine production in response to LPS. While the LPS used was from the same batch for all experiments in Chapters 3 and 4, the cells varied in passage number, which could have affected the response. For this reason, it would be more appropriate to carry out experiments using narrower passage number ranges. In Chapter 4, a large amount of information from the untargeted approach of a microarray analysis was presented. In this chapter, the main conclusion drawn was that SF at a physiologically relevant concentration was able to oppose global LPS-induced gene expression changes in THP-1 monocytes. However, a great deal of information may have been over-looked. For example, in **Table 4.10**, several genes involved in chemokine

signalling were up-regulated in response to LPS with up to a 25-fold induction, which was reduced by up to 70% in the presence of SF. Also, the genes differentially expressed in response to LPS were only presented when a minimum of 2-fold change in expression due to the vast amount of genes altered. This could however result in important collections of genes being disregarded that may have had significant functional effects following only small changes in their expression level. The potential functional importance of small expression changes was hypothesised with SF treatment on carbohydrate cell metabolism, where the fold change observed was as low as 1.2-fold, yet due to the fact that a collection of genes were linked by pathway interactions, these genes were still included. It may also be important to follow up these gene expression differences at a protein level to ensure that there are functional consequences.

In Chapter 5, the main limitation was that the research was carried out in a cell-free system with the use of a recombinant form of the TLR4 protein. While concentrations of SF were used at 5µM and above, the amount of protein used would have been far higher than the ratio of SF to TLR4 *in vitro* and *in vivo*. It is very difficult to translate the results to the potential effects demonstrated *in vitro* (Chapters 3 and 4) due to the crude experimental design. While the modification of the TLR4 by SF was investigated *in vitro*, no conclusion was able to be established as a result of technical difficulties. These experiments would need to be repeated, however, it may be difficult to identify potential SF-TLR4 adducts using the IP technique due to the reversible nature of SF binding.

#### **9.4. Future research**

The data presented in this thesis provides evidence that SF is able to target pro-inflammatory signalling at physiologically relevant concentrations by targeting monocytes in circulation and also macrophages, which in turn impacted on the inflammatory status of adipocytes (**Figure 9.1**). In terms of furthering this project, a number of extensions could be made to the experimental design. Firstly, the *in vitro* model of adipose tissue inflammation could be further improved to increase the level of relevance to *in vivo* situations by co-culturing the SGBS adipocytes with macrophages, either THP-1 or primary human macrophages. This experimental design has been previously used in several studies [258, 268]. To further the hypothesis that SF is able to significantly suppress adipose tissue inflammation, the SGBS adipocytes could be co-cultured with THP-1 macrophages that had been pre-treated with SF and measure whether there was a reduction in pro-inflammatory cytokine production by adipocytes. However, as previously discussed a limitation of the *in vitro* work is that it is

difficult to translate into an *in vivo* situation. For this reason, the findings within this thesis could be translated into an *in vivo* study design. An animal study could be carried out using a diet-induced obese (DIO) mouse model in which the effect of broccoli as a means of providing SF could be investigated. Collection of plasma and PBMCs would establish whether SF has any effect on levels of pro-inflammatory cytokines and in addition, collection of adipose tissue could allow comparison of the levels of macrophage infiltration and the expression levels of pro-inflammatory mediators.

One issue however with animal studies is the concentration of SF hoped to be achieved as well as the delivery method of choice. **Table 9.1** presents several animal studies that have involved SF supplementation, with a delivery method of either diet supplementation or oral gavage, to ensure SF is still subjected to the digestive tract.

**Table 9.1. Animal studies using SF supplementation**

Study	SF dose ( $\mu\text{mol}/\text{day}$ )*	Duration of supplementation	Broccoli consumption (g/day)**
Choi <i>et al.</i> 2014 [161]	28.2	6 weeks	22.6
Davidson <i>et al.</i> 2013 [179]	3	12 weeks	2.4
Abbaoui <i>et al.</i> 2012 [274]	7.4	2 weeks	5.6
Traka <i>et al.</i> 2010 [303]	0.5 or 5	4 or 8 weeks	0.4 or 4
Myzak <i>et al.</i> 2006 [304]	2500	16 weeks	2000

\*In order to calculate  $\mu\text{mol}/\text{day}$  two assumptions were made; the body weight of a mouse is approximately 25g and each mouse consumes around 5g of food per day.

\*\*Using the assumption that there is 0.8 $\mu\text{mol}$  of glucoraphanin per g of broccoli fresh weight with 100% conversion to SF (according to method used within the research group).

**Table 9.1** demonstrates that there is a large amount of variation in the levels of SF used in animal studies and when put into perspective of the amount of broccoli that would need to be consumed to achieve the levels, it is clear that there is a need for more studies utilising physiologically relevant concentrations. Previous studies that have employed more physiologically relevant levels of SF such as that by Davidson and colleagues, found significant effects on inflammation and the expression of key metalloproteinases implicated in osteoarthritis, another example of a chronic inflammatory disease [179]. However, Myzak and colleagues investigated the effects of SF on histone deacetylase *in vivo* using a concentration far out of the range of physiological relevance and almost 100 times higher than used within the study by Choi and colleagues, who found significant attenuation of weight gain and insulin resistance in obese models [161, 304].

The disadvantages of mouse models include the difficulty of translating the dose of SF used in the animal to the levels needed for human consumption and also the potential for species differences. As discussed by Keuper and colleagues, there are a number of different combinations of adipocytes and macrophages used either from mouse or human in order to study the effects of adipose tissue inflammation and large differences were seen, suggesting it may be difficult to achieve representative effects of human adipose tissue inflammation using studies in a mouse model [258].

Alternatively, a human intervention study could be carried out in which the effect of physiologically relevant concentrations of SF could be investigated in a targeted population for example, obese individuals compared to lean individuals. This would allow a comparison of the effect obesity on the pro-inflammatory state, in addition to any beneficial effects following an intervention with broccoli or SF supplements. It may be advantageous to use a more elderly population, based on the findings of elevated pro-inflammatory cytokines compared to that recorded in younger populations [21]. Study endpoints could include collection of plasma to monitor the levels of pro-inflammatory mediators, isolation of PBMCs to measure their inflammatory potential *ex vivo*, plus collection of adipose tissue samples to monitor the varying levels of macrophage infiltration between the lean and obese subjects and also in response to the supplementation of SF. While the collection of blood and PBMCs are less invasive procedures, the collection of adipose tissue from both obese and lean subjects would still be possible practically. Obese subjects that were undergoing a gastric band procedure, abdominoplasty and breast reductions could be prime candidates and similarly, individuals with a normal BMI could also be considered if undergoing routine abdominal surgery or indeed cosmetic procedures.

When determining the experimental design for potential human intervention studies, it is important to decide upon the method of SF delivery. SF itself is unstable and therefore the precursor of SF, glucoraphanin would be the appropriate source. Glucoraphanin could potentially be delivered as either a supplement or via the use of broccoli. In the US, a number of broccoli extracts are available which are designed to deliver a dose of glucoraphanin, and by relying on the myrosinase-like behaviour of the gut microbiota, SF could be delivered. By using a supplement it may be possible to potentially deliver higher concentrations of SF as opposed to that achieved using broccoli.

Nonetheless, the concentrations of 2-10 $\mu$ M SF used within this thesis would be achievable via consumption of broccoli within the diet. With standard broccoli, 2 $\mu$ M SF was achieved

in circulation after 2 hours of consuming broccoli [129]. However, with the development of a high-GSL broccoli, the possibility to achieve three times the amount of SF at a level of 7.4 $\mu$ M was achieved with the same portion size as that of standard broccoli [129]. This high-GSL broccoli, commercially known as Beneforté®, was produced as a result of a selective breeding process which results in the expression of a Myb-related protein-28 (*Myb28*) transcription factor from *Brassica villosa*, enabling increased production of glucoraphanin [305]. This provides the ability to deliver higher concentrations of glucoraphanin within the same portion size as that usually consumed with standard broccoli.

In conclusion, this thesis provides evidence that physiologically relevant concentrations of SF are able to suppress pro-inflammatory signalling in models of a low-grade state of inflammation, a condition linked to chronic disease. For this reason, it is logical to progress these studies into *in vivo* models and determine whether a suppression of pro-inflammatory signalling can be achieved in humans suffering from chronic inflammation. While a health claim is yet to be established for broccoli, these results could provide support for increasing the levels of standard broccoli consumption or the commercially available high-GSL Beneforté® broccoli within the diet.

---

## References

1. Barton, G.M., *A calculated response: control of inflammation by the innate immune system*. J Clin Invest, 2008. **118**(2): p. 413-20.
2. Nathan, C., *Neutrophils and immunity: challenges and opportunities*. Nat Rev Immunol, 2006. **6**(3): p. 173-82.
3. Medzhitov, R., *Origin and physiological roles of inflammation*. Nature, 2008. **454**(7203): p. 428-35.
4. Takeuchi, O. and S. Akira, *Pattern recognition receptors and inflammation*. Cell, 2010. **140**(6): p. 805-20.
5. Kawai, T. and S. Akira, *The role of pattern-recognition receptors in innate immunity: update on Toll-like receptors*. Nat Immunol, 2010. **11**(5): p. 373-84.
6. Zarembek, K.A. and P.J. Godowski, *Tissue expression of human Toll-like receptors and differential regulation of Toll-like receptor mRNAs in leukocytes in response to microbes, their products, and cytokines*. J Immunol, 2002. **168**(2): p. 554-61.
7. Akira, S., S. Uematsu, and O. Takeuchi, *Pathogen recognition and innate immunity*. Cell, 2006. **124**(4): p. 783-801.
8. Park, B.S., et al., *The structural basis of lipopolysaccharide recognition by the TLR4-MD-2 complex*. Nature, 2009. **458**(7242): p. 1191-5.
9. Endemann, G., et al., *CD36 is a receptor for oxidized low density lipoprotein*. J Biol Chem, 1993. **268**(16): p. 11811-6.
10. Hoebe, K., et al., *CD36 is a sensor of diacylglycerides*. Nature, 2005. **433**(7025): p. 523-7.
11. Jimenez-Dalmaroni, M.J., et al., *Soluble CD36 ectodomain binds negatively charged diacylglycerol ligands and acts as a co-receptor for TLR2*. PLoS One, 2009. **4**(10): p. e7411.
12. Chavez-Sanchez, L., et al., *The role of TLR2, TLR4 and CD36 in macrophage activation and foam cell formation in response to oxLDL in humans*. Human Immunology, 2014. **75**(4): p. 322-9.
13. Zeytun, A., et al., *Induction of Cytokines and Chemokines by Toll-like Receptor Signaling: Strategies for Control of Inflammation*. Critical Reviews in Immunology, 2010. **30**(1): p. 53-67.
14. Zughaier, S.M., et al., *Differential induction of the toll-like receptor 4-MyD88-dependent and -independent signaling pathways by endotoxins*. Infect Immun, 2005. **73**(5): p. 2940-50.
15. Strober, W., et al., *Signalling pathways and molecular interactions of NOD1 and NOD2*. Nat Rev Immunol, 2006. **6**(1): p. 9-20.

16. Gupta, D.K., et al., *Comparison of biosynthesis and subcellular distribution of lysozyme and lysosomal enzymes in U937 monocytes*. *Biochim Biophys Acta*, 1985. **847**(2): p. 217-22.
17. Vavricka, S.R., et al., *hPepT1 transports muramyl dipeptide, activating NF-kappaB and stimulating IL-8 secretion in human colonic Caco2/bbe cells*. *Gastroenterology*, 2004. **127**(5): p. 1401-9.
18. Grimes, C.L., et al., *The innate immune protein Nod2 binds directly to MDP, a bacterial cell wall fragment*. *J Am Chem Soc*, 2012. **134**(33): p. 13535-7.
19. Inohara, et al., *NOD-LRR proteins: role in host-microbial interactions and inflammatory disease*. *Annu Rev Biochem*, 2005. **74**: p. 355-83.
20. Pawelec, G., D. Goldeck, and E. Derhovanessian, *Inflammation, ageing and chronic disease*. *Curr Opin Immunol*, 2014. **29C**: p. 23-28.
21. Singh, T. and A.B. Newman, *Inflammatory markers in population studies of aging*. *Ageing Res Rev*, 2011. **10**(3): p. 319-29.
22. Balkwill, F. and A. Mantovani, *Inflammation and cancer: back to Virchow?* *Lancet*, 2001. **357**(9255): p. 539-45.
23. Karin, M., *NF-kappaB as a critical link between inflammation and cancer*. *Cold Spring Harb Perspect Biol*, 2009. **1**(5): p. a000141.
24. Pikarsky, E., et al., *NF-kappaB functions as a tumour promoter in inflammation-associated cancer*. *Nature*, 2004. **431**(7007): p. 461-6.
25. Aggarwal, B.B., et al., *Inflammation and cancer: How hot is the link?* *Biochemical Pharmacology*, 2006. **72**(11): p. 1605-1621.
26. Heikkila, K., S. Ebrahim, and D.A. Lawlor, *Systematic review of the association between circulating interleukin-6 (IL-6) and cancer*. *Eur J Cancer*, 2008. **44**(7): p. 937-45.
27. Heikkila, K., et al., *Associations of circulating C-reactive protein and interleukin-6 with cancer risk: findings from two prospective cohorts and a meta-analysis*. *Cancer Causes & Control*, 2009. **20**(1): p. 15-26.
28. Lu, H., W. Ouyang, and C. Huang, *Inflammation, a key event in cancer development*. *Mol Cancer Res*, 2006. **4**(4): p. 221-33.
29. Il'yasova, D., et al., *Circulating levels of inflammatory markers and cancer risk in the health aging and body composition cohort*. *Cancer Epidemiol Biomarkers Prev*, 2005. **14**(10): p. 2413-8.
30. Xu, Y., et al., *Expression and function of toll-like receptors in multiple myeloma patients: toll-like receptor ligands promote multiple myeloma cell growth and*

- survival via activation of nuclear factor-kappaB*. Br J Haematol, 2010. **150**(5): p. 543-53.
31. Beckett, N., M. Nunes, and C. Bulpitt, *Is it advantageous to lower cholesterol in the elderly hypertensive?* Cardiovasc Drugs Ther, 2000. **14**(4): p. 397-405.
32. Cesari, M., et al., *Inflammatory markers and cardiovascular disease (The Health, Aging and Body Composition [Health ABC] Study)*. Am J Cardiol, 2003. **92**(5): p. 522-8.
33. Kumar, D.V., et al., *A study on interleukin -1beta and lipid profile as markers of cardiovascular risk in rheumatoid arthritis*. J Clin Diagn Res, 2013. **7**(7): p. 1298-302.
34. Cesari, M., et al., *Inflammatory markers and onset of cardiovascular events: results from the Health ABC study*. Circulation, 2003. **108**(19): p. 2317-22.
35. Rodondi, N., et al., *Markers of atherosclerosis and inflammation for prediction of coronary heart disease in older adults*. Am J Epidemiol, 2010. **171**(5): p. 540-9.
36. Edfeldt, K., et al., *Expression of toll-like receptors in human atherosclerotic lesions: a possible pathway for plaque activation*. Circulation, 2002. **105**(10): p. 1158-61.
37. Wiedermann, C.J., et al., *Association of endotoxemia with carotid atherosclerosis and cardiovascular disease: prospective results from the Bruneck Study*. J Am Coll Cardiol, 1999. **34**(7): p. 1975-81.
38. Liu, S., et al., *A prospective study of inflammatory cytokines and diabetes mellitus in a multiethnic cohort of postmenopausal women*. Arch Intern Med, 2007. **167**(15): p. 1676-85.
39. Bertoni, A.G., et al., *Inflammation and the incidence of type 2 diabetes: the Multi-Ethnic Study of Atherosclerosis (MESA)*. Diabetes Care, 2010. **33**(4): p. 804-10.
40. Figaro, M.K., et al., *Diabetes, inflammation, and functional decline in older adults: findings from the Health, Aging and Body Composition (ABC) study*. Diabetes Care, 2006. **29**(9): p. 2039-45.
41. Pickup, J.C., et al., *Plasma interleukin-6, tumour necrosis factor alpha and blood cytokine production in type 2 diabetes*. Life Sci, 2000. **67**(3): p. 291-300.
42. Mojtaba, E., *Serum interleukin-1 beta plays an important role in insulin secretion in type II diabetic*. International Journal of Biosciences, 2011. **1**(3): p. 93-99.
43. Pradhan, A.D., et al., *C-reactive protein, interleukin 6, and risk of developing type 2 diabetes mellitus*. JAMA, 2001. **286**(3): p. 327-34.
44. Ahmad, R., et al., *Elevated expression of the toll like receptors 2 and 4 in obese individuals: its significance for obesity-induced inflammation*. J Inflamm (Lond), 2012. **9**(1): p. 48.

45. Creely, S.J., et al., *Lipopolysaccharide activates an innate immune system response in human adipose tissue in obesity and type 2 diabetes*. Am J Physiol Endocrinol Metab, 2007. **292**(3): p. E740-7.
46. Al-Attas, O.S., et al., *Changes in endotoxin levels in T2DM subjects on anti-diabetic therapies*. Cardiovasc Diabetol, 2009. **8**: p. 20.
47. Sanchez-Munoz, F., A. Dominguez-Lopez, and J.K. Yamamoto-Furusho, *Role of cytokines in inflammatory bowel disease*. World J Gastroenterol, 2008. **14**(27): p. 4280-8.
48. Hausmann, M., et al., *Toll-like receptors 2 and 4 are up-regulated during intestinal inflammation*. Gastroenterology, 2002. **122**(7): p. 1987-2000.
49. Cario, E. and D.K. Podolsky, *Differential alteration in intestinal epithelial cell expression of toll-like receptor 3 (TLR3) and TLR4 in inflammatory bowel disease*. Infect Immun, 2000. **68**(12): p. 7010-7.
50. Szebeni, B., et al., *Increased expression of Toll-like receptor (TLR) 2 and TLR4 in the colonic mucosa of children with inflammatory bowel disease*. Clin Exp Immunol, 2008. **151**(1): p. 34-41.
51. Tsianos, E.V., K.H. Katsanos, and V.E. Tsianos, *Role of genetics in the diagnosis and prognosis of Crohn's disease*. World J Gastroenterol, 2011. **17**(48): p. 5246-59.
52. van Heel, D.A., et al., *Muramyl dipeptide and toll-like receptor sensitivity in NOD2-associated Crohn's disease*. Lancet, 2005. **365**(9473): p. 1794-6.
53. Meylan, E., J. Tschopp, and M. Karin, *Intracellular pattern recognition receptors in the host response*. Nature, 2006. **442**(7098): p. 39-44.
54. Ferguson, L.R., et al., *Genes, diet and inflammatory bowel disease*. Mutat Res, 2007. **622**(1-2): p. 70-83.
55. Hong, J., et al., *TLR2, TLR4 and TLR9 polymorphisms and Crohn's disease in a New Zealand Caucasian cohort*. J Gastroenterol Hepatol, 2007. **22**(11): p. 1760-6.
56. Ouburg, S., et al., *The toll-like receptor 4 (TLR4) Asp299Gly polymorphism is associated with colonic localisation of Crohn's disease without a major role for the Saccharomyces cerevisiae mannan-LBP-CD14-TLR4 pathway*. Gut, 2005. **54**(3): p. 439-40.
57. Franchimont, D., et al., *Deficient host-bacteria interactions in inflammatory bowel disease? The toll-like receptor (TLR)-4 Asp299gly polymorphism is associated with Crohn's disease and ulcerative colitis*. Gut, 2004. **53**(7): p. 987-92.
58. Brand, S., et al., *The role of Toll-like receptor 4 Asp299Gly and Thr399Ile polymorphisms and CARD15/NOD2 mutations in the susceptibility and phenotype of Crohn's disease*. Inflamm Bowel Dis, 2005. **11**(7): p. 645-52.

- 
59. Gazouli, M., et al., *Association between polymorphisms in the Toll-like receptor 4, CD14, and CARD15/NOD2 and inflammatory bowel disease in the Greek population.* World J Gastroenterol, 2005. **11**(5): p. 681-5.
  60. Arnott, I.D., et al., *NOD2/CARD15, TLR4 and CD14 mutations in Scottish and Irish Crohn's disease patients: evidence for genetic heterogeneity within Europe?* Genes Immun, 2004. **5**(5): p. 417-25.
  61. Lakatos, P.L., et al., *Toll-like receptor 4 and NOD2/CARD15 mutations in Hungarian patients with Crohn's disease: phenotype-genotype correlations.* World J Gastroenterol, 2005. **11**(10): p. 1489-95.
  62. Shen, X., et al., *The Toll-like receptor 4 D299G and T399I polymorphisms are associated with Crohn's disease and ulcerative colitis: a meta-analysis.* Digestion, 2010. **81**(2): p. 69-77.
  63. Calle, E.E., et al., *Overweight, obesity, and mortality from cancer in a prospectively studied cohort of U.S. adults.* N Engl J Med, 2003. **348**(17): p. 1625-38.
  64. Renehan, A.G., et al., *Body-mass index and incidence of cancer: a systematic review and meta-analysis of prospective observational studies.* Lancet, 2008. **371**(9612): p. 569-78.
  65. De Pergola, G. and F. Silvestris, *Obesity as a major risk factor for cancer.* J Obes, 2013. **2013**: p. 291546.
  66. Hubert, H.B., et al., *Obesity as an independent risk factor for cardiovascular disease: a 26-year follow-up of participants in the Framingham Heart Study.* Circulation, 1983. **67**(5): p. 968-77.
  67. Manson, J.E., et al., *A prospective study of obesity and risk of coronary heart disease in women.* N Engl J Med, 1990. **322**(13): p. 882-9.
  68. Cho, E., et al., *A prospective study of obesity and risk of coronary heart disease among diabetic women.* Diabetes Care, 2002. **25**(7): p. 1142-8.
  69. Dorn, J.M., et al., *Body mass index and mortality in a general population sample of men and women. The Buffalo Health Study.* Am J Epidemiol, 1997. **146**(11): p. 919-31.
  70. Guh, D.P., et al., *The incidence of co-morbidities related to obesity and overweight: a systematic review and meta-analysis.* BMC Public Health, 2009. **9**: p. 88.
  71. Kahn, S.E., R.L. Hull, and K.M. Utzschneider, *Mechanisms linking obesity to insulin resistance and type 2 diabetes.* Nature, 2006. **444**(7121): p. 840-6.
  72. Nic Suibhne, T., et al., *High prevalence of overweight and obesity in adults with Crohn's disease: associations with disease and lifestyle factors.* J Crohns Colitis, 2013. **7**(7): p. e241-8.

73. Mendall, M.A., et al., *Is obesity a risk factor for Crohn's disease?* Dig Dis Sci, 2011. **56**(3): p. 837-44.
74. Harper, J.W., M.N. Sinanan, and T.L. Zisman, *Increased body mass index is associated with earlier time to loss of response to infliximab in patients with inflammatory bowel disease.* Inflamm Bowel Dis, 2013. **19**(10): p. 2118-24.
75. Veronica, G. and R.R. Esther, *Aging, metabolic syndrome and the heart.* Aging Dis, 2012. **3**(3): p. 269-79.
76. Basen-Engquist, K. and M. Chang, *Obesity and cancer risk: recent review and evidence.* Curr Oncol Rep, 2011. **13**(1): p. 71-6.
77. Sjostrom, L., et al., *Effects of bariatric surgery on cancer incidence in obese patients in Sweden (Swedish Obese Subjects Study): a prospective, controlled intervention trial.* Lancet Oncology, 2009. **10**(7): p. 653-62.
78. Adams, T.D., et al., *Cancer incidence and mortality after gastric bypass surgery.* Obesity (Silver Spring), 2009. **17**(4): p. 796-802.
79. Chen, Y., et al., *Association between body mass index and cardiovascular disease mortality in east Asians and south Asians: pooled analysis of prospective data from the Asia Cohort Consortium.* BMJ, 2013. **347**: p. f5446.
80. Kwok, C.S., et al., *Bariatric surgery and its impact on cardiovascular disease and mortality: a systematic review and meta-analysis.* Int J Cardiol, 2014. **173**(1): p. 20-8.
81. Lavie, C.J., R.V. Milani, and H.O. Ventura, *Obesity and cardiovascular disease: risk factor, paradox, and impact of weight loss.* J Am Coll Cardiol, 2009. **53**(21): p. 1925-32.
82. van Harmelen, V., et al., *Effect of BMI and age on adipose tissue cellularity and differentiation capacity in women.* Int J Obes Relat Metab Disord, 2003. **27**(8): p. 889-95.
83. Weisberg, S.P., et al., *Obesity is associated with macrophage accumulation in adipose tissue.* J Clin Invest, 2003. **112**(12): p. 1796-808.
84. Guilherme, A., et al., *Adipocyte dysfunctions linking obesity to insulin resistance and type 2 diabetes.* Nat Rev Mol Cell Biol, 2008. **9**(5): p. 367-77.
85. Savage, D.B., K.F. Petersen, and G.I. Shulman, *Disordered lipid metabolism and the pathogenesis of insulin resistance.* Physiol Rev, 2007. **87**(2): p. 507-20.
86. Boden, G., *Role of fatty acids in the pathogenesis of insulin resistance and NIDDM.* Diabetes, 1997. **46**(1): p. 3-10.

87. Kelley, D.S., et al., *Dietary alpha-linolenic acid alters tissue fatty acid composition, but not blood lipids, lipoproteins or coagulation status in humans*. *Lipids*, 1993. **28**(6): p. 533-7.
88. Zhang, L., et al., *Role of fatty acid uptake and fatty acid beta-oxidation in mediating insulin resistance in heart and skeletal muscle*. *Biochim Biophys Acta*, 2010. **1801**(1): p. 1-22.
89. Ramsay, R.R. and V.A. Zammit, *Carnitine acyltransferases and their influence on CoA pools in health and disease*. *Mol Aspects Med*, 2004. **25**(5-6): p. 475-93.
90. Wang, Z., et al., *Saturated fatty acids activate microglia via Toll-like receptor 4/NF-kappaB signalling*. *Br J Nutr*, 2012. **107**(2): p. 229-41.
91. Schaeffler, A., et al., *Fatty acid-induced induction of Toll-like receptor-4/nuclear factor-kappaB pathway in adipocytes links nutritional signalling with innate immunity*. *Immunology*, 2009. **126**(2): p. 233-45.
92. Hotamisligil, G.S., N.S. Shargill, and B.M. Spiegelman, *Adipose expression of tumor necrosis factor-alpha: direct role in obesity-linked insulin resistance*. *Science*, 1993. **259**(5091): p. 87-91.
93. Fried, S.K., D.A. Bunkin, and A.S. Greenberg, *Omental and subcutaneous adipose tissues of obese subjects release interleukin-6: depot difference and regulation by glucocorticoid*. *J Clin Endocrinol Metab*, 1998. **83**(3): p. 847-50.
94. Visser, M., et al., *Elevated C-reactive protein levels in overweight and obese adults*. *JAMA*, 1999. **282**(22): p. 2131-5.
95. Fain, J.N., et al., *Resistin release by human adipose tissue explants in primary culture*. *Biochem Biophys Res Commun*, 2003. **300**(3): p. 674-8.
96. Fain, J.N., S.W. Bahouth, and A.K. Madan, *TNFalpha release by the nonfat cells of human adipose tissue*. *Int J Obes Relat Metab Disord*, 2004. **28**(4): p. 616-22.
97. O'Rourke, R.W., et al., *Hypoxia-induced inflammatory cytokine secretion in human adipose tissue stromovascular cells*. *Diabetologia*, 2011. **54**(6): p. 1480-90.
98. Ye, J., et al., *Hypoxia is a potential risk factor for chronic inflammation and adiponectin reduction in adipose tissue of ob/ob and dietary obese mice*. *Am J Physiol Endocrinol Metab*, 2007. **293**(4): p. E1118-28.
99. Trayhurn, P., B. Wang, and I.S. Wood, *Hypoxia and the endocrine and signalling role of white adipose tissue*. *Arch Physiol Biochem*, 2008. **114**(4): p. 267-76.
100. Xu, H., et al., *Chronic inflammation in fat plays a crucial role in the development of obesity-related insulin resistance*. *J Clin Invest*, 2003. **112**(12): p. 1821-30.

101. Canello, R., et al., *Reduction of macrophage infiltration and chemoattractant gene expression changes in white adipose tissue of morbidly obese subjects after surgery-induced weight loss*. Diabetes, 2005. **54**(8): p. 2277-86.
102. van Beek, L., et al., *Increased systemic and adipose tissue inflammation differentiates obese women with T2DM from obese women with normal glucose tolerance*. Metabolism, 2014. **63**: p. 492-501.
103. Li, A.C. and C.K. Glass, *The macrophage foam cell as a target for therapeutic intervention*. Nat Med, 2002. **8**(11): p. 1235-42.
104. Bastard, J.P., et al., *Variations in plasma soluble tumour necrosis factor receptors after diet-induced weight loss in obesity*. Diabetes Obes Metab, 2000. **2**(5): p. 323-5.
105. Bastard, J.P., et al., *Elevated levels of interleukin 6 are reduced in serum and subcutaneous adipose tissue of obese women after weight loss*. J Clin Endocrinol Metab, 2000. **85**(9): p. 3338-42.
106. Esposito, K., et al., *Effect of weight loss and lifestyle changes on vascular inflammatory markers in obese women: a randomized trial*. JAMA, 2003. **289**(14): p. 1799-804.
107. Poitou, C., et al., *Relationship between single nucleotide polymorphisms in leptin, IL6 and adiponectin genes and their circulating product in morbidly obese subjects before and after gastric banding surgery*. Obes Surg, 2005. **15**(1): p. 11-23.
108. Clement, K., et al., *Weight loss regulates inflammation-related genes in white adipose tissue of obese subjects*. FASEB J, 2004. **18**(14): p. 1657-69.
109. Roberts, C.K. and R.J. Barnard, *Effects of exercise and diet on chronic disease*. J Appl Physiol (1985), 2005. **98**(1): p. 3-30.
110. McCullough, M.L., et al., *Diet quality and major chronic disease risk in men and women: moving toward improved dietary guidance*. Am J Clin Nutr, 2002. **76**(6): p. 1261-71.
111. Boeing, H., et al., *Critical review: vegetables and fruit in the prevention of chronic diseases*. Eur J Nutr, 2012. **51**(6): p. 637-63.
112. Higdon, J.V., et al., *Cruciferous vegetables and human cancer risk: epidemiologic evidence and mechanistic basis*. Pharmacol Res, 2007. **55**(3): p. 224-36.
113. Verhoeven, D.T., et al., *Epidemiological studies on brassica vegetables and cancer risk*. Cancer Epidemiol Biomarkers Prev, 1996. **5**(9): p. 733-48.
114. Herr, I. and M.W. Buchler, *Dietary constituents of broccoli and other cruciferous vegetables: Implications for prevention and therapy of cancer*. Cancer Treatment Reviews, 2010. **36**(5): p. 377-383.

115. Zhang, X., et al., *Cruciferous vegetable consumption is associated with a reduced risk of total and cardiovascular disease mortality*. *Am J Clin Nutr*, 2011. **94**(1): p. 240-6.
116. Lockheart, M.S., et al., *Dietary patterns, food groups and myocardial infarction: a case-control study*. *Br J Nutr*, 2007. **98**(2): p. 380-7.
117. Cornelis, M.C., A. El-Sohemy, and H. Campos, *GSTT1 genotype modifies the association between cruciferous vegetable intake and the risk of myocardial infarction*. *Am J Clin Nutr*, 2007. **86**(3): p. 752-8.
118. Kurotani, K., et al., *Vegetable and fruit intake and risk of type 2 diabetes: Japan Public Health Center-based Prospective Study*. *Br J Nutr*, 2013. **109**(4): p. 709-17.
119. Schulze, M.B., et al., *Dietary pattern, inflammation, and incidence of type 2 diabetes in women*. *Am J Clin Nutr*, 2005. **82**(3): p. 675-84; quiz 714-5.
120. Jiang, Y., et al., *Cruciferous Vegetable Intake Is Inversely Correlated with Circulating Levels of Proinflammatory Markers in Women*. *J Acad Nutr Diet*, 2014. **114**(5): p. 700-708 e2.
121. Moreno, D.A., et al., *Chemical and biological characterisation of nutraceutical compounds of broccoli*. *J Pharm Biomed Anal*, 2006. **41**(5): p. 1508-22.
122. Verkerk, R., et al., *Glucosinolates in Brassica vegetables: The influence of the food supply chain on intake, bioavailability and human health*. *Molecular Nutrition & Food Research*, 2009. **53**: p. S219-S265.
123. Fahey, J.W., A.T. Zalcman, and P. Talalay, *The chemical diversity and distribution of glucosinolates and isothiocyanates among plants*. *Phytochemistry*, 2001. **56**(1): p. 5-51.
124. Cottaz, S., B. Henrissat, and H. Driguez, *Mechanism-based inhibition and stereochemistry of glucosinolate hydrolysis by myrosinase*. *Biochemistry*, 1996. **35**(48): p. 15256-15259.
125. Saha, S., et al., *Isothiocyanate concentrations and interconversion of sulforaphane to erucin in human subjects after consumption of commercial frozen broccoli compared to fresh broccoli*. *Mol Nutr Food Res*, 2012. **56**(12): p. 1906-16.
126. Dosz, E.B. and E.H. Jeffery, *Modifying the processing and handling of frozen broccoli for increased sulforaphane formation*. *J Food Sci*, 2013. **78**(9): p. H1459-63.
127. Zhang, Y.S. and P. Talalay, *Mechanism of differential potencies of isothiocyanates as inducers of anticarcinogenic phase 2 enzymes*. *Cancer Research*, 1998. **58**(20): p. 4632-4639.

128. Ye, L., et al., *Quantitative determination of dithiocarbamates in human plasma, serum, erythrocytes and urine: pharmacokinetics of broccoli sprout isothiocyanates in humans*. Clin Chim Acta, 2002. **316**(1-2): p. 43-53.
129. Gasper, A.V., et al., *Glutathione S-transferase M1 polymorphism and metabolism of sulforaphane from standard and high-glucosinolate broccoli*. American Journal of Clinical Nutrition, 2005. **82**(6): p. 1283-1291.
130. Zhang, Y.S., *Role of glutathione in the accumulation of anticarcinogenic isothiocyanates and their glutathione conjugates by murine hepatoma cells*. Carcinogenesis, 2000. **21**(6): p. 1175-1182.
131. Zhang, Y.S., et al., *Reversible conjugation of isothiocyanates with glutathione catalyzed by human glutathione transferases*. Biochemical and Biophysical Research Communications, 1995. **206**(2): p. 748-755.
132. Shapiro, T.A., et al., *Safety, tolerance, and metabolism of broccoli sprout glucosinolates and isothiocyanates: A clinical phase I study*. Nutrition and Cancer-an International Journal, 2006. **55**(1): p. 53-62.
133. Shapiro, T.A., et al., *Human metabolism and excretion of cancer chemoprotective glucosinolates and isothiocyanates of cruciferous vegetables*. Cancer Epidemiology Biomarkers & Prevention, 1998. **7**(12): p. 1091-1100.
134. Hayes, J.D., J.U. Flanagan, and I.R. Jowsey, *Glutathione transferases*. Annu Rev Pharmacol Toxicol, 2005. **45**: p. 51-88.
135. Kolm, R.H., et al., *Isothiocyanates as substrates for human glutathione transferases: structure-activity studies*. Biochemical Journal, 1995. **311**: p. 453-459.
136. Traka, M., et al., *Broccoli Consumption Interacts with GSTM1 to Perturb Oncogenic Signalling Pathways in the Prostate*. PLoS One, 2008. **3**(7).
137. Joseph, M.A., et al., *Cruciferous vegetables, genetic polymorphisms in glutathione S-transferases M1 and T1, and prostate cancer risk*. Nutrition and Cancer-an International Journal, 2004. **50**(2): p. 206-213.
138. Spitz, M.R., et al., *Dietary intake of isothiocyanates: Evidence of a joint effect with glutathione S-transferase polymorphisms in lung cancer risk*. Cancer Epidemiology Biomarkers & Prevention, 2000. **9**(10): p. 1017-1020.
139. Wang, L.I., et al., *Dietary intake of Cruciferous vegetables, Glutathione S-transferase (GST) polymorphisms and lung cancer risk in a Caucasian population*. Cancer Causes & Control, 2004. **15**(10): p. 977-985.
140. Bonnesen, C., I.M. Eggleston, and J.D. Hayes, *Dietary indoles and isothiocyanates that are generated from cruciferous vegetables can both stimulate apoptosis and*

- confer protection against DNA damage in human colon cell lines.* Cancer Res, 2001. **61**(16): p. 6120-30.
141. Hu, R., et al., *In vivo pharmacokinetics and regulation of gene expression profiles by isothiocyanate sulforaphane in the rat.* J Pharmacol Exp Ther, 2004. **310**(1): p. 263-71.
142. Ritz, S.A., J. Wan, and D. Diaz-Sanchez, *Sulforaphane-stimulated phase II enzyme induction inhibits cytokine production by airway epithelial cells stimulated with diesel extract.* Am J Physiol Lung Cell Mol Physiol, 2007. **292**(1): p. L33-9.
143. Thimmulappa, R.K., et al., *Identification of Nrf2-regulated genes induced by the chemopreventive agent sulforaphane by oligonucleotide microarray.* Cancer Research, 2002. **62**(18): p. 5196-5203.
144. Wagner, A.E., et al., *Sulforaphane but not ascorbigen, indole-3-carbinole and ascorbic acid activates the transcription factor Nrf2 and induces phase-2 and antioxidant enzymes in human keratinocytes in culture.* Exp Dermatol, 2010. **19**(2): p. 137-44.
145. Liu, H., et al., *Sulforaphane can protect lens cells against oxidative stress: implications for cataract prevention.* Invest Ophthalmol Vis Sci, 2013. **54**(8): p. 5236-48.
146. Chambers, K.F., et al., *Gene expression profile of primary prostate epithelial and stromal cells in response to sulforaphane or iberin exposure.* Prostate, 2009. **69**(13): p. 1411-21.
147. Traka, M., et al., *Transcriptome analysis of human colon Caco-2 cells exposed to sulforaphane.* J Nutr, 2005. **135**(8): p. 1865-72.
148. Dinkova-Kostova, A.T., et al., *Induction of the phase 2 response in mouse and human skin by sulforaphane-containing broccoli sprout extracts.* Cancer Epidemiol Biomarkers Prev, 2007. **16**(4): p. 847-51.
149. Barrera, L.N., et al., *TrxR1 and GPx2 are potently induced by isothiocyanates and selenium, and mutually cooperate to protect Caco-2 cells against free radical-mediated cell death.* Biochim Biophys Acta, 2012. **1823**(10): p. 1914-24.
150. Warwick, E., et al., *Effect of phytochemicals on phase II enzyme expression in infant human primary skin fibroblast cells.* Br J Nutr, 2012. **108**(12): p. 2158-65.
151. Bacon, J.R., et al., *Dual action of sulforaphane in the regulation of thioredoxin reductase and thioredoxin in human HepG2 and Caco-2 cells.* J Agric Food Chem, 2007. **55**(4): p. 1170-6.

- 
152. Vauzour, D., et al., *Sulforaphane protects cortical neurons against 5-S-cysteinyl-dopamine-induced toxicity through the activation of ERK1/2, Nrf-2 and the upregulation of detoxification enzymes*. *Mol Nutr Food Res*, 2010. **54**(4): p. 532-42.
153. Wang, W., et al., *Sulforaphane, erucin, and iberin up-regulate thioredoxin reductase 1 expression in human MCF-7 cells*. *J Agric Food Chem*, 2005. **53**(5): p. 1417-21.
154. McMahon, M., et al., *Keap1-dependent proteasomal degradation of transcription factor Nrf2 contributes to the negative regulation of antioxidant response element-driven gene expression*. *J Biol Chem*, 2003. **278**(24): p. 21592-600.
155. Jeong, W.S., M. Jun, and A.N. Kong, *Nrf2: a potential molecular target for cancer chemoprevention by natural compounds*. *Antioxid Redox Signal*, 2006. **8**(1-2): p. 99-106.
156. Hu, C., et al., *Modification of keap1 cysteine residues by sulforaphane*. *Chem Res Toxicol*, 2011. **24**(4): p. 515-21.
157. Hong, F., M.L. Freeman, and D.C. Liebler, *Identification of sensor cysteines in human Keap1 modified by the cancer chemopreventive agent sulforaphane*. *Chemical Research in Toxicology*, 2005. **18**(12): p. 1917-1926.
158. Ahn, Y.H., et al., *Electrophilic tuning of the chemoprotective natural product sulforaphane*. *Proc Natl Acad Sci U S A*, 2010. **107**(21): p. 9590-5.
159. Zhang, D.D. and M. Hannink, *Distinct cysteine residues in Keap1 are required for Keap1-dependent ubiquitination of Nrf2 and for stabilization of Nrf2 by chemopreventive agents and oxidative stress*. *Mol Cell Biol*, 2003. **23**(22): p. 8137-51.
160. Agyeman, A.S., et al., *Transcriptomic and proteomic profiling of KEAP1 disrupted and sulforaphane-treated human breast epithelial cells reveals common expression profiles*. *Breast Cancer Res Treat*, 2011.
161. Choi, K.M., et al., *Sulforaphane attenuates obesity by inhibiting adipogenesis and activating the AMPK pathway in obese mice*. *J Nutr Biochem*, 2014. **25**(2): p. 201-7.
162. Li, Q., et al., *Sulforaphane inhibits mammary adipogenesis by targeting adipose mesenchymal stem cells*. *Breast Cancer Res Treat*, 2013. **141**(2): p. 317-24.
163. Lee, J.H., et al., *Sulforaphane induced adipolysis via hormone sensitive lipase activation, regulated by AMPK signaling pathway*. *Biochem Biophys Res Commun*, 2012. **426**(4): p. 492-7.
164. Choi, K.M., et al., *Sulforaphane inhibits mitotic clonal expansion during adipogenesis through cell cycle arrest*. *Obesity (Silver Spring)*, 2012. **20**(7): p. 1365-71.

- 
165. Kahn, B.B., et al., *AMP-activated protein kinase: ancient energy gauge provides clues to modern understanding of metabolism*. Cell Metab, 2005. **1**(1): p. 15-25.
166. Armah, C.N., et al., *A diet rich in high-glucoraphanin broccoli interacts with genotype to reduce discordance in plasma metabolite profiles by modulating mitochondrial function*. Am J Clin Nutr, 2013. **98**(3): p. 712-22.
167. Rodriguez-Cantu, L.N., et al., *Broccoli ( Brassica oleracea var. italica) sprouts and extracts rich in glucosinolates and isothiocyanates affect cholesterol metabolism and genes involved in lipid homeostasis in hamsters*. J Agric Food Chem, 2011. **59**(4): p. 1095-103.
168. Singh, S.V., et al., *Sulforaphane-induced G2/M phase cell cycle arrest involves checkpoint kinase 2-mediated phosphorylation of cell division cycle 25C*. J Biol Chem, 2004. **279**(24): p. 25813-22.
169. Herman-Antosiewicz, A., et al., *Induction of p21 protein protects against sulforaphane-induced mitotic arrest in LNCaP human prostate cancer cell line*. Mol Cancer Ther, 2007. **6**(5): p. 1673-81.
170. Cho, S.D., et al., *Involvement of c-Jun N-terminal kinase in G2/M arrest and caspase-mediated apoptosis induced by sulforaphane in DU145 prostate cancer cells*. Nutr Cancer, 2005. **52**(2): p. 213-24.
171. Parnaud, G., et al., *Mechanism of sulforaphane-induced cell cycle arrest and apoptosis in human colon cancer cells*. Nutrition and Cancer-an International Journal, 2004. **48**(2): p. 198-206.
172. Roy, S.K., R.K. Srivastava, and S. Shankar, *Inhibition of PI3K/AKT and MAPK/ERK pathways causes activation of FOXO transcription factor, leading to cell cycle arrest and apoptosis in pancreatic cancer*. J Mol Signal, 2010. **5**: p. 10.
173. Clarke, J.D., R.H. Dashwood, and E. Ho, *Multi-targeted prevention of cancer by sulforaphane*. Cancer Letters, 2008. **269**(2): p. 291-304.
174. Myzak, M.C., et al., *Sulforaphane inhibits histone deacetylase activity in BPH-1, LnCaP and PC-3 prostate epithelial cells*. Carcinogenesis, 2006. **27**(4): p. 811-9.
175. Traka, M.H., et al., *Involvement of KLF4 in sulforaphane- and iberin-mediated induction of p21(waf1/cip1)*. Nutr Cancer, 2009. **61**(1): p. 137-45.
176. Shan, Y., et al., *Effect of sulforaphane on cell growth, G(0)/G(1) phase cell progression and apoptosis in human bladder cancer T24 cells*. Int J Oncol, 2006. **29**(4): p. 883-8.
177. Singh, A.V., et al., *Sulforaphane induces caspase-mediated apoptosis in cultured PC-3 human prostate cancer cells and retards growth of PC-3 xenografts in vivo*. Carcinogenesis, 2004. **25**(1): p. 83-90.

178. Gamet-Payraastre, L., et al., *Sulforaphane, a naturally occurring isothiocyanate, induces cell cycle arrest and apoptosis in HT29 human colon cancer cells*. *Cancer Res*, 2000. **60**(5): p. 1426-33.
179. Davidson, R.K., et al., *Sulforaphane represses matrix-degrading proteases and protects cartilage from destruction in vitro and in vivo*. *Arthritis Rheum*, 2013. **65**(12): p. 3130-40.
180. Kwon, J.S., et al., *Sulforaphane inhibits restenosis by suppressing inflammation and the proliferation of vascular smooth muscle cells*. *Atherosclerosis*, 2012. **225**(1): p. 41-9.
181. Yehuda, H., et al., *Isothiocyanates inhibit psoriasis-related proinflammatory factors in human skin*. *Inflamm Res*, 2012. **61**(7): p. 735-42.
182. Guo, S., et al., *Synergistic anti-inflammatory effects of nobiletin and sulforaphane in lipopolysaccharide-stimulated RAW 264.7 cells*. *J Agric Food Chem*, 2012. **60**(9): p. 2157-64.
183. Kim, J.Y., et al., *Sulforaphane suppresses vascular adhesion molecule-1 expression in TNF-alpha-stimulated mouse vascular smooth muscle cells: involvement of the MAPK, NF-kappaB and AP-1 signaling pathways*. *Vascul Pharmacol*, 2012. **56**(3-4): p. 131-41.
184. Brandenburg, L.O., et al., *Sulforaphane suppresses LPS-induced inflammation in primary rat microglia*. *Inflammation Research*, 2010. **59**(6): p. 443-450.
185. Lin, W., et al., *Sulforaphane suppressed LPS-induced inflammation in mouse peritoneal macrophages through Nrf2 dependent pathway*. *Biochem Pharmacol*, 2008. **76**(8): p. 967-73.
186. Woo, K.J. and T.K. Kwon, *Sulforaphane suppresses lipopolysaccharide-induced cyclooxygenase-2 (COX-2) expression through the modulation of multiple targets in COX-2 gene promoter*. *Int Immunopharmacol*, 2007. **7**(13): p. 1776-83.
187. Wierinckx, A., et al., *Detoxication enzyme inducers modify cytokine production in rat mixed glial cells*. *J Neuroimmunol*, 2005. **166**(1-2): p. 132-43.
188. Shan, Y., et al., *p38 MAPK plays a distinct role in sulforaphane-induced up-regulation of ARE-dependent enzymes and down-regulation of COX-2 in human bladder cancer cells*. *Oncol Rep*, 2010. **23**(4): p. 1133-8.
189. Shan, Y., et al., *Sulforaphane down-regulates COX-2 expression by activating p38 and inhibiting NF-kappaB-DNA-binding activity in human bladder T24 cells*. *Int J Oncol*, 2009. **34**(4): p. 1129-34.

190. Zakkar, M., et al., *Activation of Nrf2 in endothelial cells protects arteries from exhibiting a proinflammatory state*. *Arterioscler Thromb Vasc Biol*, 2009. **29**(11): p. 1851-7.
191. Kivela, A.M., et al., *Sulforaphane inhibits endothelial lipase expression through NF-kappaB in endothelial cells*. *Atherosclerosis*, 2010. **213**(1): p. 122-8.
192. Heiss, E., et al., *Nuclear factor kappa B is a molecular target for sulforaphane-mediated anti-inflammatory mechanisms*. *J Biol Chem*, 2001. **276**(34): p. 32008-15.
193. Nallasamy, P., et al., *Sulforaphane reduces vascular inflammation in mice and prevents TNF-alpha-induced monocyte adhesion to primary endothelial cells through interfering with the NF-kappaB pathway*. *J Nutr Biochem*, 2014.
194. Xu, C., et al., *Suppression of NF-kappaB and NF-kappaB-regulated gene expression by sulforaphane and PEITC through IkappaBalpha, IKK pathway in human prostate cancer PC-3 cells*. *Oncogene*, 2005. **24**(28): p. 4486-95.
195. Youn, H.S., et al., *Sulforaphane Suppresses Oligomerization of TLR4 in a Thiol-Dependent Manner*. *Journal of Immunology*, 2010. **184**(1): p. 411-419.
196. Koo, J.E., et al., *Sulforaphane inhibits the engagement of LPS with TLR4/MD2 complex by preferential binding to Cys133 in MD2*. *Biochem Biophys Res Commun*, 2013. **434**(3): p. 600-5.
197. Rice, J.B., et al., *Low-level endotoxin induces potent inflammatory activation of human blood vessels: inhibition by statins*. *Arterioscler Thromb Vasc Biol*, 2003. **23**(9): p. 1576-82.
198. Tsuchiya, S., et al., *Establishment and characterization of a human acute monocytic leukemia cell line (THP-1)*. *Int J Cancer*, 1980. **26**(2): p. 171-6.
199. Tsuchiya, S., et al., *Induction of maturation in cultured human monocytic leukemia cells by a phorbol diester*. *Cancer Res*, 1982. **42**(4): p. 1530-6.
200. Wabitsch, M., et al., *Characterization of a human preadipocyte cell strain with high capacity for adipose differentiation*. *Int J Obes Relat Metab Disord*, 2001. **25**(1): p. 8-15.
201. Smyth, G.K., *Linear models and empirical bayes methods for assessing differential expression in microarray experiments*. *Stat Appl Genet Mol Biol*, 2004. **3**: p. Article3.
202. Huang da, W., B.T. Sherman, and R.A. Lempicki, *Systematic and integrative analysis of large gene lists using DAVID bioinformatics resources*. *Nat Protoc*, 2009. **4**(1): p. 44-57.
203. Huang da, W., et al., *Extracting biological meaning from large gene lists with DAVID*. *Curr Protoc Bioinformatics*, 2009. **Chapter 13**: p. Unit 13 11.

- 
204. Smith, P.K., et al., *Measurement of protein using bicinchoninic acid*. *Anal Biochem*, 1985. **150**(1): p. 76-85.
205. Scrivo, R., et al., *Inflammation as "common soil" of the multifactorial diseases*. *Autoimmun Rev*, 2011. **10**(7): p. 369-74.
206. Zhang, J.M. and J. An, *Cytokines, inflammation, and pain*. *Int Anesthesiol Clin*, 2007. **45**(2): p. 27-37.
207. Pine, S.R., et al., *Increased levels of circulating interleukin 6, interleukin 8, C-reactive protein, and risk of lung cancer*. *J Natl Cancer Inst*, 2011. **103**(14): p. 1112-22.
208. Cho, Y.A., et al., *Prognostic role of interleukin-6, interleukin-8, and leptin levels according to breast cancer subtype*. *Cancer Res Treat*, 2013. **45**(3): p. 210-9.
209. Heikkila, K., et al., *Associations of circulating C-reactive protein and interleukin-6 with survival in women with and without cancer: findings from the British Women's Heart and Health Study*. *Cancer Epidemiol Biomarkers Prev*, 2007. **16**(6): p. 1155-9.
210. Fernandez-Real, J.M., et al., *Insulin resistance, inflammation, and serum fatty acid composition*. *Diabetes Care*, 2003. **26**(5): p. 1362-8.
211. Bermudez, E.A., et al., *Interrelationships among circulating interleukin-6, C-reactive protein, and traditional cardiovascular risk factors in women*. *Arterioscler Thromb Vasc Biol*, 2002. **22**(10): p. 1668-73.
212. Dunlay, S.M., et al., *Tumor necrosis factor-alpha and mortality in heart failure: a community study*. *Circulation*, 2008. **118**(6): p. 625-31.
213. Oh, D.J., et al., *Profile of Human beta-Defensins 1,2 and Proinflammatory Cytokines (TNF-alpha, IL-6) in Patients with Chronic Kidney Disease*. *Kidney Blood Press Res*, 2013. **37**(6): p. 602-10.
214. Henderson, R.B., et al., *Rapid recruitment of inflammatory monocytes is independent of neutrophil migration*. *Blood*, 2003. **102**(1): p. 328-35.
215. Ingersoll, M.A., et al., *Monocyte trafficking in acute and chronic inflammation*. *Trends Immunol*, 2011. **32**(10): p. 470-7.
216. Tse, G. and G.D. Eslick, *Cruciferous vegetables and risk of colorectal neoplasms: a systematic review and meta-analysis*. *Nutr Cancer*, 2014. **66**(1): p. 128-39.
217. Liu, B., et al., *Cruciferous vegetables intake and risk of prostate cancer: a meta-analysis*. *Int J Urol*, 2012. **19**(2): p. 134-41.
218. Liu, B., et al., *The association of cruciferous vegetables intake and risk of bladder cancer: a meta-analysis*. *World J Urol*, 2013. **31**(1): p. 127-33.

- 
219. Liu, B., et al., *Cruciferous vegetables consumption and risk of renal cell carcinoma: a meta-analysis*. *Nutr Cancer*, 2013. **65**(5): p. 668-76.
220. Liu, X. and K. Lv, *Cruciferous vegetables intake is inversely associated with risk of breast cancer: a meta-analysis*. *Breast*, 2013. **22**(3): p. 309-13.
221. Wu, Q.J., et al., *Cruciferous vegetables consumption and the risk of female lung cancer: a prospective study and a meta-analysis*. *Ann Oncol*, 2013. **24**(7): p. 1918-24.
222. Wu, Q.J., et al., *Cruciferous vegetable consumption and gastric cancer risk: a meta-analysis of epidemiological studies*. *Cancer Sci*, 2013. **104**(8): p. 1067-73.
223. Cheung, K.L., T.O. Khor, and A.N. Kong, *Synergistic effect of combination of phenethyl isothiocyanate and sulforaphane or curcumin and sulforaphane in the inhibition of inflammation*. *Pharm Res*, 2009. **26**(1): p. 224-31.
224. Innamorato, N.G., et al., *The transcription factor Nrf2 is a therapeutic target against brain inflammation*. *J Immunol*, 2008. **181**(1): p. 680-9.
225. Heo, S.K., et al., *LPS induces inflammatory responses in human aortic vascular smooth muscle cells via Toll-like receptor 4 expression and nitric oxide production*. *Immunology Letters*, 2008. **120**(1-2): p. 57-64.
226. Blomkalns, A.L., et al., *Low level bacterial endotoxin activates two distinct signaling pathways in human peripheral blood mononuclear cells*. *J Inflamm (Lond)*, 2011. **8**: p. 4.
227. Stoll, L.L., et al., *Regulation of endotoxin-induced proinflammatory activation in human coronary artery cells: expression of functional membrane-bound CD14 by human coronary artery smooth muscle cells*. *J Immunol*, 2004. **173**(2): p. 1336-43.
228. Traka, M.H. and R.F. Mithen, *Plant science and human nutrition: challenges in assessing health-promoting properties of phytochemicals*. *Plant Cell*, 2011. **23**(7): p. 2483-97.
229. Qin, Z., *The use of THP-1 cells as a model for mimicking the function and regulation of monocytes and macrophages in the vasculature*. *Atherosclerosis*, 2012. **221**(1): p. 2-11.
230. Schildberger, A., et al., *Monocytes, peripheral blood mononuclear cells, and THP-1 cells exhibit different cytokine expression patterns following stimulation with lipopolysaccharide*. *Mediators Inflamm*, 2013. **2013**: p. 697972.
231. Bhamre, S., et al., *Temporal changes in gene expression induced by sulforaphane in human prostate cancer cells*. *Prostate*, 2009. **69**(2): p. 181-90.
232. Gross-Steinmeyer, K., et al., *Sulforaphane- and phenethyl isothiocyanate-induced inhibition of aflatoxin B1-mediated genotoxicity in human hepatocytes: role of*

- GSTM1* genotype and *CYP3A4* gene expression. *Toxicol Sci*, 2010. **116**(2): p. 422-32.
233. Wamelink, M.M., E.A. Struys, and C. Jakobs, *The biochemistry, metabolism and inherited defects of the pentose phosphate pathway: a review*. *J Inherit Metab Dis*, 2008. **31**(6): p. 703-17.
234. Brooks, J.D., V.G. Paton, and G. Vidanes, *Potent induction of phase 2 enzymes in human prostate cells by sulforaphane*. *Cancer Epidemiology Biomarkers & Prevention*, 2001. **10**(9): p. 949-954.
235. Ellertsen, L.K., et al., *Effect of a medicinal extract from Agaricus blazei Murill on gene expression in a human monocyte cell line as examined by microarrays and immuno assays*. *Int Immunopharmacol*, 2006. **6**(2): p. 133-43.
236. Melchini, A., et al., *Enhanced in vitro biological activity of synthetic 2-(2-pyridyl) ethyl isothiocyanate compared to natural 4-(methylsulfinyl) butyl isothiocyanate*. *J Med Chem*, 2012. **55**(22): p. 9682-92.
237. Kim, H.M., et al., *Crystal structure of the TLR4-MD-2 complex with bound endotoxin antagonist Eritoran*. *Cell*, 2007. **130**(5): p. 906-17.
238. Han, J., et al., *Structure-based rational design of a Toll-like receptor 4 (TLR4) decoy receptor with high binding affinity for a target protein*. *PLoS One*, 2012. **7**(2): p. e30929.
239. Zhang, Y., et al., *A major inducer of anticarcinogenic protective enzymes from broccoli: isolation and elucidation of structure*. *Proc Natl Acad Sci U S A*, 1992. **89**(6): p. 2399-403.
240. Zhao, L., J.Y. Lee, and D.H. Hwang, *Inhibition of pattern recognition receptor-mediated inflammation by bioactive phytochemicals*. *Nutr Rev*, 2011. **69**(6): p. 310-20.
241. Walsh, D., et al., *Pattern recognition receptors--molecular orchestrators of inflammation in inflammatory bowel disease*. *Cytokine Growth Factor Rev*, 2013. **24**(2): p. 91-104.
242. Jialal, I., et al., *Increased toll-like receptor activity in patients with metabolic syndrome*. *Diabetes Care*, 2012. **35**(4): p. 900-4.
243. Hardy, O.T., et al., *Increased Toll-like receptor (TLR) mRNA expression in monocytes is a feature of metabolic syndrome in adolescents*. *Pediatr Obes*, 2013. **8**(1): p. e19-23.
244. Manolakis, A.C., et al., *TLR4 gene polymorphisms: evidence for protection against type 2 diabetes but not for diabetes-associated ischaemic heart disease*. *Eur J Endocrinol*, 2011. **165**(2): p. 261-7.

245. Franchi, L., et al., *Function of Nod-like receptors in microbial recognition and host defense*. Immunol Rev, 2009. **227**(1): p. 106-28.
246. Galluzzo, S., et al., *Association between NOD2/CARD15 polymorphisms and coronary artery disease: a case-control study*. Human Immunology, 2011. **72**(8): p. 636-40.
247. Liu, J., et al., *NOD2 polymorphisms associated with cancer risk: a meta-analysis*. PLoS One, 2014. **9**(2): p. e89340.
248. Arbour, N.C., et al., *TLR4 mutations are associated with endotoxin hyporesponsiveness in humans*. Nat Genet, 2000. **25**(2): p. 187-91.
249. Pierik, M., et al., *Toll-like receptor-1, -2, and -6 polymorphisms influence disease extension in inflammatory bowel diseases*. Inflamm Bowel Dis, 2006. **12**(1): p. 1-8.
250. Geisse, S. and B. Voedisch, *Transient expression technologies: past, present, and future*. Methods Mol Biol, 2012. **899**: p. 203-19.
251. Bonen, D.K., et al., *Crohn's disease-associated NOD2 variants share a signaling defect in response to lipopolysaccharide and peptidoglycan*. Gastroenterology, 2003. **124**(1): p. 140-6.
252. Inohara, N., et al., *Host recognition of bacterial muramyl dipeptide mediated through NOD2. Implications for Crohn's disease*. J Biol Chem, 2003. **278**(8): p. 5509-12.
253. Nair, R.P., et al., *Lack of association between NOD2 3020InsC frameshift mutation and psoriasis*. J Invest Dermatol, 2001. **117**(6): p. 1671-2.
254. Lecine, P., et al., *The NOD2-RICK complex signals from the plasma membrane*. J Biol Chem, 2007. **282**(20): p. 15197-207.
255. Despres, J.P. and I. Lemieux, *Abdominal obesity and metabolic syndrome*. Nature, 2006. **444**(7121): p. 881-7.
256. Despres, J.P., *Intra-abdominal obesity: an untreated risk factor for Type 2 diabetes and cardiovascular disease*. J Endocrinol Invest, 2006. **29**(3 Suppl): p. 77-82.
257. Kelley, D.E., et al., *Interaction between glucose and free fatty acid metabolism in human skeletal muscle*. J Clin Invest, 1993. **92**(1): p. 91-8.
258. Keuper, M., et al., *THP-1 Macrophages and SGBS Adipocytes - A New Human in vitro Model System of Inflamed Adipose Tissue*. Front Endocrinol (Lausanne), 2011. **2**: p. 89.
259. Chorley, B.N., et al., *Identification of novel NRF2-regulated genes by ChIP-Seq: influence on retinoid X receptor alpha*. Nucleic Acids Res, 2012. **40**(15): p. 7416-29.

- 
260. Vomhof-DeKrey, E.E. and M.J. Picklo, *NAD(P)H:quinone oxidoreductase 1 activity reduces hypertrophy in 3T3-L1 adipocytes*. Free Radic Biol Med, 2012. **53**(4): p. 690-700.
261. Xu, J., et al., *Enhanced Nrf2 activity worsens insulin resistance, impairs lipid accumulation in adipose tissue, and increases hepatic steatosis in leptin-deficient mice*. Diabetes, 2012. **61**(12): p. 3208-18.
262. Zhou, R., J. Lin, and D. Wu, *Sulforaphane induces Nrf2 and protects against CYP2E1-dependent binge alcohol-induced liver steatosis*. Biochim Biophys Acta, 2014. **1840**(1): p. 209-18.
263. Souza, C.G., et al., *Chronic sulforaphane oral treatment accentuates blood glucose impairment and may affect GLUT3 expression in the cerebral cortex and hypothalamus of rats fed with a highly palatable diet*. Food Funct, 2013. **4**(8): p. 1271-6.
264. Vomhof-Dekrey, E.E. and M.J. Picklo, Sr., *The Nrf2-antioxidant response element pathway: a target for regulating energy metabolism*. J Nutr Biochem, 2012. **23**(10): p. 1201-6.
265. Yates, M.S., et al., *Genetic versus chemoprotective activation of Nrf2 signaling: overlapping yet distinct gene expression profiles between Keap1 knockout and triterpenoid-treated mice*. Carcinogenesis, 2009. **30**(6): p. 1024-31.
266. Pi, J., et al., *Deficiency in the nuclear factor E2-related factor-2 transcription factor results in impaired adipogenesis and protects against diet-induced obesity*. J Biol Chem, 2010. **285**(12): p. 9292-300.
267. Shin, S., et al., *NRF2 modulates aryl hydrocarbon receptor signaling: influence on adipogenesis*. Mol Cell Biol, 2007. **27**(20): p. 7188-97.
268. Keuper, M., et al., *An inflammatory micro-environment promotes human adipocyte apoptosis*. Mol Cell Endocrinol, 2011. **339**(1-2): p. 105-13.
269. Zagotta, I., et al., *Resveratrol suppresses PAI-1 gene expression in a human in vitro model of inflamed adipose tissue*. Oxid Med Cell Longev, 2013. **2013**: p. 793525.
270. Overman, A., C.C. Chuang, and M. McIntosh, *Quercetin attenuates inflammation in human macrophages and adipocytes exposed to macrophage-conditioned media*. Int J Obes (Lond), 2011. **35**(9): p. 1165-72.
271. Chacon, M.R., et al., *Grape-seed procyanidins modulate inflammation on human differentiated adipocytes in vitro*. Cytokine, 2009. **47**(2): p. 137-42.
272. Canello, R. and K. Clement, *Is obesity an inflammatory illness? Role of low-grade inflammation and macrophage infiltration in human white adipose tissue*. BJOG, 2006. **113**(10): p. 1141-7.

- 
273. Ghanim, H., et al., *Circulating mononuclear cells in the obese are in a proinflammatory state*. *Circulation*, 2004. **110**(12): p. 1564-71.
274. Abbaoui, B., et al., *Inhibition of bladder cancer by broccoli isothiocyanates sulforaphane and erucin: characterization, metabolism, and interconversion*. *Mol Nutr Food Res*, 2012. **56**(11): p. 1675-87.
275. Kanematsu, S., et al., *Sulforaphane inhibits the growth of KPL-1 human breast cancer cells in vitro and suppresses the growth and metastasis of orthotopically transplanted KPL-1 cells in female athymic mice*. *Oncol Rep*, 2011. **26**(3): p. 603-8.
276. Lasa, A., et al., *Resveratrol regulates lipolysis via adipose triglyceride lipase*. *J Nutr Biochem*, 2012. **23**(4): p. 379-84.
277. Lu, C., et al., *A novel effect of growth hormone on macrophage modulates macrophage-dependent adipocyte differentiation*. *Endocrinology*, 2010. **151**(5): p. 2189-99.
278. Constant, V.A., et al., *Macrophage-conditioned medium inhibits the differentiation of 3T3-L1 and human abdominal preadipocytes*. *Diabetologia*, 2006. **49**(6): p. 1402-11.
279. Yarmo, M.N., et al., *Macrophage-conditioned medium inhibits differentiation-induced Rb phosphorylation in 3T3-L1 preadipocytes*. *Exp Cell Res*, 2009. **315**(3): p. 411-8.
280. Constant, V.A., et al., *The antiadipogenic effect of macrophage-conditioned medium depends on ERK1/2 activation*. *Metabolism*, 2008. **57**(4): p. 465-72.
281. Lacasa, D., et al., *Macrophage-secreted factors impair human adipogenesis: involvement of proinflammatory state in preadipocytes*. *Endocrinology*, 2007. **148**(2): p. 868-77.
282. Curat, C.A., et al., *From blood monocytes to adipose tissue-resident macrophages: induction of diapedesis by human mature adipocytes*. *Diabetes*, 2004. **53**(5): p. 1285-92.
283. Tannahill, G.M., et al., *Succinate is an inflammatory signal that induces IL-1beta through HIF-1alpha*. *Nature*, 2013. **496**(7444): p. 238-42.
284. Bassols, J., et al., *Study of the proinflammatory role of human differentiated omental adipocytes*. *J Cell Biochem*, 2009. **107**(6): p. 1107-17.
285. O'Hara, A., et al., *Microarray analysis identifies matrix metalloproteinases (MMPs) as key genes whose expression is up-regulated in human adipocytes by macrophage-conditioned medium*. *Pflugers Arch*, 2009. **458**(6): p. 1103-14.
286. Carey, A.L. and M.A. Febbraio, *Interleukin-6 and insulin sensitivity: friend or foe?* *Diabetologia*, 2004. **47**(7): p. 1135-42.

- 
287. Kristiansen, O.P. and T. Mandrup-Poulsen, *Interleukin-6 and diabetes: the good, the bad, or the indifferent?* Diabetes, 2005. **54 Suppl 2**: p. S114-24.
288. Suganami, T., J. Nishida, and Y. Ogawa, *A paracrine loop between adipocytes and macrophages aggravates inflammatory changes: role of free fatty acids and tumor necrosis factor alpha.* Arterioscler Thromb Vasc Biol, 2005. **25**(10): p. 2062-8.
289. Gagnon, A., et al., *The role of interleukin 1beta in the anti-adipogenic action of macrophages on human preadipocytes.* J Endocrinol, 2013. **217**(2): p. 197-206.
290. Gao, D. and C. Bing, *Macrophage-induced expression and release of matrix metalloproteinase 1 and 3 by human preadipocytes is mediated by IL-1beta via activation of MAPK signaling.* J Cell Physiol, 2011. **226**(11): p. 2869-80.
291. Lagathu, C., et al., *Long-term treatment with interleukin-1beta induces insulin resistance in murine and human adipocytes.* Diabetologia, 2006. **49**(9): p. 2162-73.
292. Wang, B. and P. Trayhurn, *Acute and prolonged effects of TNF-alpha on the expression and secretion of inflammation-related adipokines by human adipocytes differentiated in culture.* Pflugers Arch, 2006. **452**(4): p. 418-27.
293. Wang, B., J.R. Jenkins, and P. Trayhurn, *Expression and secretion of inflammation-related adipokines by human adipocytes differentiated in culture: integrated response to TNF-alpha.* Am J Physiol Endocrinol Metab, 2005. **288**(4): p. E731-40.
294. Sibhatu, M.B., et al., *Expression of MRP1 and GSTP1-1 modulate the acute cellular response to treatment with the chemopreventive isothiocyanate, sulforaphane.* Carcinogenesis, 2008. **29**(4): p. 807-15.
295. Ye, L.X. and Y.S. Zhang, *Total intracellular accumulation levels of dietary isothiocyanates determine their activity in elevation of cellular glutathione and induction of Phase 2 detoxification enzymes.* Carcinogenesis, 2001. **22**(12): p. 1987-1992.
296. Zhang, Y. and E.C. Callaway, *High cellular accumulation of sulphoraphane, a dietary anticarcinogen, is followed by rapid transporter-mediated export as a glutathione conjugate.* Biochem J, 2002. **364**(Pt 1): p. 301-7.
297. Gao, X. and P. Talalay, *Induction of phase 2 genes by sulforaphane protects retinal pigment epithelial cells against photooxidative damage.* Proc Natl Acad Sci U S A, 2004. **101**(28): p. 10446-51.
298. Callaway, E.C., et al., *Cellular accumulation of dietary anticarcinogenic isothiocyanates is followed by transporter-mediated export as dithiocarbamates.* Cancer Letters, 2004. **204**(1): p. 23-31.

- 
299. Permana, P.A., C. Menge, and P.D. Reaven, *Macrophage-secreted factors induce adipocyte inflammation and insulin resistance*. *Biochem Biophys Res Commun*, 2006. **341**(2): p. 507-14.
300. Juge, N., R.F. Mithen, and M. Traka, *Molecular basis for chemoprevention by sulforaphane: a comprehensive review*. *Cellular and Molecular Life Sciences*, 2007. **64**(9): p. 1105-1127.
301. Hu, R., et al., *Gene expression profiles induced by cancer chemopreventive isothiocyanate sulforaphane in the liver of C57BL/6J mice and C57BL/6J/Nrf2 (-/-) mice*. *Cancer Lett*, 2006. **243**(2): p. 170-92.
302. Brown, K.K. and M.B. Hampton, *Biological targets of isothiocyanates*. *Biochim Biophys Acta*, 2011. **1810**(9): p. 888-94.
303. Traka, M.H., et al., *The dietary isothiocyanate sulforaphane modulates gene expression and alternative gene splicing in a PTEN null preclinical murine model of prostate cancer*. *Mol Cancer*, 2010. **9**: p. 189.
304. Myzak, M.C., et al., *Sulforaphane inhibits histone deacetylase in vivo and suppresses tumorigenesis in Apc-minus mice*. *FASEB J*, 2006. **20**(3): p. 506-8.
305. Traka, M.H., et al., *Genetic regulation of glucoraphanin accumulation in Beneforte broccoli*. *New Phytol*, 2013. **198**(4): p. 1085-95.